Rock Slopes and Gravel Beaches under Wave Attack

Jentsje W. van der Meer

Rock Slopes and Gravel Beaches under Wave Attack

Jentsje W. van der Meer

Rock Slopes and Gravel Beaches under Wave Attack

Proefschrift

ter verkrijging van de graad van doctor aan
de Technische Universiteit Delft, op gezag van
de Rector Magnificus, prof. dr. J.M. Dirken,
in het openbaar te verdedigen ten overstaan van
een commissie aangewezen door het College van
Dekanen op 26 april 1988 te 14.00 uur

door

Jentsje Wouter van der Meer,

geboren te Leeuwarden,

civiel ingenieur.

1988

Dit proefschrift is goedgekeurd door de promotor prof. dr. ir. E.W. Bijker

aan Jan, Pieter, Leen
en
aan Vronie, Wouter en Annet

Samenvatting

Stortsteen taluds en grindstranden onder golfaanval

Taluds van losgestorte materialen onder golfaanval werden onderzocht met behulp van klein en grootschalige physische modellen. Deze taluds kunnen worden onderverdeeld in stortsteen golfbrekers, stortsteen taludverdedigingen, steen- en grindstranden. De konstrukties kunnen kortweg worden verdeeld in statisch en dynamisch stabiele konstrukties.

Bij statisch stabiele konstrukties is geen of maar weinig verplaatsing van materiaal toegestaan. Als verplaatsing optreedt, wordt gesproken van **schade** aan de konstruktie. Dynamisch stabiele konstrukties kenmerken zich door het instellen van een **profiel** onder golfaanval. In dit geval is niet de schade van belang, maar het gevormde profiel. Deze studie beschrijft het gebied van "geen schade" bij statisch stabiele konstrukties tot de profielvorming van fijn (4 mm) grind onder prototype omstandigheden.

Als eerste worden variabelen behandeld die van invloed kunnen zijn op stabiliteit en profielvorming. De achtergronden en vermoedelijke invloeden van deze variabelen worden beschreven. De variabelen worden herleid tot dimensieloze grootheden. De mogelijkheden en gevaren van het gebruik van dimensieloze variabelen worden toegelicht. Uiteindelijk wordt een lijst geproduceerd met van belang zijnde dimensieloze variabelen en hun mogelijk toepassingsgebied. Hoofdstuk 2 behandelt deze materie.

Het physisch onderzoek is zodanig opgezet dat alle van belang geachtte dimensieloze variabelen werden onderzocht in een zo breed mogelijk gebied. Hierdoor zullen ook de resultaten een breed toepassingsgebied beslaan. In eerste instantie is een kwalitatieve analyse uitgevoerd op de resultaten. Bij statische stabiliteit werden invloeden op de stabiliteit beschreven met behulp van zogenaamde $H_s/\Delta D_{n}50 - \xi_m$ plots. De kwalitatieve resultaten bij dynamische stabiliteit werden geanalyseerd door profielen rechtstreeks met elkaar te vergelijken.

Funktionele verbanden werden afgeleid met als basis de resultaten van de kwalitatieve analyse. Het onderzoek naar statische stabiliteit heeft geleid tot twee stabiliteitsformules, één voor brekende en één voor niet-brekende golven, die de stabiliteit van statisch stabiele stortsteen konstrukties beschrijven. De welbekende Hudson formule, overigens impliciet verwerkt in de formules, kan hiermee worden vervangen. Hoofdstuk 3 behandelt de opzet en analyse van de statisch stabiele konstrukties.

De funktionele verbanden, gevonden voor dynamisch stabiele konstrukties, hebben geleid tot een computer model waarmee het profiel kan worden berekend dat zich vormt op een willekeurig uitgangstalud. Het model werd geverifieerd met afhankelijke en onafhankelijke proefgegevens en met prototype waarnemingen. Berm golfbrekers, die momenteel een sterk groeiende belanstelling genieten, kunnen met dit model worden ontworpen. De opzet en analyse van dynamisch stabiele konstrukties en de ontwikkeling van het model worden in hoofdstuk 4 behandeld.

Abstract

Rock slopes and gravel beaches under wave attack

The stability of slopes consisting of loose materials under wave attack have been investigated with the aid of small and large scale physical models. These slopes can be divided into rubble mound breakwaters, rubble mound revetments, rock beaches and gravel or shingle beaches. The structures may be treated as either statically or dynamically stable.

No displacement of material or only very little is allowed for statically stable structures. Displacement of stones is called **damage**. Dynamically stable structures are characterized by the forming of a **profile** under wave attack. In this case damage is not important, but the developed profile. This study describes the range from "no damage" to statically stable structures up to the profile development of very small (4 mm) shingle under prototype circumstances.

Governing variables on stability and profile development were treated first. The basic background and possible influences of these variables were described. The variables were transformed into dimensionless governing variables. The possibilities and disadvantages of using dimensionless variables were highlighted. A list of governing variables with their possible range of application was given finally. Chapter 2 deals with these aspects.

The physical investigation was set up in such a way that all listed governing variables were studied in a range as wide as possible. This means that the results will cover a wide range of possible applications too. In a previous stage a qualitative analysis was performed on the results. The influences on static stability were described by so-called $H_s/\Delta D_{n50} - \xi_m$ plots. The results of the dynamically stable structures were qualitatively analyzed by a direct comparison of profiles.

Functional relationships were established with the results of the qualitative analysis as a basis. The investigation on static stability resulted in two stability formulae, one for plunging and one for surging waves, which describe the stability of statically stable structures. The well-known Hudson formula, although implicitly described in the formulae, can be replaced by these formulae. Chapter 3 deals with the set-up and analysis of statically stable structures.

The functional relationships established for dynamically stable structures resulted in a computer model which is able to compute the profile that will be developed under wave attack on an arbitrary initial slope. The model was verified with dependent and independent test results and with prototype measurements. Berm breakwaters which gain increasing interest, can be designed with the aid of this model. The set-up and analysis of dynamically stable structures and the development of the model are described in Chapter 4.

Acknowledgements

CONTENTS

Samenvatting

Abstract

Acknowledgements

CONTENTS (continued)

CONTENTS (continued)

References

List of symbols

List of tables

List of figures

Curriculum Vitae

ROCK SLOPES AND GRAVEL BEACHES UNDER WAVE ATTACK

1. Introduction

1.1 Introduction to stability

Most breakwaters and revetments are designed in such a way that no or only little damage is allowed for in the design criteria, damage being defined as the displacement of the structure as a whole (caisson) or the displacement of armour units. This criterion leads to large concrete structures or large and heavy rock or artificial concrete elements for armouring. A more economic solution can be a structure with smaller elements, where profile development is being allowed in order to reach a stable profile.

In recent years, there has been an increasing demand for reliable design formulae, to cope with the ever growing dimensions of the structures and the necessity to move into more hostile environments. Moreover, the alternative structures with high economical potential, such as S-shaped and berm breakwaters, required new design techniques.

The $H/\Delta D$ parameter can be used to give the relationship between different structures. Here: H = wave height, Δ = relative mass density and D = characteristic diameter of structure, armour unit, stone, gravel or sand. Structures such as caissons or structures with large armour units are characterized by small values of $H/\Delta D$. Large values imply gravel beaches and sand beaches. Examples of types of structures with corresonding $H/\Delta D$ values are shown in Figure 1.1.

Figure 1.1 gives the following rough classification:

- $H/\Delta D < 1$ **Caissons or seawalls**
  No damage is allowed, for these fixed structures. The diameter, D, can be the height or width of the structure.

- $H/\Delta D = 1 - 4$ **Stable breakwaters**
  Generally, uniform slopes are applied with heavy artificial armour units or natural rock. Only little damage (displacement) is allowed under severe design conditions. The diameter is a characteristic diameter of the unit, such as the nominal diameter.

- $H/\Delta D = 3 - 6$ **S-shaped and berm breakwaters**
  These structures are characterized by more or less steep slopes above and
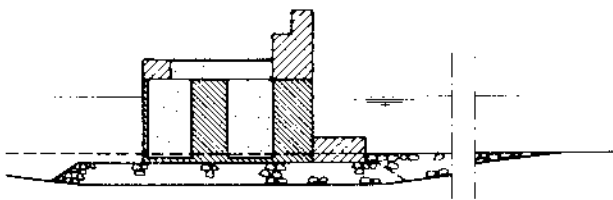
caisson
H/ΔD < 1
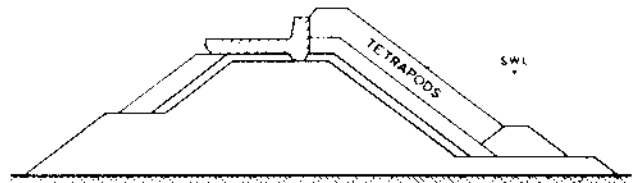
rubble mound breakwater
H/ΔD = 1 - 4
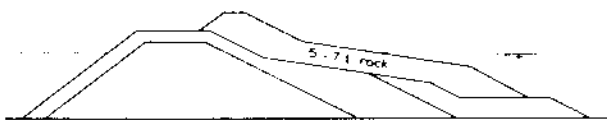
S-shaped breakwater
H/ΔD = 3 - 6
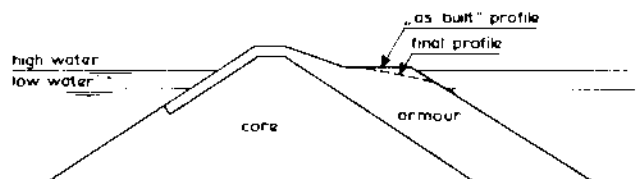
berm breakwater
H/ΔD = 3 - 6
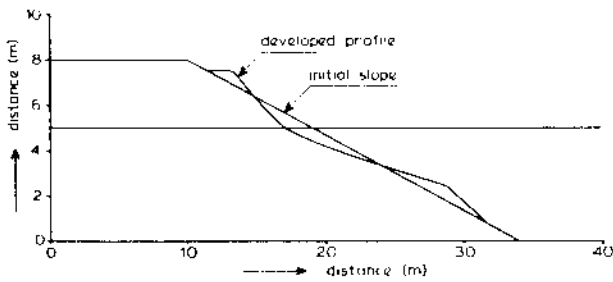
rock beach
H/ΔD = 6 - 20
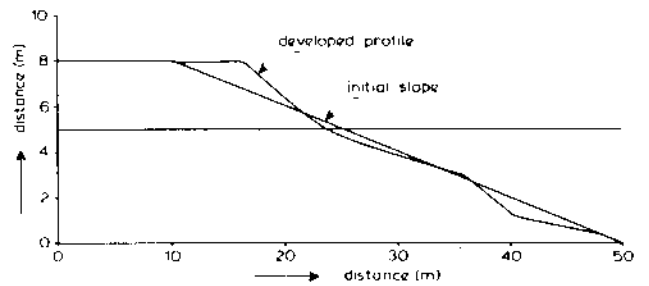
gravel beach
H/ΔD = 20 - 500
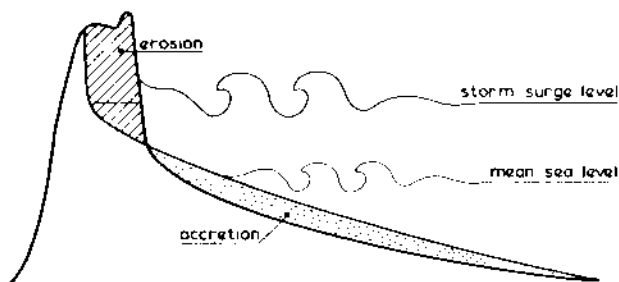
dune erosion (sand beach)
H/ΔD > 500

Figure 1.1   Type of structure as a function of H/ΔD

below the still water level with a more gently intermediate part. This gentle slope reduces the wave forces on the armour units. Berm breakwaters are designed with a rather steep seaward slope and a horizontal berm just above the still water level or tidal area. The first storms develop a more gentle profile which does not change later on. The profile changes to be expected are important.

- $H/\Delta D = 6 - 20$ **Rock slopes / beaches**
  The diameter of the rock is relatively small. The structure cannot withstand severe wave attack without displacement of material. The profile which is being developed under different wave boundary conditions is the design objective.

- $H/\Delta D = 15 - 500$ **Gravel beaches**
  Grain sizes, between ten centimeters and four millimeters, can be classified as gravel. Gravel beaches will change continuously under varying wave conditions and water levels (tide). Again the development of the profile is one of the design objectives.

- $H/\Delta D > 500$ **Sand beaches and dunes**
  Material with very small diameters can withstand severe wave attack. The Dutch coast is partly protected by sand dunes. The dune erosion and profile development during storm surge are the main design parameters. Extensive basic research has been performed on this topic (Vellinga, 1986).

Structures, designed to protect coasts or harbours against wave attack, can be classified by the $H/\Delta D$ parameter described above. These structures can be classified into statically stable structures and dynamically stable structures, depending on the behaviour under design conditions.

Statically stable structures are structures where no or minor damage is allowed under design conditions. Damage is defined as displacement of armour units. The mass of individual units must be large enough to withstand the wave forces during design conditions. Caissons and traditionally designed breakwaters belong to the group of statically stable structures. The design is based on an optimum solution between design conditions, allowable damage and costs for construction and maintenance. Static stability is characterized by the design parameter **damage**, and can roughly be classified by $H/\Delta D < 4$.

Dynamically stable structures are structures where profile development is accepted. Units (stones, gravel or sand) are displaced by wave action until a profile is reached where the transport capacity along the profile is reduced

to a minimum. Material around the still water level is continuously moving during each run-up and run-down of the waves, but when the net transport capacity has become zero the profile has reached an equilibrium. Dynamic stability is characterized by the design parameter **profile**, and can roughly be classified by $H/\Delta D > 6$.

Rock slopes and gravel beaches can be divided into statically and dynamically stable structures. Stability of individual stones is concerned in the case of static stability. For dynamic stability the transport capacity along the slope is important. The intermediate range where static stability passes into dynamic stability is the most difficult area to describe. Both the stability of individual stones and the transport capacity along the slope must be taken into account.

The design of statically stable rubble mound (rock) breakwaters and revetments and dynamically stable rock slopes and gravel beaches will be discussed in this theses. This encompasses a range of $H/\Delta D$ values from $1 - 500$. Rubble mound structures armoured with artificial concrete units and structures such as caissons will not be considered.

Only the behaviour of the cross-section perpendicular to the alignment of the structure will be described. This is the damage for statically stable structures and the profile for dynamically stable structures. The aspect of longshore transport of material due to oblique wave attack or currents has not been considered during the research and has also not been considered in this thesis.

In IAHR/PIANC (1986) a list of sea state parameters was produced. In their preface it was stated: "Active use of the recommended parameters and their symbols can significantly reduce the possibility of serious misunderstandings, and prevent further confusion. It is sincerely hoped that this document, recommended for use by IAHR and PIANC, will benefit the maritime research and engineering community". The notation of symbols in the present thesis is accordingly to the IAHR/PIANC list, as far as possible. This means that notation in this thesis may differ slightly from the notation in earlier publications of the author.

1.2 Background of the research

Stability of loose materials under wave attack has been investigated all over the world during the past fifty years. Initially monochromatic waves were applied, investigations with random waves in the model facilities started

about twenty years ago. Many design formulae are still based on monochromatic wave tests, however.

As far as static stability tests under **monochromatic waves** are concerned the widely used Hudson formula (Hudson, 1959) will be discussed and the work of Hedar (1960), Losada and Giménez-Curto (1979a) and the large scale tests of Ahrens (1975) on riprap slopes. Thompson and Shuttler (1975) have performed an extensive research on static stability of riprap slopes under **random wave** attack. Their work has been used as a starting point for this basic research on static stability of rubble mound breakwaters and revetments under random wave attack.

Dynamic stability of gravel beaches has been investigated at DELFT HYDRAU-LICS during the past fifteen years. Summarized results have been published by Van Hijum (1974, 1976), Van Hijum and Pilarczyk (1982) and Pilarczyk and Den Boer (1983). Van Hijum and Pilarczyk (1982) developed a model which described the dynamically stable profile of gravel beaches in the range $H/\Delta D = 12 - 35$. Their work has partly been the basis for an extensive literature review in order to study the validity of the model beyond the range tested, (DELFT HYDRAULICS-M1809, (1984)).

The latter literature study included also static stability of breakwaters and one objective of the study was to identify "blank spots" in the knowledge of statically and dynamically stable rock slopes and gravel beaches. The results of this study were used to set-up an extensive model investigation which was performed by the author, (DELFT HYDRAULICS-M1983, (1988a and b)).

First tests were performed in September 1983, the final tests were completed in December 1986. In total about 500 tests have been performed, divided into three parts:

● small scale tests on static stability
● small scale tests on dynamic stability
● large scale tests on scale effects and extrapolation of dynamic stability up to the transition to sand beaches.

The latter research and the study of Thompson and Shuttler (1975), and the work of Van Hijum and Pilarczyk (1982) have been the basis of this thesis. The methodology, the philosophy of approach and the governing variables for stability are described in Chapter 2. Static stability is described in Chapter 3, including the large scale tests on scale effects. Finally, dynamic stability is described in Chapter 4.

1.3 Conclusions and recommendations

1.3.1 Static stability

1. The stability of statically stable rock slopes is determined by a large number of variables. The main governing variables are:

The significant wave height at the structure:	H_s
The average wave period:	T_m
The storm duration or number of waves:	N
The water depth at the structure:	h
The nominal diameter of the stone:	D_{n50}
The relative mass density:	Δ
The slope angle of the front slope:	$\cot\alpha$
The permeability of the structure:	P

2. A number of variables investigated had no or only minor influence on stability. Amongst them are the spectral shape parameter, κ , and the grading of the stones, D_{85}/D_{15}.

3. A clearly defined damage level, S, was introduced by coupling the cross-sectional eroded area, A, to the nominal diameter of the armour stones, D_{n50}.

$$S = A/D_{n50}^2 \tag{2.4}$$

For the "no damage" criterion of Hudson (1959), S is taken generally to be between 1 and 3. The lower and upper damage levels, that is the onset of damage and failure (filter layer visible), were determined from the investigation. These damage levels should be considered in the design of a two diameter thick armour layer.

	DAMAGE LEVEL $S = A/D_{50}^2$	
$\cot\alpha$	start of damage	filter layer visible (2D_{50} thick layer)
1.5	2	8
2.0	2	8
3.0	2	12
4.0	3	17
6.0	3	17

4. The relation between the damage, S, and the number of waves, N, can be described by $S/\sqrt{N}$ (N < 8500). The surf similarity parameter, ξ_m, describes the influence of wave steepness and slope angle in a proper way, but only for plunging (breaking) waves. For surging waves the dependency of slope angle and wave steepness on stability is different from that described by ξ_m. The wave height, H_s, relative mass density, Δ, and nominal diameter, D_{n50}, can be combined to the dimensionless wave height or stability number, $H_s/\Delta D_{n50}$. The permeability of the structure can be described by the permeability coefficient P. The lower boundary of P is given by an impermeable core (P = 0.1) and the upper boundary by a homogeneous structure (P = 0.6).

5. The dimensionless governing variables on static stability can be summarized as follows:

$S/\sqrt{N}$

$H_s/\Delta D_{n50}$

ξ_m

$\cot\alpha$

P

6. The relationship between the governing variables can be given by two stability formulae, one for plunging waves and the other for surging waves.

For plunging waves:

$$H_s/\Delta D_{n50} * \sqrt{\xi_m} = 6.2 \ P^{0.18} \ (S/\sqrt{N})^{0.2} \tag{3.23}$$

For surging waves:

$$H_s/\Delta D_{n50} = 1.0 \ P^{-0.13} \ (S/\sqrt{N})^{0.2} \ \sqrt{\cot\alpha} \ \xi_m^P \tag{3.24}$$

The transition from plunging to surging waves is described by the intersection of both formulae:

$$\xi_m = (6.2 \ P^{0.31} \ \sqrt{\tan\alpha}) \ 1/(P + 0.5) \tag{3.25}$$

7. The influence of the truncation of the wave height exceedance curve on stability, due to depth limitation, can be described by using the $H_{2\%}$ wave height in the formulae. This means that only the highest waves during a storm will influence stability. Formulae with $H_{2\%}$ instead of H_s are given by Equations 3.26 and 3.27.

8. The reliability of the stability formulae can be expressed by considering the coefficients 6.2 and 1.0 in Equations 3.23 and 3.24 as stochastic variables. Assuming a normal distribution for these coefficients, the standard deviation of the coefficient 6.2 amounted to 0.4 (6.5%). For the coefficient 1.0 this amounted to 0.08 (8%). These values can be used in a probabilistic design.

9. Large scale tests confirmed the validity of the above stability formulae. Physical model investigation on stability of rock armoured slopes is not influenced by the Reynolds number if Re is between 4.10^4 and 7.10^5. The value of 4.10^4 is not necessarily the lowest boundary to avoid scale effects.

10. The permeability coefficient, P, can be related to the volume of water that is stored (dissipated) in the core of the structure. This dissipated volume was computed in a first attempt by the computer program HADEER. It is possible, therefore, to establish P for each actual structure on the basis of computations. It is recommended to extend research in this field.

11. The stone shape, being more or less cubical throughout the investigation was not considered to be a governing variable on stability. Test results indicate, however, that the shape of the stone, described by the roundness and the surface texture, have large influence on stability. Further research is strongly recommended, using recently developed techniques to measure shape descriptors.

1.3.2 Dynamic stability

1 Dynamic stability is described in terms of 6 length or height parameters and 2 slope angles, characterizing the profile under wave action. These profiles were described in the range of $H_s/\Delta D_{n50} = 3 - 500$. The curved profile around the still water level is described by two power functions. The length and height parameters are related to the water level or to the local origin of the profile (the intersection with the still water level). This means that the profile description is independent of the initial slope and of the location of the profile itself. The location of the profile is finally determined from the mass balance. The schematic profile is given in Figure 4.20.

2. The governing variables for dynamic stability are:

The nominal diameter: D_{n50}

The relative mass density of the stone: Δ

The significant wave height at the structure: H_S

The average wave period: T_m

The storm duration or number of waves: N

The water depth at the structure: h

The angle of wave attack: ψ

3. From the analysis of the profiles it followed that:

- Wave height and period have similar effects on the profile formation. This is expressed by the combined dimensionless wave height - wave period parameter, H_oT_o, which is described by:

$$H_oT_o = H_s/\Delta D_{n50} * \sqrt{g/D_{n50}} \, T_m$$

where:

$H_o = H_s/\Delta D_{n50}$ = dimensionless wave height parameter

$T_o = \sqrt{g/D_{n50}} \, T_m$ = dimensionless wave period parameter, related to D_{n50}

- The storm duration has influence up to a very large number of waves.
- The spectral shape has no influence on the profile, using T_m as the wave period.
- For $H_s/\Delta D_{n50} < 15 - 20$ the developed profile is influenced by the initial slope. A method to establish an equivalent slope angle was introduced, therefore.
- The initial slope has no influence on the profile for $H_s/\Delta D_{n50} > 15-20$.
- The shape of the material, cubical, long and flat, or rounded has no influence on the profile.
- The profile is influenced by the angle of wave attack, ψ. The length and height parameters should be reduced by $\cos\psi$ (except for one parameter).
- The profile below the still water level becomes steeper when the structure is situated in shallow water.

4. The profile parameters were related to the boundary conditions and a computer program was developed to compute the profiles. The profile can be computed for an arbitrary initial slope. A sequence of storms with varying water levels can be simulated by taking the last computed profile as the initial profile for the next computation.

5. The verification of the model with both dependent and independent data showed good agreement between computation and measurement.

6. Possible applications of the model are:

- Computation of the behaviour of rock slopes and gravel beaches.
- Design of a berm or mass armoured breakwater.
- Design of an S-shaped breakwater.
- Prediction of the behaviour of filter layers and core of breakwaters under construction, for yearly storm conditions.
- Performance of a sensitivity analysis on a designed profile.

2. Governing variables

2.1 Methodology

2.1.1 Overall view

Basic research in engineering is often based on numerical and/or physical modeling of processes. It depends largely on the process to be investigated whether numerical or physical modeling will be applied. Two aspects are important in this case. First the **availability of theoretical descriptions** of the process and the possibility of solving these descriptions. Secondly the **possibility of physical modeling** of the process.

The possibility of solving a large amount of equations increases tremendously with the aid of the fast increasing capacity of super computers. The development of a lot of numerical models is based on this increased capacity of the computer. This is especially so in areas where physical modeling is not or hardly possible. Breakthroughs in engineering have been realized. Sophisticated hindcast wave models are a good example of this.

Numerical models have been developed in many area's where physical models were applied before. Expensive physical models are replaced by cheaper and faster numerical models. Wave penetration into harbours is an example.

Stability of coastal structures has mostly been studied by means of physical modeling. One of the main reasons for this is the relatively easy way of modeling the structures and its loads by small scale models based on Froude's law. Another reason is the large number of governing variables involved in the processes. Only a part of them can be described by theoretical descriptions or equations.

A disadvantage of physical models is the possibility of model and scale effects. Scale effects occur if physical properties can not be scaled properly. The Reynolds number is one of the most important proporties which is not scaled correctly. Large scale investigation (in the Delta Flume) might, however, overcome this problem. Model effects result from an improper schematization of the processes, with respect to nature. Common effects are parasitic reflection from model boundaries and wave board, basin resonance, etc. By applying modern wave generation techniques, these parasitic effects have been eliminated.

The processes involved with stability of coastal structures under wave attack are given in a basic scheme in Figure 2.1. The environmental conditions

```
┌─────────────────────────────┐     ┌─────────────────────┐
│ A.  Environmental parameters │     │ B.  Structural      │
│     describing the water motion│   │     parameters      │
│     in front of the structure│     │                     │
└─────────────────────────────┘     └─────────────────────┘
```

┌─────────────────────────────┐   ┌─────────────────────┐
│   C. LOADS   │   │ D. STRENGTH   │
│ External water motion   │   │ Resistance against │
│ Internal water motion   │   │ wave loads   │
└─────────────────────────────┘   └─────────────────────┘

┌─────────────────────────────────┐
│ E. Description of static and   │
│   dynamic stability: │
│   damage, profile   │
└─────────────────────────────────┘
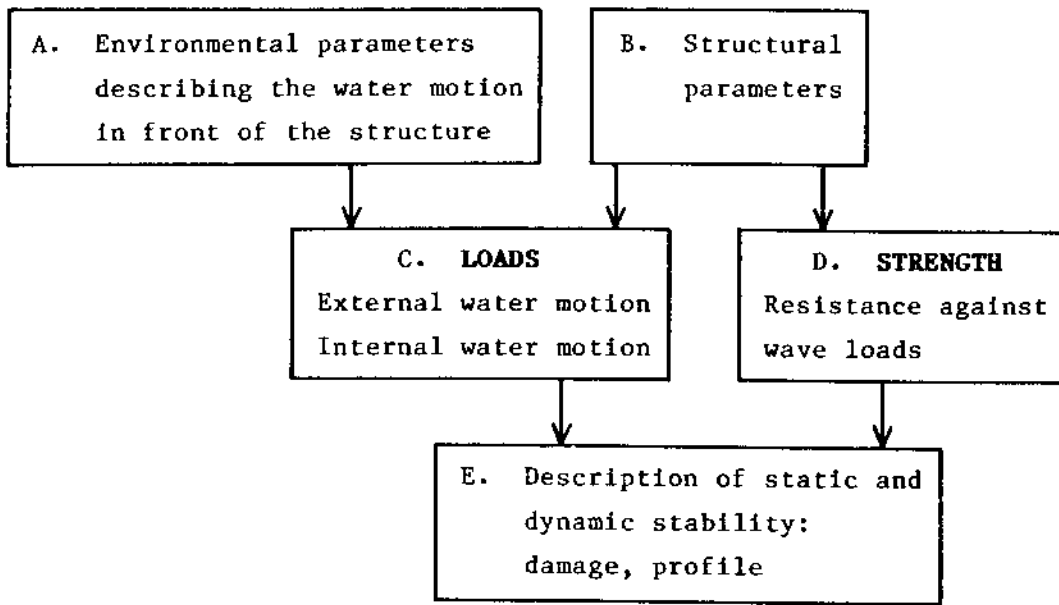
Figure 2.1 Basic scheme of coastal structures under wave attack

lead to a number of parameters which describe the water motion in front of the structure. These parameters are not influenced by the structure itself, and generally, the designer of a structure has no influence on these parameters. Wave height, period and water depth are the main environmental parameters. The structure can be described by a large number of structural parameters. Some important structural parameters are the slope of the structure, the mass and mass density of the rock, and the dimensions of the structure.

The loads on the structure or on structural elements are given by both the environmental and the structural parameters. These loads can be divided into loads due to external water motion on the slope and loads generated by internal water motion in the structure. The external water motion is affected by amongst others the deformation of the wave (breaking or not breaking), the run-up and run-down, reflection and overtopping. The internal water motion describes the penetration or dissipation of water into the structure, the variation of pore pressures and the variation of the freatic line.

Almost all structural parameters might have some or large influence on the loads. Size, shape and grading of armour stones have influence on the roughness of the slope, and therefore on run-up and run-down. Filter size and grading, together with the above mentioned characteristics of the armour stones, have an influence on the permeability of the structure, and hence on the internal water motion.

The resistance against the wave loads can be called the strength of the structure. All structural parameters together describe the strength of the structure. Most of them have influence too on the loads, as described above.

Finally, the behaviour of the structure (strength) under the water motion (loads) leads to a description of static and dynamic stability, given by the threshold of motion or the subsequent profile deformation, respectively.

Figure 2.1 can be used too in order to describe the various ways of physical and numerical modelling of the stability of coastal structures. A black box method is used if the environmental parameters (A in Fig. 2.1) and the structural parameters (B in Fig. 2.1) are modelled physically, and the results (E in Fig. 2.1) are given in graphs or formulae. Description of water motion (C) and influence on strength (D) is not considered.

A grey box method is used if parts of the loads (C) are described by theoretical formulations or numerical models which are related to the strength (D) of the structure by means of a failure criterion or reliability function. The theoretical derivation of a stability formula might be the simplest example of this.

With regard to numerical modelling the recent work of Kobayashi et al (1985, 1986 and 1987) should be mentioned. He developed a numerical model of wave motion on a slope and coupled the water velocities with stability criteria for rubble. In this way stability curves for monochromatic waves were derived solely with a numerical model. But even with this model it is difficult to incorporate for instance the influence of random waves, storm duration and permeability on stability, which means that it does not describe the loads (C) and strength (D) completely.

Other numerical work has been described by Barends (1985) and Hölscher and Barends (1986) who developed the computer code HADEER. This model is able to compute the internal water motion in the structure for given hydrodynamic boundary conditions on the slope.

Finally, a white box is used if all relevant loads and failure criteria can be described by theoretical formulations or numerical models. It is obvious that it will take a long time and a tremendous research effort before coastal structures can be designed by means of a white box.

Therefore, the grey box method was described in this thesis. The behaviour of the structure was studied by means of an extensive physical model investi-

gation. However, in addition qualitative descriptions of processes were given wherever possible, including the computer code HADEER which was used to establish the permeability of the structure with regard to stability. Finally, scale effects were studied by means of large scale tests.

2.1.2 Philosophy of approach

Based on literature a list of governing variables can be composed and an approximation can be made of the qualitative influences of these variables on stability. As it is hardly feasible to investigate all variables, a selection is made again based on the work of other researchers.

The model investigation is performed on a small scale. Direct results, therefore, will be available in model units. Application into prototype design is possible by using scale relations, generally based on Froude's law. Another possibility is to describe the variables in a dimensionless way.

A warning with respect to the use of dimensionless variables should be given here. The choice of the length parameter in dimensional analysis defines the shape of most dimensionless variables. The choice of this parameter, therefore, is extremely important and should in fact be the most governing variable in the processes considered. The investigation should cover these variables in a wide range of possible application. If this requirement is not met, application of results is hardly possible and can lead to large errors.

Overtopping on a structure can be used as an example. If the water depth is used as the length parameter, the dimensionless crest height is directly related to the water depth. If the investigation is focussed on variation of wave height, period, and crest height and not on water depth, the dimensionless expressions found can hardly be used in situations with another water depth.

The choice of the length parameter with respect to governing stability variables is not difficult. The diameter of the stone defines the behaviour of the structure, as described in Section 1.1. Large diameters give statically stable structures as conventional breakwaters. Smaller diameters give dynamically stable structures as rock and gravel beaches. The diameter classifies the structure and will therefore be used as the characteristic length with regard to stability.

Other processes are not influenced by the diameter of the armour stone. The description of the waves and the overtopping with regard to the crest height, are examples of this. The choice of the length parameter in this case is ob-

viously the wave height. Therefore it depends on the process considered which length parameter (diameter or wave height) is chosen in composing dimensionless variables.

Another aspect of using dimensionless variables to be considered, is the extrapolation of results beyond the range tested. Therefore, the range tested should be given together with the possible range of application. Final results presented in a dimensionless way should be given together with the range of application. It is essential that the set-up of the investigation covers a large part of possible applications. If this requirement is met the final results can be applied in a wide range of applications.

The results of the investigation will give quantitative measures for the governing variables. Unexpected phenomena should be considered in more detail in order to find the basic background.

Finally the quantitative results have to be described by formulae in order to make the results applicable for other researchers or designers. If possible, formulae should be based on theoretical backgrounds, using for instance lower and upper boundaries. In a lot of cases, however, a theoretical relationship is not available. Then curve fitting with a presumed functional relationship might be used.

Most warnings described for the use of dimensionless variables yield for curve fitting too. Extrapolation of the curve beyond the range tested, but within the range of possible application should be considered. If the investigation, however, covers lower and upper boundaries of variables, curve fitting can be performed on a sound basis. The set-up of the investigation, therefore, is extremely important and should cover a wide range of application, as said before.

The functional relationship to be used for curve fitting might be a linear, exponential, logarithmic or power function. In this thesis the power function is used in most cases. This relationship has the advantage that variables can be combined in relatively simple equations. The power coefficient for each variable expresses clearly the influence of that variable and the relationship with the other variables. The other coefficient can still be a function of other variables. In this way the number of (curve fitted) coefficients will be minimized. The procedure of curve fitting will be treated in more detail in the relevant sections (Sections 3.4 and 4.4).

Based on the procedures and comments described in this Section the philosophy of approach of the study can be summarized as follows:

1. Select the governing variables and describe the expected qualitative influences on the process using a qualitative description of phenomena. Describe the governing variables in a dimensionless form. Give the possible range of application of each variable. Chapter 2 deals with these aspects.

2. Set up the investigation on the basis of the governing variables selected and try to cover the range of application of each variable. Sections 3.1 and 3.2 give this set-up for static stability and Section 4.1 for dynamic stability.

3. Analyze the qualitative results of the tests and try to find basic backgrounds of the processes involved. For static stability this is described in Section 3.3 and for dynamic stability in Sections 4.2 and 4.3.

4. Try to derive functional relationships between the governing variables on the basis of the results of the analysis on the qualitative results. These sections on curve fitting are described in Sections 3.4 and 4.4 for static and dynamic stability, respectively.

5. Verify the formulae derived on (dependent) test results and if possible on independent data. Sections 3.5 and 4.6 deal with this aspect.

The following part of this Chapter deals first with the description and definition of the basic governing variables or descriptors of static and dynamic stability: damage (Section 2.2.1) and profile (Section 2.2.2). The main environmental parameters (A in Fig. 2.1) are described in more detail in Section 2.3. These are the wave height, the wave period, the spectral shape and the storm duration. A list of governing variables is produced in Section 2.4.1 and dimensionless variables are composed with the diameter and wave height as characteristic length parameters (Section 2.4.2). Finally the lists of governing variables is reviewed, resulting in separate lists for static (Section 2.4.3) and dynamic (Section 2.4.4) stability. The range of possible application is given for each variable.

2.2 Descriptors of static and dynamic stability

2.2.1 Damage

Armour layers of statically stable structures consist of loose materials, such as large rock or artificial concrete units. Normal wave conditions are not able to move or displace stones or units of such armour layers. Only under design conditions wave forces can become so large that individual stones or units can start moving (rocking) or can be displaced.

For large structures with heavy artificial concrete units, especially slender units such as Dolosse, rocking can lead to breakage of the units. This breakage can cause an early failure of the armour layer. A lot of research has been performed in recent years in order to describe the impact forces, caused by rocking (DELFT HYDRAULICS-M1968 (1983a and b), Hall et al (1984), Baird et al (1986), Nishigori et al (1986) and Scott et al (1986)). Other research was focussed on the strength of concrete armour units under impact loading (Desai (1976), Burcharth (1980, 1981b, 1984), Timco (1983a and b, 1984)).

The maximum size of rock in armour layers of breakwaters and revetments is limited by the available material in the quarry used. In almost all cases where good quality rock is used, the strength of the rock is large enough to withstand the impact loads caused by rocking. Therefore, the influence of rocking on stability of armour layers, consisting of rock, is usually not taken into account.

The design process of a statically stable rubble mound breakwater or revetment should result in a unit mass for the armour layer. This mass is based on an economically optimum solution, where construction costs (higher for heavier rock) are compared with maintenance costs (higher for smaller rock). The amount of displacement of rock to be expected in the structures lifetime and under design conditions, is an essential parameter in the design process. This amount of displacement is called damage.

Damage after a storm (or test) can be measured by counting the number of displaced stones, or by comparing the initial profile of the slope with the profile after the event.

Hudson (1959) measured damage with a rod equipped with a circular foot with a diameter equal to one-half the average diameter of the armour stones. Hedar (1960) counted the number of stones displaced. Ahrens (1975) used the same method as Hudson (1959) for his large wave tank tests. The survey pattern was a square grid with points 2 by 2 feet apart in the horizontal plane. This resulted in 6 parallel profiles along the slope. Broderick (1984) used exactly the same method. Thompson and Shuttler (1975) used also a rod equipped with a circular foot with a diameter equal to one half of the average diameter of the armour stones. A survey consisted of recordings over a square grid of positions (in plan) one average diameter apart. Ten profiles parallel along the slope were measured.

Summarizing, the method of measuring damage by using a rod with a circular foot is used by many authors. The accuracy, i.e. the distance between the mea-

sured points and the number of parallel profiles along the slope, differs in most investigations.

Both the method of using a surface profiler and the method of counting the number of displaced stones result in a damage which has to be related to the structure used. Hudson (1959) defined the "no damage criterion" as less than 1% of displaced stones, where the actual number of stones was related to the total number of armour stones. Hedar (1960) defined that the slope was considered stable until some of the stones were just about to move. Ahrens (1975) defined "no damage" as a loss of the riprap layer erosion zone of 1.5 cubic feet per foot tank width. As Ahrens used three different stone sizes, this definition gives a larger tolerable number of displaced stones, using smaller stones.

Thompson and Shuttler (1975) defined a damage parameter, N_Δ, as "the number of D_{50} sized spherical stones eroded from a $9D_{50}$ width of slope which was obtained by dividing the product of the bulk density, ρ_b and the eroded volume by the size of a spherical stone". The figure $9D_{50}$ was applied as the average profile was measured with 10 sounding rods, placed one D_{50} apart, resulting in a width of $9D_{50}$. The bulk density was used to take into account the porosity of the armour layer. In fact a damage parameter was defined which should give an estimation of the actual number of displaced stones. This more exact, but also more difficult definition of damage can be expressed by:

$$N_\Delta = A \, \rho_b \, 9D_{50}/(\rho_a \, D_{50}^3 \, \pi/6) \tag{2.1}$$

where:

N_Δ = damage parameter

A = erosion area in a cross-section

ρ_b = bulk density of material as laid on the slope.

D_{50} = diameter of stone which exceeds the 50% value of the sieve curve

ρ_a = mass density of stone

The advantage of a damage parameter as N_Δ is that the damage is independent of the size of the armour layer (length above and below water level and thickness), compared to a percentage of damage. The parameter, N_Δ, is directly related to the erosion area and to the stone size. A problem can be the measurement of the bulk density in prototype. Another disadvantage is the use of the sieve diameter instead of the actual mass of the stone. Broderick (1984) deletes the bulk density and defines the damage, S, as the erosion area divided by the cube-root squared of the median stone mass, W_{50}, divided by the mass density of the stone, ρ_a.

$$S = A/(W_{50}/\rho_a)^{2/3} \tag{2.2}$$

In fact, the damage, S, is directly related to the diameter of the stone used. By introduction of the nominal diameter, D_{n50}, where:

$$D_{n50} = (W_{50}/\rho_a)^{1/3} \tag{2.3}$$

damage (Equation 2.2) can be changed to:

$$S = A/D_{n50}^2 \tag{2.4}$$

A physical description of the damage, S, in Equation 2.4 is the number of squares with a side D_{n50} which fit into the erosion area, see Figure 2.2. An other description of S is the number of cubic stones with a side of D_{n50}, eroded within a width of one D_{n50}. The actual number of stones eroded within this width of one D_{n50} can be more or less than S, depending on the porosity, the grading of the armour stones and the shape of the stone. But generally, the actual number of stones eroded within a width of one D_{n50} is equal to 0.7 to 1 times the damage, S.
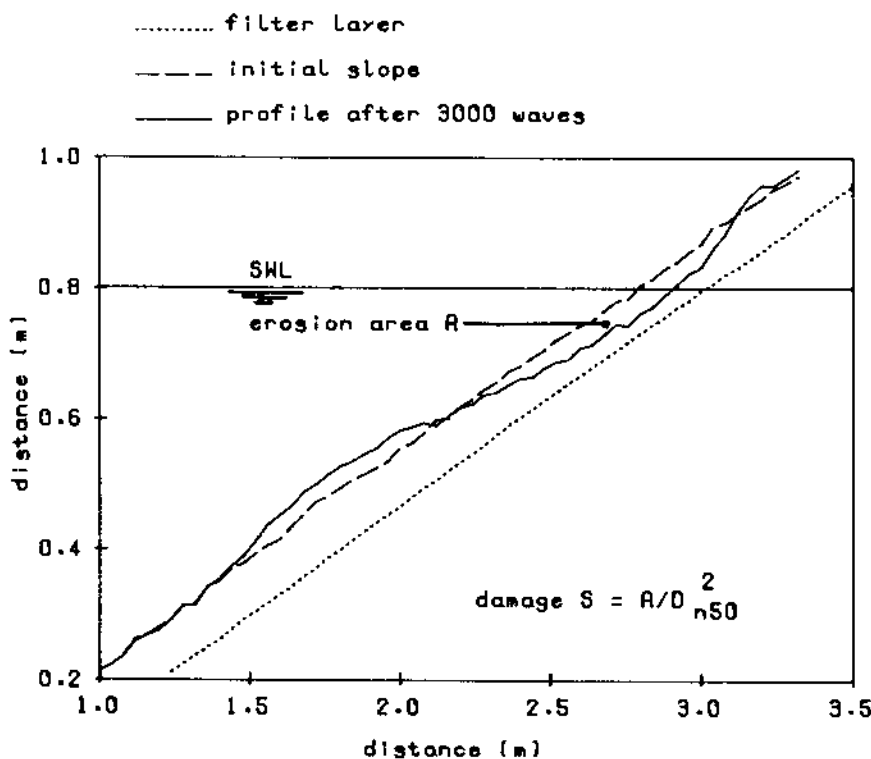
Figure 2.2 Damage, S, based on erosion area, A.

Broderick (1984) states that S = 2 is the lowest level of damage that can be consistently detected in the survey data, using the average of 6 parallel pro-

files. Thompson and Shuttler (1975) use an average of 10 parallel profiles and a smaller sounding interval of one D_{n50}. They detected S values smaller than 0.5. Depending on the size of the armour layer and the definition, the "no damage" criterion of Hudson (1959) and Ahrens (1975) is taken generally to be when S is between 1 and 3. Broderick (1984) defines "no damage" as S = 2.

Equation 2.4 gives a clearly defined damage level parameter, S. A clearly defined "no damage" criterion is found when S is set at a certain low level.

2.2.2 Profile

Static stability is described by using the damage level, S. This damage level is based on the average profiles of a certain number of parallel profiles (see Section 2.2.1). The erosion part of the average profile is used for calculating S, and the accretion part(s), (below and/or above the water level) are less important.

Dynamic stability is defined by the formation of a profile which can deviate substantially from the initial profile. Now all the changes of the slope have to be taken into account. Interesting areas are for instance, the upper and lower points of movement, the depth of the erosion part and the amount and direction of transport of material. In fact the profile itself is important together with the position of the profile with regard to the initial profile.

In order to describe a dynamically stable profile the profile has to be schematized into profile parameters. Early work has been done by Popov (1960), who described a profile under monochromatic wave attack by four heights related to the still water level and by three angles. His tests were performed for a 1:3 uniform initial slope and described only profiles where material is transported downwards.

Van Hijum and Pilarczyk (1982) schematized the profile by a number of length and height parameters and angles, as shown in Figure 2.3. Initial slopes were mainly 1:5 and 1:10 uniform slopes. Profile parameters were established for monochromatic and random waves and for perpendicular and oblique wave attack. Some parameters were related to the uniform initial slope which means that it is difficult to describe the dynamic profile for initial slopes with a more irregular shape. The model describes the "equilibrium" profile which is formed after a fairly long storm duration. Consequently the effect of short storm durations with varying water levels can not be described correctly. A difference between Popov (1960) and Van Hijum and Pilarczyk (1982) is the formation of a "step" for the gentler slopes of Van Hijum and Pilarczyk, see Figure 2.3.
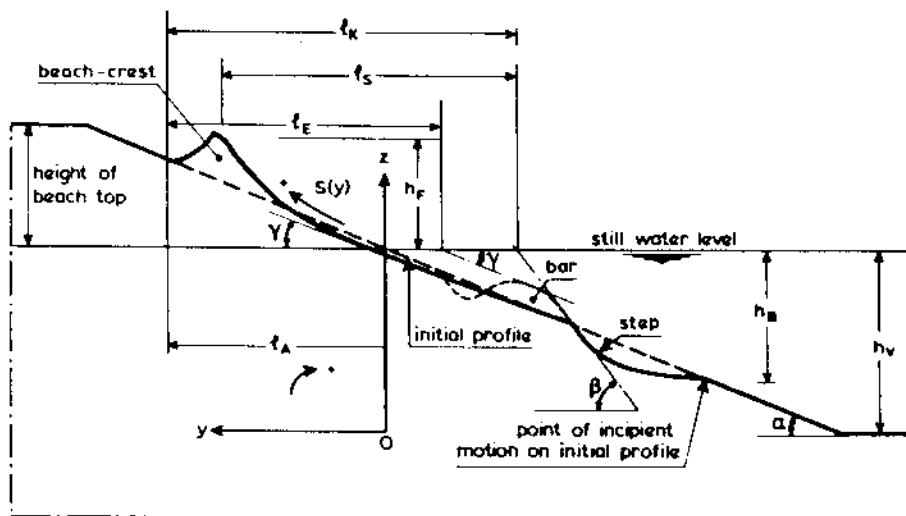
Figure 2.3 Model for dynamically stable profile (Van Hijum and Pilarczyk (1982)). Symbols given in this Figure are not described in the text or list of symbols.

Recently, Powell (1986) performed a small scale investigation on shingle beaches. The tests were run with **monochromatic** waves on a 1:5.5 initial slope. Small diameters of 2 and 4 mm were used where scale effects were present. The research covered the same range as the research of Van Hijum (1974) with monochromatic waves ($H_s/\Delta D_{n50}$ = 13 - 30) and gives no additional data with regard to profile formation.

Powell (1986) defined the profile by two power curves. The upper curve started at the crest and described the run-up and run-down area, up to the transition to the steep part (line with angle β in Figure 2.3). The lower curve started at this transition and described the step (see Figure 2.3). The profile was completely described with a further definition of a crest height, a length for the upper curve and a depth for the lowest point of incipient motion.

As the research of Powell was based on monochromatic wave testing, the data will not be used here. Powell (1986-pp. 334, 335) gave the following recommendations for further research: random wave testing, including research on the influence of shingle shape and grading, the time dependent formation of the profile and scale effects. It is worth noting that all these recommendations were effected in the present research (described in Chapter 4).

Static stability is described by damage and dynamic stability by the profile. The profile can be schematized by profile parameters such as height and length parameters and angles.

2.3 Main environmental parameters

2.3.1 Wave height

The International Commission for the study of Waves (PIANC, 1976) gave an overview of existing stability formulae for static stability of rock slopes. Generally, a stability formula can be developed by assuming incipient instability of an armour unit, subjected to certain wave forces. Depending on the schematisation of resisting forces and wave forces, numerous formulae can be developed, as shown by the Commission mentioned above.

Most stability formulae, however, have a common part. And this part can be regarded as very important for stability of rock slopes, but also for stability of artificial armour units and for stability of placed block revetments. A general development of a stability formula will be given first.

Figure 2.4 shows a part of an armour layer. The slope angle is given by α, the natural angle of repose by ϕ and the boyant mass of the stone by W', where:

$$W' = (\rho_a - \rho) \, D_{n50}^3 \qquad (2.5)$$
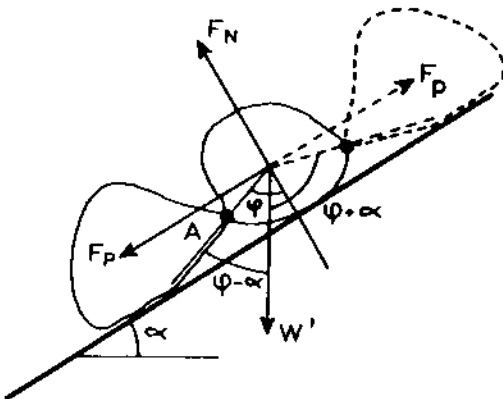
Figure 2.4 Schematisation of incipient instability

The wave forces are schematized by two forces, one parallel to the slope, F_p, and the other normal to the slope, F_N. The same assumptions were made by Sigurdsson (1962). Assuming incipient instability the momentum equation for the point A gives:

$$F_N \sin\phi \, D/2 + F_p \cos\phi \, D/2 = g \, W' \sin(\phi-\alpha) \, D/2 \qquad (2.6)$$

Generally, wave forces as F_p and F_N are related to the wave height (Hudson (1959)) by the following equation:

$$F = \rho \, g \, C \, D^2 H \qquad (2.7)$$

where:

F = wave force

C = coefficient

D = diameter of the stone

Assuming a coefficient C_1 for the normal wave force, F_N, a coefficient C_2 for the parallel wave force, F_P, and assuming $D = K D_{n50}$, (K = coefficient), Equation 2.6 becomes with 2.7:

$$\rho g \, C_1 D_{n50}^3 \, H \, \sin\phi \, K^3/2 + \rho g \, C_2 D_{n50}^3 \, H \, \cos\phi \, K^3/2 = g(\rho_a - \rho) D_{n50}^4 \, \sin(\phi - \alpha) K^4/2 \quad (2.8)$$

Equation 2.8 can be elaborated to:

$$H/\Delta D_{n50} = K \sin(\phi - \alpha)/(C_1 \sin\phi + C_2 \cos\phi) \qquad (2.9)$$

with:

$$\Delta = (\rho_a - \rho)/\rho \qquad (2.10)$$

Defining the friction coefficient, μ, (Iribarren (1950)) as $\mu = \tan\phi$, Equation 2.9 can finally be rewritten to:

$$H/\Delta D_{n50} = K(\mu\cos\alpha - \sin\alpha)/(\mu C_1 + C_2) \qquad (2.11)$$

Equation 2.11 was already developed by Sigurdsson (1962). The $H/\Delta D_{n50}$ is the same as the often used stability number, N_s, (Hudson (1959)). In fact $H/\Delta D_{n50}$ is a combination of two dimensionless variables, the H/D_{n50} and the relative mass density, Δ. The $H/\Delta D_{n50}$ appears in a lot of stability formulae.

In fact the ΔD_{n50} determines the stability of a stone under wave action. In Section 1.1 the $H/\Delta D_{n50}$ parameter (with $D_{n50} = D$) was used to distinguish between various types of structures. Statically stable structures have $H/\Delta D_{n50}$ values between 1 and 4, and dynamically stable structures between 6 and 500. As described in Section 1.2 this thesis will deal with the range of $H/\Delta D_{n50} = 1 - 500$, which is the complete range for rock slopes and gravel beaches.

Artificial armour units can be described by the nominal diameter, D_n, where $D_n = (W/\rho_a)^{1/3}$. In that case $H/\Delta D_n$ can be used. An important design parameter for placed block revetments is the thickness of the blocks, D. With this definition of D, the parameter becomes $H/\Delta D$. It is obvious that by using a nominal diameter for a mass and a thickness for a block, the stability of different

structures under wave attack can be compared by using the parameter $H/\Delta D$ as a reference. Moreover, structures under steady flow regimes are often described by the Shields parameter, $u^2/g\Delta D_{n50}$. Assuming $H :: u^2/g$, the agreement between $H/\Delta D_{n50}$ and the Shields parameter becomes clear.

Equation 2.11 can be rewritten to some well known formulae. Assuming that only a parallel force exists, ($C_1 = 0$), Equation 2.11 becomes Iribarren's formula:

$$H/\Delta D_{n50} = K_1(\mu\cos\alpha - \sin\alpha) \tag{2.12}$$

with:
$K_1 = K/C_2$

Assuming only a normal force ($C_2 = 0$), Equation 2.11 becomes Iribarren's formula, modified by Hudson (1959):

$$H/\Delta D_{n50} = K_2 (\mu\cos\alpha - \sin\alpha)/\mu \tag{2.13}$$

with:
$K_2 = K/C_1$

Hudson (1959) assumed for rubble structures $\phi = 1$, which reduces Equation 2.11 to:

$$H/\Delta D_{n50} = K(\cos\alpha - \sin\alpha)/(C_1 + C_2) \tag{2.14}$$

Hudson combined all coefficients to one coefficient, K_D, and replaced the term $\cos\alpha - \sin\alpha$ by $(\cot\alpha)^{1/3}$. This reduces Equation 2.14 to the well-known Hudson formula, although written in a more simple equation:

$$H/\Delta D_{n50} = (K_D \cot\alpha)^{1/3} \tag{2.15}$$

Summarizing, $H/\Delta D_{n50}$ is an important variable in a stability formula. Different types of structures can be compared using this variable.

The nominal diameter, D_{n50} (Equation 2.3), and the relative mass density, Δ (Equation 2.10), have clearly been defined. The remaining part in the $H/\Delta D_{n50}$ variable is the wave height, H. The first statement to be made is that the wave height to be used in stability formulae is always the wave height in front of the structure.

Wave heights in a random sea state in deep water can be described by the Rayleigh probability distribution. This means that with one significant value of a wave height the probability of exceedance of other values can be calculated. A well known value is the significant wave height, H_s, defined by the average of the highest one third of the waves in a time series, or defined by $4 \sqrt{m_0}$, where m_0 is the zeroth moment of the wave energy density spectrum. Other significant values are the root mean square value, $H_{rms} = 2 \sqrt{2} \sqrt{m_0} = 1/\sqrt{2} \, H_s$, and the H_{10} (Coastal Engineering Research Center - SPM (1984)), where H_{10} is the average of the highest 10 percent of the waves in a time series. Assuming a Rayleigh distribution for the wave heights, H_{10} can be described by $H_{10} = 1.27 \, H_s = 1.79 \, H_{rms}$.

Most structures are not situated in deep water which means that the assumption of a Rayleigh distribution of the wave height in front of the structure can not often be made. Highest waves will break on the foreshore and this will reduce the wave forces on the structure. Instability of armour units is caused by the highest wave forces and therefore by the highest waves. Beforehand it is not possible to say which characteristic value of the wave height will describe stability in the most proper way.

For this thesis the significant wave height in front of the structure, H_s, will be used. This means that the dimensionless wave height is described by $H_s/\Delta D_{n50}$. The value to be taken when the wave heights are not Rayleigh distributed will be discussed during the analysis of the test results (Section 3.3).

2.3.2 Wave period

Random waves will be described by the significant wave height, H_s, as described in the previous Section. Random waves, however, have also to be characterized by one or more wave periods. Three characteristic wave periods are the peak period of the spectrum, T_p, the significant period, T_s, and the average period of the zero crossings, T_m. The average period, T_m, can also be calculated from the spectrum by $T_m = \sqrt{m_0/m_2}$. Depending on the spectral shape the ratio of T_p/T_s, T_p/T_m and T_s/T_m can vary roughly from 1.0 to 1.5.

Random waves are described by the (significant) wave height, the (peak, significant, or average) wave period and a spectral shape parameter. It might be possible that by choosing the right wave period, the influence of the spectral shape will reduce or will even become negligible. This means that the choice of the wave period has an impact on the influence of the spectral shape on the phenomenon described (stability, profile, run-up, reflection). Therefore, the comparison of results for different spectra must give the answer whether a certain wave period can describe the influence of different spectral shapes.

As long as one spectral shape is used for testing it is not necessary to use T_p, T_s and T_m simultaneously. Relationships established by using T_m can easily be rewritten to relationships with T_p or T_s, using the ratio T_p/T_m or T_s/T_m which is fairly constant for a given spectrum. The average zero up-crossing wave period, T_m, will be used in this thesis without any basic background for choosing this period.

In the previous Section the wave height, H_s, was related to the relative mass density, Δ, and the nominal diameter, D_{n50}, resulting in the wave height parameter $H_s/\Delta D_{n50}$. The wave period is often written as a wave length and related to the wave height, resulting in the wave steepness. The wave steepness, s, can be defined by using the deep water wave length, $L = gT^2/2\pi$:

$$s = 2\pi H/gT^2 \tag{2.16}$$

If the wave height in front of the structure is used in Equation 2.16, a fictitious wave steepness is obtained. This steepness is fictitious because H is the wave height in front of the structure and L is the wave length on deep water. The wave steepness belongs to the group of environmental parameters, given by part A in Figure 2.1.

Iribarren (1950) defined the similarity parameter, ξ, in which the wave steepness, s, is related to the slope angle of the structure, $\tan\alpha$:

$$\xi = \tan\alpha/\sqrt{s} \tag{2.17}$$

In fact, the similarity parameter belongs to part C of Figure 2.1, as the environmental parameter, s, is related to the structural parameter, $\cot\alpha$.

Battjes (1974a) described possible breaker types as a function of this parameter and called it the surf similarity parameter. The parameter gives answer to the question whether the waves will break and how the waves will break. Figure 2.5 was taken from Battjes (1974a) and shows the main types of breaking waves which are surging, collapsing, plunging and spilling. Battjes related the surf similarity parameter, ξ, to a number of characteristic surf parameters: the breaker criterion, the breaker type, the breaker height-to-depth ratio, the number of waves in the surf zone, the reflection coefficient, and the relative importance of set-up and run-up.

In fact the surf similarity parameter has been used since then by many authors. Run-up and run-down were described by a function of ξ by Günbak (1979) and Losada and Giménez-Curto (1981). Stability of rubble mound break-

waters or revetments were described by a function of ξ by Ahrens (1975), Losada and Giménez-Curto (1979a and b) and Pilarczyk and den Boer (1983).
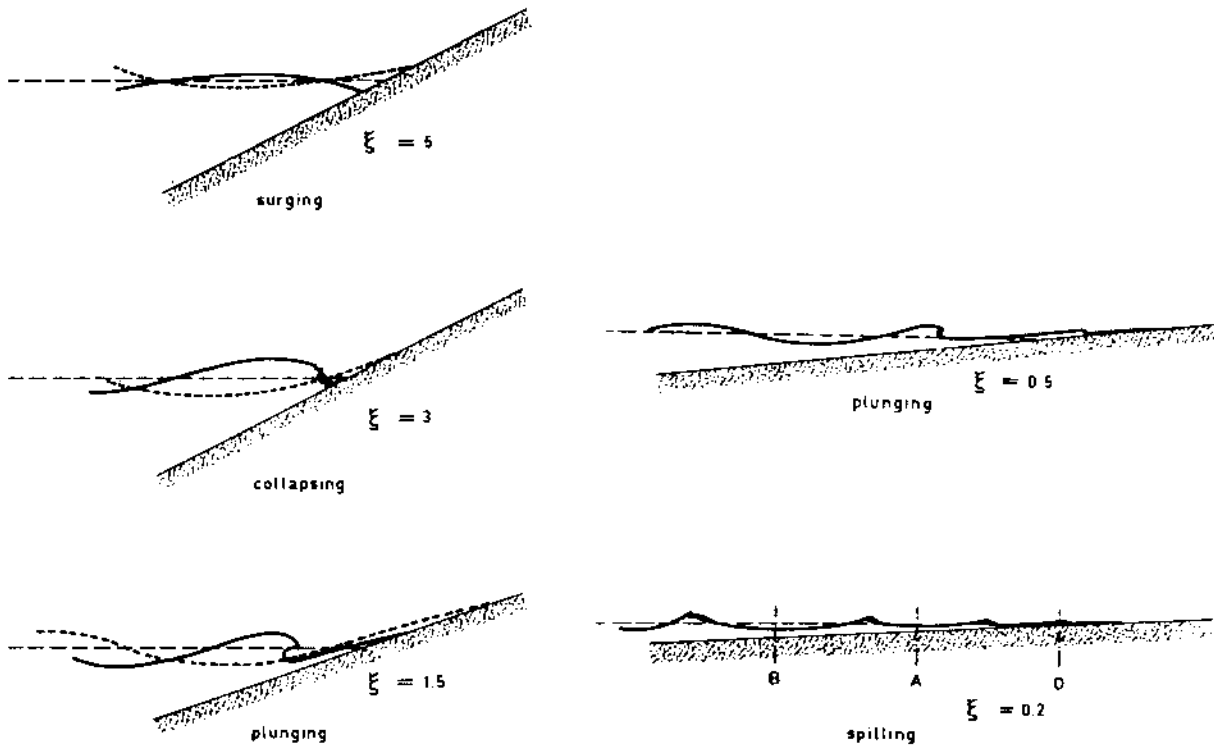
Figure 2.5 Breaker types as a function of ξ, Battjes (1974a)

Summarizing, the wave period, T, can be described by the dimensionless variables s and ξ.

The use of H_s and T_m leads to the following dimensionless variables for the wave period:

$$s_m = 2\pi H_s/gT_m^2 \tag{2.18}$$

$$\xi_m = \tan\alpha/\sqrt{s_m} \tag{2.19}$$

These variables will be used to describe the influence of the wave period on static stability (damage) and dynamic stability (profile).

2.3.3 Spectral shape

In Sections 2.3.1 and 2.3.2 a choice was made to use the significant wave height, H_s, and the average wave period, T_m. Both can be calculated from the spectrum (frequency domain) or from the wave signal (time domain). The wave height and period, however, do not describe the shape of the energy density spectrum and the groupiness of the waves.

Various parameters were developed to describe the width of the spectrum. Well known parameters are ϵ (Cartwright and Longuet Higgens (1956)) and Q_p (Goda (1970)). Other parameters were based on the wave signal and described the groupiness of the waves in the time domain. The mean length, $\overline{j_1}$ (H), and the mean total length $\overline{j_2}$ (H) of the wave groups (Goda (1970)) and the groupiness factor, GF (Funke and Mansard (1980)), are some of these parameters. None of these parameters, however, can be computed in both the time and frequency domain.

Based on the bivariate Rayleigh probability density function derived by Uhlenbeck (1943) and Rice (1945) the parameter, κ, was developed. Battjes (1974a - Appendix 1) gives some details of this function. The parameter, κ, is defined by:

$$\kappa_f^2 \, m_0^2 = \left[\int_0^\infty S(f)\cos(2\pi f\tau)df \right]^2 + \left[\int_0^\infty S(f)\sin(2\pi f\tau)df \right]^2 \qquad (2.20)$$

where:

κ_f = parameter of bivariate Rayleigh probability density function

m_n = n-th spectral moment of S(f) about f=0

S(f) = spectral density as a function of f

f = wave frequency

τ = time lag; in this case $\tau = T_m = \sqrt{m_0/m_2}$

The bivariate Rayleigh probability density function is based on the statistical properties of the amplitude envelope of a narrow band Gaussian process. The subscript f in κ_f is used, as the parameter is defined in the frequency domain.

The amplitude envelope theory mentioned above can be used to describe the correlation coefficient between wave heights. Arhan and Ezraty (1978) assume, therefore, that the amplitude envelope on an arbitrary time, R(t), can be transformed to R(t) = $\frac{1}{2}$ H(t), that is the wave height envelope. This means that the envelope theory (the bivariate Rayleigh distribution) can be applied to wave heights.

Battjes (1974a) showed that κ^2 equals the coefficient of linear correlation of X^2 and Y^2, the stochastic variables, X and Y both having a marginal Rayleigh distribution. The parameter κ, based on successive wave heights, can then be defined by (Arhan and Ezraty (1978)):

$$\kappa_{HH.t}^2 = \frac{\dfrac{1}{N-1} \sum_{n=1}^{N-1} (H_n^2 - \overline{H^2})(H_{n+1}^2 - \overline{H^2})}{\dfrac{1}{N} \sum_{n=1}^{N} (H_n^2 - \overline{H^2})^2} \qquad (2.21)$$

where:

$\kappa_{HH.t}$ = parameter in bivariate Rayleigh distribution, based on successive wave heights in the time domain

N = number of zero-upcrossings in a given time interval

H = wave height - height of highest maximum of the time signal above lowest minimum between successive zero-upcrossings

$\overline{H^2}$ = average of the squared wave heights

Equation 2.20 gives κ in the frequency domain (κ_f) and Equation 2.21 gives this parameter in the time domain ($\kappa_{HH.t}$), the latter based on successive wave heights. In fact κ_f and $\kappa_{HH.t}$ should give similar values. Battjes and Van Vledder (1984) concluded that (based on prototype measurements) the correlation coefficient of successive wave heights, and therefore $\kappa_{HH.t}$, is consistently larger than κ_f.

A further comparison of κ_f and $\kappa_{HH.t}$ was performed by Stam (1988) who used data from small scale wave flumes and data from computer simulations. His results will be considered in more detail, as a part of the data was based on the investigation described in this thesis.

Figures 2.6 - 2.8 show the spectra used by Stam (1988). Figure 2.6 gives three spectra with almost the same significant wave height and average period. Shown are a very narrow spectrum, a Pierson Moskowitz spectrum and a rather wide spectrum. These three spectra were used in the present investigation.

Figure 2.7 shows besides a Jonswap and a Pierson Moskowitz spectrum also two double peaked spectra. Again the wave heights and average periods are more or less the same for all four spectra. The spectra were applied in the model investigation DELFT HYDRAULICS-H24 (1987).

Figure 2.8 shows various stages of the Jonswap spectrum for which time histories were simulated by computer.

Time signals were measured or simulated for all spectra shown in Figure 2.6 - 2.8. The parameters κ_f and $\kappa_{HH.t}$ were computed for all data and are shown in Figure 2.9. The same tendency as found by Battjes and Van Vledder (1984) is present in this Figure. The $\kappa_{HH.t}$ is consistently larger than κ_f.

Stam (1988) analyzed the assumptions for both theories of κ_f and $\kappa_{HH.t}$ and found that one of the assumptions made by Arhan and Ezraty (1978) caused the difference. The amplitude envelope, R(t), was transformed to the wave height envelope, assuming R(t) = ½ H(t). This assumption implies that the correlation

between successive amplitudes is the same as the correlation between successive wave heights. Probably this assumption yields only for very narrow spectra, as can be seen in Figure 2.9.

In order to verify the assumption mentioned above, Stam (1988) calculated the parameter $\kappa_{aa.t}$ based on successive amplitudes. $\kappa_{aa.t}$ is then defined, according to Equation 2.21:
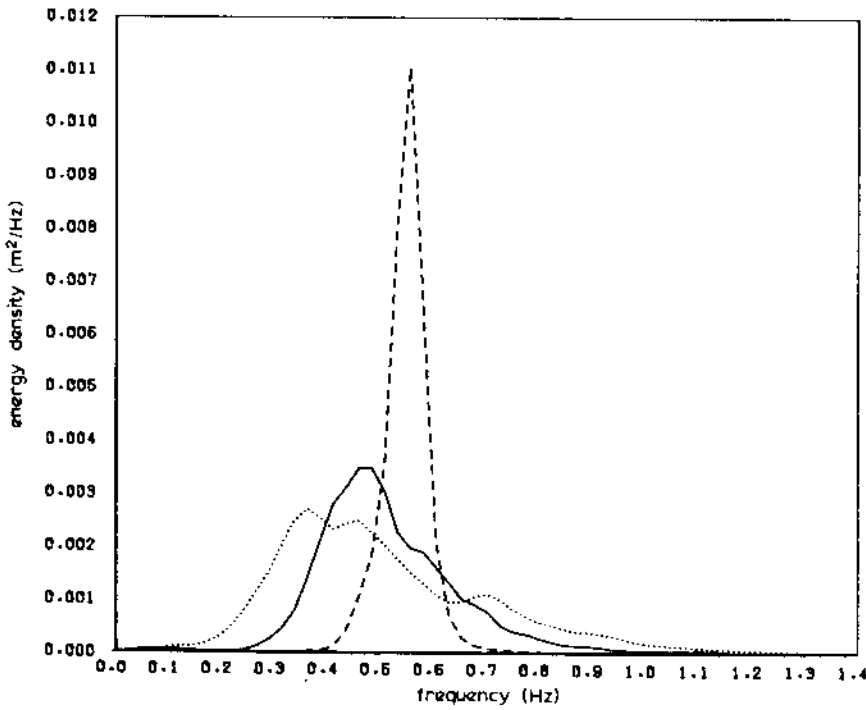
Spectrum	H_s (m)	T_m (s)	T_p (s)	κ_f	$\kappa_{HH.t}$
·············· wide	0.122	1.81	2.67	0.25	0.48
————— PM	0.116	1.84	2.17	0.47	0.62
——————— narrow	0.119	1.79	1.79	0.90	0.92

Figure 2.6 Spectra with the same H_s and T_m (present research)
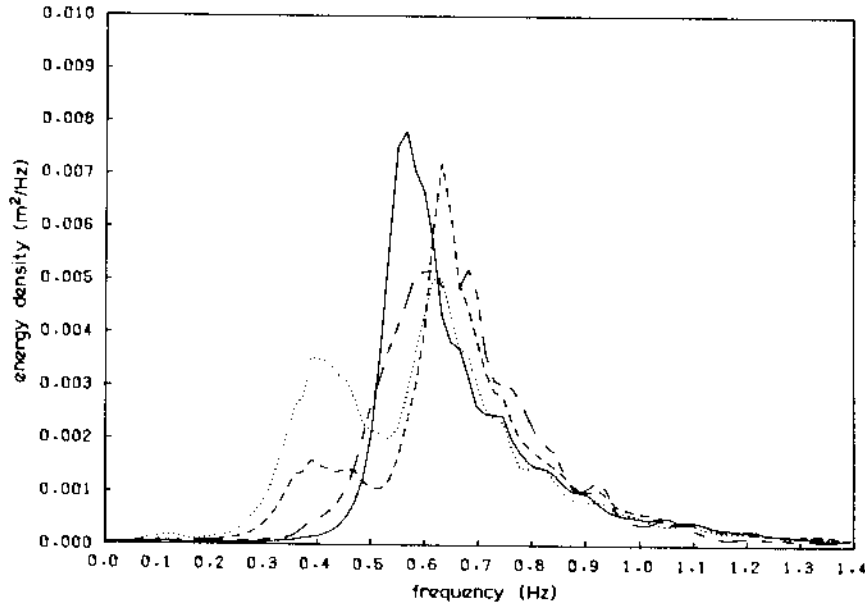
Spectrum		H_S (m)	T_m (s)	T_p (s)	κ_f	$\kappa_{HH \cdot t}$
—————	Jonswap	0.147	1.42	1.80	0.56	0.63
— — — —	PM	0.148	1.43	1.57	0.47	0.48
··············	double peak	0.149	1.54	1.61	0.36	0.50
— — — — —	double peak	0.140	1.40	1.61	0.20	0.42

Figure 2.7 Spectra with the same H_S and T_m (Delft Hydraulics-H24 (1987))
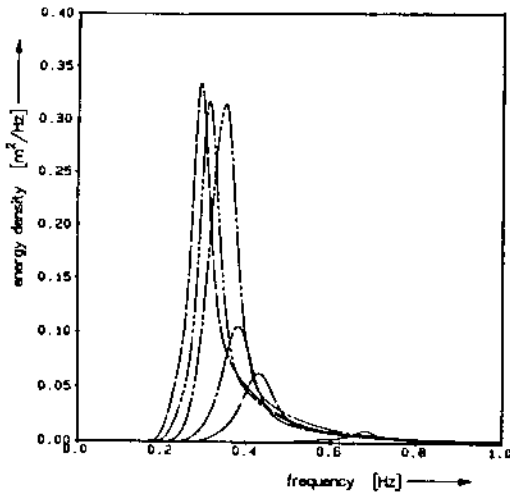
	H_S (m)	T_m (s)	T_p (s)	κ_f	$\kappa_{HH \cdot t}$
—————————	0.19	1.20	1.47	0.48	0.59
———— ————	0.38	1.91	2.33	0.58	0.70
———— — ————	0.46	2.18	2.63	0.61	0.71
———— — — ————	0.73	2.46	2.86	0.65	0.71
— — — — ————	0.68	2.63	3.23	0.61	0.72
— — — —	0.71	2.72	3.45	0.55	0.68

Figure 2.8 Jonswap spectra used for computer simulated time series (Stam (1988))
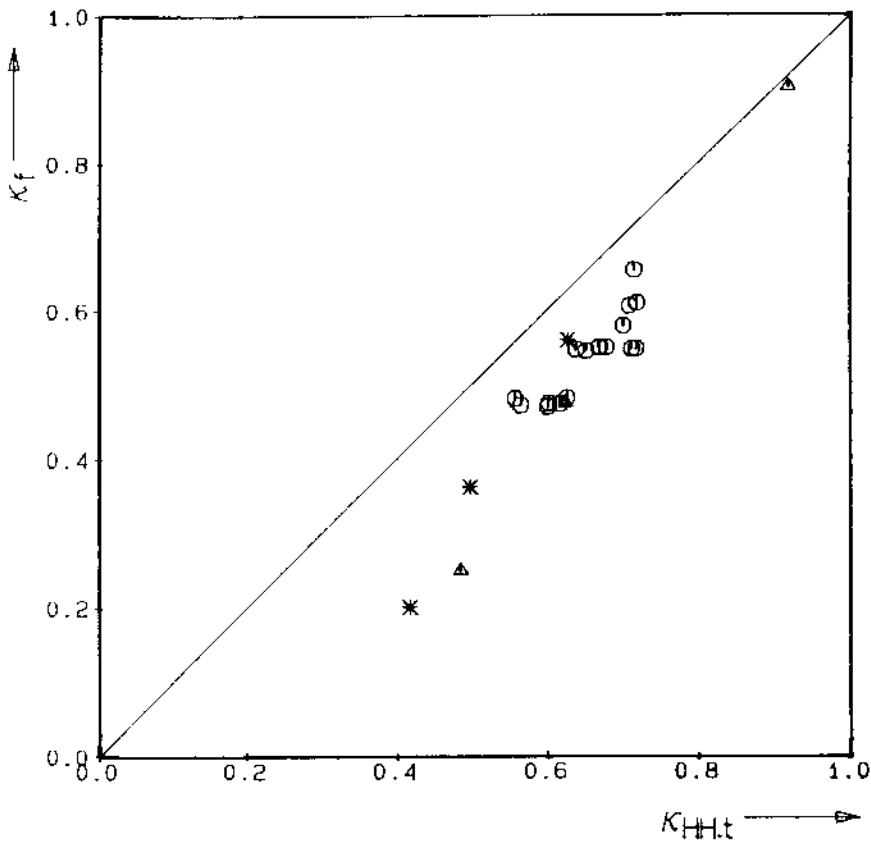
Δ   present research (Fig. 2.6)

∗   Delft Hydraulics H24 (Fig. 2.7)

Ⓞ   Simulations of JONSWAP spektra (Fig. 2.8)

Figure 2.9 Comparison of κ_f and $\kappa_{HH.t}$ (Stam (1988))

$$\kappa_{aa.t} = \frac{\dfrac{1}{N-1} \displaystyle\sum_{n=1}^{N-1} (a_n^2 - \overline{a^2})(a_{n+1}^2 - \overline{a^2})}{\dfrac{1}{N} \displaystyle\sum_{n=1}^{N} (a_n^2 - \overline{a^2})^2} \tag{2.22}$$

where:

$\kappa_{aa.t}$ = parameter in bivariate Rayleigh distribution, based on successive amplitudes in the time domain

a   = the amplitude − height of highest maximum of the time signal above the still water level between two successive zero-upcrossings

The results for $\kappa_{aa.t}$ (based on wave crests) are shown in Figure 2.10. Similar results were found for $\kappa_{aa.t}$ based on wave troughs. The agreement in Figure 2.10 between κ_f and $\kappa_{aa.t}$ is very good, except for a very wide and a

double peaked spectrum. Based on this Figure it can be concluded that the cor-relation between successive amplitudes is less than between successive wave heights.
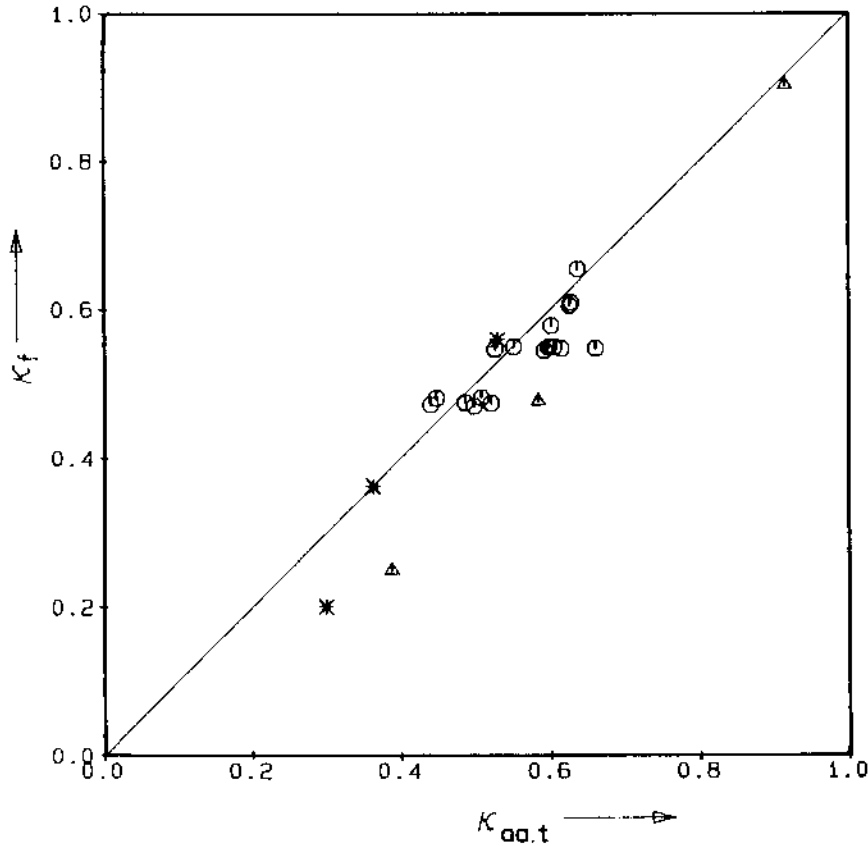
△	present research (Fig 2.6)
*	Delft Hydraulics H24 (Fig 2.7)
℗	Simulations of JONSWAP spektra (Fig 2.8)

Figure 2.10   Comparison of κ_f and $\kappa_{aa.t}$ (Stam (1988))

The parameters κ_f and $\kappa_{aa.t}$ calculated in the frequency domain (Equation 2.20) and in the time domain (Equation 2.22) respectively, and based on the amplitude envelope, give similar values. The parameter κ_f, however, underesti-mates the groupiness of wave heights, calculated by $\kappa_{HH.t}$ (Equation 2.21), unless an empirical relationship is derived between κ_f and $\kappa_{HH.t}$, based on Figure 2.9. No attempt is made to explain theoretically the differences in correlation between amplitudes and wave heights. Both κ_f and $\kappa_{HH.t}$ will be used, whenever necessary.

The main conclusion from the analysis given above, is that the parameter of the bivariate Rayleigh probability density function, κ, can be calculated from the spectral shape and is in agreement with calculation of κ (based on amplitudes) in the time domain. In fact, the spectral shape determines the groupiness in the time domain.

The accuracy of $\kappa_{HH.t}$ or $\kappa_{aa.t}$ depends largely on the duration of the time signal. Short durations (for instance 20 minutes in prototype recordings) will give a large variation of $\kappa_{HH.t}$ and $\kappa_{aa.t}$. The accuracy of these parameters, based on about 1000 waves, can be seen in Figures 2.9 and 2.10. Various time signals were simulated for two spectral shapes, giving the data points in horizontal order in the Figures. It can be concluded that κ, computed in the time domain, is influenced by the length of the records.

2.3.4 The storm duration

Monochromatic waves generate the same wave forces on a structure during each single wave. This caused a rather fast response to these repeated forces, and in most cases an equilibrium was reached in a short time. Tests on static stability with monochromatic waves (Hudson (1959), and Ahrens (1975)) had durations not exceeding 1000 waves. Therefore, the storm duration was never mentioned as a governing variable in static or dynamic stability.

Random waves cause a wide spectrum of wave forces on the structure. It can be expected therefore, that it will take much longer before an equilibrium is reached which represents also the response to less frequently occurring high wave groups.

Van Hijum and Pilarczyk (1982) used monochromatic waves as well as random waves. Random wave tests were stopped after reaching an "equilibrium profile". The average duration of a random wave test varied between 3000 and 6000 waves. Thompson and Shuttler (1975) performed more than 100 tests on static stability of riprap slopes under random wave attack. Damage was measured after every 1000 waves, up to 5000 waves. Some long duration tests were performed up to 15,000 waves. Also some measurements were made after 500 waves.

The results of Thompson and Shuttler were reanalyzed by the author in order to show the importance of the storm duration on static stability. All tests were selected where the damage was measured up to 5000 waves. Tests, where the filter layer became visible within 5000 waves, were omitted. Tests where the damage was very small after 5000 waves (S < 2 - 3) were omitted too. This procedure resulted in a total of about 50 available tests.

All damages were related to the final damage after 5000 waves. This ratio, S(N)/S(5000), is shown as a function of the number of waves, N, in Figure 2.11. Data points between N = 1000 - 5000 are generally based on 50 tests and are independent of slope angle, wave period and damage level. The standard deviation for the ratio, S(N)/S(5000), in this region is about 0.1 and is independent of the number of waves.

Thompson and Shuttler performed five long duration tests, with N up to 15,000. These data are also given in Figure 2.11 together with the data of 14 tests with N = 500.

$$S(N)/S(5000) = 1.3(1-exp(-0.0003N))$$

$$S(N)/S(5000) = 0.014\sqrt{N}$$
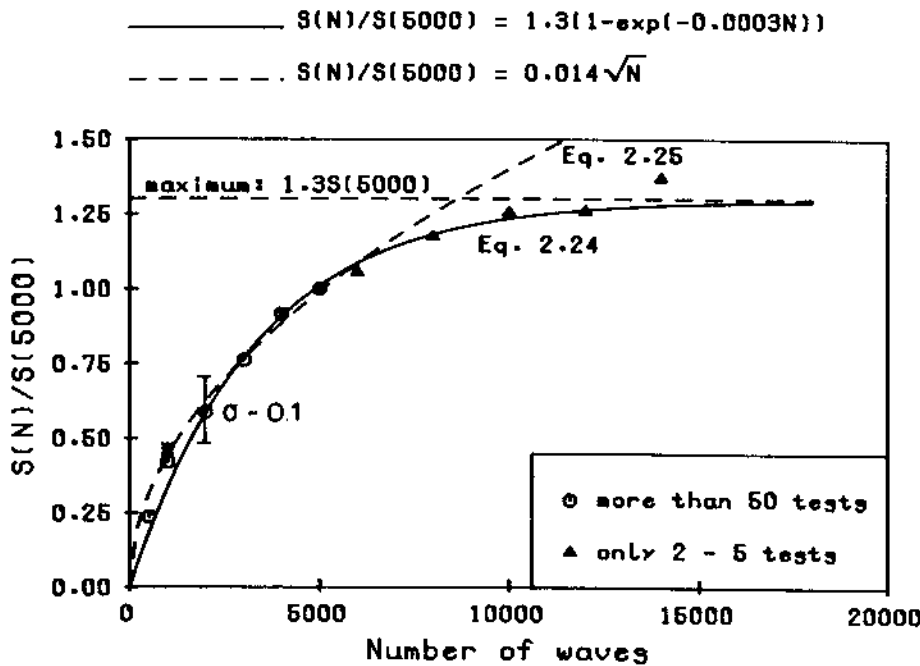
Figure 2.11 Influence of number of waves on damage.

A function which describes the influence of the storm duration on static stability completely, should meet the following theoretical requirements:

● From N = 0 to N = 500 or 1000 the function should be almost linear as only high wave groups will cause the first damage. It may be expected that after about 500-1000 waves a longer duration will reduce the increase of damage, partly due to changes of the initial slope.
● For large N numbers a limit to the damage should be reached (equilibrium).

A function which meets this requirements is:

$$f(S) = a [1 - exp(-bN)], \qquad (2.23)$$

where a and b are curve-fitting coefficients and $f(S) = S(N)/S(5000)$. Based on the data of Figure 2.11 the coefficients, a and b, are found to be 1.3 and 3.10^{-4} respectively. The influence of the storm duration on stability for the whole range of N can therefore be described by:

$$f(S) = S(N)/S(5000) = 1.3 \ [1 - \exp \ (-3.10^{-4} \ N)] \tag{2.24}$$

Equation 2.24 is also shown in Figure 2.11. The damage is limited to 1.3 times the damage found after $N = 5000$.

Another relationship between damage, S, and number of waves, N, can be established if only the most important region is considered, i.e. $N < 7000-10,000$. A square root function can be established, see Figure 2.11:

$$S = 0.014 \ \sqrt{N} \tag{2.25}$$

Equation 2.25 was also plotted in Figure 2.11. For the range given above, the influence of number of waves on stability can be described simply by the parameter group $S/\sqrt{N}$. The limiting factor of 1.3 in Equation 2.24 is also found using $N = 8500$ in the $S/\sqrt{N}$ relation, Equation 2.25. The parameter group $S/\sqrt{N}$ covers a large part of the area of interest and will, for sake of simplicity be included as governing variable. For $N > 8500$ the maximum damage can be set at $S = 1.3 \ S(5000)$.

2.4 Final list of governing variables

2.4.1 Overall list

Stability of rubble mound breakwaters, revetments, rock slopes and gravel beaches can be described by static stability or dynamic stability. The governing variable for static stability is the damage, S, as described in Section 2.2.1. The variable for dynamic stability is the profile which can be described by profile parameters as lengths and angles, Section 2.2.2.

Following Sections resulted in the dimensionless wave height parameter, $H_s/\Delta D_{n50}$ (Section 2.3.1), the dimensionless wave period parameters, wave steepness s_m and surf similarity parameter, ξ_m (Section 2.3.2), the spectral parameter, κ (Section 2.3.3) and for static stability the damage as function of the number of waves, $S/\sqrt{N}$ (Section 2.3.4).

Generally, governing variables can be divided into variables related to environmental conditions and variables related to the structure, see Figure

2.1, the parts A and B. Various authors gave a list of these governing variables, (amongst others Hudson (1959), Raichlen (1974), Thompson and Shuttler (1975)). This Section gives an overview of most governing variables and these variables will be made dimensionless in a following Section by means of a dimensional analysis procedure. The advantages and disadvantages of using dimensional analysis and dimensionless variables were described in Section 2.1.2. Using dimensionless variables, the range of possible application should be taken into account.

Generally, environmental conditions are boundary conditions which firstly can not be influenced by the designer. The wave height, H_s, and the wave period, T_m, are obviously environmental variables. Random waves can be described by the (directional) spectral shape and the groupiness of the waves. The storm duration is important for random waves as shown by Thompson and Shuttler (1975). The storm duration can be described by the number of waves, N, which attack the structure during a storm. The angle of wave attack is described by ψ.

Other variables are the water depth, h, tide and the shape of the foreshore. In fact, these three variables can be described by the water depth, $h(x,t)$, if h is a function of time (tide) and place (foreshore). Finally, the mass density of water, ρ, the dynamic fluid viscosity, ν, and the acceleration of gravity, g, belong to the group of environmental variables (as they can not be influenced by the designer).

Summarizing, the environmental variables are given by:
The wave height, H_s
The wave period, T_m
The (directional) spectral shape and groupiness of waves
The number of waves, N
The angle of wave attack, ψ
The water depth, $h(x,t)$
The mass density of water, ρ
The dynamic fluid viscosity, ν
The acceleration of gravity, g

Structural variables (see Figure 2.1 part B), related to the armour stone, are the mass of the stone, W_{50}, the grading of the stone, D_{85}/D_{15}, the mass density of the stone, ρ_a, the natural angle of repose, ϕ, including friction and interlocking, and the shape of the stone and the mechanical strength of the stone.

The mass of the stone, W_{50}, can also be described by the nominal diameter, D_{n50}, (Equation 2.3) which is a characteristic dimension of an armour unit. The grading, D_{85}/D_{15}, is characterized by the 85 and 15 percent values of the sieve curves. Uniform stone is given by small values of D_{85}/D_{15} (smaller than 1.2 - 1.3) and riprap by large values (roughly between 1.5 and 2.5). Hedar (1960) established the natural angle of repose, ϕ by tilting a box filled with armour stones until the angle at which the first stones commenced rolling down the slope.

The shape of the stone can be described by the roundness (Allsop et al (1985)) or by other descriptors (Latham and Poole (1987)). The mechanical strength of the stone can be described by various engineering tests or by specially developed laboratory roller mill tests (Allsop et al (1985)).

Other variables which are related to the structure, are the ratio of armour stone size and filter stone size, D_{50} (armour)/D_{50} (filter), the grading of the filter layer, D_{85}/D_{15} (filter), the slope angle of the structure, $\cot\alpha$, the armour layer thickness, t_a, the crest height or relative freeboard related to the water level, R_c, the crest width, w_c, the construction method and the permeability of the structure, P.

Summarizing, the structural variables are given by:

The nominal diameter, Eq. 2.3, D_{n50}
The grading of the stone, D_{85}/D_{15}
The mass density of the stone, ρ_a
The natural angle of repose, ϕ
The shape of the stone
The mechanical strength of the stone
The ratio D_{50} (armour)/D_{50} (filter)
The grading of the filter, D_{85}/D_{15} (filter)
The slope angle, $\cot\alpha$
The thickness of the armour layer, t_a
The height of the crest, R_c
The width of the crest, w_c
The permeability of the structure, P
The construction method

2.4.2 Dimensionless variables

A long list of governing variables was produced in the previous Section. Descriptors of static and dynamic stability were given in Section 2.2, resul-

ting in the damage, S, and the profile schematized by height and length parameters and angles, respectively.

The main environmental variables were discussed in Section 2.3 which resulted in the dimensionless wave height parameter, $H_s/\Delta D_{n50}$, the dimensionless wave period parameters, s_m, and ξ_m, and the spectral shape and groupiness parameter, κ.

Waves in nature can be described by a directional spectrum. Tests described in the present research were performed, however, in a wave flume or in a wave basin with long crested waves. Directional spectra, were not considered, therefore, and are not treated in more detail here. It is assumed that the spectral shape and groupiness of waves can solely be described by the parameter, κ.

It may be assumed that shape and strength of the stone and construction method can be described by one or more dimensionless variables. Possible dimensionless variables are a roundness measure for the shape of the stone (Allsop et al (1985)), percentage of weight loss in a roller mill for strength of stones (Allsop et al (1985)), and packing densities for the construction method. The group of dimensionless variables becomes now:

$H_s/\Delta D_{n50}$, s_m, ξ_m, κ, N, ψ, D_{85}/D_{15}, ϕ, shape of stone, strength of the stone, D_{50} (armour)/D_{50} (filter), D_{85}/D_{15} (filter), $\cot\alpha$, P and construction method.

The remaining group consists of variables with a certain dimension. This group is listed by:

$h(x,t)$, ν, t_a, R_c and w_c.

The variables ρ and g were used in Section 2.3 to define the dimensionless parameters $H_s/\Delta D_{n50}$, s_m and ξ_m. The relative mass density, Δ, was defined by Equation 2.10. The wave height, H_s, was related to the nominal diameter, D_{n50}. The wave period was related to H_s. As described in Section 2.1, the length parameter to be used in dimensionless analysis depends on the phenomenon considered. The wave height, H_s, is a good length parameter for the environmental parameters (part A in Figure 2.1).

Water depth, $h(x,t)$ and relative crest height, R_c, can be related to the wave height, H_s. This results in the variables $h(x,t)/H_s$ and R_c/H_s. The crest width may be related to H_s or D_{n50} which results in w_c/H_s or w_c/D_{n50}. A final choice is difficult to make. The armour layer thickness can be related to the

nominal diameter, resulting in t_a/D_{n50}. The remaining variable, ν, can be related to both H_s and D_{n50}. This results in the Reynolds number, $Re = \sqrt{g\ H_s}\ D_{n50}/\nu$.

Finally a list can be constructed which consists of only dimensionless variables related to stability of rock slopes and gravel beaches. This list is given by:

The wave height parameter,	$H_s/\Delta D_{n50}$
The wave period parameter,	s_m and ξ_m
The water depth,	$h(x,t)/H_s$
The armour layer thickness,	t_a/D_{n50}
The crest height,	R_c/H_s
The crest width,	w_c/D_{n50} or w_c/H_s
The Reynolds Number,	Re
The number of waves,	N
The slope angle,	$\cot\alpha$
The natural angle of repose,	ϕ
The angle of wave attack,	ψ
The grading of the stone,	D_{85}/D_{15}
The ratio,	D_{50} (armour)$/D_{50}$ (filter)
The grading of the filter,	D_{85}/D_{15} (filter)
The permeability of the structure,	P
The spectral shape and groupiness of waves,	κ
The shape of the stone (roundness)	
The strength of the stone (weight loss in roller mill)	
The construction method (packing density)	

This general list is related to both static and dynamic stability. Following Sections deal in more detail with the variables and a final list of variables will be considered for static and dynamic stability separately. The lists will be reduced on the basis of existing knowledge of the variables. The range of application of each variable will be discussed for these final lists.

2.4.3 Final list for static stability

The water depth, $h(x,t)/H_s$ is a function of the location on the foreshore and of the changing water level due to tide. Damage will occur around the still water level for statically stable slopes. A variation of the water level on a uniform slope will cause a variation in the location of the damage, but not in the amount of damage. Therefore it is stated that the stability of statically stable uniform slopes is not a function of the water level. Moreover,

the wave height to be used was defined to be the wave height just in front of the structure (Section 2.3.1). This means that the variation of the wave height due to the foreshore should have been established before any stability calculation is made. The program ENDEC (DELFT HYDRAULICS-ENDEC (1986)) gives for example the opportunity to compute this wave height in front of the structure in a sophisticated way.

A foreshore might give a reduction of the wave heights in front of the structure, as waves will break. Then the Rayleigh distribution of the wave heights can no longer be applied. This implies a check whether the significant wave height, H_s, is the governing wave height which counts for this effect or that another value (for example the 1% on 2% value) has to be taken. The parameter $h(x,t)/H_s$ can be deleted if this is kept in mind.

The height of the crest, R_c/H_s becomes important when the crest is so low that wave energy can pass over the crest (overtopping). The front slopes of low crested structures and revetments are more stable than non-overtopped structures. The stability of the crest and the rear becomes important in this case. The influence of the crest height can not be ignored.

The crest width, w_c is only important when overtopping structures are considered. As only the stability of the seaward slope will be the subject for this thesis, the stability of the rear and the stability of the crest itself, therefore, will be ignored. This means that the crest width parameter, w_c/D_{n50} or w_c/H_s can be deleted.

Thompson and Shuttler (1975) performed tests on (viscous) scale effects, to check the influence of the Reynolds number, Re, on stability. Tests were performed on stones with diameters of 20, 30 and 40 mm respectively. They concluded that within the scatter of the results, the tests showed no clear dependency of the erosion damage on the Reynolds number.

The effect of the Reynolds number on stability was investigated or mentioned by various other researchers, Dai and Kamel (1969), Thomsen et al (1972), Broderick and Ahrens (1982), Jensen and Klinting (1983), Sörensen and Jensen (1985) and Burcharth and Frigaard (1987). Although results are not throughout consistent, lowest values for which no scale effects will be present can be set at Re = $\sqrt{gH_s}\ D_{n50}/v$ = 1.10^4 - 4.10^4. The range of Reynolds numbers used in the present investigation on static stability was about 4.10^4 - 8.10^4. Therefore, the Reynolds number will be ignored as being not a governing variable in this case.

The difference between 20 - 40 mm diameter stones and prototype dimensions is still large, however. Large scale tests on (almost) prototype scale, therefore, would support the small scale investigations, if the same results are obtained. The large Delta flume gives the opportunity to facilitate this problem. Therefore some tests were repeated in this Delta flume on a larger scale. These tests will be described in more detail in Section 3.6.

The natural angle of repose, ϕ, appears in a lot of stability formulae. This angle varies, depending on the shape of the (artificial) armour unit used and the friction coefficient between the units (Klein Breteler and Van der Meer (1984)). The natural angle of repose was measured as described by Hedar (1960). Hedar measured for rock a natural angle of repose of $\phi = 48° ± 0.9°$. Klein Breteler and Van der Meer (1984) measured ϕ for uniform stones, riprap and large shingle. The natural angles of repose were $\phi = 50°$, $53°$, and $47°$ respectively. It can be concluded that the natural angle of repose for rock is more or less independent of grading and shape. Therefore ϕ is not considered to be a governing variable.

Perpendicular wave attack is often regarded as the most severe condition for the stability of a trunk section of a breakwater or revetment. Some interlocking units as Dolosse, however, seem to be less stable for an angle of wave attack of about $\psi = 30°$ (Price (1978)). For rock slopes it is assumed that an angle of wave attack which is different from perpendicular attack, will show the same or a better stability than for perpendicular wave attack. The angle of wave attack, ψ, will therefor not be treated further.

The difference between armour stone size and filter stone size is given by the ratio D_{50} (armour)/D_{50} (filter). Thompson and Shuttler (1975) used different ratios and concluded that this ratio had no influence on stability, using ratios between 4.5 and 12 and using an impermeable core. Large ratios of D_{50} (armour)/D_{50} (filter), however, had the finer material drawn through the riprap. A filter with a D_{50} (armour)/D_{50} (filter) ratio of 4.5 was not removed by erosion through the riprap. As the stability of the armour layer was not influenced by the size of the filter layer, the parameter D_{50} (armour)/D_{50} (filter) will no longer be taken into account.

Thompson and Shuttler found the same conclusion for the grading of the filter, D_{85}/D_{15} (filter). A wide grading of fine filter stones showed no influence on stability of the armour layer (D_{85}/D_{15} (filter) = 3 and D_{50} (armour)/D_{50} (filter) = 12). The fine filter material came out through the riprap layer with ease. It can be concluded that if the size of the filter material is not too small in relation with the size of the armour stones, that is to say if

fine material can not erode through the armour layer, the stability of the armour layer is not influenced by the grading and size of the filter layer (D_{50} (armour)/D_{50} (filter) $< 5 - 8$).

Both conclusions on filter size and filter grading were found for an impermeable core. If the filter stone size is only a little smaller than the armour stone size, which is often the case for breakwaters, and if the structure is more permeable, above stated conclusions are maybe not applicable. A relatively large filter layer will influence the permeability of the structure and, therefore, stability.

The permeability of the structure, P, has large influence on stability as shown by Hedar (1960) and (1984) and Thompson and Shuttler (1975). The permeability is influenced by the thickness of the armour layer, the sizes of the filter layers and the size of the core material. The influence of the thickness of the armour layer, t_a/D_{n50}, on stability can be included in the permeability parameter, P. This permeability parameter, P, will be described in more detail in Chapter 3.

Lower and upper boundaries for permeability can be assumed to be a coastal protection with an impermeable core and a homogeneous structure, respectively.

The shape of the stone can be characterized by the ratio of maximum/minimum dimensions. It is assumed that for most designs of breakwaters and coastal structures more or less angular stones are required and that the use of very flat and long or rounded rock is prohibited, unless special placing procedures are applied. Therefore the shape of the stone will not be regarded to be a governing variable on static stability.

The quality (or mechanical strength) of the stone might be a problem in prototype design using poor qualities. Since the mechanical strength was not part of the model investigation on static stability, the effect is ignored here.

Finally the construction method has to be considered. Randomly placed stones will be less stable than stones placed with special care, especially when flat and long stones are placed with the longitudinal axis perpendicular to the slope (Bruun and Johanneson (1974)). Even the method of placing stones randomly in the model can effect stability and repeatability, as was shown by Thompson and Shuttler (1975) during their preliminary tests. During their main test program the method adopted gave repeatable results within a scatter which is to be expected with random waves attacking randomly placed stone. The same method was used for the tests which are described in Chapter 3. Other construction methods will not be taken into account in this thesis.

Above given review has reduced the list of governing variables for static stability. The final list of governing variables will be treated in more detail now. In Section 2.1.2 the philosophy of approach of the investigation was discussed. The advantages, but also the disadvantages of using dimensionless variables were mentioned. One of the requirements for using dimensionless variables was the consideration of the possible ranges of application of those variables. If the complete range is covered by investigation, the results can be applied widely. If only a small range is investigated, extrapolation may cause unacceptable errors. Therefore the range of possible application of the remaining governing variables will be dealt with.

The wave height parameter $H_s/\Delta D_{n50}$ must be related to the damage, S. The wave height-damage curves are the basic results of stability investigations. $H_s/\Delta D_{n50}$ values should be applied from no damage (S = 1 - 3) upto failure of the slope (depending on the slope angle, S = 10 - 20). The range S = 1 - 20 can be considered as the range of possible application. Depending on the slope angle (gentle slopes are more stable, resulting in higher $H_s/\Delta D_{n50}$ values), the possible range of application for $H_s/\Delta D_{n50}$ is about 1 - 4.

The wave period is strongly related to the wave steepness, s_m. The maximum wave steepness is about s_m = 0.06 - 0.07. Steeper waves will break due to instability. Long waves are considered for s_m = 0.005 - 0.02. The possible range of application for the wave steepness is about s_m = 0.01 - 0.06.

The surf similarity parameter, ξ_m, depends on both the slope angle and the wave steepness. Rubble mound (rock) slopes will practically not be steeper than $\cot\alpha$ = 1.5. Very flat slopes are assumed for $\cot\alpha$ = 5 - 6. Based on a range of $\cot\alpha$ = 1.5 - 6 and a wave steepness of s_m = 0.01 - 0.06, the range for ξ_m becomes ξ_m = 0.7 - 7.

Uniform stones are characterized by $D_{85}/D_{15} < 1.25$. Riprap has gradings between D_{85}/D_{15} = 1.75 - 2.50. A grading with D_{85}/D_{15} = 2.5 can be considered to be extremely wide for armour stone. The ratio of W_{85}/W_{15}, in which W is the weight of the stone, becomes more than 15 in this latter case. A stone class of 0.5 - 15 tons has approximately a grading of D_{85}/D_{15} = 2.2 - 2.5. The range of possible application can be set at about D_{85}/D_{15} = 1 - 2.5.

The damage, S, was related to the number of waves by the parameter $S/\sqrt{N}$ (Section 2.3.4). The damage should lay between S = 1 - 20. The influence of the number of waves was evaluated on the results of Thompson and Shuttler (1975). The number of waves ranged from 500 upto 20,000 which can be regarded as the complete range of possible application. Based on the relationship $S/\sqrt{N}$

It is acceptable to decrease the number of waves to be performed in further testing. The range of N = 1000 - 3000 can be considered to be satisfactory in this case. Taking N = 500 as a minimum and S = 20 as a maximum, gives $S/\sqrt{N}$ < 0.9.

The permeability of the structure, P, can be enclosed between two boundaries. The upper boundary can be assumed to be a homogeneous structure consisting of only armour stones. A practical lower boundary is found for a two diameters thick armour layer on a thin filter layer and with an impermeable core (clay or sand in prototype and concrete in model). At least both boundaries (homogeneous and impermeable) should be considered with a structure with a permeable core in between.

Theoretical boundaries for the spectral shape parameter, κ, are 0 (white noise) and 1 (a spectrum with only one frequency). Practical boundaries (see Figure 2.9) are κ = 0.3 - 0.9.

A non-overtopped structure is assumed when R_c/H_s is in the order of R_c/H_s > 1 - 2. The crest is well below the water level when R_c/H_s < - 1. The range to be investigated, therefore, must cover roughly - 1 < R_c/H_s < 2.

The final list of governing variables with the range to be considered can now be summarized:

variable	expression	range
The wave height parameter	$H_s/\Delta D_{n50}$	1 - 4
The wave period parameters, wave steepness, and	s_m	0.01 - 0.06
surf similarity parameter	ξ_m	0.7 - 7
The damage as a function of the number of waves	$S/\sqrt{N}$	< 0.9
The slope angle	$\cot\alpha$	1.5 - 6
The grading of the armour stones	D_{85}/D_{15}	1 - 2.5
The permeability of the structure	P	imperm.- hom.
The spectral shape parameter	κ	0.3 - 0.9
The crest height	R_c/H_s	-1 - 2

2.4.4 Final list for dynamic stability

The surf similarity parameter, ξ_m, is a function of the slope angle. Dynamically stable profiles have varying and curved slopes and can not be characterized by one slope angle. This means that the dimensionless wave period parameter is given by the fictitious wave steepness s_m.

The water depth in front of the structure determines whether the lowest point of movement is influenced by this depth, or that the water depth is large enough to form a profile which is independent on the water depth. A variation in water level (tide) will also have an influence on the position of the profile for given wave boundary conditions. The wave height is again defined as the wave height just in front of the structure, which means that the shape of the foreshore must be taken into account in order to determine this wave height, before profile calculations can be made. It is important to investigate the influence of the water depth just in front of the structure on the formation of the profile. The governing variable can be given by $h(x=toe,t)/H_s$.

The wave height can be limited by the water depth. Water depths should be applied from this depth limited conditions (roughly $h/H_s = 1.2 - 2$) up to depths where the profile is no longer influenced by changes in depths. Water depths in this case should be larger than the lowest point of the developed profile.

The crest height, R_c/H_s, has influence on the profile if the crest is relatively low. Generally, the range to be investigated should lay between the still water level and the maximum runup which is in the order of $1 - 2$ H_s. As the stability of the rear of a low crested structure will not be taken into account, the crest width, w_c/D_{n50} or w_c/H_s, will be ignored. It is assumed that the crest width is large enough to avoid damage to the rear.

Scale effects become important if too small rock or gravel is used. Van Hijum and Pilarczyk (1982) found no scale effects in a small scale investigation for $D_{90} > 4 - 6$ mm in the model, D_{90} being the 90% value of the sieve curve. The transition from sand to gravel can be laid at 4 mm. Small diameters of gravel, therefore, cannot be scaled down without introducing scale effects. Large scale tests on (almost) prototype scale can tackle this problem. Therefore tests in the large Delta flume were performed on fine shingle.

The natural angle of repose, ϕ, is nearly the same for rock and gravel and is less important for dynamically stable profiles where a lot of material is continuously moving.

The angle of wave attack, ψ, has an influence on the profile as wave run-up, run-down and breaking vary with varying angles of wave attack. Van Hijum and Pilarczyk (1982) have investigated gravel beaches for $\psi = 30°$. Their results will be reanalyzed in this thesis. Generally, the range should roughly be between $\psi = 0° - 50°$.

A rock slope or gravel beach is a more or less homogeneous structure without filter layers and core. The parameters D_{50} (armour)/D_{50} (filter) and D_{85}/D_{15} (filter) are not relevant therefor for dynamic stability. The thickness of the armour layer t_a/D_{n50}, can also be deleted. As the structure is homogeneous, the permeability coefficient, P, is the same for all structures. For berm breakwaters with only 3 - 10 layers of armour stones the permeability of the armour layer (and core) might vary, and therefore, might have some influence on the profile.

Rock is more or less angular, where gravel (shingle) is rounded. The shape of the material can not be ignored beforehand for dynamically stable slopes. More or less angular stones, flat and long stones and rounded stones (shingle) give the range to be investigated. The description of the stone shapes will be given in Chapter 3.

The method of construction of the structure is not considered to be a governing variable, as small material for testing dynamically stable profiles is dumped in the model facility without any special care on the method of placing.

The mechanical strength (or quality) of stones has to be considered in prototype designs, especially for dynamically stable structures with large stones, as berm breakwaters. The quality of the stones is less important for small scale investigation and will not be considered.

Most statically stable structures are designed as a uniform slope, characterized by the slope angle, cotα. Dynamically stable profiles can not be described by the slope angle. Only for model tests a uniform initial slope can be considered and characterized by cotα. In most cases the initial slope will have an arbitrary shape.

Finally, the profile itself can be described by a number of height and length parameters which can be related to the nominal diameter, D_{n50}, or to the wave height, H_s.

The remaining governing variables for dynamic stability will be treated in more detail, as was done for statically stable slopes, in order to establish possible ranges of application.

The wave height parameter $H_s/\Delta D_{n50}$ was described already in Section 1.1 to classify various types of structures (simply reduced to H/ΔD). The lower values of $H_s/\Delta D_{n50}$ should be the same as the higher values for static stability

$(H_s/\Delta D_{n50} = 3 - 4)$. The maximum value for dynamic stability is determined by the smallest possible diameter $(D_{n50} = 4$ mm) and the largest (prototype) wave heights. Assuming $H_s = 3 - 4$ m and $\Delta = 1.7$ the maximum value will be in the order of $H_s/\Delta D_{n50} = 450 - 600$. The maximum value which can be investigated in the Delta flume becomes with $H_s = 1.7$ m, $H_s/\Delta D_{n50} = 250$. Values higher than 250 can only be investigated under prototype conditions. The range of wave steepness will be again $s_m = 0.01 - 0.06$.

The influence of the number of waves on profile development will probably differ from statically stable slopes (the parameter $S/\sqrt{N}$). It can be expected that profile development will occur faster than the development of damage, as the resistance to wave action is much smaller for the smaller grains used in dynamically stable structures. Although most reshaping of the profile will have been occurred after 1000 - 3000 waves, some long duration tests upto 10,000 waves are valuable. Also measurements after short durations ($N = 250 - 1000$) should be considered. The possible range of application can roughly be defined between $N = 250 - 10,000$.

Initial slopes can be uniform or can have an arbitrary shape. A developed profile can even be the initial profile for another storm condition. As described for statically stable structures the grading can be defined between $D_{85}/D_{15} = 1 - 2.5$. The spectral shape parameter, κ, is again defined by $\kappa = 0.3 - 0.9$.

The final list of governing variables for dynamically stable rock slopes and gravel beaches with the possible range of application is given by:

variable	expression	range
The wave height parameter	$H_s/\Delta D_{n50}$	3 - 500
The wave period parameter (wave steepness)	s_m	0.01 - 0.06
The profile parameters	-	-
The number of waves	N	250 - 10,000
The initial slope	$\cot\alpha$ or arbitrary shape	-
The grading of the material	D_{85}/D_{15}	1 - 2.5
The shape of the stone	-	angular, rounded, flat
The spectral shape parameter	κ	0.3 - 0.9
The crest height	R_c/H_s	SWL - runup
The water depth in front of the structure	$h(x=toe,t)/H_s$	-
The angle of wave attack	ψ	$0° - 50°$

3. Static stability

3.1 Earlier work

Static stability of rubble mound structures is described by so-called stability formulae. Some formulae were described in Section 2.3.1 and an overview of existing stability formulae was given by the International Commission for the study of Waves (PIANC (1976)). A well known and widely used formula is the formula of Hudson (Equation 2.15), which became so popular due to its simple form.

The Hudson formula, however, as has been found by many users, has a lot of shortcomings. It does not include, for example, the influence of the wave period and was not developed with random waves. The study of Ahrens (1975) in a large wave tank showed the importance of the wave period on the stability of riprap. The tests, however, were also performed with regular waves. Figure 3.1 shows the results of Ahrens (1975), where the $H/\Delta D_{n50}$ value is plotted against the surf similarity parameter, ξ. This parameter, ξ, gives almost the same curves for different slope angles if the waves are of the plunging type ($\xi <$ 2.5 - 3.0). Minimum of stability is found for collapsing waves, (see also Figure 2.5 for types of breakers). The surf similarity parameter gives different curves for different slopes if the waves are of the surging type ($\xi >$ 2.5 - 3.0).
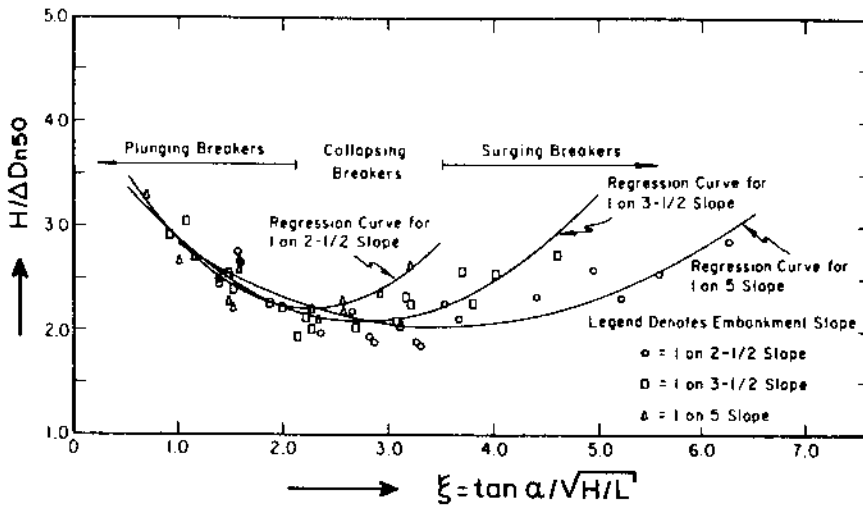
Figure 3.1 Stability of riprap for regular waves, Ahrens (1975).

Evaluation of Ahrens' data by Pilarczyk and Den Boer (1983) produced stability formulae which included the wave period. A replot of above mentioned data with the developed formulae is shown in Figure 3.2. The formulae derived were:

for plunging waves - the left curves in Figure 3.2:

$$H/\Delta D_{n50} = 2.25 \; \xi^{-0.5} \; S_R \qquad (3.1)$$

for surging waves - the right curves in Figure 3.2:

$$H/\Delta D_{n50} = 0.54 \; \sqrt{\cot\alpha} \; \xi^{0.5} \; S_R = 0.54 \; (H/L)^{-0.25} \; S_R \qquad (3.2)$$

where:

$S_R = \mu\cos\alpha + \sin\alpha$ (see also Equation 2.11).
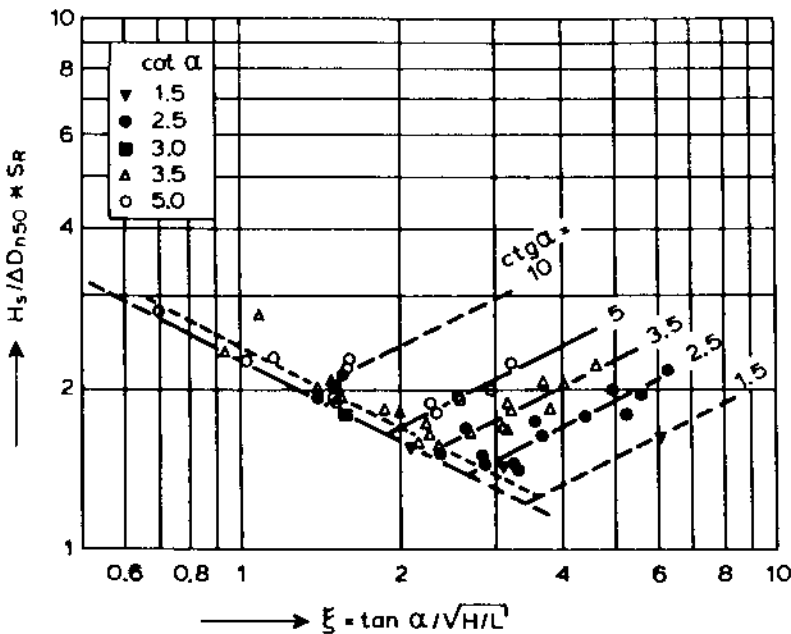
Figure 3.2 Replot of Ahrens' data by Pilarczyk and Den Boer (1983).

Losada and Giménez-Curto (1979a) gave formulae for the stability of rubble mound slopes under regular wave attack which also included the wave period. Figure 3.3 was taken from Losada and Giménez-Curto (1979a) and shows the parameter Q as a function of ξ, where Q is the inverse of the cubic value of $H/\Delta D_{n50}$ ($Q = (H/\Delta D_{n50})^{-3}$). The curves show also minimum stability for $\xi = 2 - 4$. The same kind of plots were given for parallelopipedic blocks and tetrapods.

Hedar (1960, 1986) showed the importance of the permeability of the structure, but again for regular waves. Figure 3.4 was taken from Hedar (1986) and shows k/H_b plotted versus $\cot\alpha$ for the no damage criterion (k/H_b equals about $1/(H/\Delta D_{n50})$).
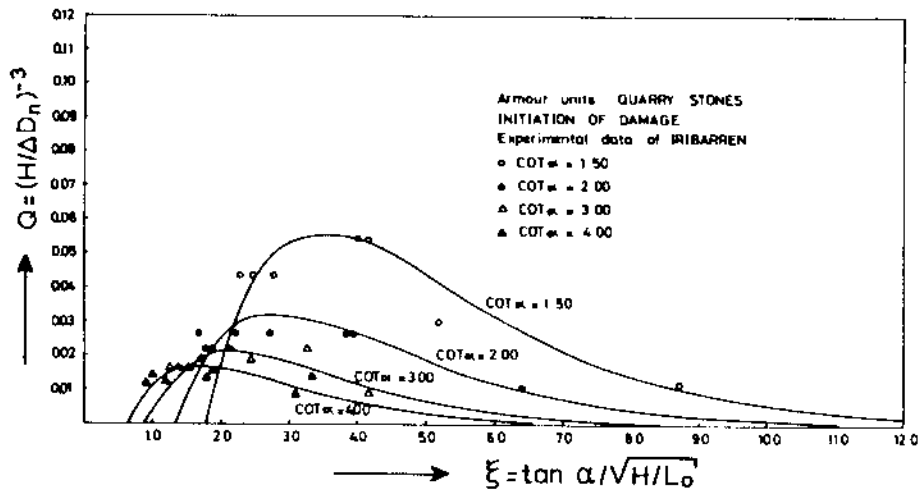
Figure 3.3 Influence of the wave period on stability for regular waves, Losada and Giménez-Curto (1979a).
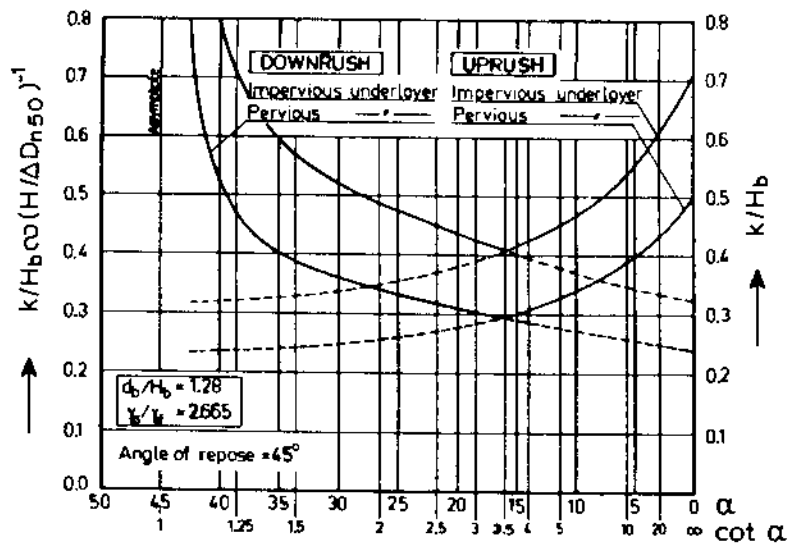
Figure 3.4 Influence of permeability on stability, Hedar (1986).

Hedar considered two types of structures, an impermeable and a permeable one. Figure 3.4 shows that a permeable structure has the highest stability.

An extensive investigation was performed by Thompson and Shuttler (1975) on the stability of rubble mound (riprap) slopes under random waves, as described already in Chapter 2. Their main results are shown in Figures 3.5 - 3.8. Damage, N_Δ (Equation 2.1), is plotted against the parameter H_s/D_{50}. Results are shown for N = 1000 and 3000 and for four slope angles (cotα = 2, 3, 4 and 6).
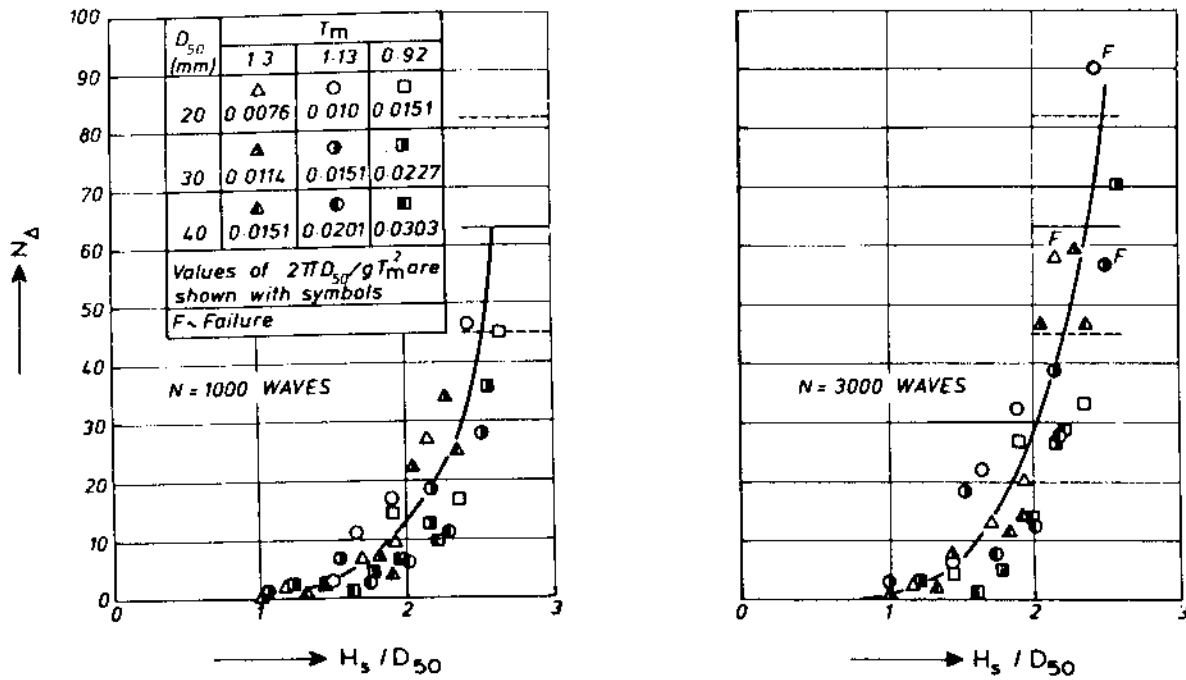
Figure 3.5 Damage curves for random waves, Thompson and Shuttler (1975); cotα = 2
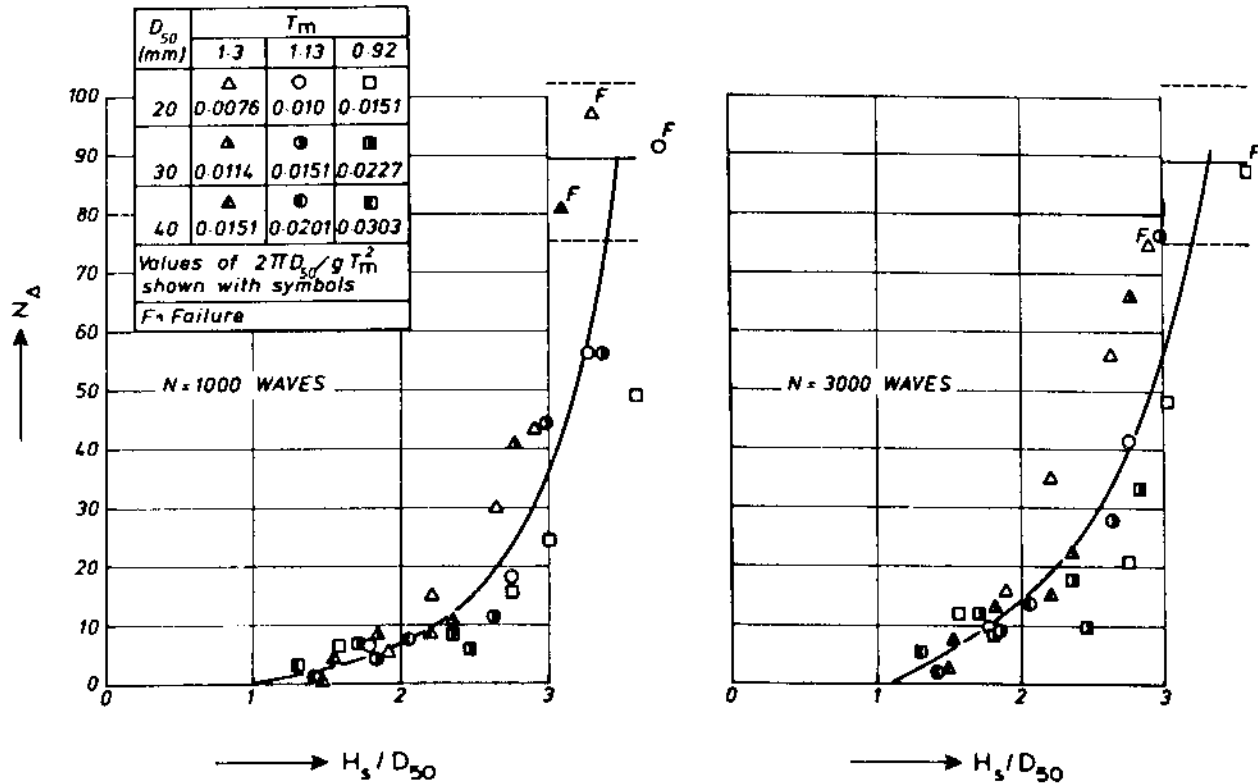
Figure 3.6 Damage curves for random waves, Thompson and Shuttler (1975); cot α = 3
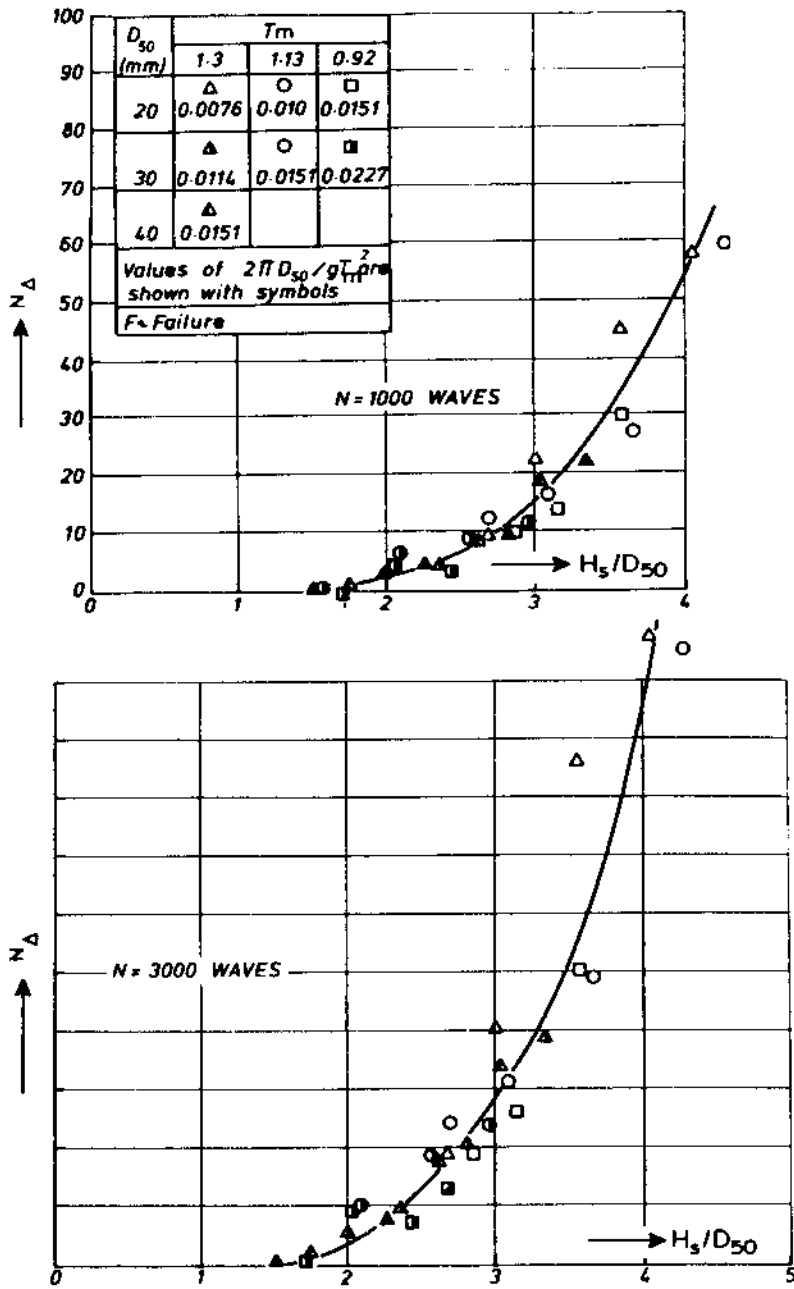
Figure 3.7 Damage curves for random waves, Thompson and Shuttler (1975); cotα = 4

One of their main conclusions was that, within the scatter of the results, the erosion damage showed no clear dependence on the wave period. By re-arranging their data, however, it can be found, that in fact there is a clear dependence on the wave period. This re-analysis was done in the following way: Damage curves were plotted for each wave period used, and the damage parameter N_Δ was transformed into the damage S. From all these damage curves the H_s/D_{50} values were taken for different fixed damage levels. With these H_s/D_{50} values, the wave periods, T_m, the slope angles and the given relative mass density, Δ,

It is possible to calculate the $H_s/\Delta D_{n50}$ and ξ_m values for different damage levels. Figure 3.9 shows the results of this re-analysis. The $H_s/\Delta D_{n50}$ and ξ_m values are given for the damage levels S = 3 (start of damage) and S = 8 (moderate damage).
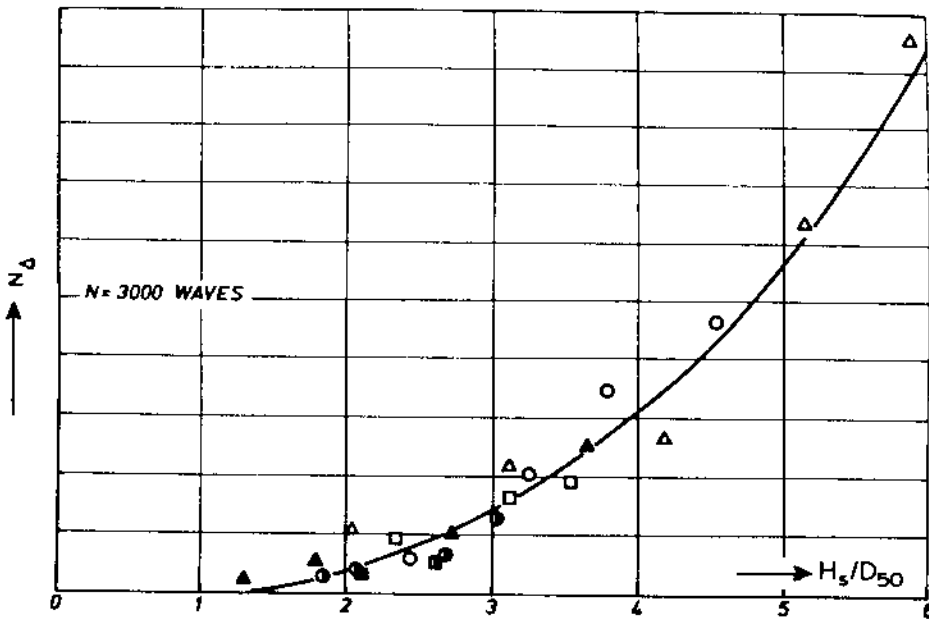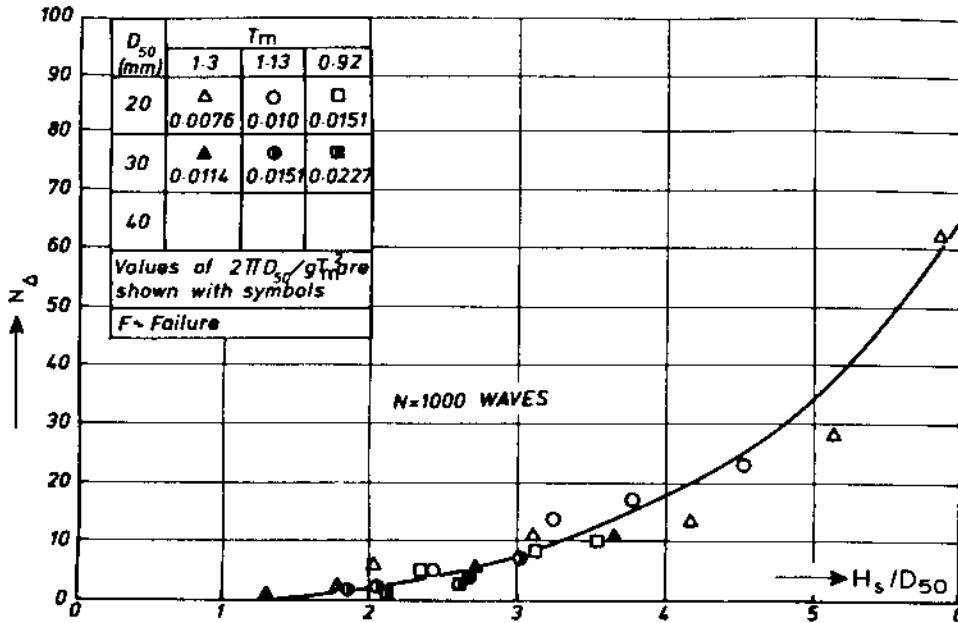
Figure 3.8 Damage curves for random waves, Thompson and Shuttler (1975); cotα = 6

The same trend is found as for regular waves, see Figure 3.1. A longer wave period gives lower stability, in the area which was investigated. In fact only plunging waves (high wave steepnesses) were used by Thompson and Shuttler. The

minimum of stability for collapsing waves was never reached. The work of Thompson and Shuttler can be used, therefore, as a starting point for an extensive model research program.
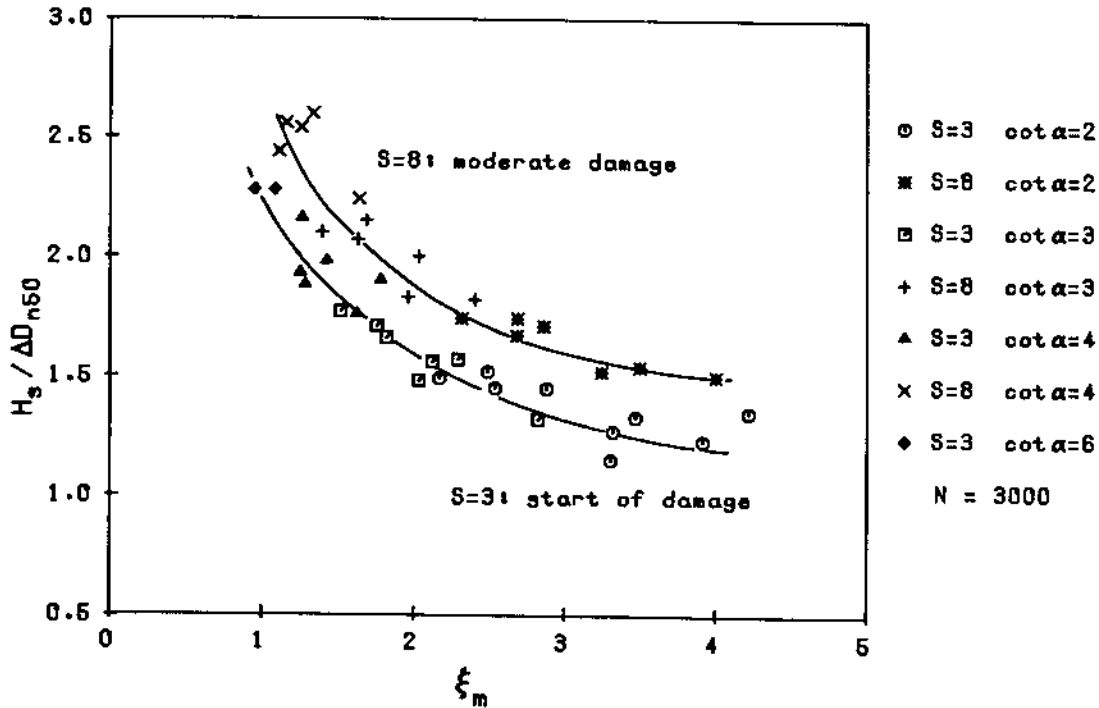
Figure 3.9 Re-analysis of the data of Thompson and Shuttler (1975), showing the influence of the wave period on damage.

3.2 Test equipment, materials, procedure and test program

Almost all tests were conducted in a 1.0 m wide, 1.2 m deep and 50.0 m long wave flume with the test section installed about 44 m from the random wave generator. A system developed by DELFT HYDRAULICS was used to measure and compensate for reflected waves at the wave board. With this system standing waves and basin resonance were avoided. The incident significant wave height was measured with the structure in the flume, by means of two wave gauges placed about a quarter of a wave length apart. In this way the incident and reflected spectra were determined.

For the investigation a surface profiler was developed with nine gauges placed 0.10 m apart on a computer controlled-carriage. The surface along the slope was measured every 0.040 m. Depending on the slope angle every survey consisted between 500 and 1600 data points. Successive soundings were taken at exactly the same points using the relocatability of the profiler. An average profile was calculated and plotted by computer and used for determining the erosion damage, S, see Figure 2.2.

100 90 85 80 70 60 50 40 30 20 15 10 0

percent passing by weight

uniform stones $D_{85}/D_{15} = 1.25$

filter

riprop $D_{85}/D_{15} = 2.25$

4 6 8 10 20 40 60 80

sieve diameter (mm)

Figure 3.10 Sieve curves.
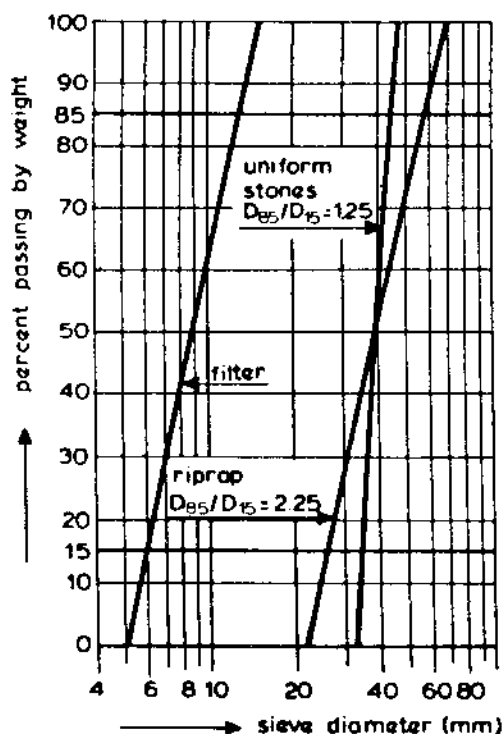
Crushed stone was used for the armour layer, the main characteristics of which were: W_{50} = 0.123 kg; ρ_a = 2620 kg/m³; D_{n50} = 0.036 m; layer thickness 0.080 m. The sieve analysis curves were straight lines on a log-linear plot, see Figure 3.10. Two gradings were used: D_{85}/D_{15} = 2.25 (riprap) and 1.25 (uniform stones) respectively. The filter layer was defined by: D_{50} (armour)/D_{50} (filter) = 4.5 and D_{85}/D_{15} = 2.25, according to the tests of Thompson and Shuttler (1975). The thickness of the filter layer was 0.02 m.

When an impermeable core was tested the filter layer was placed directly on a slope constructed of mortar. When a permeable core was tested the armour layer was placed directly on the core, without a special filter layer. During the tests with a permeable core the grading of the core was: D_{85}/D_{15} = 1.50 with D_{n50} = 0.011 m. This means that for the tests with a permeable core, D_{50} (armour)/D_{50} (core) = 3.2, or W_{50} (armour)/W_{50} (core) = 33.

Figures 3.11 - 3.14 show the various structures investigated in the small scale flume. Figure 3.11 shows the model with an impermeable core, Figure 3.12 the permeable core, Figure 3.13 a homogeneous structure and Figure 3.14 shows the structure with a sloping foreshore of 1 : 30.

Thompson and Shuttler performed tests with the duration, the number of waves, N, up to 5000. They measured damage every 1000 waves. The influence of the number of waves on damage was analyzed in Section 2.3.4, using the results of Thompson and Shuttler. Based on these results the procedure was changed for the present tests.

Each complete test consisted of a pre-test sounding, a test of 1000 waves, an inter-mediate sounding, a test of 2000 more waves, a final sounding. After each complete test the armour layer was removed and rebuilt. A test series consisted generally of five tests with the same wave period, but different significant wave heights. Wave heights ranged from 0.05 m to 0.26 m and wave periods from 1.3 to 3.2 seconds. A water depth of 0.80 m was applied for all tests.
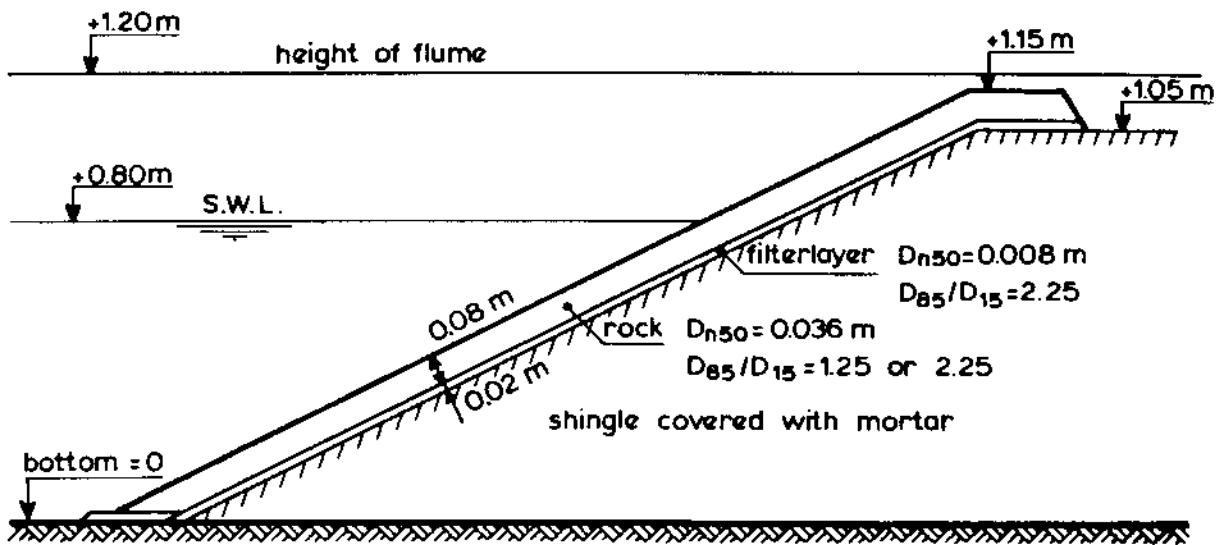
Figure 3.11 Tested structure with an impermeable core.
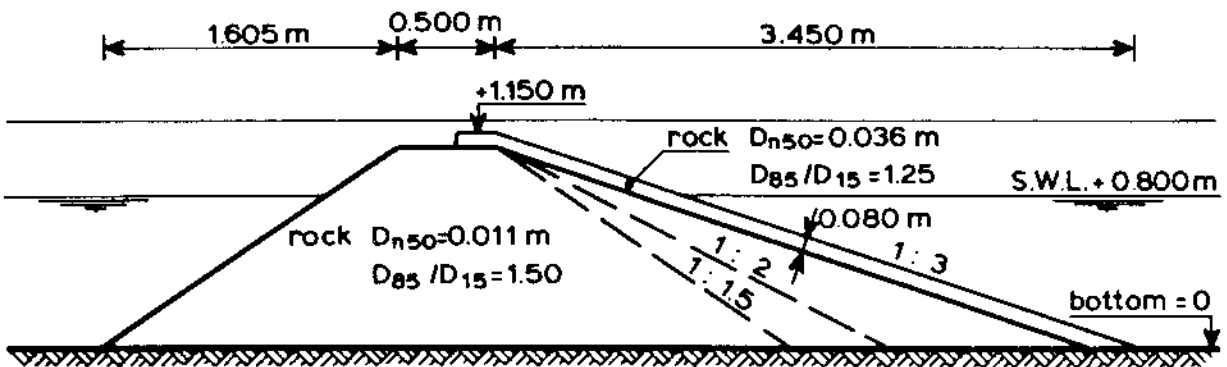
Figure 3.12 Tested structure with a permeable core.
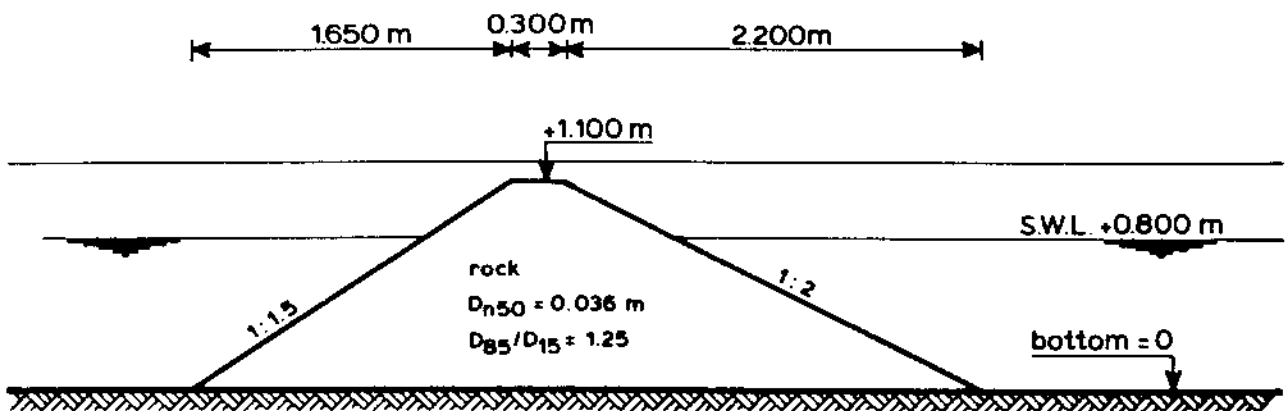
Figure 3.13 Tested homogeneous structure.
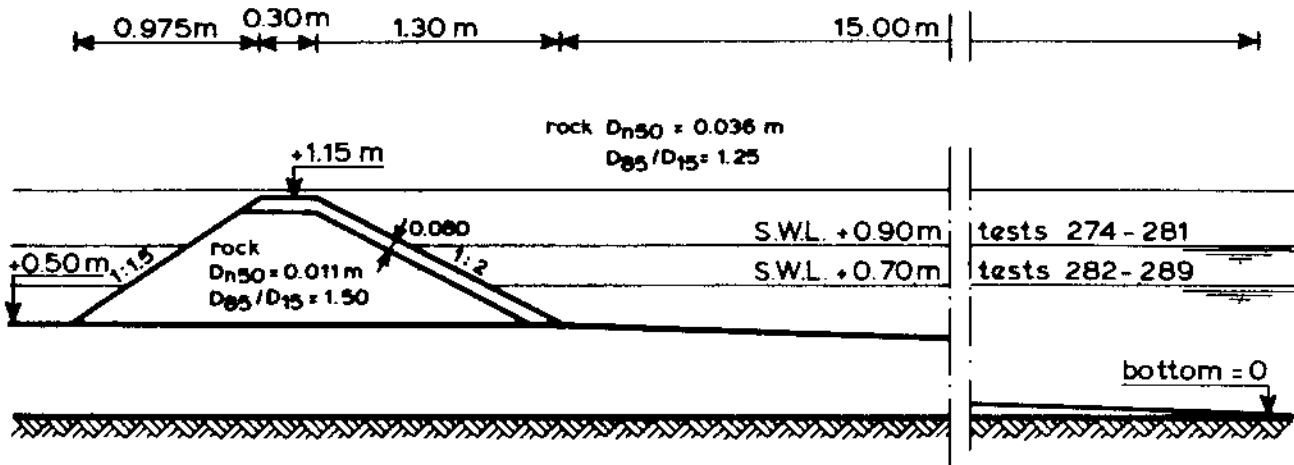
Figure 3.14 Tested structure with a 1 : 30 foreshore.

A damage curve was drawn for N = 1000 and N = 3000, for each test series, as shown in Figure 3.15. An average curve was drawn through the measured points. The $H_s/\Delta D_{n50}$ values were taken from these curves for different fixed damage levels. Damage levels were chosen at S = 2, 3, 5, 8, 12 and 17. The damage levels S = 3 (start of damage) and S = 8 (moderate damage) will be elaborated here as an example, using Figure 3.15. The $H_s/\Delta D_{n50}$ values obtained from Figure 3.15, are:

S	N	$H_s/\Delta D_{n50}$
3	1000	1.64
3	3000	1.42
8	1000	2.04
8	3000	1.77
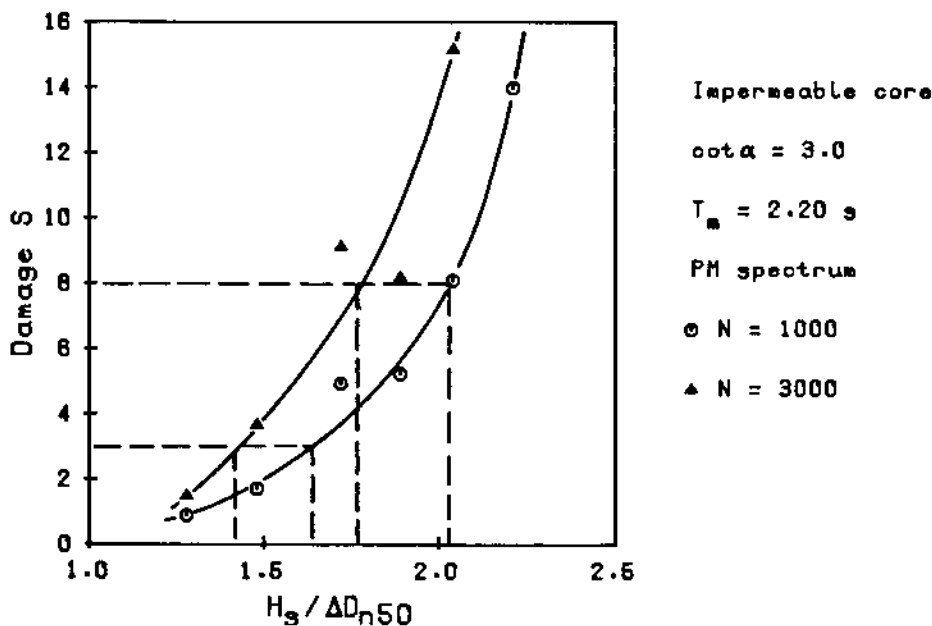
Figure 3.15 Typical damage curves

With $\Delta = 1.615$, $D_{n50} = 0.036$ m, $T_m = 2.20$ s and cot$\alpha = 3$, the surf simila-
rity parameter, ξ_m (Equation 2.19), can be calculated for each $H_s/\Delta D_{n50}$ value
shown above. These values are:

$H_s/\Delta D_{n50}$	ξ_m
1.64	2.97
1.42	3.19
2.04	2.66
1.77	2.86

All derived combinations of $H_s/\Delta D_{n50}$ and ξ_m of all the tests were plotted in
$H_s/\Delta D_{n50} - \xi_m$ plots and were used for analysis of the test results. Some se-
lected plots will be used in the next sections in order to describe the influ-
ence of governing variables on stability.

The test program was based on the governing dimensionless variables and
their possible range of application established in Section 2.4.3. First the
research of Thompson and Shuttler (1975) was extended with longer wave peri-
ods. Four slope angles were investigated (cot$\alpha = 2$, 3, 4 and 6) with riprap as
armour stone ($D_{85}/D_{15} = 2.25$) and an impermeable core. Uniform stones with
$D_{85}/D_{15} = 1.25$ were then used on slopes with cot$\alpha = 3$ and 4. These gradings
are both near the upper and lower boundaries of $D_{85}/D_{15} = 1 - 2.5$, established
in Section 2.4.3. A wide and a very narrow spectrum were used on a slope with
cot$\alpha = 3$. These spectra are shown in Figure 2.6 and cover the range of $\kappa = 0.4$
- 0.9.

Structures with a permeable core had slopes with cot$\alpha = 1.5$, 2 and 3. A
homogeneous structure was tested only for cot$\alpha = 2$. Armour stones with both a
very low relative mass density ($\Delta = 0.95$) and also with a high relative mass
density ($\Delta = 2.05$) were used on a structure with cot$\alpha = 2$ and a permeable
core. Finally a 1:30 foreshore was constructed, with waves breaking on the
foreshore due to depth limitations. A permeable structure with cot$\alpha = 2$ and
also low crested structures were tested with this 1:30 foreshore.

The test program is summarized in Table 3.1. Groups of tests are given, cha-
racterized by the slope angle, the grading, the spectral shape, the permeabi-
lity of the underlaying structure, and the relative mass density. Each group
of tests generally consists of about 20 tests which covers the total range of
possible application of $H_s/\Delta D_{n50}$ and s_m as established in Section 2.4.3. The
ranges investigated are shown too in Table 3.1. The first two groups in Table
3.1 (cot$\alpha = 2$ and 3, impermeable core) show only a range of $s_m = 0.005 -
0.024$, i.e. only long waves. The higher wave steepnesses were investigated by
Thompson and Shuttler (1975).

Comparison of Table 3.1 with the final list of governing variables given in Section 2.4.3 shows that almost the complete possible range of application is covered by the test program.

slope angle cotα	grading D_{85}/D_{15}	spectral shape	core permeability	relative mass density	number of tests	range $H_s/\Delta D_{n50}$	range s_m
2	2.25	PM	none	1.63	19	0.8-1.6	0.005-0.016
3	2.25	PM	none	1.63	20	1.2-2.3	0.006-0.024
4	2.25	PM	none	1.63	21	1.2-3.3	0.005-0.059
6	2.25	PM	none	1.63	26	1.2-4.4	0.004-0.063
3*	1.25	PM	none	1.62	21	1.4-2.9	0.006-0.038
4	1.25	PM	none	1.62	20	1.2-3.4	0.005-0.059
3	2.25	narrow	none	1.63	19	1.0-2.8	0.004-0.054
3	2.25	wide	none	1.63	20	1.0-2.4	0.004-0.043
3*	1.25	PM	permeable	1.62	19	1.6-3.2	0.008-0.060
2	1.25	PM	permeable	1.62	20	1.5-2.8	0.007-0.056
1.5	1.25	PM	permeable	1.62	21	1.5-2.6	0.008-0.050
2	1.25	PM	homogeneous	1.62	16	1.8-3.2	0.008-0.059
2	1.25	PM	permeable	0.95	10	1.7-2.7	0.016-0.037
2	1.25	PM	permeable	2.05	10	1.6-2.5	0.014-0.032
2**	1.25	PM	permeable	1.62	16	1.6-2.5	0.014-0.031
2***	1.25	PM	permeable	1.62	31	1.4-5.9	0.010-0.046

PM   = Pierson Moskowitz spectrum

*   = some tests repeated in Delta flume

** = foreshore 1 : 30

*** = low crested structure with foreshore 1:30

Table 3.1   Test program.

Some tests were repeated in the large Delta flume after completion of the small scale tests described above, in order to evaluate scale effects on stability of the armour layer. All dimensions of the small scale model were scaled up to the Delta flume according to Froude's law by a linear factor 6.25. This means that the dimensions of filter and core material were also scaled with this factor and that different flow regimes were present in the structure for the small and large scale tests.

The dimensions of the Delta flume are: length 230 m, width 5 m and depth 7 m. The same system to measure and compensate for reflected waves at the wave board was present in the Delta flume. Also a similar surface profiler was developed with nine gauges on a carriage.

All relevant parameters measured for each test are given in Appendix I. Established values of $H_s/\Delta D_{n50}$ and ξ_m for fixed damage levels are given in

Appendix II, including results obtained from the tests of Thompson and Shuttler (1975). These data will be elaborated in more detail in the following Sections.

3.3 Qualitative analysis of results

3.3.1 Results on damage levels and storm duration

Almost all tests were performed on a two diameter thick armour layer (except for the homogeneous structure). The extent of damage depends on the slope angle. More stones have to be displaced or moved for gentler slopes before the "no damage" criterion or the failure criterion (filter layer visible) is reached. This is due to the larger amount of stones around the water level for a gentler slope. The lower and upper damage levels, that is the onset of damage and failure, were determined from the investigation and are shown in Table 3.2. The damage limits in Table 3.2 should be considered when a statically stable structure of rock is designed with a two diameter thick armour layer.

DAMAGE LEVEL $S = A/D_{n50}^2$		
$\cot\alpha$	start of damage	filter layer visible ($2D_{50}$ thick layer)
1.5	2	8
2.0	2	8
3.0	2	12
4.0	3	17
5.0	3	17

Table 3.2 Lower and upper damage levels for rock slopes

The influence of the storm duration on stability was investigated by Thompson and Shuttler (1975). Analysis of their results (Section 2.3.4) showed that the influence of the storm duration on damage could be described by $S/\sqrt{N}$.
Using this relationship the ratio of damage after 3000 and after 1000 waves should be $S(3000)/S(1000) = \sqrt{3} = 1.73$. The ratio of the 50 tests of Thompson and Shuttler, analyzed in Section 2.3.4, amounted to $S(3000)/S(1000) = 1.81$. The ratio of the present test series (about 200 tests) amounted to $S(3000)/S(1000) = 1.64$ with a standard deviation of 0.30. This is close to the value of 1.73. The ratio was calculated under the restriction $2 < S < 17$.

It can be concluded that the variable, $S/\sqrt{N}$, was confirmed by the present tests and can be considered to be a variable which describes the influence of the storm duration on damage in a proper way.

3.3.2 Influence of wave height, wave period and slope angle

The influence of various variables will be shown by $H_s/\Delta D_{n50} - \xi_m$ plots. The influence of the wave height is shown by the $H_s/\Delta D_{n50}$ parameter. The wave period and the slope angle are combined in the surf similarity parameter, ξ_m.
The influence of wave height, wave period and slope angle on stability will be shown for structures with an impermeable core, with a permeable core and for a homogeneous structure. Plots are given for the damage levels S = 3 (start of damage) and S = 8 (moderate damage).

Figure 3.16 shows the results for an impermeable core with cotα = 2, 3, 4 and 6. Figure 3.17 shows the data for a permeable core with slope angles of cotα = 1.5, 2 and 3. The results for a homogeneous structure (cotα = 2) are
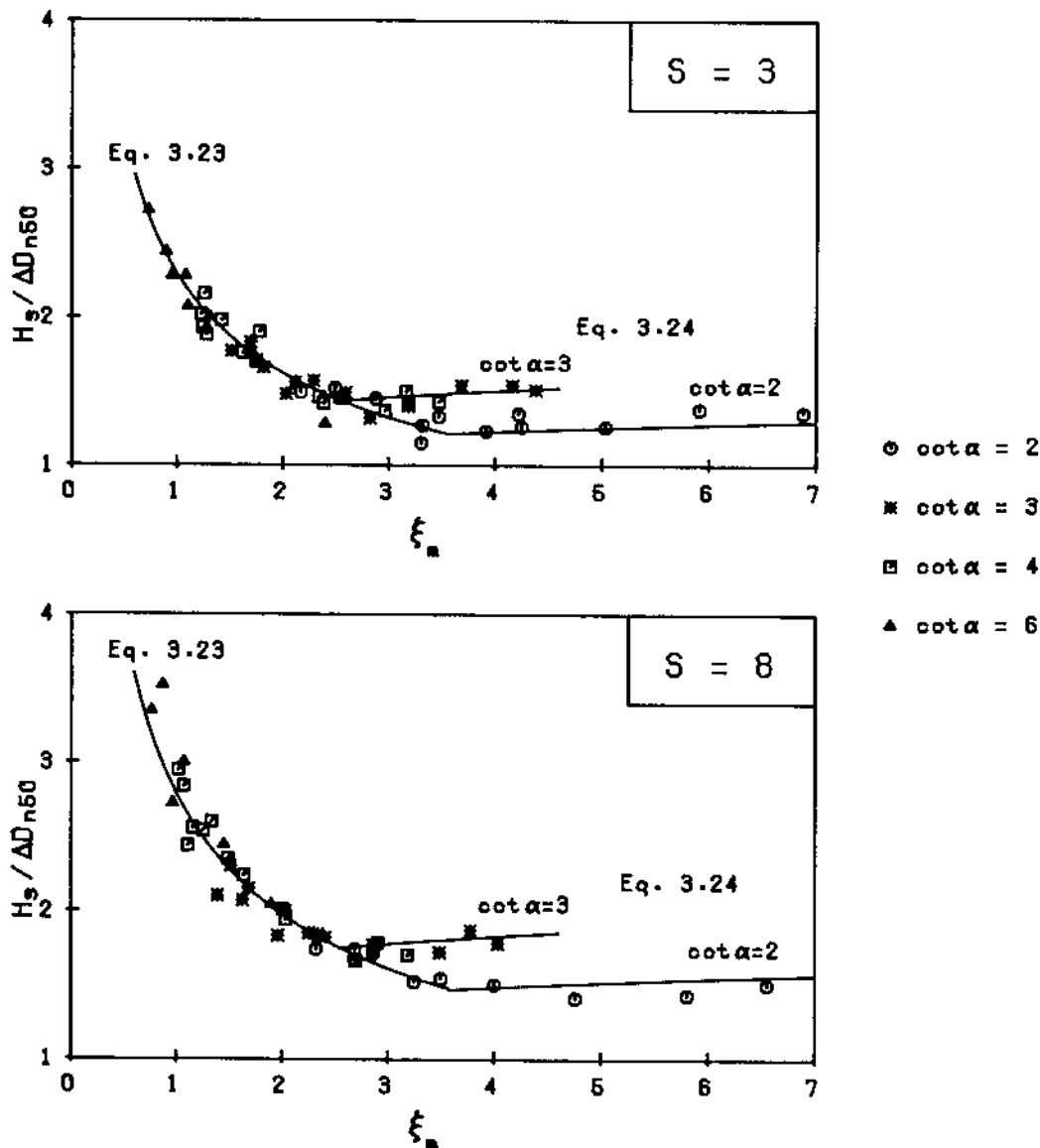
Figure 3.16 Results for an impermeable core, S = 3 and 8.
(N = 3000, P = 0.1).

shown in Figure 3.18. All data points are given in Appendix II. The curves are the stability formulae 3.23 and 3.24 which are derived later on in this Chapter.
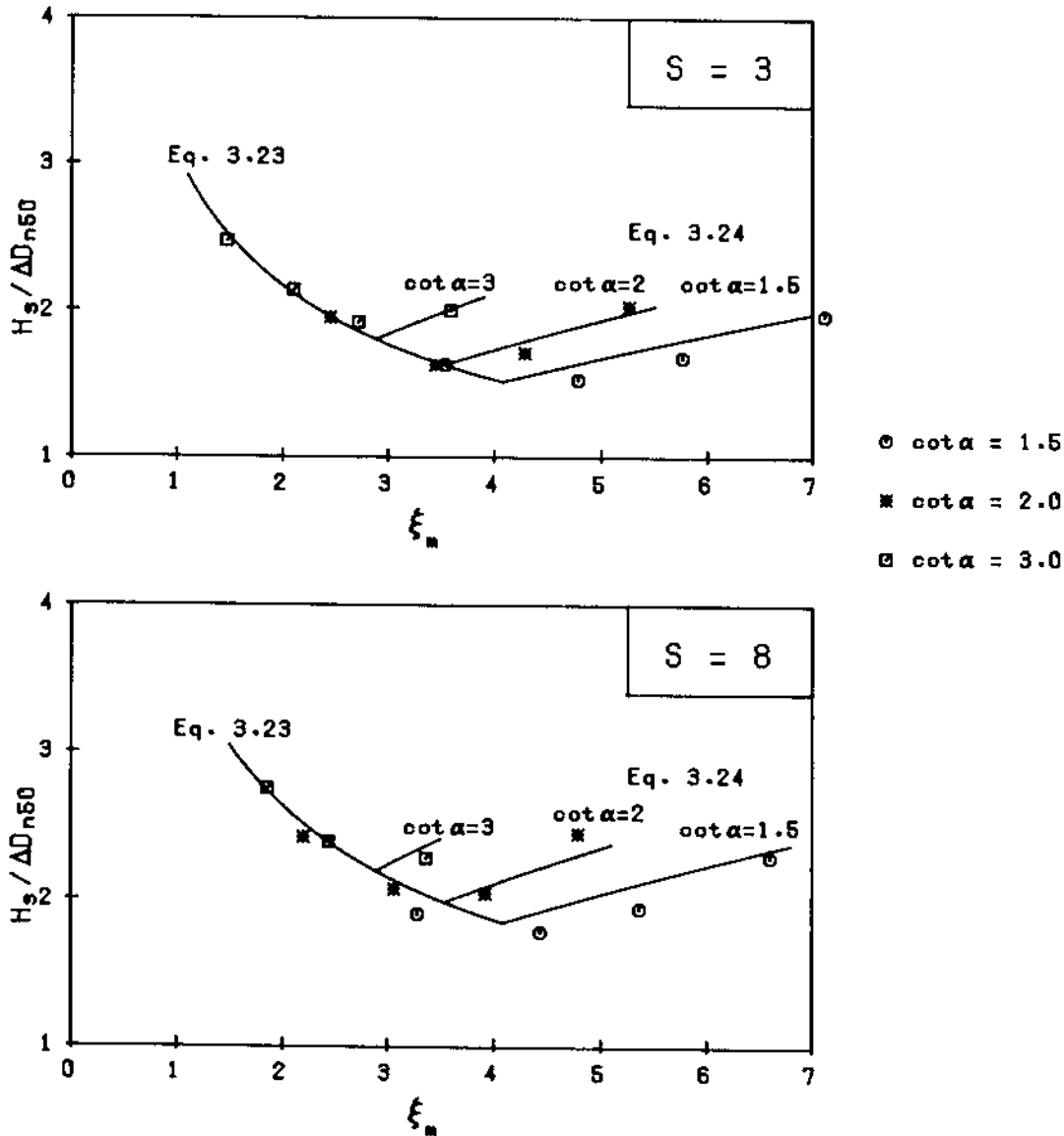
Figure 3.17   Results for a permeable core, S = 3 and 8. (N = 3000, P = 0.5).

Figures 3.16 - 3.18 show the same trend as that found by Ahrens (1975) for regular waves, see Figures 3.1 and 3.2. Plunging waves are present on the left side of the figures for ξ_m < 2.5 - 4. Surging waves are shown when ξ_m > 2.5 - 4. Minimum stability is found for the transition from plunging to surging waves, referred to as collapsing waves.

The trends shown in Figures 3.16 - 3.18 and also in Figure 3.1 and 3.2 can be explained physically as follows. In the plunging region the fast wave run-up after breaking of the wave is decisive for stability and in the surging

region wave run-down. In the collapsing region both run-up and run-down forces are high which causes the minimum of stability.

For plunging (breaking) waves the surf similarity parameter, ξ_m, or breaker parameter gives a good description of the influence of slope angle and wave steepness on stability, as results for different slopes form one curve. For surging waves on the right side of Figures 3.16 and 3.17, different curves are shown for different slope angles. The transition from plunging to surging waves shifts to the right (larger ξ_m value) for steeper slopes. The surf similarity parameter, therefore, does not show the influence of the slope angle and wave steepness in a proper way for surging waves.
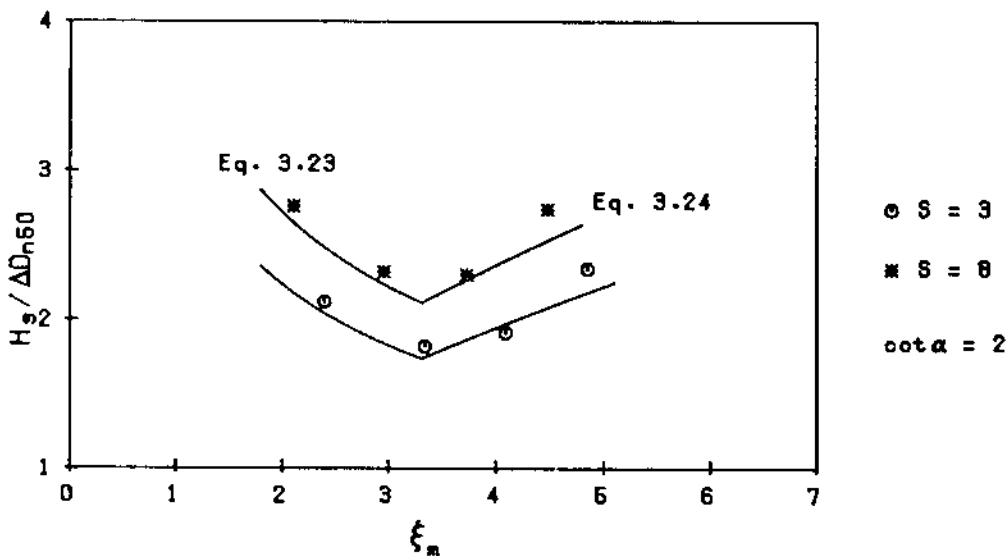
Figure 3.18 Results for a homogeneous structure, S = 3 and 8.
(N = 3000, P = 0.6, cotα =2).

3.3.3 Influence of armour grading

Tests were carried out at slopes with cotα = 3.0 and cotα = 4.0 with widely graded riprap, D_{85}/D_{15} = 2.25, and uniform stones, D_{85}/D_{15} = 1.25. Tests results are shown on Figure 3.19 for both slopes and for three different damage levels. The damage to both gradings was found to be the same for both slope angles. It can be concluded that the grading of the armour within the range tested has no or only minor influence on the stability and that, within this range, the armour layer can be described simply by the nominal diameter, D_{n50}.

3.3.4 Influence of spectral shape and groupiness of waves

The main part of the present series of tests was conducted with a Pierson Moskowitz (PM) spectrum. The test series with a slope angle of cotα = 3.0 was
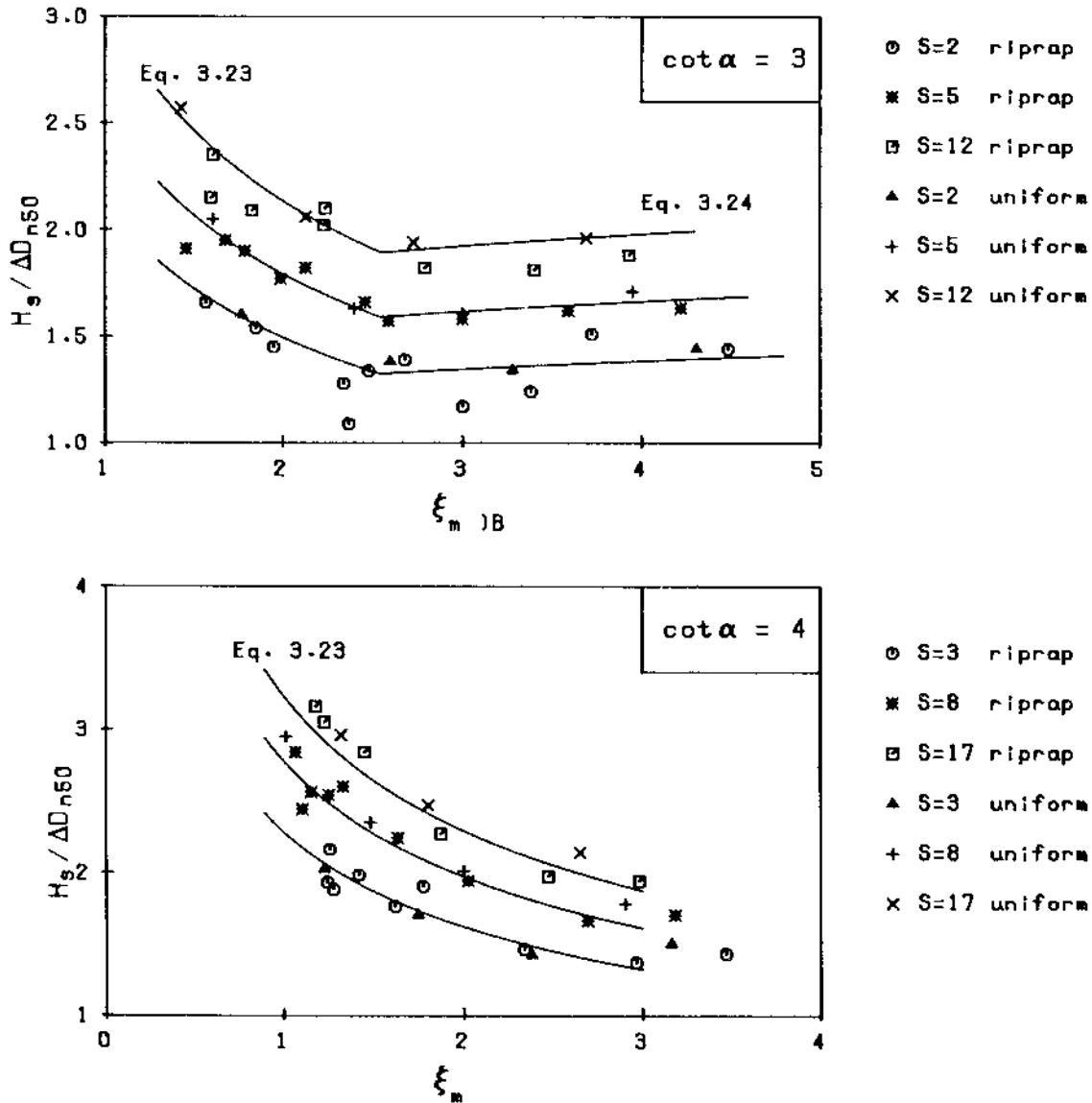
Figure 3.19 Influence of grading for cotα = 3 and 4.

performed with a very narrow spectrum and also with a wide spectrum. The spectra have already been described in Section 2.3.3 (Figure 2.6). The parameter κ which describes the spectral shape and groupiness is respectively $\kappa_f = 0.90$ and $\kappa_{HH.t} = 0.92$ for the narrow spectrum, $\kappa_f = 0.47$ and $\kappa_{HH.t} = 0.62$ for the PM spectrum and $\kappa_f = 0.25$ and $\kappa_{HH.t} = 0.48$ for the wide spectrum. The ratio of peak period to average period amounted to $T_p/T_m = 1.01$ for the very narrow spectrum, $T_p/T_m = 1.15$ for the PM spectrum and $T_p/T_m = 1.42$ for the wide spectrum.

The wave period which should be used to describe different spectral shapes, can not be stated beforehand if this period is used to minimize the influence of the spectral shape, as described in Section 2.3.2. The choice of the wave period has influence on the results between different spectral shapes. It

might be possible to minimize the influence of the spectral shape on stability, just by choosing the characteristic wave period for the spectra which show this minimum influence. If the wave period is selected beforehand, influences found between various spectral shapes have to be described by the parameter κ.

A choice for the average period, T_m, was made arbitrarily when discussing results for one spectral shape. Here results will be given both for the peak period and average period. Figure 3.20 shows the results for the narrow and wide spectrum for two damage levels (S = 2 and 12) which can be considered as the lower and upper boundaries, i.e. "no damage" and "filter layer visible".
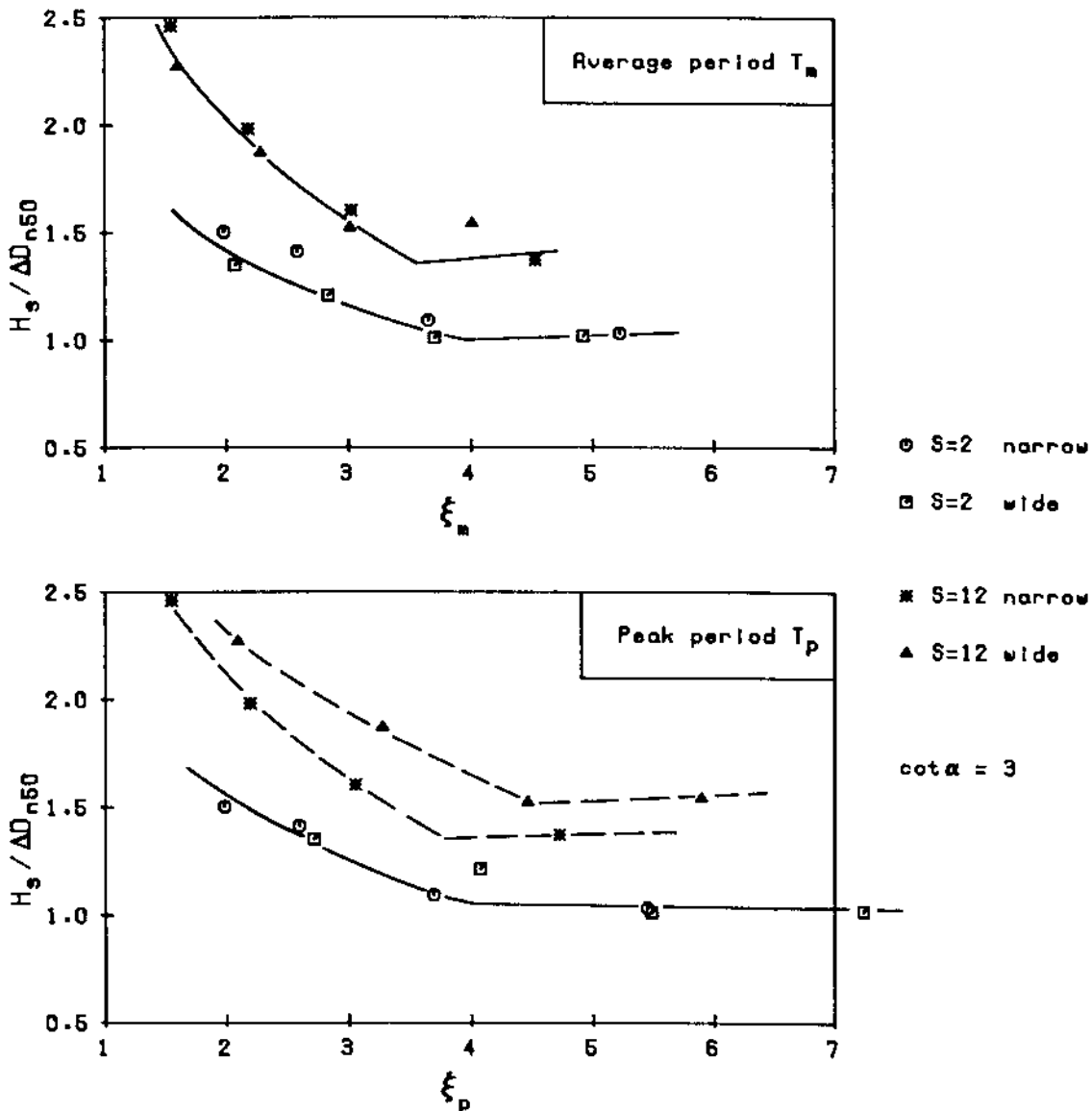
Figure 3.20   Influence of spectral shape on stability.

The average period, T_m, was used in calculating $\xi_m = \tan\alpha/\sqrt{2\pi H_s/gT_m^2}$ for the upper figure. The results of the lower figure were plotted by using the peak period, T_p, in calculating $\xi_p = \tan\alpha/\sqrt{2\pi H_s/gT_p^2}$.

The upper plot of Figure 3.20, using T_m in ξ_m, shows good agreement between the two spectra for both damage levels. The lower plot, using T_p in ξ_p, shows a more complex situation. For S = 2 the agreement is the same, or even better, than using T_m (the upper plot), except for ξ_p = 4. For the damage level S = 12 differences between the spectra are much larger in the lower than the upper plot of Figure 3.20. For example, the damage level S = 12 for ξ_p = 3 is reached for $H_s/\Delta D_{n50}$ = 2.10 for the narrow spectrum and for $H_s/\Delta D_{n50}$ = 2.45 for the wide spectrum. This is a difference of about 17%.

Based on Figure 3.20 the following conclusion can be drawn. For start of damage (S = 2) the influence of the spectral shape is negligible for both a characteristic wave period T_m and T_p. For higher damage levels (S = 12) the influence of the spectral shape is much smaller for the characteristic period T_m. Therefore preference should be given for using T_m in describing static stability of rock slopes. In that case the influence of the spectral shape on stability is very small and might be ignored.

Another conclusion, and a very surprising one, can be drawn form Figure 3.20. Comparison of this Figure with the upper plot of Figure 3.19 (results for Pierson Moskowitz spectrum) shows that the curves in Figure 3.20 are lower, especially for ξ_m > 4. As a wide and a narrow spectrum give more or less the same results, it is not expected that a Pierson Moskowitz spectrum, with κ values between the values for the wide and narrow spectrum, will give much better results on stability. Some aspects were verified in order to explain the differences between Figures 3.19 and 3.20.

a. If the difference is not caused by the difference in spectral shape, as was concluded from Figure 3.20, a repetition of a test with a Pierson Moskowitz spectrum should give much more damage for this repetition test. Test 189 is a repetition of test 32. The wave boundary conditions are almost equal for both tests, see Appendix I. The damage found for test 32 amounted to S = 4.43 (N = 1000) and S = 8.70 (N = 3000). For test 189 the damage was S = 11.43 and S = 20.65 respectively. This means that the damage in test 189 is 2.5 times higher than in test 32 and is consistent with the results with the narrow and wide spectrum.

It can be concluded therefore, that the difference in stability is not caused by the spectral shape. The conclusion on the influence of the spectral shape on stability is not affected.

b. Lower stability in Figure 3.20 can be caused by a stone class around the still water level which is (accidently) smaller than in previous tests. This grading was checked, but showed no difference with the previous tests ($D_{n50} = 0.036$ m, $D_{85}/D_{15} = 2.25$).

c. The stones of the armour layer were frequently handled. After each test the stones were placed in buckets and the armour layer was rebuilt. Stones rolled during this handling. Stones rolled also during tests where damage occurred. For a few tests this procedure may not cause a problem. The stones of the riprap were used in more than 150 tests, however. Moreover, the riprap was painted again after test 151 which is before the tests with a narrow and wide spectrum. Painting was performed by rolling the stones in a concrete mill with the paint.

The frequent handling of the stones and probably especially the painting by using a concrete mill caused rounding of the stones. The stones were more rounded in the tests with the narrow and wide spectrum. The rounding, however, did not influence the grading of the stone (no loss of weight), see above described point b. It might be possible that stability of rock slopes is influenced by the roundness of the stones. And, according to Figure 3.20, the possible influence of the roundness is more pronounced for the surging wave region ($\xi_m > 3 - 4$) where rundown is decisive for stability.

It should be remembered that the overall shape of the stones, i.e. the ratio of maximum/minimum dimensions was not changed. The roundness describes the roughness of the surface and this parameter might have caused the difference in stability between Figures 3.19 and 3.20.

Bergh (1984) found that nicely rounded stones showed much lower stability. The $H_s/\Delta D_{n50}$ value for start of damage was even 50% lower than for cubical stones. This means a difference of a factor 8 in stone mass. For the failure criterion the $H_s/\Delta D_{n50}$ was 77% of that for cubical stones (factor 2.2 in stone mass). Other researchers (Hudson (1959) and Thomsen et al (1972)) found no influence, however. More investigation is required to solve the influence of roundness of stones on stability.

Allsop et al (1985) defined a parameter which describes the roundness. Further research on shape descriptors is still in progress (Latham and Poole (1987)). It is recommended to include the results of these investigations for further research on the influence of roundness of stones on stability.

Further testing (after test 197) was performed with a new made stone class, which was not painted.

3.3.5 Influence of permeability

Three structures have been tested: A revetment with an impermeable core, clay or sand in nature and concrete in model, tested first, see Figure 3.11. A structure with a permeable core (breakwater) tested second, see Figure 3.12. This structure was much more stable than the impermeable core. A homogeneous structure consisting only of armour stones which is an upper boundary, as far as permeability is concerned, tested third, see Figure 3.13. The impermeable core can be regarded as a lower boundary of permeability. The coefficient P described later in this Chapter, was introduced to take account of permeability.

Results for the three structures mentioned above and for all slope angles investigated have already been discussed in this Chapter, Figures 3.16 - 3.18. A comparison of the three structures is shown in Figure 3.21.
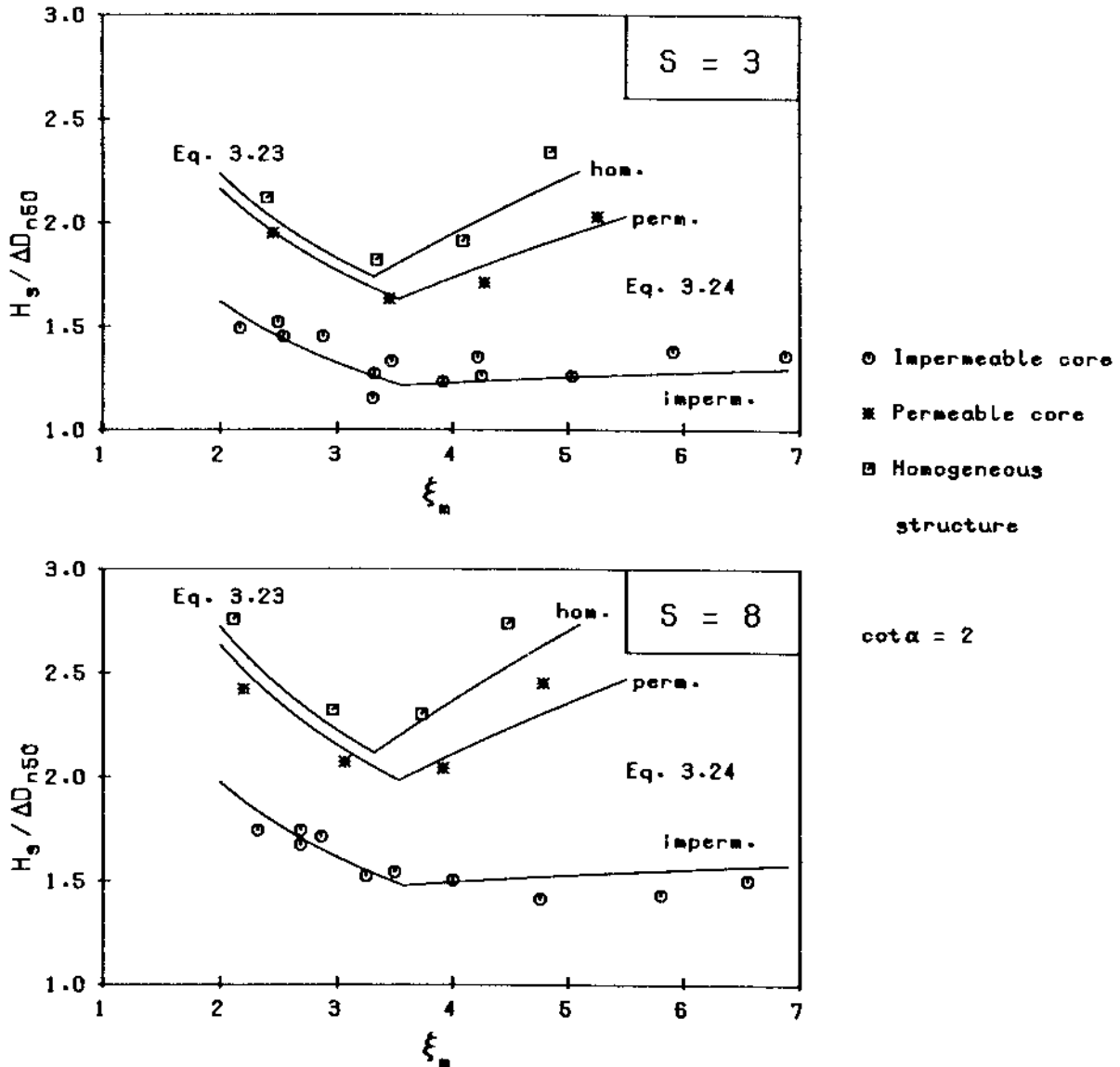
Figure 3.21 Influence of permeability.

Results are shown for a slope with cotα = 2, damage levels of S = 3 and 8 and after 3000 waves. The influence of the wave period for plunging waves (left side of figures) shows the same trend for all three structures, although a more permeable structure is more stable. A more permeable structure is also more stable for surging waves ($\xi_m > 3.5$), but the stability increases with larger wave periods. The curves are steeper for larger permeability.

This phenomenon can be explained in physical terms by the difference in water motion on the slope. For a slope with an impermeable core the flow is concentrated in the armour layer causing large forces on the stones during run-down. For a slope with a permeable core the water dissipates into the core and the flow becomes less violent. With longer wave periods (larger ξ_m) more water can percolate and flow down through the core. This reduces the forces and stabilizes the slope.

The stability increases by more than 35 percent for plunging waves in relation to the wave height as the permeability shifts from an impermeable core to a homogeneous structure. This means a difference of a factor 2.5 in mass of stone for the same design wave height. And this is only caused by a difference in permeability. The trend for the influence of permeability on stability is the same as that found by Hedar (1960 and 1986) for regular waves, see Figure 3.4.

3.3.6 Influence of relative mass density

Tests were performed with stones having different mass densities. The light stones (crushed bricks) had a mass density of 1950 kg/m^3 and the heavy stones (basalt) of 3050 kg/m^3. Normal stones had a mass density of 2620 kg/m^3.
Results for light, normal and heavy stones are shown in Figure 3.22 for S = 3 and 8. Both the light and heavy stones are relatively (in dimensionless terms) a little more stable than the normal stones.

The difference can not be explained in terms of scatter. The trend is not consistent, however, as both the light and the heavy stones are more stable than the normal stones (which is in between the range of Δ).

The difference is probably again caused by differences in roundness of the stones, see also Section 3.3.4 on influence of spectral shape. Both the broken bricks and the basalt had more sharp edges than the normal stones. Moreover, the surface texture of the light stones was more rough than for the basalt and normal stones. It might be possible that, besides the roundness, the surface texture has influence on stability too.

If it is accepted that the differences in Figure 3.22 are caused by differences in roundness and surface texture, it can be concluded that the influence of the mass density on stability can be described correctly by the Δ in the parameter $H_s/\Delta D_{n50}$.
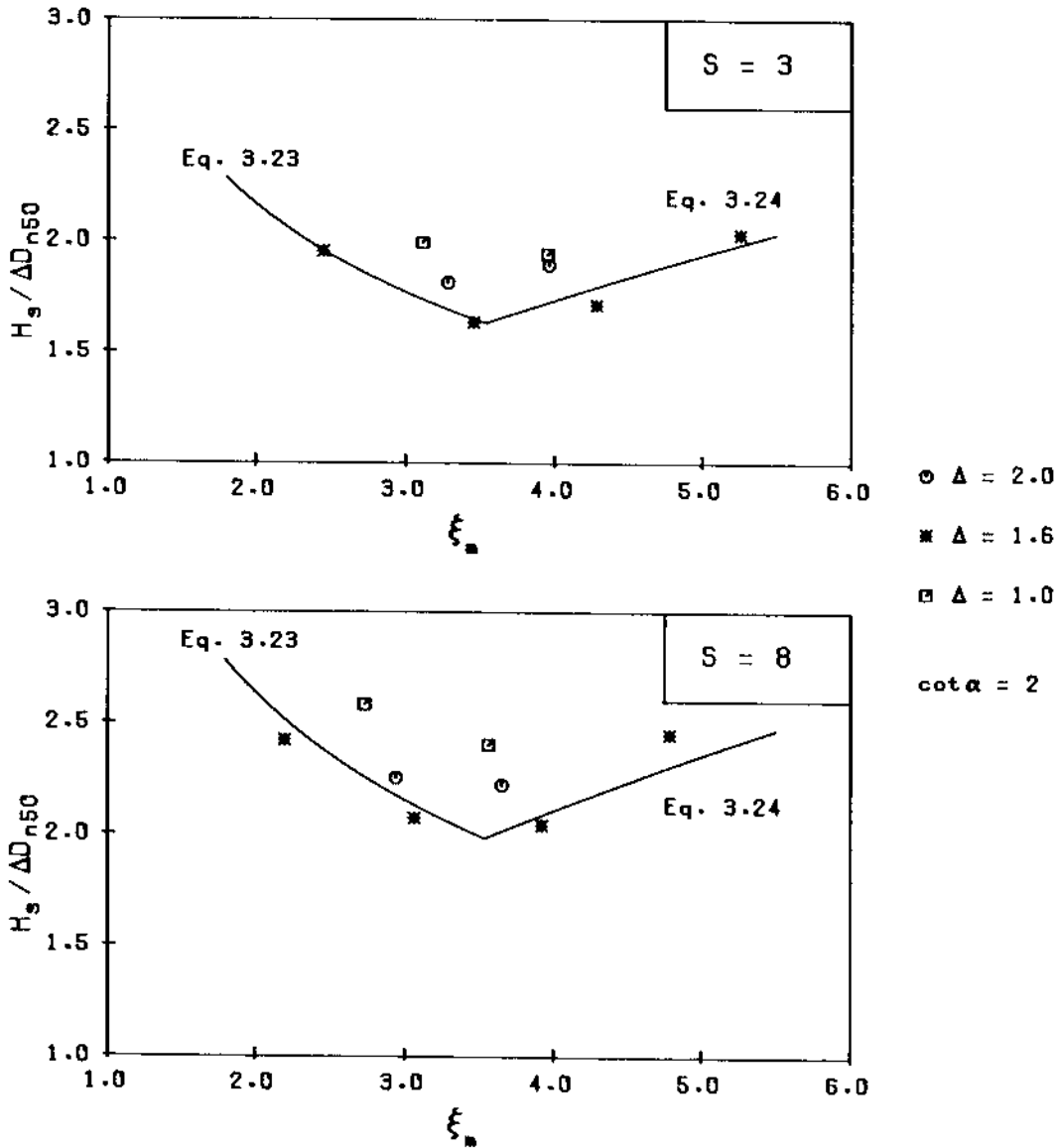
Figure 3.22 Influence of relative mass density for S = 3 and 8.

3.3.7 Influence of water depth

Tests were performed in the small scale flume with a sloping 1:30 foreshore in front of the structure, see Figure 3.14. The length of the foreshore was 15 m and the toe of the structure was situated 0.5 m above the bottom of the flume. The water depth during the previous tests was 0.80 m.

Two different water levels were used with this foreshore in the flume. The water depths in front of the foreshore were 0.90 m and 0.70 m, respectively, resulting in water depths at the structure of 0.40 m and 0.20 m. The significant wave heights at the structure ranged roughly from 0.10 - 0.15 m, which means that only high waves were breaking with a water depth of 0.40 m in front of the structure. A large part of the waves were breaking on the foreshore with a water depth of 0.20 m in front of the structure. In both cases the wave heights were not Rayleigh distributed. The wave heights were measured at the toe of the structure when the structure itself was not present in the flume.

Figure 3.23 shows the usual plots, for S = 3 and S = 8, using the significant wave height at the toe of the structure, H_s, in the $H_s/\Delta D_{n50}$ parameter.
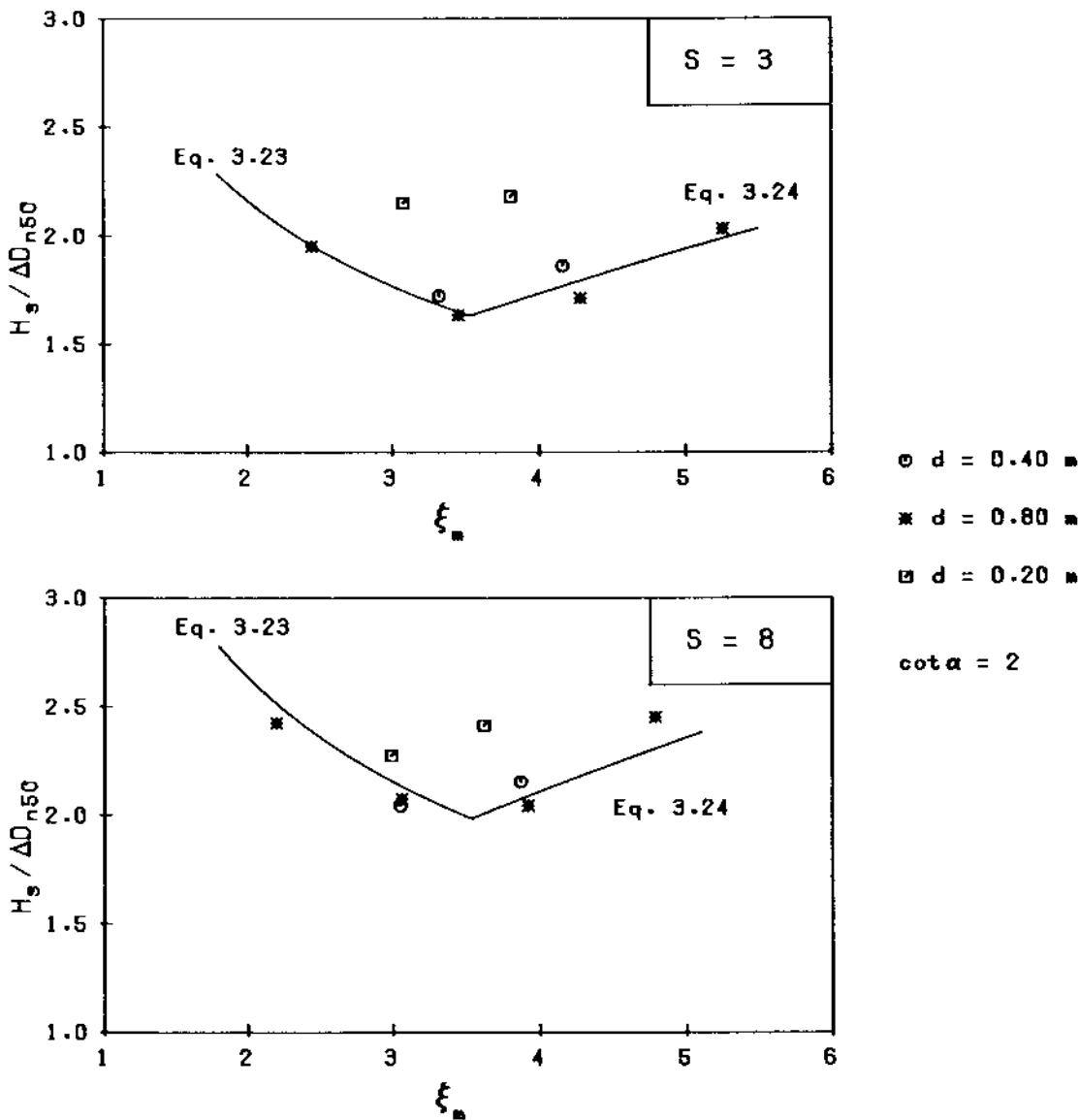
Figure 3.23 Influence of water depth on stability for S = 3 and 8, using the significant wave height, H_s, at the toe of the structure.

The results with a water depth of 0.40 m are more or less similar to the results with a water depth of 0.80 m. The stability of the structure with a water depth of 0.20 m in front of it, is higher than with a water depth of 0.80 m. Highest waves broke on the foreshore and this resulted in lower wave forces on the structure. It can be concluded on the basis of Figure 3.23 that the significant wave height does not take into account the effect of heavy wave breaking on the foreshore.

Figure 3.24 shows again the stability plots of the structures with different water depths, but now using the two percent wave height, $H_{2\%}$, of the wave height exceedance curve instead of the significant wave height. The $H_{2\%}$ is chosen in relation with the often used 2% value for run-up. The parameter on
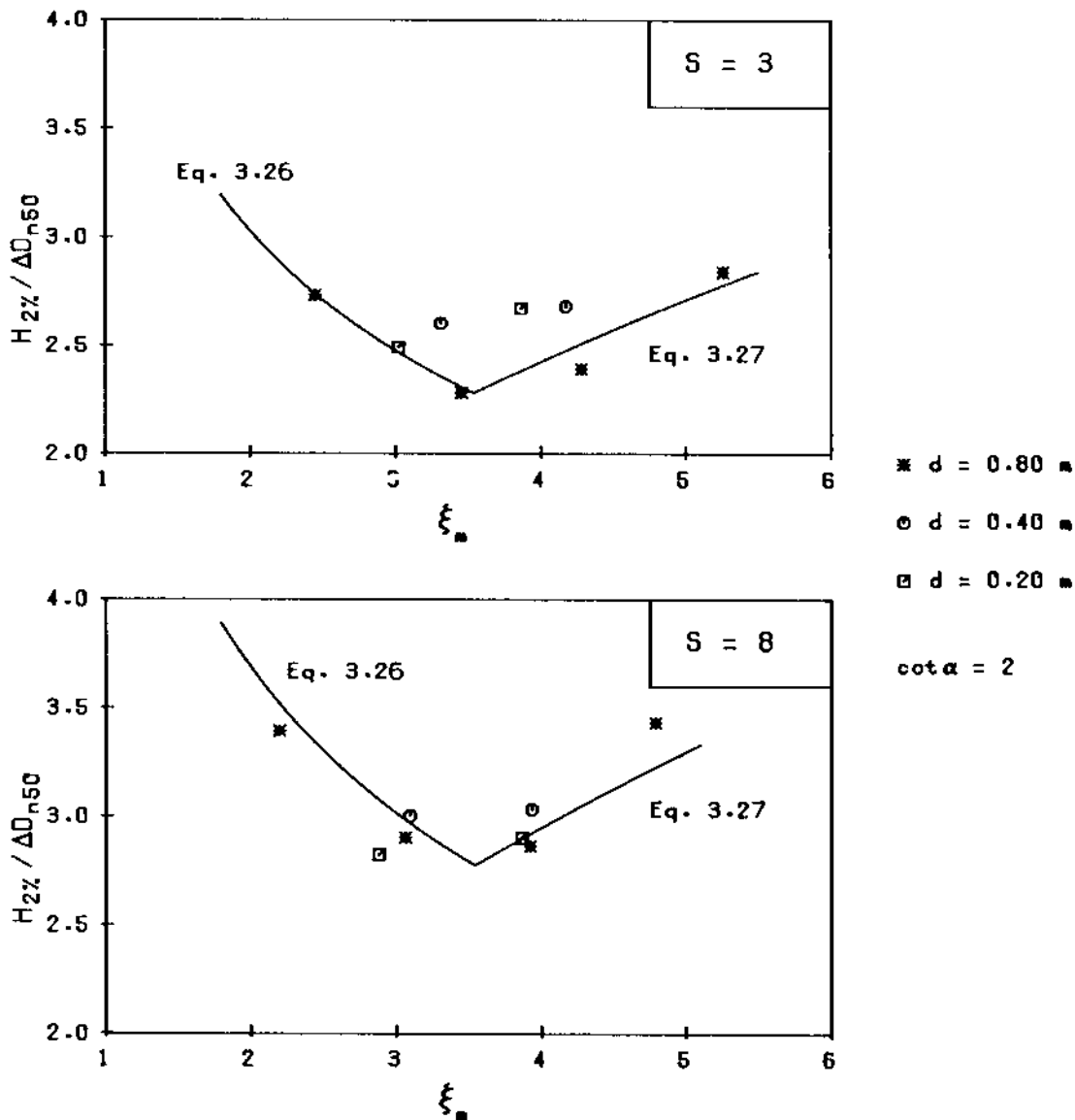
Figure 3.24 Influence of water depth on stability for S = 3 and 8, using the two percent wave height, $H_{2\%}$, at the toe of the structure.

the vertical axis is now $H_{2\%}/\Delta D_{n50}$. As the ratio $H_{2\%}/H_s$ is smallest for the smallest water depth of 0.20 m, the stability results come closer to the results for larger water depth.

From Figure 3.24 it can be concluded that the two percent wave height takes into account the effect of wave breaking. It can be concluded that the two percent wave height is a good parameter, although also the one or five percent wave height will give similar results.

As the significant wave height is often used in stability design, this wave height will be used in derivation of stability formulae. The effect of a non-Rayleigh distribution of the wave heights can be taken into account by using the ratio $H_{2\%}/H_s$ or a similar one with $H_{1\%}$ or $H_{5\%}$.

3.4 Derivation of stability formulae

3.4.1 Governing variables

A list was provided of governing variables for static stability in Section 2.4.3 This list with the possible range of application was given by:

variable	expression	range
The wave height parameter	$H_s/\Delta D_{n50}$	1 - 4
The wave period parameters, wave steepness,	s_m	0.01 - 0.06
and surf similarity parameter,	ξ_m	0.7 - 7
The damage as a function of the number of waves	$S/\sqrt{N}$	< 0.9
The slope angle	$\cot\alpha$	1.5 - 6
The grading of the armour stones	D_{85}/D_{15}	1 - 2.5
The permeability of the structure	P	imperm. - hom.
The spectral shape parameter	κ	0.3 - 0.9
The crest height	R_c/H_s	-1 - 2

In Section 3.2 it was concluded that above mentioned range of possible application is almost completely covered by the test program. The list of variables can be shortened using the qualitative results described in the previous Section.

The influence of the number of waves can be given by $S/\sqrt{N}$. The influence of the relative mass density is given correctly by $H_s/\Delta D_{n50}$. The wave period parameter which was used throughout this study and which has shown its validity is the surf similarity parameter, ξ_m. The surf similarity parameter describes the influence of the slope angle and the wave steepness. Stability of

rock slopes under breaking (plunging) waves ($\xi_m < 3 - 4$) is indeed described correctly by this parameter, ξ_m. Different results are found for different slope angles under non-breaking (surging) waves (shifted curves). On the basis of the results of Section 3.3 the surf similarity parameter, ξ_m, will be used and, if necessary, a combination with cotα.

It is preferred to use the average period T_m. In that case the influence of the spectral shape (parameter κ) on stability is small and can be ignored. Armour grading, has practically no influence on the stability, and the stone class can be described by the nominal diameter D_{n50} only. The influence of the water depth will be taken into account by using the ratio $H_{2\%}/H_s$.

The results on low crested structures will be described later on. Although not considered to be a governing variable, the roundness and surface texture of the stones might have influence on stability. This influence was not investigated in more detail and should be a topic for further research. This means that in this Section stability formulae will be derived for non-overtopped structures with a uniform slope and consisting of angular rock.

The stability of rubble mound revetments and breakwaters can then be described by the following dimensionless variables:

$H_s/\Delta D_{n50}$; ξ_m; cotα; $S/\sqrt{N}$; permeability P

All results show a clear difference between plunging and surging waves, see Figures 3.16 - 3.24. A minimum is found for the transition from surging to plunging waves, referred to as collapsing waves. In Section 3.3 these trends were explained in a physical way.

In the plunging region the fast wave run-up after breaking of the wave is decisive for stability. The forces during run-down are relatively small. In the surging region the wave does not break and forces during run-up are small. Instability in this region is caused by run-down. In the collapsing region both run-up and run-down forces are high which causes the minimum of stability. Based on these trends two stability formulae have been considered, one for plunging waves and one for surging waves.

3.4.2 Example of curve fitting procedure

The results shown in Figures 3.16 - 3.24 and described in Section 3.3 should be described by functional relationships, in order to make the research applicable in practice. The philosophy of approach of the investigation was descri-

bed in Section 2.1.2, mentioning the use of curve fitting procedures in order to find the functional relationships. Many types of functions can be applied for curve fitting.

As the range of possible application of the governing variables is almost completely covered by the test program, the relationships will cover a wide range of application too. In this case where results for the complete range are available, the application of a power function has an advantage. The power coefficient describes the trend of the results (curved, increasing or decreasing) and the other coefficient describes the location of the curve. As shown in Figures 3.16 - 3.24 some trends are consistent using various parameters. It can be expected, therefore, that this trend can be described by only one (rounded) power coefficient. The other coefficient will still be a function of all other variables. Once the power coefficient has been established, the other coefficient can be analysed in more detail.

Above described procedure will be used in an example. Results on stability were shown in $H_s/\Delta D_{n50} - \xi_m$ plots (Figures 3.16 - 3.24) and clear trends are found in these Figures. Consider for instance the plunging wave region ($\xi_m < 3 - 4$). A curved trend is found, as $H_s/\Delta D_{n50}$ is decreasing with increasing ξ_m values, regardless of the other variables, such as damage level, storm duration and permeability. The following power function can be defined:

$$H_s/\Delta D_{n50} = a_1 \, \xi_m^{b_1} \qquad \text{with} \qquad a_1 = f(S/\sqrt{N}, P) \qquad (3.3)$$

As $H_s/\Delta D_{n50}$ is decreasing with increasing ξ_m, a negative value of b_1 will be found. The coefficient b_1 can be established for various groups with the same S, N and P. For fixed damage levels, S, the corresponding values for $H_s/\Delta D_{n50}$ and ξ_m have been tabulated in Appendix II. For simplicity only the permeable core tests will be considered which means that P is fixed. The coefficient b_1 was established for various combinations of S and N and is shown in Table 3.3. The data used for regression analysis can be found in Appendix II - numbers 236 - 288. Most b_1 coefficients in Table 3.3 are based on 5 - 6 data points.

damage level S	b_1 for N = 1000	b_1 for N = 3000
2	-0.50	-0.42
3	-0.54	-0.52
5	-0.57	-0.57
8	-0.50	-0.52
12	-0.42	-0.53

Table 3.3 b_1 values for permeable core tests.

The b_1 values in Table 3.3 are very consistent and the average is $b_1 = 0.51$ with a standard deviation of $\sigma = 0.05$. The same procedure can be applied for the impermeable core tests and the tests with the homogeneous structure. Data points are given in Appendix II – numbers 1 – 235 and numbers 289 – 308 respectively. The average values of b_1 were -0.54 for the impermeable core and -0.51 for the homogeneous structure. This means that b_1 is independent of the permeability of the structure, the damage level and the storm duration.

For practical use the value of b_1 should be a round figure. Within the scatter a value of $b_1 = -0.50$ is acceptable. Equation 3.3 can now be written as:

$$H_s/\Delta D_{n50} * \sqrt{\xi_m} = a_1 \qquad \text{with} \qquad a_1 = f(S/\sqrt{N}, P) \qquad (3.4)$$

Now the whole procedure can be repeated with $H_s/\Delta D_{n50} * \sqrt{\xi_m}$ as one parameter and S, N or P as the others. Further elaboration will be performed separately for the plunging and the surging wave region. The intersection between the two functional relationships will give the transition from plunging to surging waves.

3.4.3 Plunging waves

The first analysis on the plunging wave region led to a functional relationship between $H_s/\Delta D_{n50}$ and ξ_m (Equation 3.4). The coefficient a_1 is still a function of S, N and P. The damage level and number of waves can be described by $S/\sqrt{N}$, as was shown in Sections 2.3.4 and 3.3. This influence of the damage level and the number of waves can then be described by the power function:

$$H_s/\Delta D_{n50} * \sqrt{\xi_m} = a_2 \ (S/\sqrt{N})^{b_2} \qquad \text{with} \qquad a_2 = f(P) \qquad (3.5)$$

where a_2 and b_2 are again regression coefficients. In this case the value of the coefficient, b_2, was 0.22, 0.17 and 0.19 for the impermeable core, permeable core and homogeneous structure, respectively. An average value of $b_2 = 0.2$ can be chosen. This changes Equation 3.5 into:

$$H_s/\Delta D_{n50} * \sqrt{\xi_m} = a_3 \ (S/\sqrt{N})^{0.2} \qquad \text{with} \qquad a_3 = f(P) \qquad (3.6)$$

The coefficient, a_3, is only dependent on the permeability of the structure. The following formulae were derived for the three structures tested:

impermeable core: $\qquad H_s/\Delta D_{n50} * \sqrt{\xi_m} = 4.1 \ (S/\sqrt{N})^{0.2} \qquad\qquad (3.7)$

permeable core: $\qquad H_s/\Delta D_{n50} * \sqrt{\xi_m} = 5.3 \ (S/\sqrt{N})^{0.2} \qquad\qquad (3.8)$

homogeneous structure: $H_s/\Delta D_{n50} * \sqrt{\xi_m} = 5.7 \ (S/\sqrt{N})^{0.2}$ (3.9)

Formulae 3.7 - 3.9 can be combined into one formula when the permeability coefficient, P, is introduced.

3.4.4 Surging waves

A similar procedure can be followed for surging waves, although the breaker parameter does not cover the influence of the slope angle. The influence of the wave steepness can again be described by:

$H_s/\Delta D_{n50} = a_1 \ \xi_m^{b1}$ with $a_1 = f(S/\sqrt{N}, \ P, \ cot\alpha)$ (3.3)

For the three structures tested, impermeable core, permeable core and homogeneous structure, the value of the coefficient b_1, was 0.1, 0.5 and 0.6, respectively. The increasing value of b_1 shows the increasing influence of wave steepness with increasing permeability. This reflected in the steeper curves found on the $H_s/\Delta D_{n50}$ - ξ_m plot, see Figure 3.21. Equation 3.3 becomes:

$H_s/\Delta D_{n50} = a_4 \ \xi_m^{0.1}$ (3.10)

$H_s/\Delta D_{n50} = a_5 \ \xi_m^{0.5}$ (3.11)

$H_s/\Delta D_{n50} = a_6 \ \xi_m^{0.6}$ (3.12)

with a_4 to $a_6 = f(S/\sqrt{N}, \ P, \ cot\alpha)$

The influence of the slope angle can be described for the impermeable and permeable core only, as for the homogeneous structure only one slope angle was tested. The influence can be described by:

impermeable core: $H_s/\Delta D_{n50} = a_7 \ \xi_m^{0.1} \ cot\alpha^{b7}$ (3.13)

permeable core: $H_s/\Delta D_{n50} = a_8 \ \xi_m^{0.5} \ cot\alpha^{b8}$ (3.14)

where a_7, a_8 and b_7 and b_8 are regression coefficients. The coefficients b_7 and b_8 in Equations 3.13 and 3.14 were found to be 0.46 and 0.54, respectively. A round figure of 0.5 was selected for the present study which resulted in the parameter $\sqrt{cot\alpha}$. The influence of damage level and number of waves is the last variable to be taken into account:

impermeable core: $H_s/\Delta D_{n50} = a_9 \ (S/\sqrt{N})^{b9} \ \sqrt{cot\alpha} \ \xi_m^{0.1}$ (3.15)

permeable core:
$$H_s/\Delta D_{n50} = a_{10} \ (S/\sqrt{N})^{b10} \ \sqrt{\cot\alpha} \ \xi_m^{0.5} \tag{3.16}$$

homogeneous structure:
$$H_s/\Delta D_{n50} = a_{11} \ (S/\sqrt{N})^{b11} \ \sqrt{\cot\alpha} \ \xi_m^{0.6} \tag{3.17}$$

with a_9 to $a_{11} = f(P)$

The coefficients, $b_9 - b_{11}$ in Equations 3.15 - 3.17 were found to be 0.17, 0.19 and 0.25, respectively. A value of 0.2 was selected for the present study which brings all coefficients $b_9 - b_{11}$ together. The coefficients $a_9 - a_{11}$ in Equations 3.15 - 3.17 are only dependent on the permeability of the structure. The following formulae were derived for the three structures tested, by curve-fitting of the coefficients $a_9 - a_{11}$ in Equations 3.15 - 3.17 and using $b_9 = b_{10} = b_{11} = 0.2$:

impermeable core:
$$H_s/\Delta D_{n50} = 1.35 \ (S/\sqrt{N})^{0.2} \ \sqrt{\cot\alpha} \ \xi_m^{0.1} \tag{3.18}$$

permeable core:
$$H_s/\Delta D_{n50} = 1.07 \ (S/\sqrt{N})^{0.2} \ \sqrt{\cot\alpha} \ \xi_m^{0.5} \tag{3.19}$$

homogeneous structure:
$$H_s/\Delta D_{n50} = 1.10 \ (S/\sqrt{N})^{0.2} \ \sqrt{\cot\alpha} \ \xi_m^{0.6} \tag{3.20}$$

3.4.5 Introduction of the permeability coefficient, P

A permeability coefficient, P, was introduced into the stability formulae to take into account the permeability of the structure. This permeability coefficient has no physical meaning, but was introduced to ensure that permeability is taken into account. In Equations 3.18 - 3.20 the power coefficient of ξ_m has a value, dependent on the permeability of the structure, of 0.1, 0.5 and 0.6 respectively. Therefore, P is defined by P = 0.1 for the impermeable core, 0.5 for the permeable core, and 0.6 for the homogeneous structure. Now the coefficients 0.1, 0.5 and 0.6 in Equations 3.18 - 3.20 can be replaced by this P.

Four structures are shown in Figure 3.25 for which three P values, 0.1, 0.5 and 0.6. The other structure has an assumed value of 0.4. In the absence of other information the selection of the P-value is left to the engineers judgement. Further research is in progress and can probably provide a more physical definition of P, as P can then be calculated for each particular structure. First results of this further research will be described in Section 3.5.3.
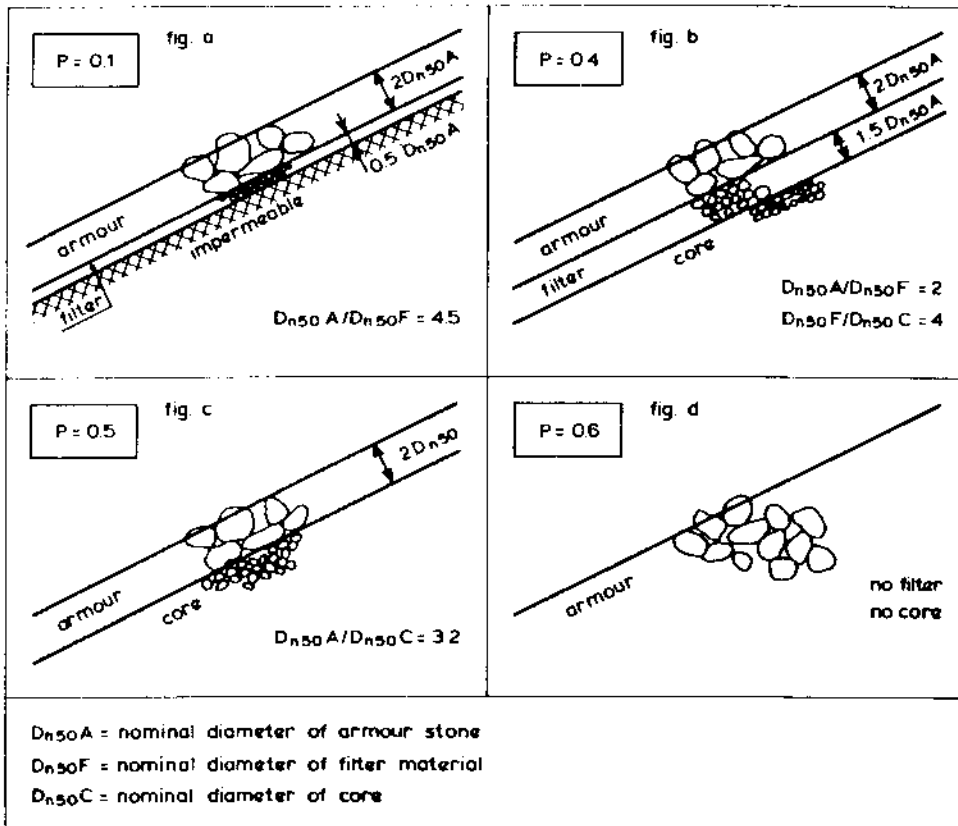
Figure 3.25 Permeability coefficient assumptions for various structures.

3.4.6 Final formulae

The coefficients a_3, 4.1, 5.3 and 5.7 in Formulae 3.7 - 3.9 and a_9 - a_{11}, 1.35, 1.07 and 1.10 in Formulae 3.18 - 3.20 can now be described as a function of the permeability coefficient, P. It must be remembered that the impermeable structure and the homogeneous structure are in fact lower and upper boundaries of permeability. The permeable core is a structure laying between the boundaries. The permeability coefficient can be included in the formulae as follows:

$$H_s/\Delta D_{n50} * \sqrt{\xi_m} = a_{12}\ P^{b12}\ (S/\sqrt{N})^{0.2} \qquad \text{for plunging waves, and:} \qquad (3.21)$$

$$H_s/\Delta D_{n50} = a_{13}\ P^{b13}\ (S/\sqrt{N})^{0.2}\ \sqrt{\cot\alpha}\ \xi_m^P \qquad \text{for surging waves} \qquad (3.22)$$

Curve fitting of $a_{12}\ P^{b12}$ and $a_{13}\ P^{b13}$ in Equations 3.21 and 3.22 to the established P-values and the coefficients in Equations 3.7 - 3.9 and 3.18 - 3.20 gives the final formulae. In total 600 points were used for this curve fitting.

The final formulae are:

for plunging waves,

$$H_s/\Delta D_{n50} * \sqrt{\xi_m} = 6.2 \ P^{0.18} \ (S/\sqrt{N})^{0.2}$$

(3.23)

for surging waves,

$$H_s/\Delta D_{n50} = 1.0 \ P^{-0.13} \ (S/\sqrt{N})^{0.2} \ \sqrt{\cot\alpha} \ \xi_m^P$$

(3.24)

The coefficient -0.13 in Formula 3.24 suggests that stability will decrease with increasing permeability. This is in contrast to the results found in model tests. The influence of the permeability, in the surging waves region is, however, described by the factor $P^{-0.13} \ \xi_m^P$, a factor which increases in this region with increasing P.

Formulae 3.23 and 3.24 are shown in most figures of this Chapter. The formula for plunging waves is shown on the left side of the $H_s/\Delta D_{n50} - \xi_m$ plots and the formula for surging waves on the right side. Collapsing waves are present at the intersection of both curves. This intersection can be derived from Equations 3.23 and 3.24 and is given by:

$$\xi_m = (6.2 \ P^{0.31} \ \sqrt{\tan\alpha})^{1/(P + 0.5)}$$

(3.25)

Depending on slope angle and permeability the transition lays between $\xi_m = 2.5$ to 4.

The influence of a non-Rayleigh distribution of the wave heights, can be taken into account by using the ratio $H_{2\%}/H_s$. For a Rayleigh distribution this ratio becomes $H_{2\%}/H_s = 1.40$. The actual value of $H_{2\%}$ with a foreshore in front of the structure can be derived from the Shore Protection Manual (1984) or in a more sophisticated way from ENDEC calculations (DELFT HYDRAULICS - ENDEC (1986)), or can be measured in a physical model, or in prototype. The ratio 1.40 for a Rayleigh distribution can be multiplied with the coefficients 6.2 and 1.0 in Equations 3.23 and 3.24. Equations 3.23 and 3.24 become with $H_{2\%}$ instead of H_s in the $H_s/\Delta D_{n50}$ parameter:

for plunging waves,

$$H_{2\%}/\Delta D_{n50} * \sqrt{\xi_m} = 8.7 \ P^{0.18} \ (S/\sqrt{N})^{0.2}$$

(3.26)

for surging waves,

$$H_{2\%}/\Delta D_{n50} = 1.4 \ P^{-0.13} \ (S/\sqrt{N})^{0.2} \ \sqrt{\cot\alpha} \ \xi_m^P$$

(3.27)

The Shore Protection Manual (1984) introduced the H_{10}, being the characteristic wave height. H_{10} is defined as the average of the highest ten percent of the waves. For a Rayleigh distribution H_{10} is equal to $H_{4\%}$, $H_{4\%}$ being the 4% value of the wave height exceedance curve. In Section 3.3 the $H_{2\%}$ was used to describe the influence of a truncated wave height exceedance curve due to depth limitations. It was concluded there that a $H_{5\%}$ or $H_{1\%}$ would give similar results. It can be concluded therefore, that H_{10} can characterize this influence too in a proper way.

In a similar way as described above for the $H_{2\%}$, the H_{10} can be included in the stability formulae. For a Rayleigh distribution the ratio H_{10}/H_s becomes $H_{10}/H_s = 1.27$. Using this ratio in Equations 3.23 and 3.24 gives:

for plunging waves:

$$H_{10}/\Delta D_{n50} * \sqrt{\xi_z} = 7.9 \ P^{0.18} \ (S/\sqrt{N})^{0.2} \tag{3.28}$$

for surging waves:

$$H_{10}/\Delta D_{n50} = 1.3 \ P^{-0.13} \ (S/\sqrt{N})^{0.2} \ \sqrt{\cot\alpha} \ \xi_z^P \tag{3.29}$$

3.5 Comparison and validity of formulae and results

3.5.1 The Hudson formula

The Hudson formula, Equation 2.15, only considers the "no-damage" criterion. The Shore Protection Manual (1984 - Table 7-9), however, gives the influence of the damage level on the K_D factor. Using the data for rough quarry stone the Hudson formula can be transformed into an expression which takes into account the damage level. The data from SPM - Table 7-9 and for rough quarry stone are:

Damage in percent	$H/H_{D=0}$	corresponding S level
0 - 5	1.00	2
5 - 10	1.08	6
10 - 15	1.19	10
15 - 20	1.27	14
20 - 30	1.37	20
30 - 40	1.47	28
40 - 50	1.56	36

where $H_{D=0}$ is the no damage wave height. The no damage criterion S = 2 can be assumed to be equivalent to 2.5% damage (and therefore S = 4 to 5% damage

etc.) and these damage levels are given above. Using $H_{10} = 1.27 \; H_s$ the Hudson formula:

$$H_{10}/\Delta D_{n50} = (K_D \cot\alpha)^{1/3} \tag{3.30}$$

can be rewritten to:

$$H_s/\Delta D_{n50} = 0.79 \; (K_D \cot\alpha)^{1/3} \qquad \text{(no damage)} \tag{3.31}$$

Using the results of the SPM - Table 7-9 the damage level can be included:

$$H_s/\Delta D_{n50} = a_{14} \; (K_D \cot\alpha)^{1/3} \; S^{b_{14}} \tag{3.32}$$

Regression analysis gives:

$$H_s/\Delta D_{n50} = 0.70 \; (K_D \cot\alpha)^{1/3} \; S^{0.15} \tag{3.33}$$

Formula 3.33 can directly be compared with the model test results obtained in the present investigation. Figure 3.26 shows this comparison with $K_D = 2$ and $K_D = 4$. The area of interest for the designer is roughly given by onset of damage $S = 2$ and failure by $S = 15$. It is clear that although the Hudson formula with $K_D = 4$ is, in fact, a reasonable average of the test results, it can only be used to give a rough estimate for a particular case.

Only in a few cases the damage will be under estimated using $K_D = 2$. In a lot of cases the damage will be over estimated, resulting in a too large mass of the stone.

The accuracy of the Hudson formula can be described in more detail. Consider the data points in Figure 3.26 between $S = 2$ and $S = 15$. The total number of points in this area amounts to 375. Left from the $K_D = 2$ curve 54 points are present and left from the $K_D = 4$ curve 166 points. The latter is almost the half of the total number of points which means that the curve for $K_D = 4$ is about an average of all the points.

The coefficient $K_D^{1/3}$ in Equation 3.33 determines the curve in Figure 3.26. This coefficient can be considered as a stochastic variable in order to describe the accuracy of the Hudson formula with respect to the test results. An average value and a standard deviation can be established, if a normal distribution is obtained for the coefficient $K_D^{1/3}$. From analysis of the test results it followed that $K_D^{1/3} = 1.65$ (this means $K_D = 4.5$) is the average and $\sigma = 0.30$ is the standard deviation. This results in a variation coefficient of 18%.

Hudson formula $K_D = 4$

Hudson formula $K_D = 2$

$$H_s / \Delta D_{n50} \quad * \quad \cot \alpha^{-1/3}$$
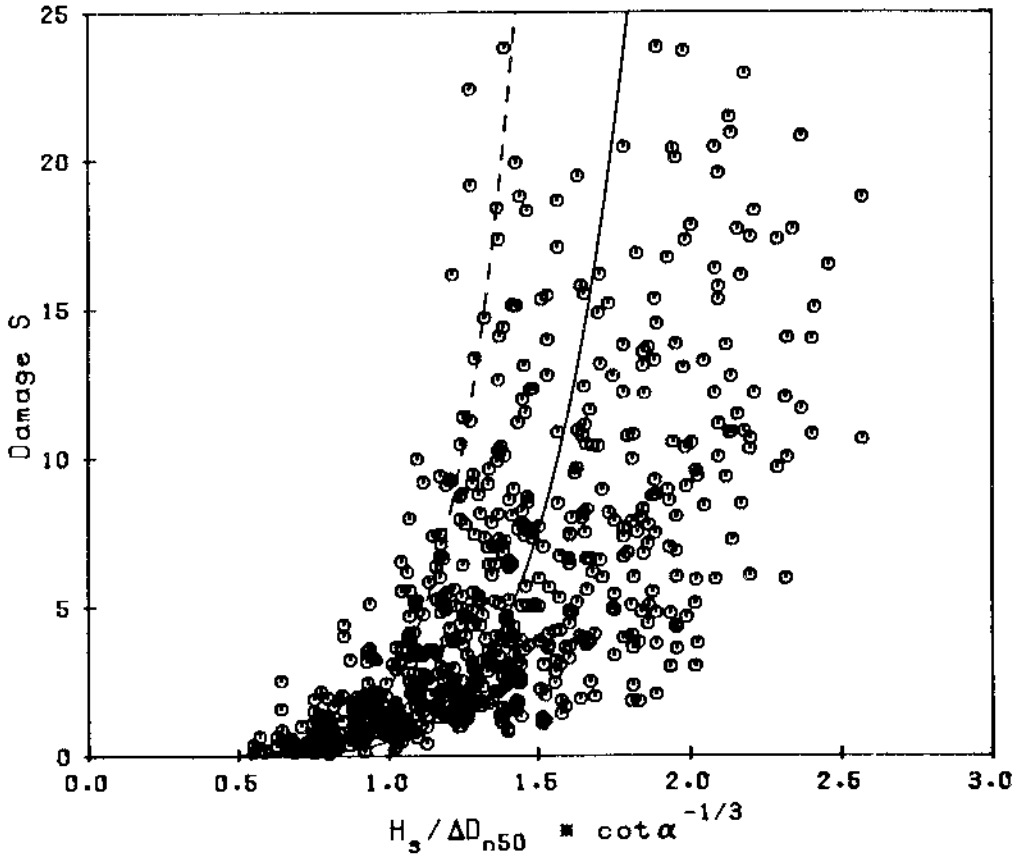
Figure 3.26 Comparison of the Hudson Formula with the test results.

3.5.2 Validity of new formulae

Formula 3.23 and 3.24 are shown on Figures 3.27 and 3.28 together with all the actual test results. On both figures the vertical axis is the parameter $S/\sqrt{N}$. A distinction is made between the data for an impermeable core, a permeable core, a homogeneous structure, and for the data of Thompson and Shuttler (1975). In total more than 650 data points have been plotted in the two figures.

The stability formulae 3.23 and 3.24 agree well with the test results and are a substantial improvement in comparison with the Hudson formula (compare Figure 3.26 with Figures 3.27 and 3.28). Still scatter is present in Figures 3.27 and 3.28. The scatter of the stability results can be due to:
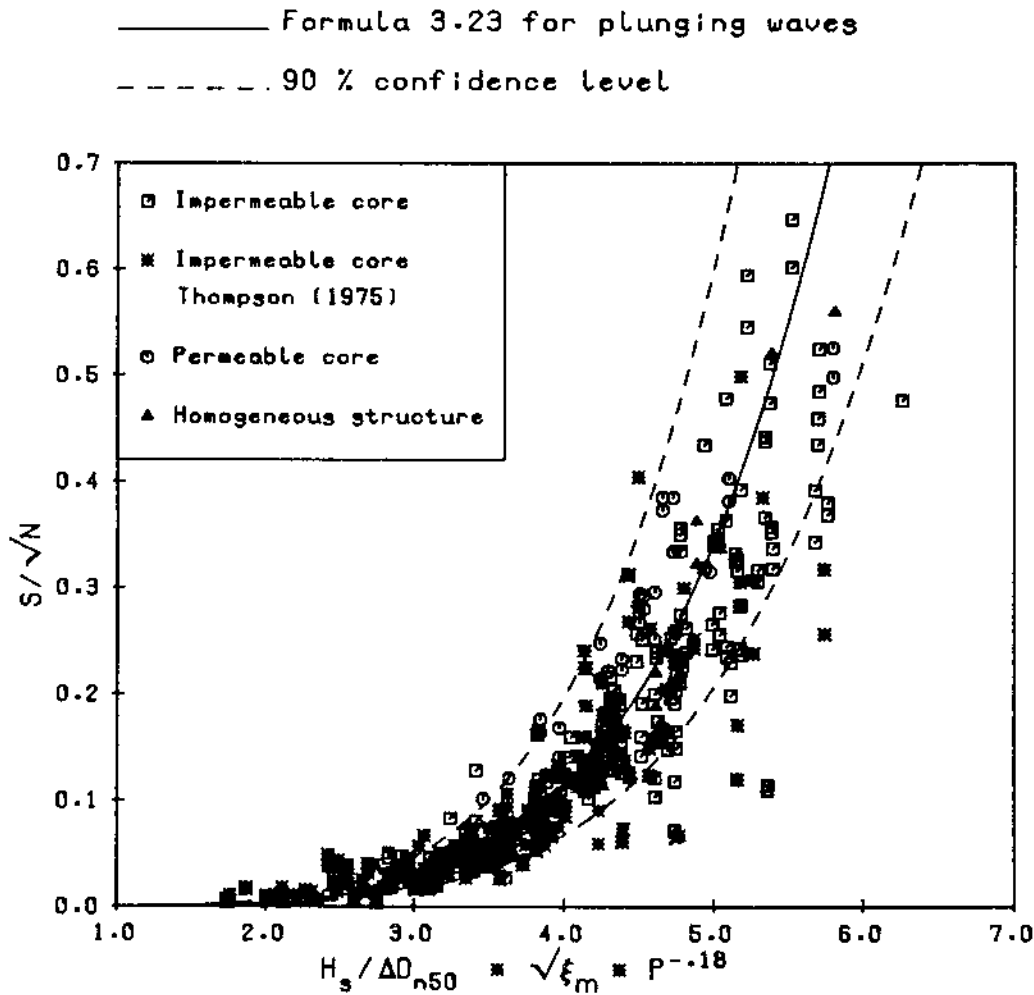
Figure 3.27 Stability Formula 3.23 for plunging waves with actual test results.

- differences due to random behaviour of rock slopes
- accuracy of measuring damage
- curve fitting

One test was repeated 4 times. These repeated tests are 98 and 105 to 107, see Appendix I. The damage S after 1000 and 3000 waves varied between 6.64 - 8.01 and 10.47 - 11.64 respectively, which gives a variation coefficient of about 5 - 10 %. Damage curves as shown in Figure 3.15 also give an impression of the scatter. Within 500 data points, for 15 cases it was found that a wave height gave more damage than a 10 - 20 % higher wave height, the other parameters being the same. In fact, Figure 3.15 shows one of these cases. Two tests in 250 gave a damage that was 70% higher than expected (tests 128 and 237, Appendix I). These tests were repeated and then gave the expected damage (tests 134 and 241).
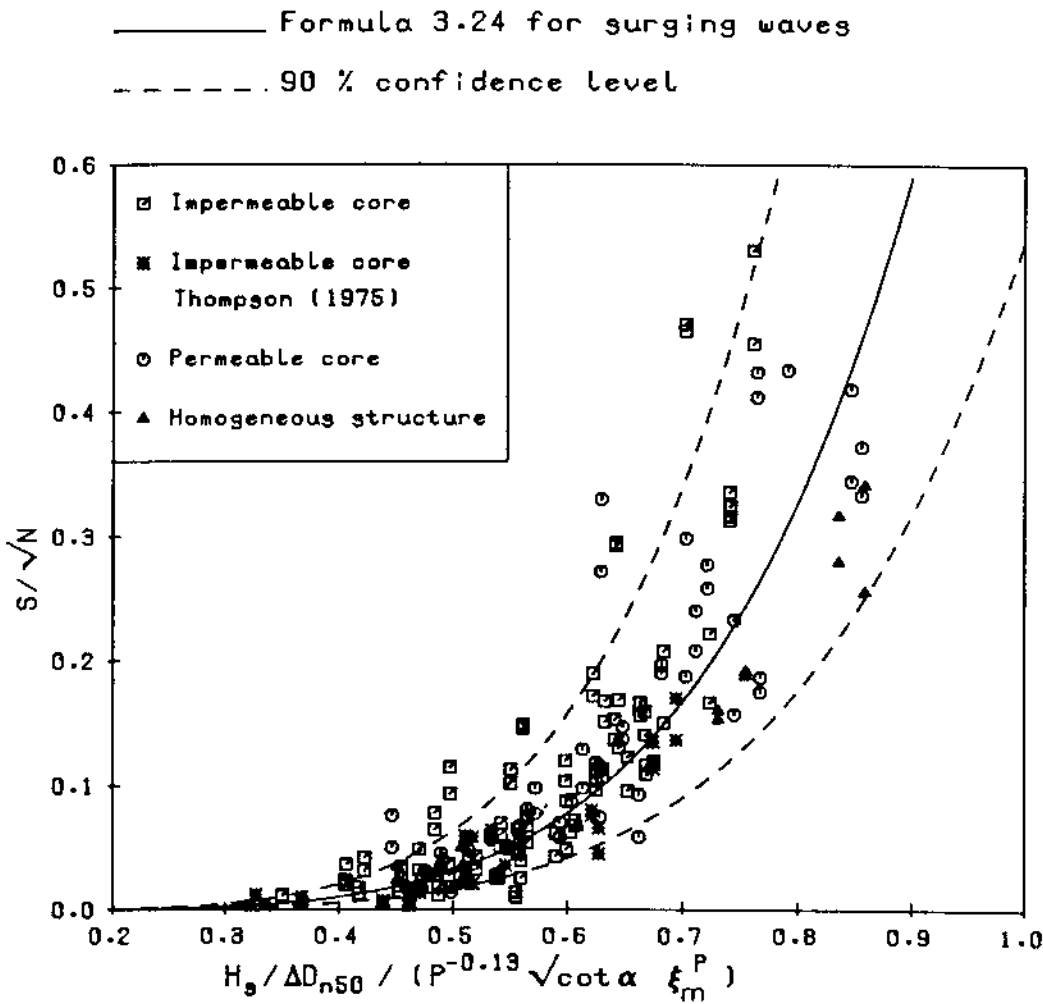
Figure 3.28 Stability Formula 3.24 for surging waves with actual test results.

Most of this scatter is due to the random behaviour of rock slopes which can also be found in nature. In fact, due to better controlled construction conditions in a laboratory flume than in nature, it might be expected that scatter in nature will be even larger.

Figures 3.27 and 3.28 give a picture of the scatter for the given stability formulae which include both the scatter to be expected in nature and the scatter due to curve fitting. This scatter can be taken into account in the stability formulae by considering the coefficients 6.2 in Equation 3.23 and 1.0 in Equation 3.24 as stochastic variables with the values as an average value. Assuming a normal distribution, the standard deviations can be established. From Figure 3.27 a standard deviation of $\sigma = 0.4$ can be established (6.5%). The standard deviation for the coefficient 1.0 in Formula 3.24 amounted to $\sigma = 0.08$ (8%). In both Figures 3.27 and 3.28 the two 90% confidence level are drawn. The variation coefficients of 6.5% and 8% can be related to that found

for the Hudson formula with $K_D^{1/3} = 1.65$. The variation coefficient for $K_D^{1/3}$ amounted to 18% which is about 2.5 times higher than found for Equation 3.23 and 3.24.

The derived standard deviations for the coefficients can be used to establish conservative assumptions for the mass required for stability. An other application is the use of it in so-called probabilistic designs (Nielsen and Burcharth (1983) and Van der Meer (1988)). The coefficients 6.2 and 1.0 in Equations 3.23 and 3.24 can be considered as stochastic variables with a normal distribution. This means that with probabilistic design the scatter due to random behaviour of rock slopes and the scatter due to curve fitting is taken into account.

3.5.3 Computation of permeability coefficient, P

The influence of the permeability of the structure on stability was discussed in Section 3.3.5 and values for the permeability coefficient P were introduced in Section 3.4.5, Figure 3.25. A first attempt will be made to give this permeability coefficient P a more physical description.

Barends (1985) described the computer model HADEER which was able to compute the flow pattern in a breakwater under wave attack. The model was improved by Hölscher and Barends (1986) and was calibrated on measurements performed in the large Delta flume. The boundary conditions for the tests with random waves in the Delta flume and the results will be described in the next Section.

During that investigation a few tests were performed with monochromatic waves in order to calibrate the HADEER model. Three tests were performed, all with a wave height of 1.0 m. The wave periods were 3.5, 4.5 and 7.0 s, respectively. The run-up and run-down were measured with a capacitance wire stretched along the slope and pore pressures were measured underneath the armour layer and in the core. The armour stones had a diameter of $D_{50} = 0.25$ m and the core stones had a diameter of $D_{50} = 0.08$ m. The slope was 1 : 3.

After calibration, the HADEER model was used to investigate the influence of permeability on the water motion in the core. The measured run-up and run-down was used as input for each computation. Computations were performed for the three monochromatic wave conditions and for various diameters of the core.

A core with D_{50} (core) = 0.25 m gives a homogeneous structure with P = 0.6 as the armour stones have the same diameter $D_{50} = 0.25$ m. This structure can be assumed as an upper boundary. An almost impermeable core is assumed with

core diameters of D_{50} (core) = 0.0125 m. All three wave conditions were compu-
ted with core diameters of D_{50} (core) = 0.25, 0.05 and 0.0125 m. Some wave
conditions were computed with D_{50} (core) = 0.10 and 0.025 m. The computations
resulted in flow velocities for each time step and each finite element.

These results were used to compute the volume of water, Q, that dissipates
into the core during each wave and per meter width. Figure 3.29 gives the com-
puted dissipation (volume of water that penetrates into the core) as a func-
tion of the wave period T (or surf similarity parameter ξ).
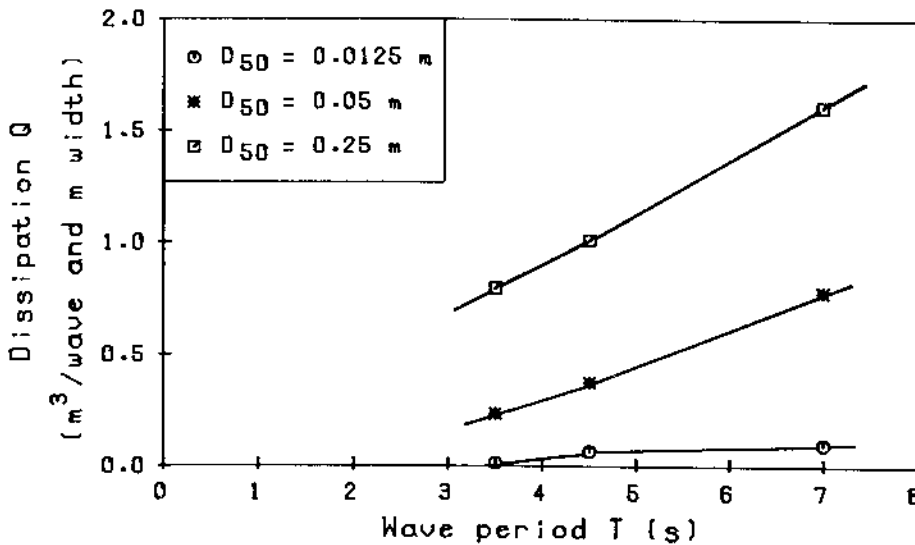
Figure 3.29 Dissipation of water into the core, Q, as a function of wave
period and core stone diameter.

From this Figure it follows indeed that a longer wave period and a higher
permeability of the structure (larger core stones) give much higher dissipa-
tion of water into the core.

Figure 3.30 shows the dissipating volume of water as a function of the dia-
meter of the core stones. The same conclusions can be drawn as for Figure
3.29, but now the values of the permeability coefficient P can be added to the
Figure for the three structures, investigated on stability. An impermeable
structure (P = 0.1) is found when the diameter of the core is zero or almost
zero. A homogeneous structure (P = 0.6) is found for a core stone diameter of
0.25 m. The permeable core (P = 0.5) in the small scale tests was defined by
D_{50} (armour)/D_{50} (core) = 3.2. For Figure 3.30 this results in a diameter of
the core of 0.08 m (diameter armour is 0.25 m).
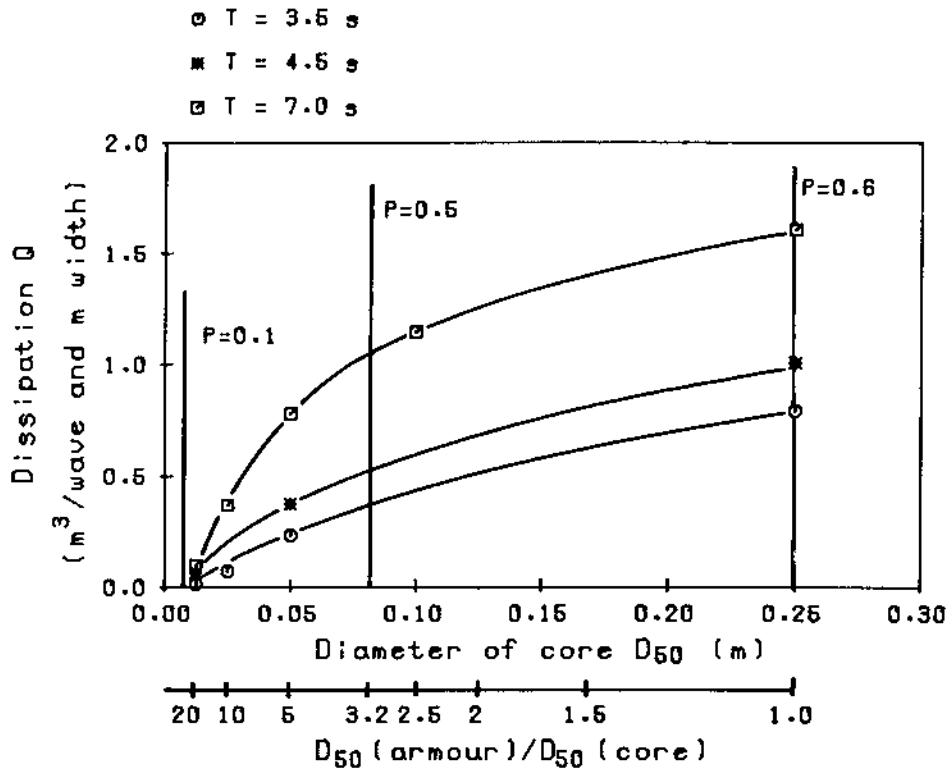
Figure 3.30 Dissipation of water into the core, Q, as a function of core stone diameter and wave period.

The maximum dissipation occurs for the homogeneous structure (P = 0.6). If the dissipation for other permeabilities is related to this maximum dissipation, a relative dissipation is defined. The relative dissipation for D_{50} (core) = 0.05 m and 0.0125 m can directly be computed from the results shown in Figure 3.30. The relative dissipation for D_{50} (core) = 0.08 m (and therefore for P = 0.5) is found by interpolation. The relative dissipation obtained from Figure 3.30 is given as a function of the permeability coefficient P in Figure 3.31.

A relative dissipation of 45% to 63% is obtained from Figure 3.30 for P = 0.5, depending on the wave period. Assuming a curve through the points for P = 0.1, 0.5 and 0.6 as shown in Figure 3.31, the permeability coefficient for a core with a diameter of 0.05 m (D_{50} (armour)/D_{50} (core) = 5) can be found. The computed relative dissipation was 29, 37 and 49%, depending on the wave period. This results in a permeability coefficient of about P = 0.43 - 0.44.

It can be concluded that the computer model HADEER can be used to make an assumption of the permeability coefficient P of a structure. In a particular case the volume of water that dissipates into the core should be computed for a homogeneous structure, for a structure with D_{50} (armour)/D_{50} (core) = 3.2

(i.e. P = 0.5) and for the particular structure. Computations should be done for various wave conditions. The results of the computations can be plotted in a similar way as in Figure 3.31 and the permeability coefficient for the particular structure can then be established.
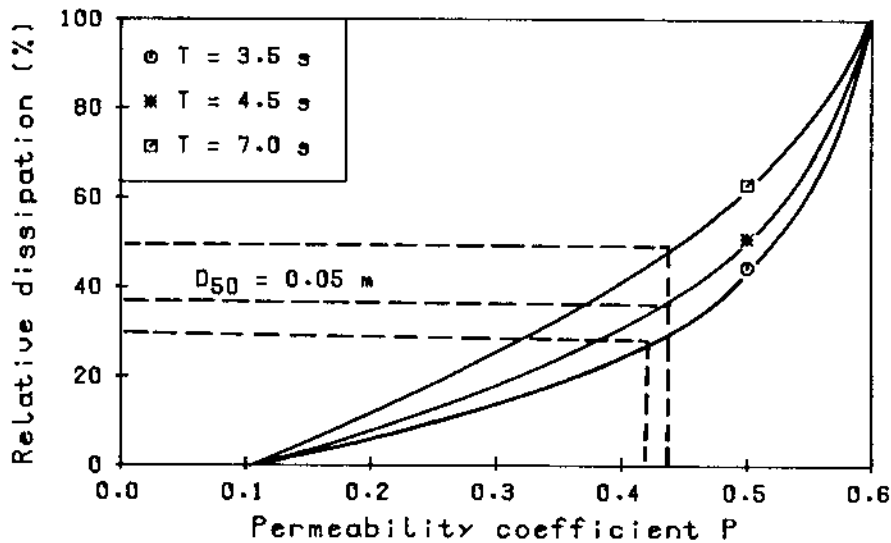
Figure 3.31 Relative dissipation into the core as a function of the permeability coefficient P.

3.6 Large scale tests

The influence of the Reynolds number on stability was discussed briefly in Section 2.4.3. It was stated that, according to various authors, no scale effects on armour stability will be present in small scale models if $Re > 10^4$ - 4.10^4. The range of Reynolds numbers of the small scale tests in the present investigation was about 4.10^4 - 8.10^4.

Some authors obtained higher boundaries for Re. Thomsen et al (1972) found no influence on stability for $Re > 2.10^5$. Shimada et al (1986) suggest a value of $Re > 4.10^5$. The results of Thomsen et al and Shimada et al were both obtained in large wave flumes with monochromatic wave attack.

In order to verify the validity of the small scale tests and the results obtained (stability formulae 3.23 and 3.24), large scale tests on stability were performed in the Delta flume. One test series with a permeable core (tests 211 - 216, Appendix I) and one with an impermeable core (tests 41 - 45) were repeated and scaled up according to Froude's law by a linear factor 6.25.

The stones used had an average mass of W_{50} = 26.5 kg, a nominal diameter of D_{n50} = 0.214 m, a mass density of 2700 kg/m^3 and a grading of D_{85}/D_{15} = 1.38.

Both a permeable and impermeable structure were tested on a slope angle with cotα = 3. The wave period was T_m = 4.4 s in all tests. In total six tests were performed on a permeable structure and five tests on an impermeable one.

All relevant parameters measured for each test are given in Appendix I. The large scale tests with a permeable core were numbered 930 - 935 and with an impermeable core 936 - 940. The Reynolds numbers varied from 5.10^5 - 7.10^5.

Results of small and large scale tests can directly be compared in a dimensionless damage curve, where $H_s/\Delta D_{n50}$ is plotted versus the damage S. Figure 3.32 gives the results of the tests with the permeable core and Figure 3.33 the results with the impermeable core. Besides the different data points of the small and large scale tests, stability formula 3.23 was plotted in the figures (the curved line).
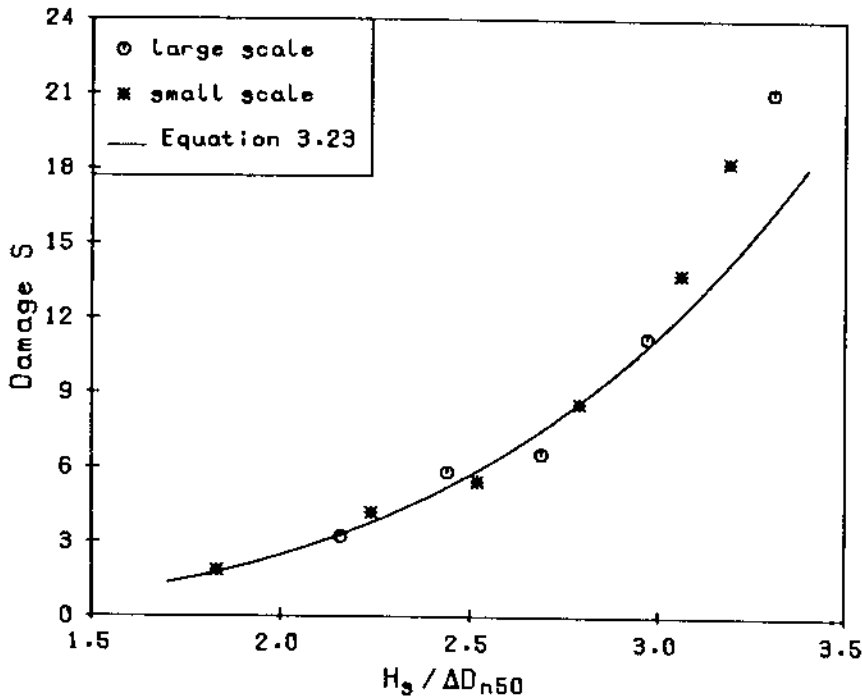
Figure 3.32 Comparison of small and large scale tests and stability formula for a permeable core.

From both Figures it can be concluded that the results of small and large scale tests are in close agreement. This confirms the validity of the stability formulae derived. The stability curve fits very well to the data, although some difference is found in Figure 3.32 for extreme damage levels, S > 12 (filter exposed). The final conclusion of the large scale tests can be stated as follows:
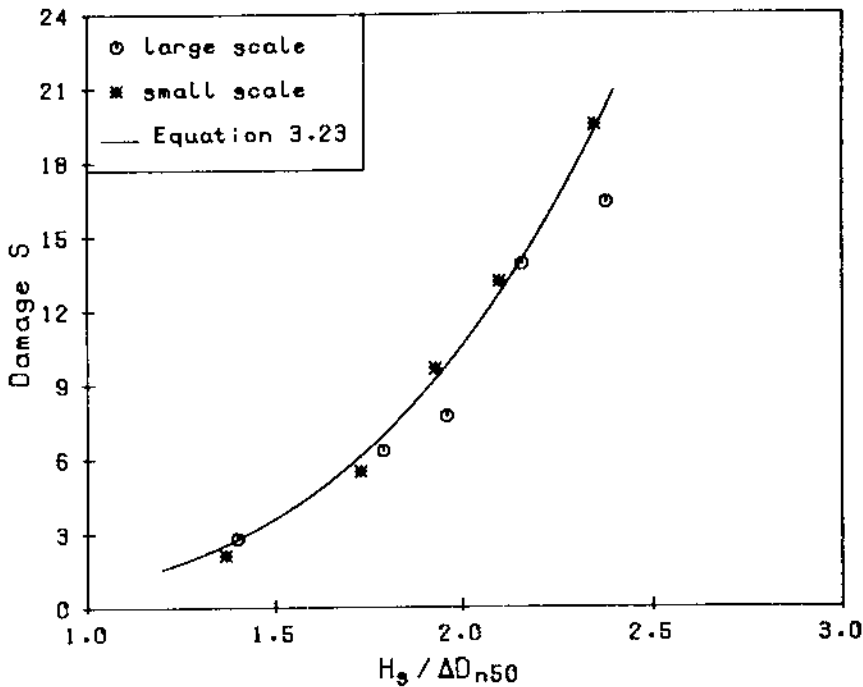
Figure 3.33 Comparison of small and large scale tests and stability formula for an impermeable core.

Large scale model tests confirmed the validity of the small scale tests. The stability of an armour layer of rock was not influenced by the Reynolds number when Re was between 4.10^4 and 7.10^5. As these figures gave the whole range of testing, the value of Re = 4.10^4 can only be regarded as an upper boundary for which scale effects on rock armour stability might start.

3.7 Low crested structure

Finally the influence of the crest height of the structure on stability will be described. Three crest heights were tested: R_c = 0.125 m above, at, and 0.10 m below SWL. The slope angle was given by $\cot\alpha$ = 2 and the structures were tested with a permeable core (P = 0.5). The damage curve was established for each structure and for two wave periods: T_m = 1.7 s and 2.2 s.

In total 31 tests were performed which were numbered 941 -971, Appendix I. The tests can directly be compared with the tests for a non-overtopped structure (tests 217 - 226, Appendix I). Non-dimensional damage curves ($H_s/\Delta D_{n50}$ versus S) are shown in Figure 3.34 for the wave period of 1.7 s.

Figure 3.34 shows that for R_c = 0.125 m the influence of the crest height on stability is small. The influence becomes substantial for R_c = 0 and is large for R_c = - 0.10 m. In fact, for R_c = - 0.10 m the $H_s/\Delta D_{n50}$ value is about a

factor 2 larger than for the non-overtopping structure, for the same damage level. This is a factor 8 in required mass for stability. It can be concluded therefore that the influence of the crest height of the structure on stability is large.
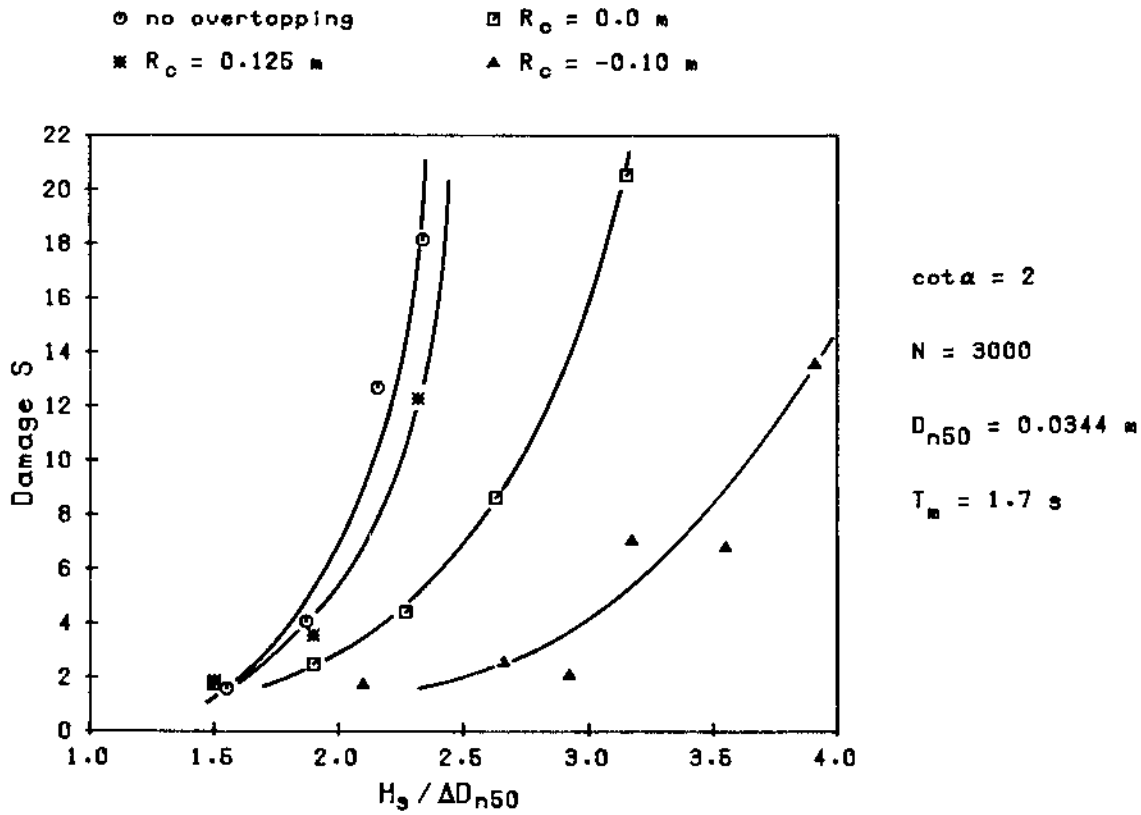
Figure 3.34 Influence of crest height on damage curves

The increase in stability can be related to the damage for a non-overtopped structure which can be calculated by Equations 3.23 and 3.24. If these Equations are used as a reference, the increase in $H_s/\Delta D_{n50}$ value for a lower crest height can be calculated, using the results of Figure 3.34. For this procedure fixed damage levels of S = 2, 3, 5, 8 and 12 were taken and the corresponding $H_s/\Delta D_{n50}$ values were established from the damage curves. With the given wave periods the corresponding ξ_m values were calculated. This procedure is according to that one described in more detail in Section 3.2. The $H_s/\Delta D_{n50}$ and ξ_m values for fixed damage levels are given in Appendix II, numbers 350 - 379.

The $H_s/\Delta D_{n50}$ values for the fixed damage levels were related to Equations 3.23 and 3.24. This ratio (called the increase in $H_s/\Delta D_{n50}$) is shown in Figure 3.35 for both wave periods and for N = 1000 and 3000, as a function of the crest height R_c/H_s.
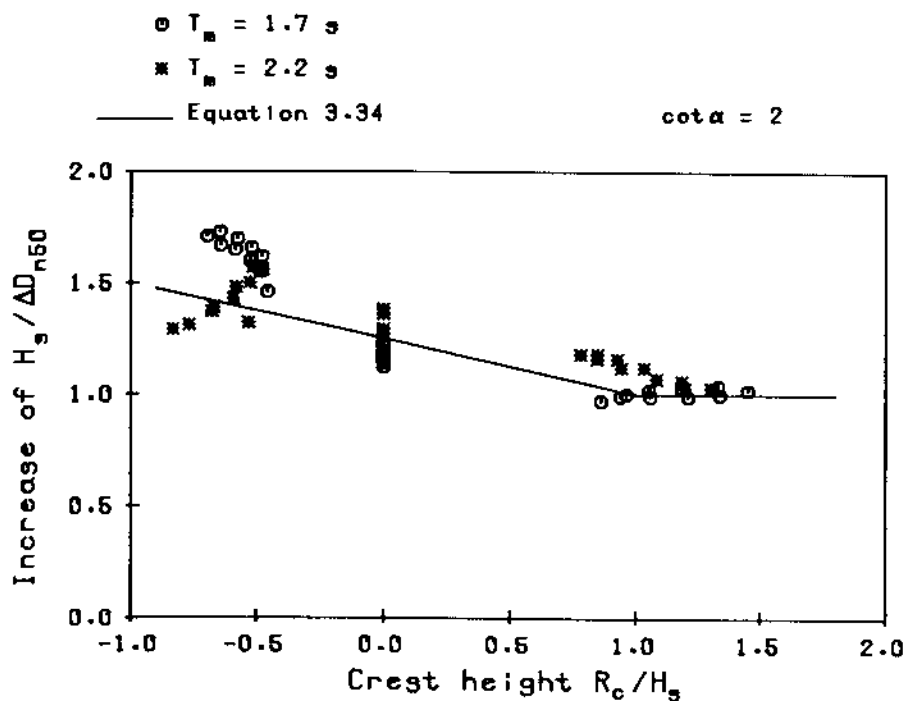
Figure 3.35 Increase in $H_s/\Delta D_{n50}$ as a function of crest height, R_c/H_s

An increase of a factor 1.0 means that the stability is the same as for a non-overtopped structure. From Figure 3.35 follows that a low crest height increases stability if $R_c/H_s < 1.0 - 1.2$. If $R_c/H_s = 1.0$ is taken as the transition where for lower values of R_c/H_s an increase in stability is gained, this increase can simply be described by a linear function, see Figure 3.35. This increase for R_c/H_s can be given by:

$$\text{Increase in } H_s/\Delta D_{n50} = 1.25 - 0.25 \ R_c/H_s \qquad \text{for } R_c/H_s < 1 \qquad (3.34)$$

Equation 3.34 was established for one slope angle (cotα = 2) and for only two wave periods. Therefore Equation 3.34 can only be used as a first estimate of the influence of a low crest on stability for extrapolation to other slope angles and wave periods or wave steepnesses. It should be remembered that only damage on the front slope is considered and not the damage on the crest and rear of the structure. The tests on this particular structure, however, showed no substancial damage on the rear.

4. Dynamic stability

4.1 Test set-up and program

Dynamic stability is characterized by the formation of a profile which can deviate substantially from the initial profile. All the changes of the slope have to be taken into account. Dynamic stability will occur if $H_s/\Delta D_{n50} > 6$. A transition area exists between static stability and dynamic stability which is given by $H_s/\Delta D_{n50}$ between 3 and 6.

Earlier work, by Van Hijum and Pilarczyk (1982), was briefly described in Section 2.2.2 (and Figure 2.3). Their model described the "equilibrium" profile which is formed after a fairly long storm duration. Consequently the effect of short storm durations which do not give the equilibrium profile were not taken into account.

The range for dynamic stability of rock slopes and gravel beaches can roughly be chosen between $H_s/\Delta D_{n50} = 6$ and 500, see Section 1.1. The tests of Van Hijum and Pilarczyk ranged between $H_s/\Delta D_{n50} = 13$ and 32. This means that their results do not cover the complete range for dynamic stability. Both the lower and the upper area were not investigated. Their work, however, is very useful and can be defined as the basis for the present research program on dynamic stability.

Tests were conducted in a small scale flume and in the large Delta flume. Both facilities have been described in Section 3.2. Also the surface profiler described in that section was used to measure the profile developed. The same test procedure was followed as for the tests on static stability. This means that each complete test consisted of a pre-test sounding, a test of 1000 waves, an inter-mediate sounding, a test of 2000 more waves, and a final sounding.

Crushed stone or shingle was used for the tests. The range of $H_s/\Delta D_{n50} = 3 - 13$ was investigated with nominal diameters $D_{n50} = 0.011$ m and 0.026 m. Normally, a grading was used with $D_{85}/D_{15} = 1.50$. Some tests were performed with gradings with $D_{85}/D_{15} = 1.25$ and with 2.25. The wave heights during these tests ranged from $H_s = 0.13$ to 0.26 m and the wave periods from $T_m = 1.3$ to 3.0 s.

The $H_s/\Delta D_{n50}$ values between 25 - 250 were investigated in the Delta flume. Gravel (shingle) was used with $D_{n50} = 0.019$ m and 0.004 m respectively. The gradings were described by $D_{85}/D_{15} = 1.64$ ($D_{n50} = 0.019$ m) and 1.85 ($D_{n50} = $

0.004 m). The wave heights ranged from H_s = 0.7 to 1.7 m and the wave periods from T_m = 2.6 to 5.9 s.

Test program

The present research on dynamic stability can be divided into four parts:

- $H_s/\Delta D_{n50}$ = 3 - 13. This range was investigated in the small scale flume. Most governing variables mentioned in Section 2.4.4 were investigated in this range.

- $H_s/\Delta D_{n50}$ = 13 - 32. This range was investigated by Van Hijum and Pilarczyk (1982). Tests were performed in the same small scale flume as for the present tests. The influence of oblique wave attack, however, was investigated in a wave basin.

- $H_s/\Delta D_{n50}$ = 7 - 21. In this range tests were performed with varying water levels and with storm surges.

- $H_s/\Delta D_{n50}$ = 25 - 250. Large scale tests in the Delta flume were performed on fine shingle. This range can only be investigated on a large scale since small scale investigations would give unacceptable diameters in the order of 1 mm and smaller, for which the fall velocity of the material is not scaled according to Froude's law.

All relevant boundary conditions for each test are given in Appendix III.

All tests of Van Hijum and Pilarczyk were performed with shingle. The lower area with $H_s/\Delta D_{n50}$ = 7 - 13, not covered by van Hijum and Pilarczyk, was investigated first for the present research with shingle. Six tests were performed (tests 301 -306, Appendix III).

The influence of wave height, wave period, diameter and initial slope for $H_s/\Delta D_{n50}$ = 3 - 13 was studied in the basic tests 307 - 341. Tests were performed with crushed stone (rock) and not with the more rounded shingle. Two diameters of stone were used: D_{n50} = 0.026 m for $H_s/\Delta D_{n50}$ < 6 and D_{n50} = 0.011 m for $H_s/\Delta D_{n50}$ > 6. Two uniform initial slopes were investigated, 1 : 5 (according to Van Hijum and Pilarczyk) and 1 : 3.

Generally nine tests were performed for each diameter and each slope angle mentioned above. These nine test conditions can be described by a matrix of wave heights and periods. Three wave heights were performed, each with three different wave periods. Wave heights and periods were chosen in such a way that series of three tests were formed with only one variable.

Summarizing these basic tests, each initial slope (1 : 5 and 1 : 3) and each diameter (D_{n50} = 0.011 m and 0.026 m) was tested with:

H_s = 0.13 m and T_m = 1.3 s, T_m = 1.8 s, T_m = 2.5 s
H_s = 0.18 m and T_m = 1.8 s, T_m = 2.5 s, T_m = 3.0 s
H_s = 0.24 m and T_m = 1.8 s, T_m = 2.5 s, T_m = 3.0 s

In total 35 tests were performed on this aspect.

Further tests were performed to investigate the influence of other variables mentioned in Section 2.4.4. First tests were performed with a very narrow spectrum (tests 342 - 347). The spectrum was described in Section 2.3.3 and Figure 2.6.

The influence of the shape of the stone was investigated in tests 348 - 356. Tests were performed with nicely rounded gravel (shingle) and with flat and long rock. The ratio of maximum/minimum dimensions was measured of 200 stones and an exceedance curve was established for gravel (shingle), angular rock and flat/long rock. These curves are shown in Figure 4.1.
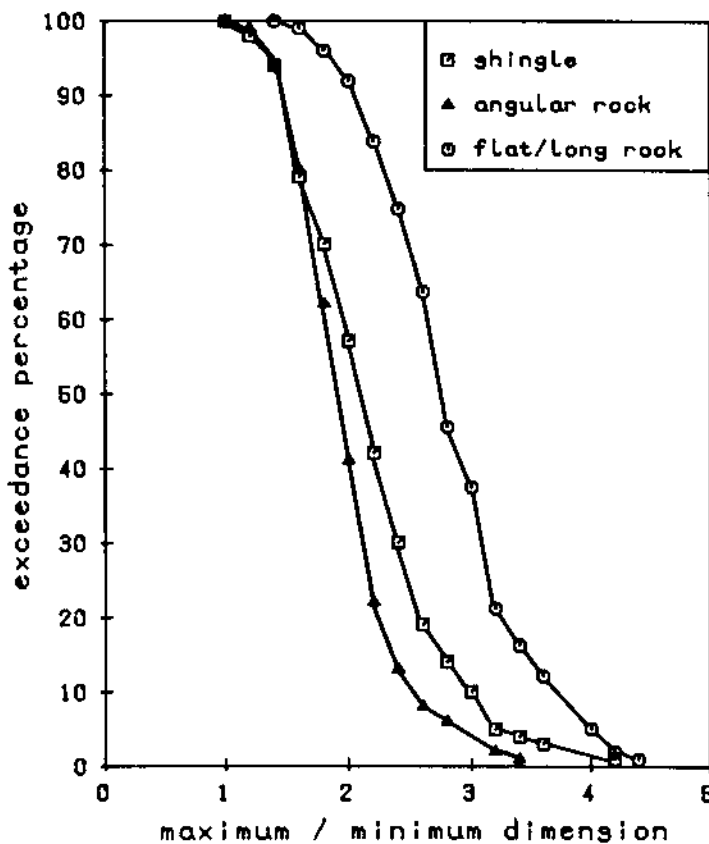
Figure 4.1 Shape of stone of shingle, angular rock and flat long rock

The concept of berm breakwaters was developed and applied by Baird and Hall (1984). The berm breakwater consists of a gentle slope above the still water level, a horizontal berm at and a rather steep slope below the water level (natural angle of repose). In total 16 tests were performed on berm breakwaters with the upper slopes of 1 : 3 and lower slopes of 1 : 1.5 (tests 380 - 395). The level of the horizontal berm was varied between 0.10 m above, on, and 0.10 m below the still water level.

In test 396 the technician who built all the models, was asked to build an arbitrary initial slope in the way he preferred. This slope was tested to verify the model, for dynamic stability.

The grading of the stone was varied in tests 397 - 408. A narrow grading with D_{85}/D_{15} = 1.25 and a wide grading with D_{85}/D_{15} = 2.25 were used.

The influence of a low crest was investigated in tests 409 - 415. The crest level was 0.05 m above the still water level. The crest width was 0.10 m (about 4 diameters) in the first part and 1.2 m in the second part of the series.

Finally a foreshore was constructed with a slope of 1 : 30. This foreshore was described in Section 3.3.7. The water depth at the toe of the structure ranged from 0.20 m to 0.40 m. Waves were breaking on this foreshore with the smallest water depths applied. The tests are described with numbers 416 - 421.

Van Hijum and Pilarczyk (1982) performed two-dimensional tests with random waves on gravel beaches. Four tests were performed with a 1 : 10 uniform slope and twenty eight tests with a 1 : 5 uniform slope. Generally a profile was measured after "equilibrium" was reached (about 2 hours of testing) and one or two intermediate soundings were taken after about 9 and 15 minutes from start of testing. Although these intermediate soundings were not reported in their work (only equilibrium profiles) the soundings were still available on magnetic tape.

Another part of the work of Van Hijum and Pilarczyk consisted of three-dimensional tests with oblique wave attack. Ten tests were performed on a 1 : 5 uniform slope.

All profiles of Van Hijum and Pilarczyk were re-analysed during the present research. Both the intermediate soundings and the final sounding (equilibrium) were used. The two-dimensional tests were numbered by test numbers 501 - 533 (Appendix III) and the three-dimensional tests by test numbers 551 - 560.

The influence of variation in water level and of storm surges on the profile was investigated during tests 360 - 377. The test procedure was different from the normal procedure (normal procedure was 1000 waves, intermediate sounding, 2000 more waves, final sounding). The tests can be divided into two types which are shown in Figure 4.2. The tests on varying water level are explained in the upper figure. The water level changed during five hours of testing, but the wave boundary conditions remained constant during the whole test. Profiles were taken after 1, 3 and 5 hours, indicated in the figure.
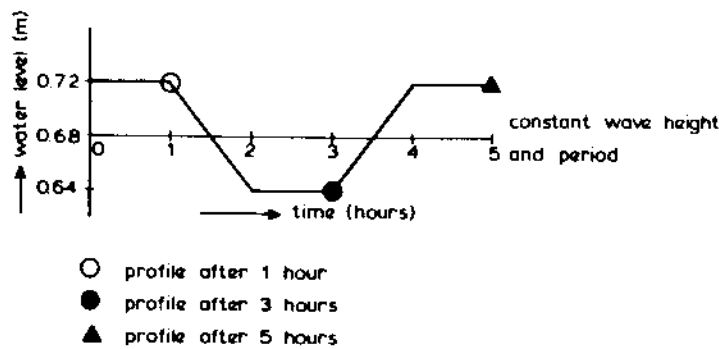
Test on varying water level
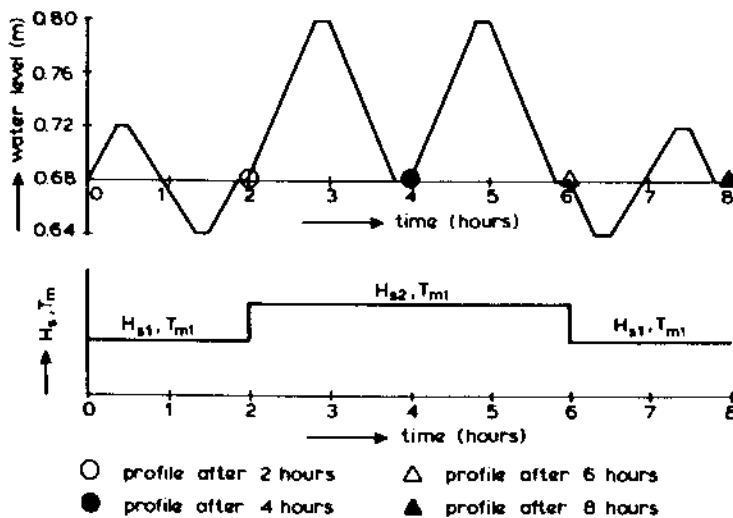
Test on storm surge

Figure 4.2 Boundary conditions for tests with varying water levels and storm surges

Tests were also performed with a storm surge as shown in the lower figure of Figure 4.2. Four tides with a (model) duration of 2 hours each were simulated. In fact, this implies that these tests were performed on a linear scale of 38, as a tide in prototype takes 12 hours and 20 minutes. The first and the fourth

tide were the same, with the same wave boundary conditions. The second and third tide simulated the peak of a storm with higher water levels and higher waves. Profiles were taken at the end of each tide (each two hours) as indicated in the figure.

The boundary conditions for each test and each tide are given in Appendix III, where the test numbers 360 - 377 are extended with one figure (1 to 4), indicating the part of the test where the waves were measured.

The present research was completed with tests in the large Delta flume. First two tests were performed in the same area as the tests of Van Hijum and Pilarczyk ($H_s/\Delta D_{n50}$ = 25 and 33), but on a larger scale (factor 4.6). These tests were performed on shingle with a nominal diameter of D_{n50} = 0.019 m. One test was added to this series with a higher wave height ($H_s/\Delta D_{n50}$ = 50). Finally 6 tests were performed on 4 mm shingle covering the area $H_s/\Delta D_{n50}$ = 90 - 250. All boundary conditions for the tests are given in Appendix III with test numbers 801 - 809.

Summarizing the test program, about 120 tests were performed on dynamic stability in the small scale flume (tests 301 - 421). The research of Van Hijum and Pilarczyk resulted in 42 tests (tests 501 - 560). Nine tests were performed in the Delta flume (tests 801 - 809).

4.2 Analysis of profiles

4.2.1 Governing variables

A final list of governing variables for dynamically stable rock slopes and gravel beaches was established in Section 2.4.4 together with the possible range of application. This list is given by:

variable	expression	range
The wave height parameter	$H_s/\Delta D_{n50}$	3 - 500
The wave period parameter (wave steepness)	s_m	0.01 - 0.06
The profile parameters	-	-
The number of waves	N	250 - 10,000
The initial slope	$\cot\alpha$ or arbitrary shape	-
The grading of the material	D_{85}/D_{15}	1 - 2.5
The shape of the stone	-	angular, rounded, flat
The spectral shape parameter	κ	0.3 - 0.9
The crest height	R_c/H_s	SWL - runup
The water depth in front of the structure	$h(x=toe,t)/H_s$	-
The angle of wave attack	ψ	$0° - 50°$

When this list is compared with the test program described in the previous section, it follows that all variables mentioned were investigated and mostly in the complete range indicated.

A first analysis was made by comparing profiles from those tests in which the same variable was changed. From this qualitative analysis conclusions can be derived on the influence of these variables on the profile. These conclusions can be used to develop a model for dynamic stability.

In fact, for each variable various sets of profiles are available for comparison. Analysis of these sets shows the trend for the variable to be described. In this thesis only one set is shown for each variable which characterizes the general trend found for all sets of comparable profiles. Most figures are compared by plotting the profiles at the same intersection with the still water level. This point is indicated by a dot in the figures. Only Figures 4.6, 4.15 and 4.16 were drawn at the original location. Some sets of profiles are shown in Figures 4.3 to 4.18.

4.2.2 Influence of wave height and period

Wave height

Figure 4.3 shows the profiles measured for three tests (tests 316, 318 and 321). The initial slope was a 1 : 5 uniform slope, the wave period was $T_m = 1.75$ s and the diameter was $D_{n50} = 0.011$ m for all tests. The significant wave heights were $H_s = 0,129$, 0.188 and 0.237 m respectively; the lowest wave height in fact produced the smallest changes in slope. From Figure 4.3 it can be concluded that the wave height has a large influence on the profile.

Wave period

Figure 4.4 shows the influence of the wave period (tests 315, 316 and 317). The initial slope was again a 1 : 5 uniform slope and the nominal diameter was $D_{n50} = 0.011$ m. The significant wave height for all three tests was $H_s = 0.13$ m. The wave periods were $T_m = 1.32$, 1.77 and 2.52 s; the shortest period in fact produced the smallest changes in slope. A similar conclusion can be drawn as for the wave height, namely that the wave period has a large influence on the profile. From Figures 4.3 and 4.4 it can be seen that the wave height and wave period have the same order of influence on the profile.
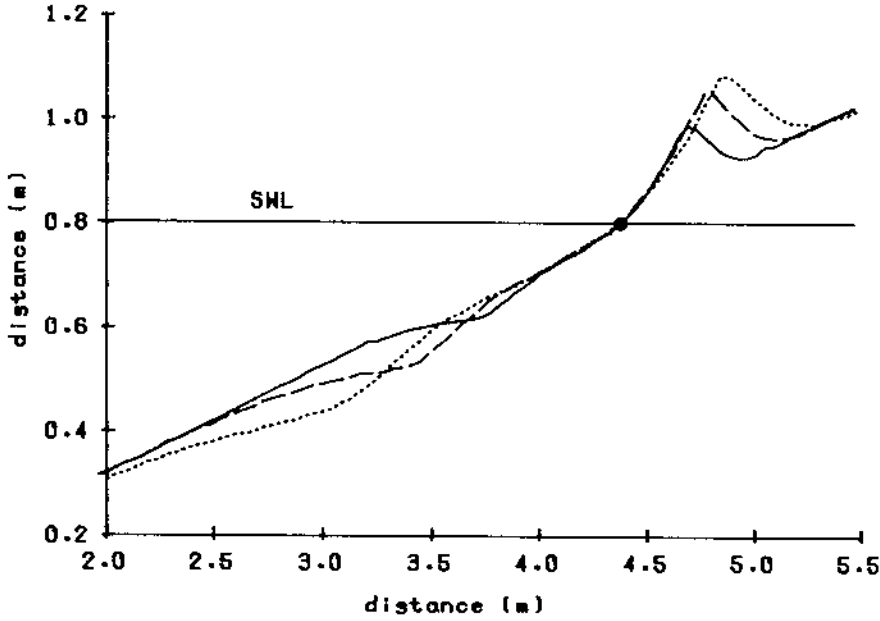
Figure 4.3   Influence of wave height
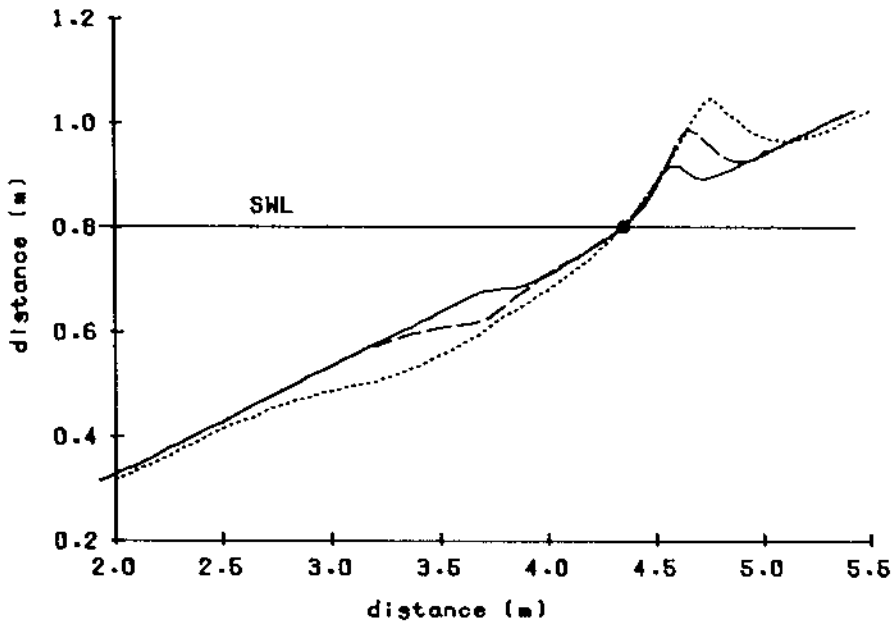
Figure 4.4   Influence of wave period

4.2.3 Influence of spectral shape and storm duration

Spectral shape

The tests 342 - 347 were performed with a very narrow spectrum (see Figure 2.6). The profiles of tests 331 (Pierson Moskowitz spectrum) and 347 are compared in Figure 4.5. From this figure it can be concluded that the influence of the spectral shape on the profile is very small.

A comparison was made by using the same average wave period, T_m. From Figure 4.4 it was concluded that a longer wave period results in a longer profile. If the same peak period was used for comparison, the PM spectrum would show a larger difference with the narrow spectrum. The narrow spectrum would remain the same as shown in Figure 4.5 as $T_p = T_m$ for this spectrum. The ratio T_p/T_m = 1.15 for the PM spectrum will result in a less high and less long profile than shown in Figure 4.5.
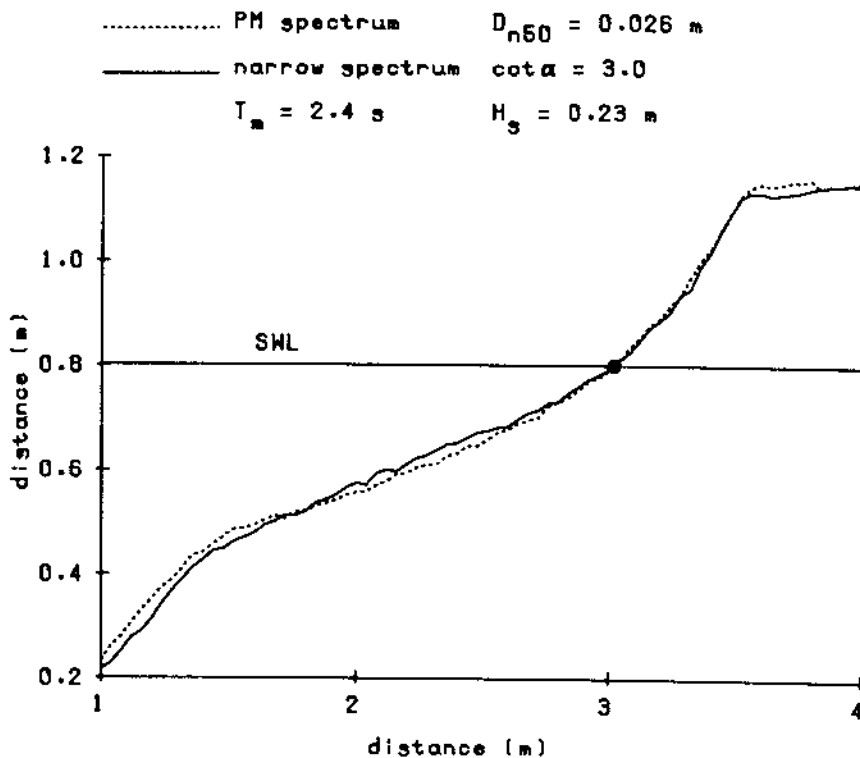
Figure 4.5 Influence of spectral shape

It can be concluded, therefore, that the spectral shape has no or only minor influence on the profile, provided that the average period is used to compare profiles. In that case random waves can be described by the significant wave height and average period only and the spectral shape parameter, κ, can be ignored.

Storm duration

Generally, profiles were measured after 1000 and 3000 waves. A small number of tests were performed with a longer storm duration and more intermediate soundings. The profiles of tests 407 and 504 are shown in Figure 4.6. Profiles for test 407 are given for 250, 500, 2000 and 5000 waves. In this case profiles were not plotted with the same intersection at the still water level, but at their original location. This was done as all profiles belong to the same test. Profiles for test 504 were established by Van Hijum and Pilarczyk (1982). Profiles are shown for 900, 8000, 17,000 and 26,000 waves.

From Figure 4.6 it can be concluded that a large part of the profile develops within the first few hundred waves. With a longer duration the crest moves up the slope and the profile becomes longer. Even after fairly long wave attack the crest still increases in height. The crest height is largely influenced by the storm duration.

4.2.4 Influence of diameter, stone shape and grading

Diameter

Figure 4.7 shows the influence of the diameter (tests 309, 318, 375 and 508). The initial slope was a 1 : 5 uniform slope, the wave height was $H_s = 0.18$ m and the wave period $T_m = 1.7$ s. The nominal diameters were $D_{n50} = 0.0257$, 0.011, 0.0062 and 0.0041 m, respectively. The largest diameters produced the smallest changes in the profile.

From Figure 4.7 it can be concluded that the nominal diameter has an influence on the profile. For small diameters ($D_{n50} = 0.0062$ and 0.0041 m), however, it can be concluded that some parts of the profile, for example the crest height, are not much affected by the diameter. The wave runup determines the crest height, more or less independent of the diameter of the material.

Stone shape

Nicely rounded gravel (shingle), angular rock and flat/long stones were used in different tests to investigate the influence of the shape of stone on the profile. Figure 4.8 shows the comparison of three profiles with different material shapes.
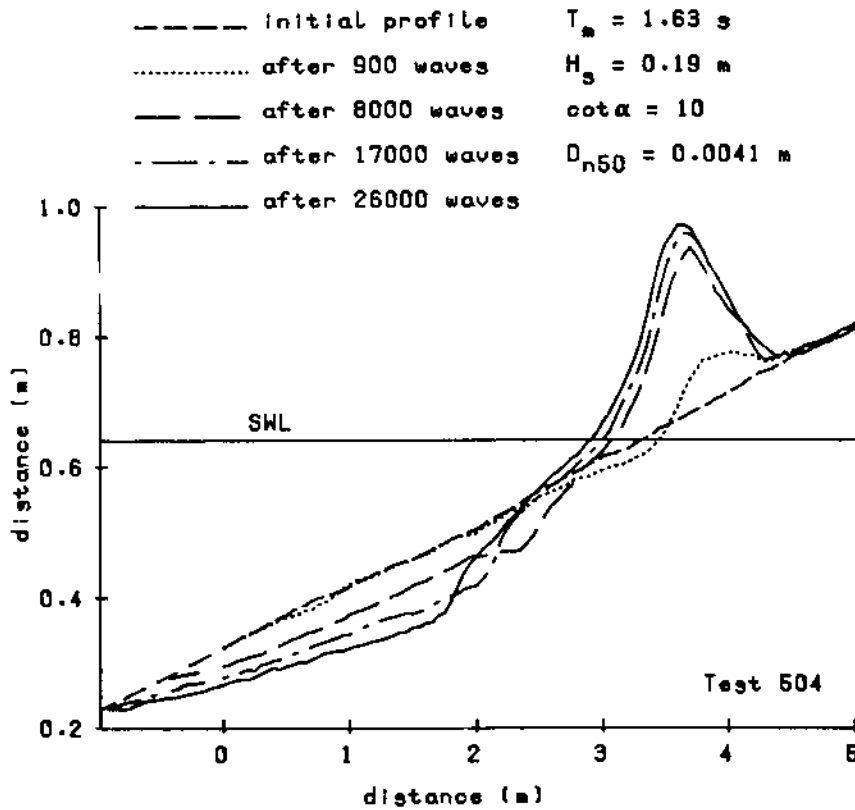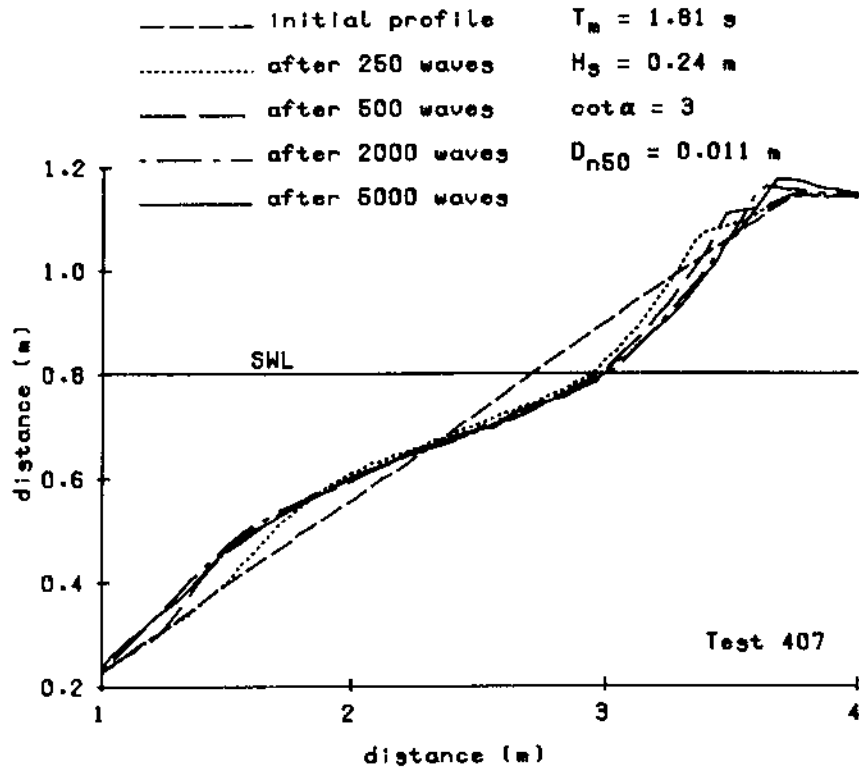
Figure 4.6 Influence of storm duration

```
------  D_n50 = 0.0041 m      cot α = 5.0
--- ---  D_n50 = 0.0062 m
.............  D_n50 = 0.0110 m      T_m = 1.75 s
---------  D_n50 = 0.0257 m      H_s = 0.18 m
```
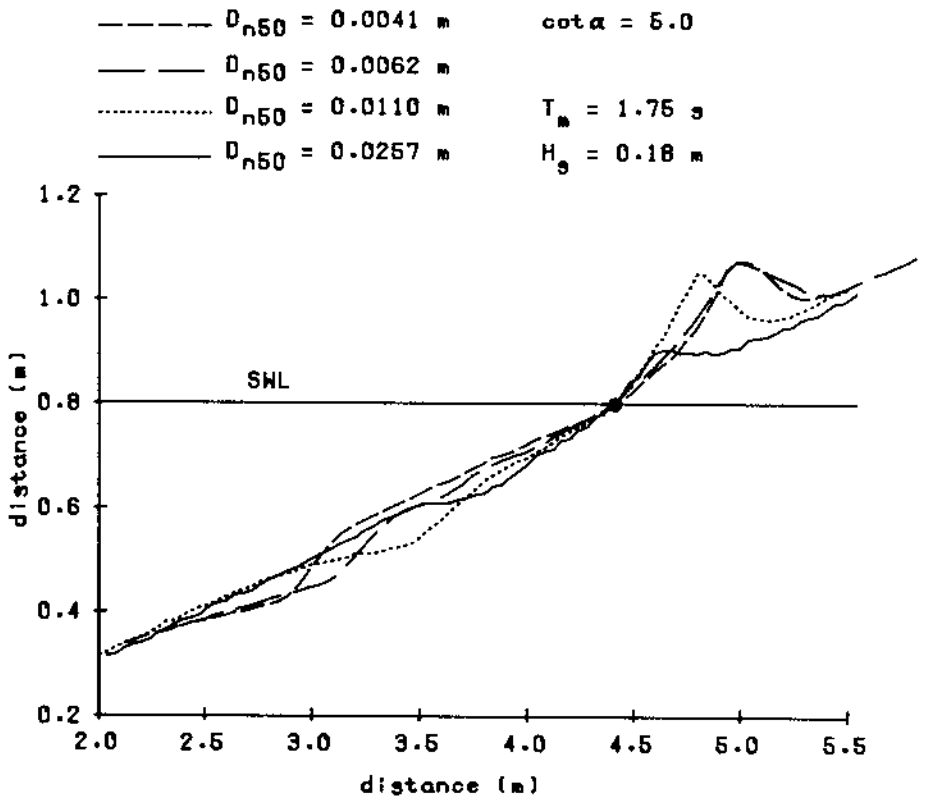

Figure 4.7 Influence of diameter

```
                          T_m = 1.8 s
.............  Angular rock     D_n50 = 0.026 m
--- ---  Shingle          cot α = 3.0
---------  Flat/long rock   H_s = 0.24 m
```
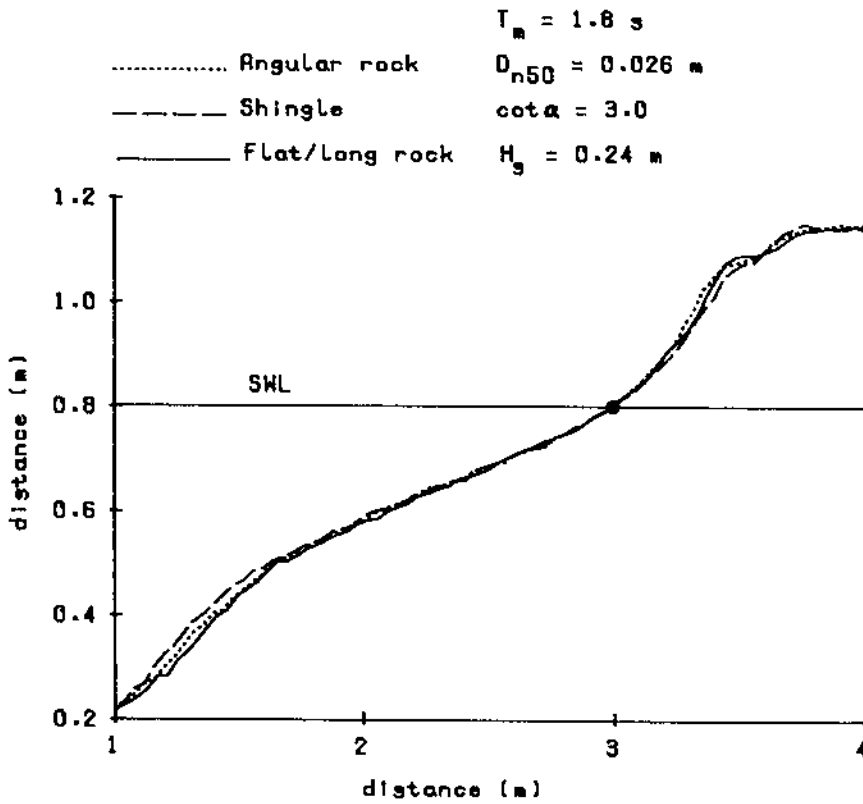

Figure 4.8 Influence of shape of stone

No difference is found between rock and flat/long stones. The rounded gravel has a tendency to form a lower crest height and a longer berm. The differences are small, however, and it can be concluded that the shape of stone has no or only minor influence on the profile.

Grading

Generally, a grading was used with D_{85}/D_{15} = 1.50. A narrow grading with D_{85}/D_{15} = 1.25 was used in tests 397 - 402 and a wide grading with D_{85}/D_{15} = 2.25 in tests 403 - 408. The profiles found for three different gradings are shown in Figure 4.9.
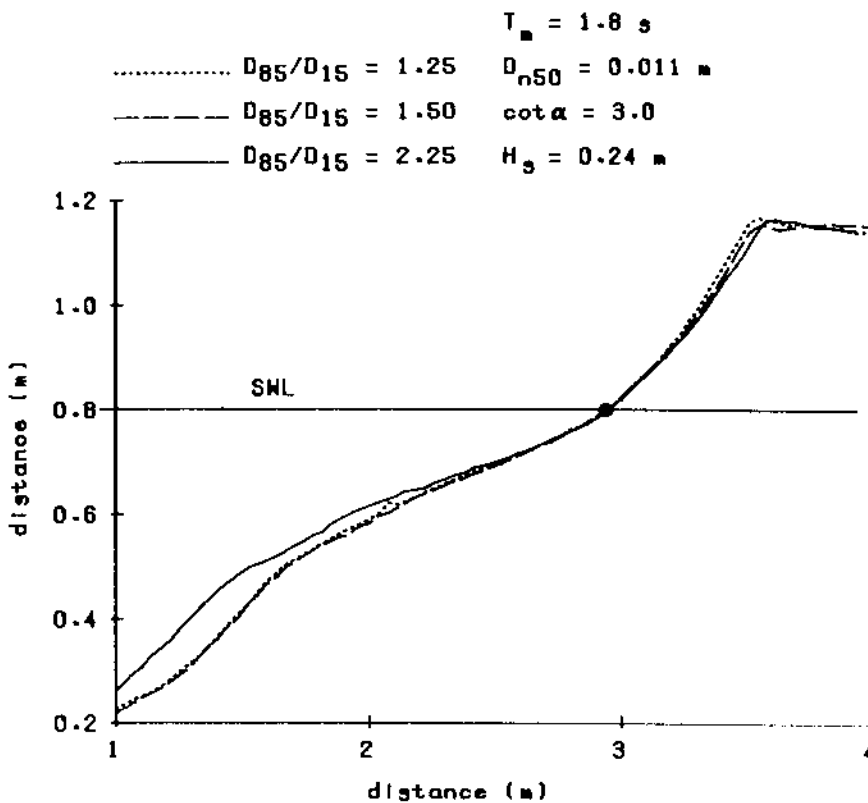
Figure 4.9 Influence of grading

From this figure it follows that the grading with D_{85}/D_{15} = 1.25 and 1.50 show almost no difference. The wide grading shows the same profile above the still water level, but has a little longer profile below this level. The influence of a wide grading on the profile below the still water level can not directly be ignored, therefore.

4.2.5 Influence of initial slope

In most tests the initial slope was a uniform slope of 1 : 3 or 1 : 5. In other tests a berm breakwater was tested with a 1 : 3 upper slope, a horizon-

tal berm above, at, or below the still water level, and a 1 : 1.5 slope for the lower part. Low crested structures were also tested. Figure 4.10 shows a comparison of two tests with the same boundary conditions, but with different initial slopes. These initial slopes were a 1 : 3 and a 1 : 5 uniform slope. Figure 4.11 shows the comparison of a 1 : 3 uniform slope and a berm profile. From these figures it can be concluded that in spite of the different initial slopes, the same profile is reached between the crest and the transition towards a steep slope (the step) at the deep water end of the profile.

Figure 4.12 shows the resultant profiles for a 1 : 5, a 1 : 3 and a 1 : 1.5 uniform initial slope. Only the upper and lower parts of the profile are in fact dependent on the initial slope (the dotted lines). The largest part of the profile (the solid line) is the same for all three initial slopes in this indicative figure. The direction of transport of material and the position of the profiles with regard to the initial slope is, of course, largely influenced by the initial slope. The 1 : 1.5 initial slope shows only erosion around the still water level, with material being transported downwards. For the 1 : 3 slope, however material is transported upwards and downwards. The 1 : 5 initial slope shows only erosion below the still water level and all the material is transported upwards.
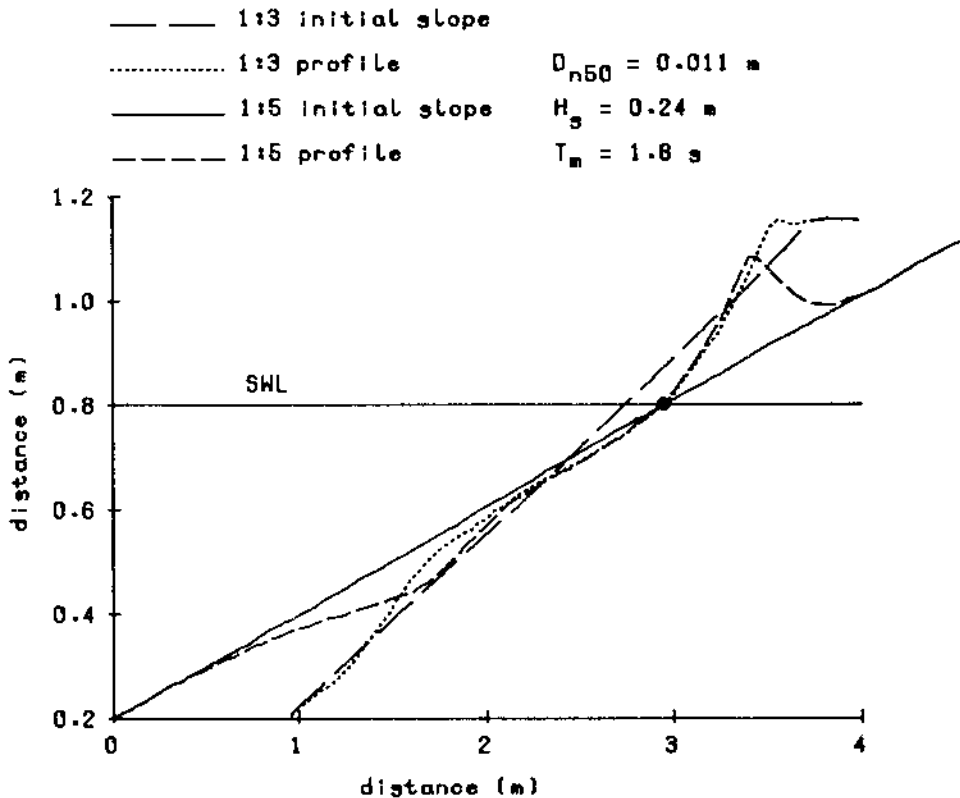
Figure 4.10 Influence of initial slope
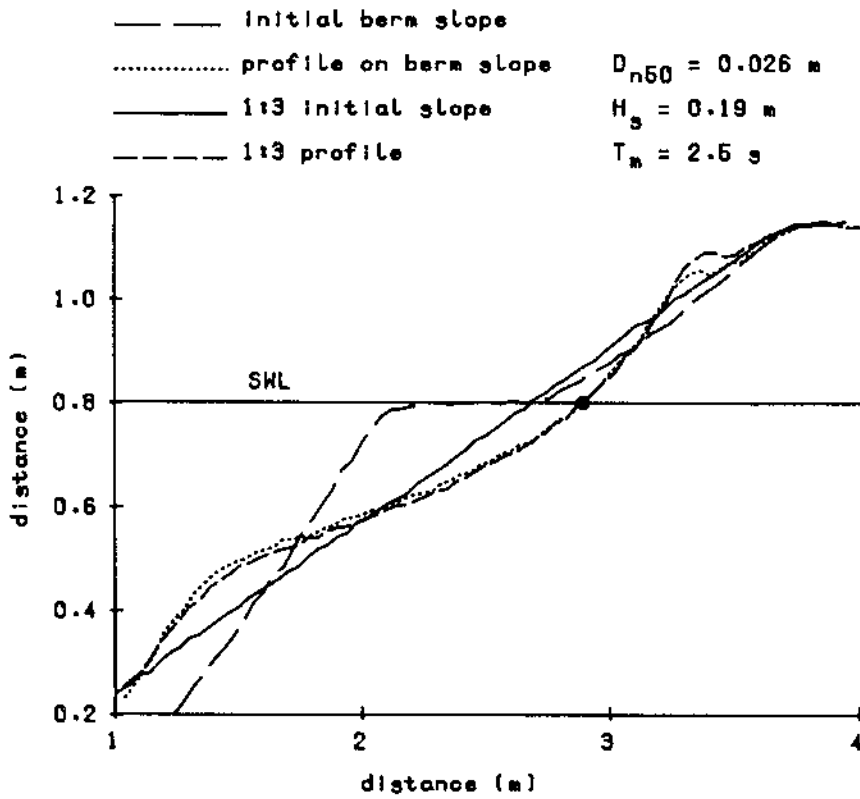
Figure 4.11 Influence of initial slope
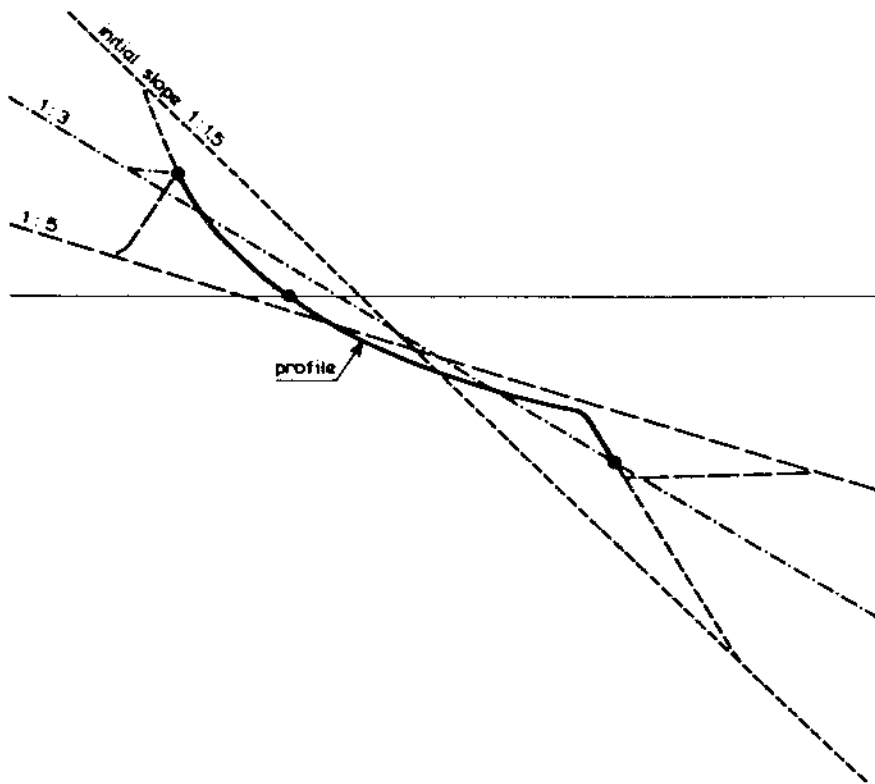
Figure 4.12 General influence of initial slope

4.2.6 Influence of crest height and water depth

Crest height

A low crest was investigated in tests 409 - 415. Tests 409 - 412 had a small crest width and the rear of the structure was attacked by overtopping waves. The crest disappeared below the still water level and the results can be compared with those of Ahrens (1984) and (1987).

Tests 413 - 415 were performed with a wider crest. Figure 4.13 shows the comparison of a test with a berm profile and a test with a low crest. A large part of the profile is the same, although the berm profile shows a higher crest and a longer berm. The wave height was also a little higher for the berm profile (0.18 against 0.19 m), however.
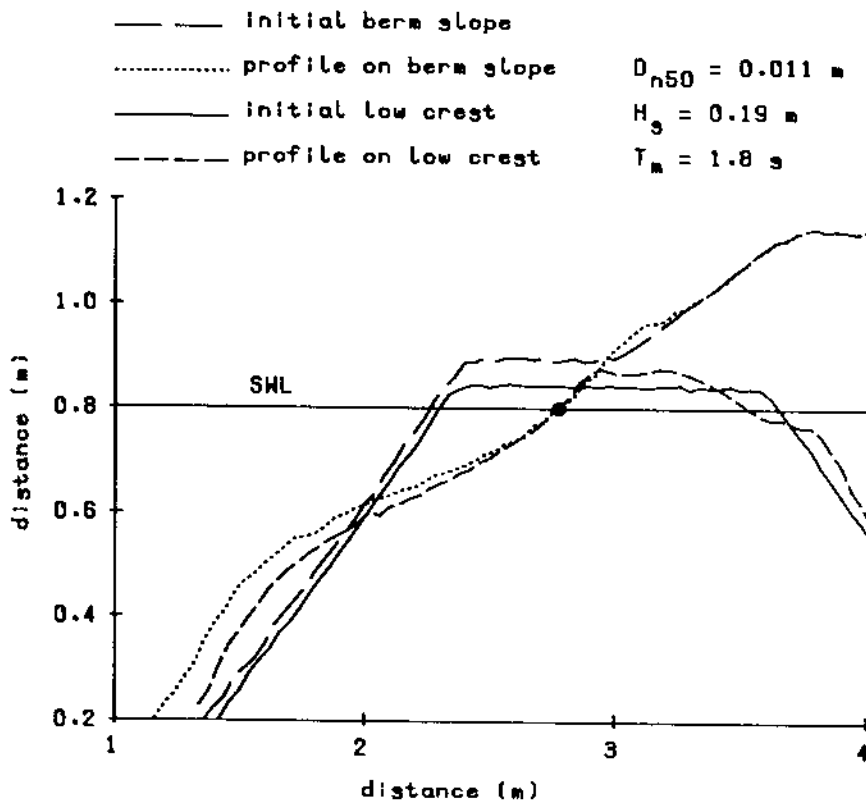
Figure 4.13 Influence of crest height

Still the same conclusion can be drawn as for the continuous initial slopes. The initial slope and the crest height have no or minor influence on the formation of a large part of the profile, provided that the crest is wide enough to avoid wave attack at the rear.

Water depth

A 1 : 30 uniform foreshore was applied in tests 416 - 421. The water depth in front of the structure ranged from 0.20 to 0.40 m, causing breaking waves on the foreshore for the smallest water depth due to depth limitations.

Figure 4.14 shows the comparison of a long 1 : 3 uniform slope with a short 1 : 3 uniform slope on a foreshore. A large part of the profile is the same. The length of the profile below the still water level decreases, however, when the length of the slope (or the water depth) is decreased. The effect of depth limited waves on the profile below the still water level can not be ignored.
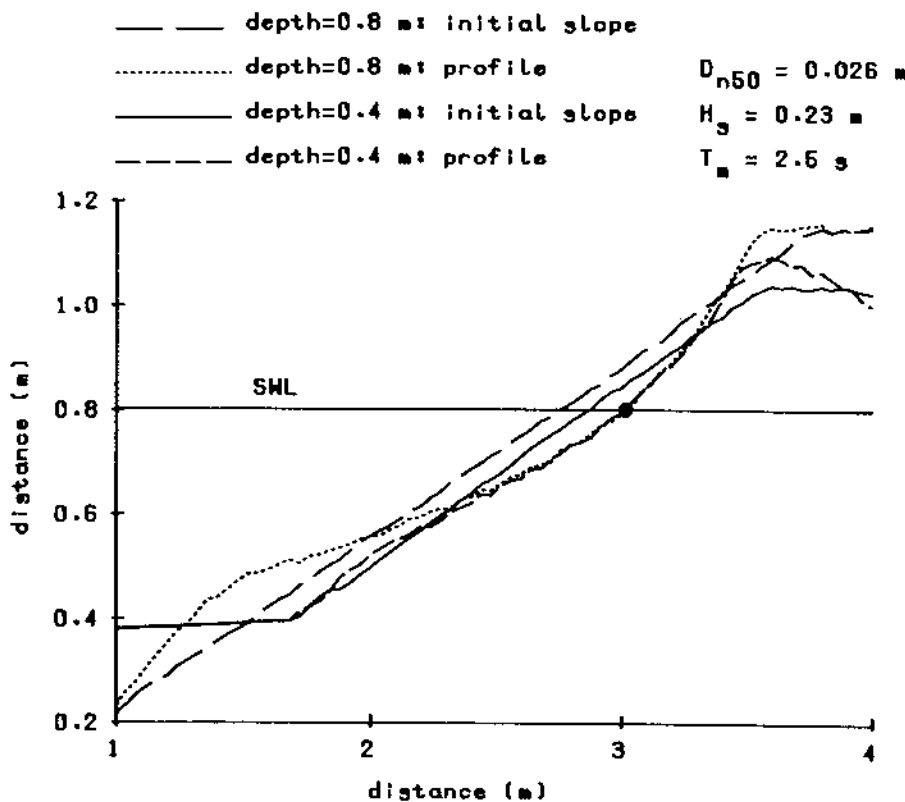
Figure 4.14 Influence of water depth

4.2.7 Influence of varying water level

The test procedure of the tests with varying water level and with a storm surge were described in Section 4.1 and Figure 4.2. The wave boundary conditions (wave height and period) remained constant during the test on varying water level, see the upper plot of Figure 4.2.

Figure 4.15 shows the profiles of one of these tests. Three profiles were measured during the test, two at high water and one at low water. The wave

height was $H_s = 0.13$ m and the period $T_m = 1.73$ s. The final profile in Figure 4.15, the second high water, is almost the same as the first, the first high water profile. In fact, the profile changed immediately with changing water level.
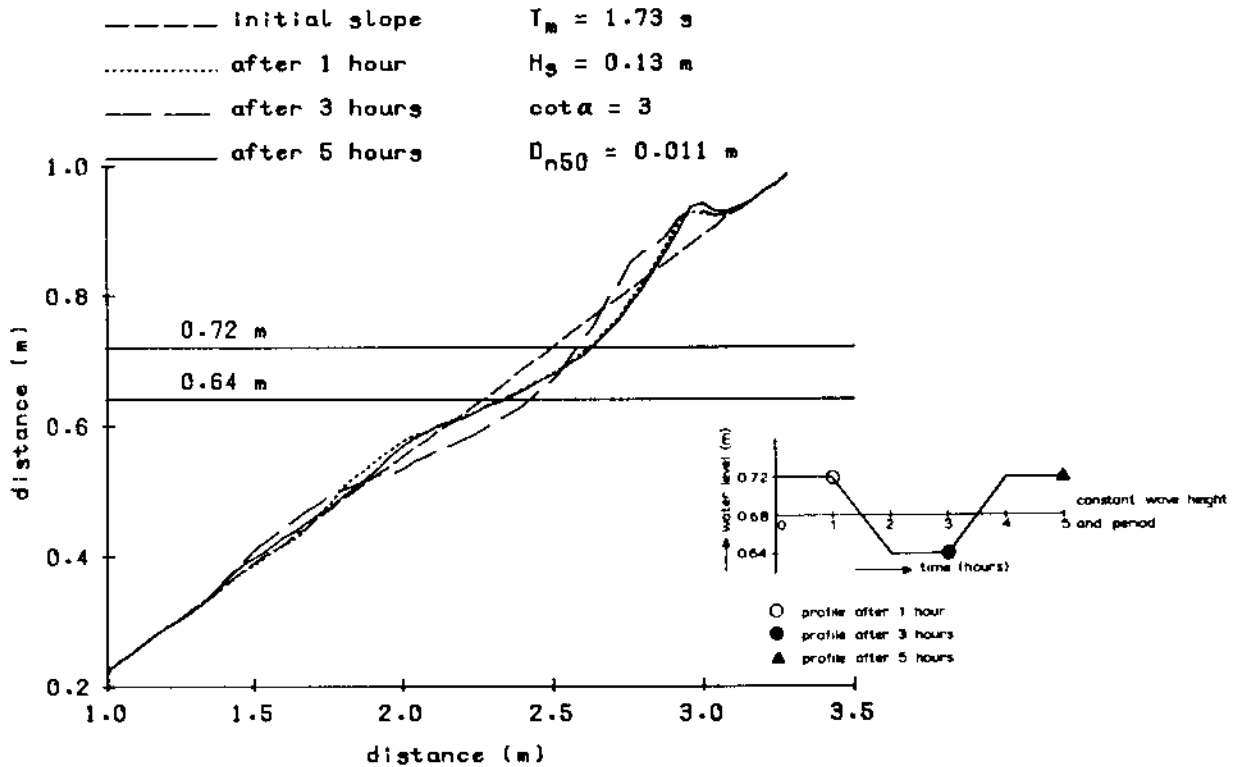
Figure 4.15 Influence of varying water level

The tests with a storm surge (lower plot of Figure 4.2) were conducted with four tides, a low one at the beginning and end of the test and two high tides in between. The wave boundary conditions were higher for the high tides than for the low tides. Profiles were measured after each tide (profiles after 2, 4, 6 and 8 hours).

Figures 4.16 and 4.17 show the results of one of the tests with storm surge. Figure 4.16 shows the profiles after the first three tides. It can be concluded from this Figure that the profile after the first tide disappeared completely during the second tide. The profile after the third tide is almost the same as after the second tide although the crest becomes a little higher.

Figure 4.17 shows the profiles after the first (low) tide and after the fourth (also low) tide. The profiles were drawn with the same intersection at the still water level. The same profile was formed for the same wave boundary conditions. It can be concluded that the profile is independent of the initial slope (a uniform slope or a formed profile) and that the profile goes up and down with the water level.
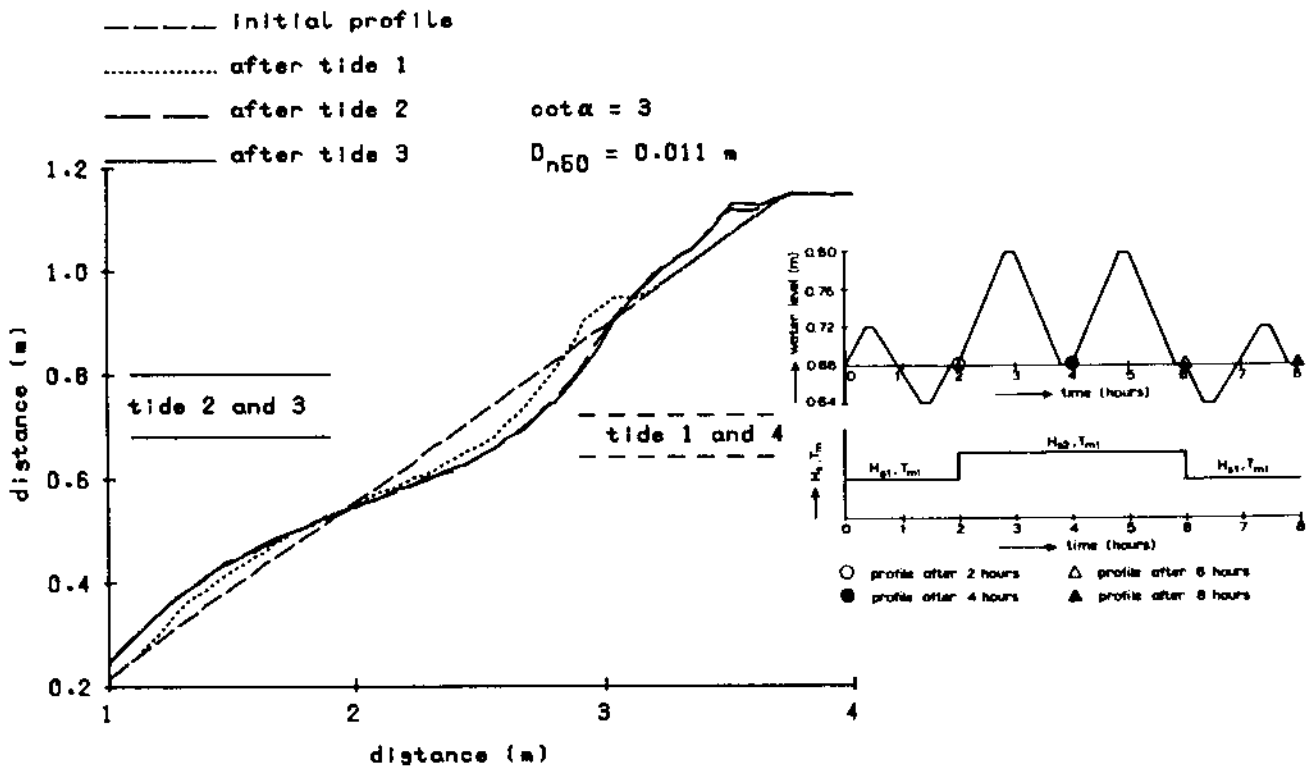
Figure 4.16 Influence of storm surge
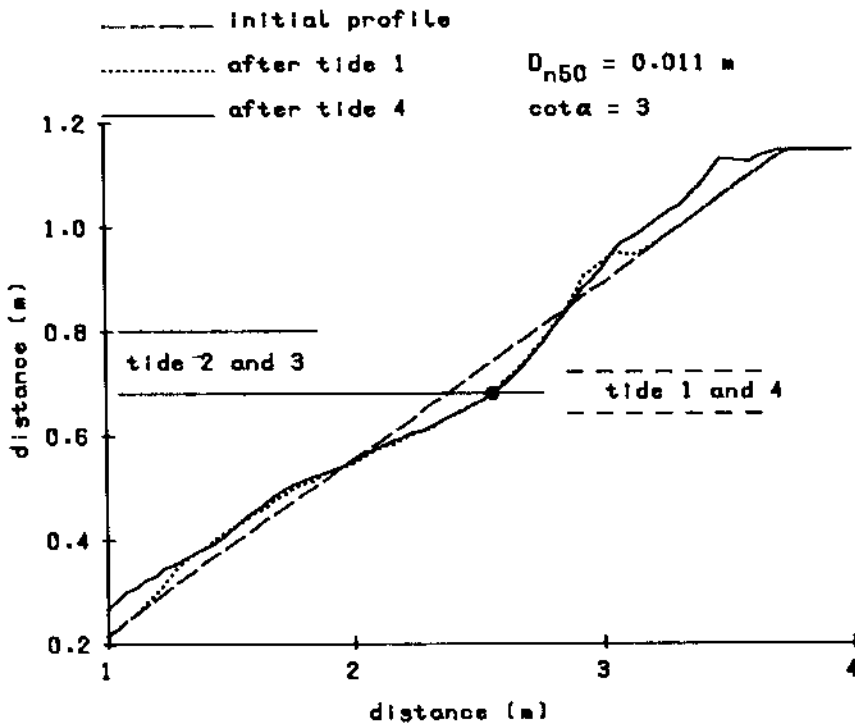
Figure 4.17 Influence of storm surge

4.2.8 Influence of angle of wave attack

The tests of Van Hijum and Pilarczyk (1982) included both perpendicular wave attack (tests 501 - 533, Appendix III) and oblique wave attack (tests 551 - 560, ψ = 30°). Two tests are compared in Figure 4.18. From this figure it can not be concluded that the profile becomes shorter with oblique wave attack. Van Hijum and Pilarczyk concluded that profile parameters should be reduced by $\sqrt{\cos\psi}$. The influence of angle of wave attack must be analyzed in more detail, however, when deriving functional relationships.
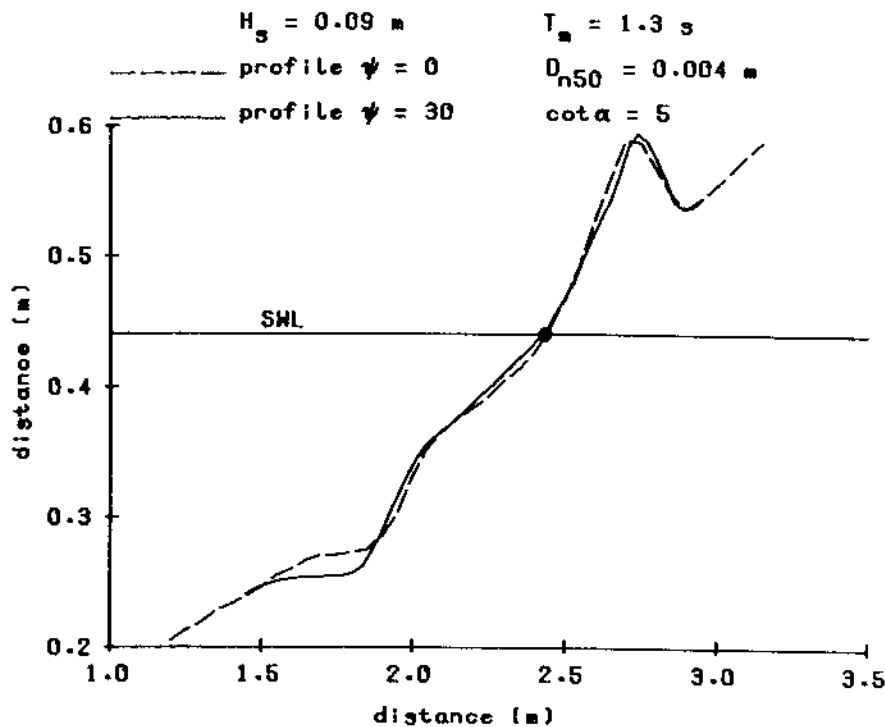
Figure 4.18 Influence of angle of wave attack

4.3 Development of model

Static stability is largely dependent on the initial slope, as is clearly expressed by the well known Hudson formula. Of course, for dynamically stable structures which are almost statically stable, the initial slope has influence on the profile too. It can be stated that, for $H_S/\Delta D_{n50}$ = 10 - 15, the initial slope has some influence on the profile and that for $H_S/\Delta D_{n50}$ < 10, the initial slope has a large influence on the profile. For $H_S/\Delta D_{n50}$ > 15 the initial slope has no influence on a large part of the profile.

From the analysis in Section 4.2 it was concluded that the influence of the spectral shape on the profile, can be described by the significant wave

height, H_s, and average period, T_m, only. The same conclusion was found in Section 3.3 for the influence on stability. No substantial difference was found for various shapes of stones and it can be concluded that the shape of the stone has no influence on the profile. The grading of the material also has no or only minor influence on the profile, using the nominal diameter, D_{n50}, as reference. Only for very wide gradings a longer profile was found below the still water level.

A structure with a low crest can be considered as a structure with a non-uniform slope. As already concluded, the initial slope has no influence on a large part of the profile and, therefore, the influence of a low crest is negligible.

The number of governing variables given in Section 4.1 can be reduced, therefore. By virtue of above mentioned conclusions, the following dimensionless variables can be ignored:

The initial slope (for $H_s/\Delta D_{n50} > 10 - 15$)
The grading of the material, D_{85}/D_{15}
The shape of the stone
The spectral shape parameter, κ
The crest height, R_c/H_s

From the qualitative comparison of profiles in Section 4.2 it was concluded that the wave height, H_s, wave period, T_m, the number of waves, N, and the nominal diameter, D_{n50}, all have influence on the dynamic profile. The water depth in front of the structure has only influence on the part below the still water level. Finally the angle of wave attack, ψ, probably has influence on the profile too. The final list of governing dimensionless variables can then be given by:

The wave height parameter, $H_s/\Delta D_{n50}$
The wave period parameter (steepness), s_m
The number of waves, N
The water depth in front of the structure, $h(x=toe)/H_s$
The angle of wave attack, ψ
The profile parameters

On the basis of the conclusions described above, a schematized model can be developed to describe the dynamic profile. Two points on the profile are very important. These are shown in Figure 4.19, where profiles for a 1 : 3 and 1 : 2 uniform slope are shown schematically. The local origin is chosen at the

intersection of the profile and the still water level. The first point, situated above the still water level, is the upper point of the beach crest. The second point, situated below the still water level, is the transition from the gentle sloping part to the steep part.
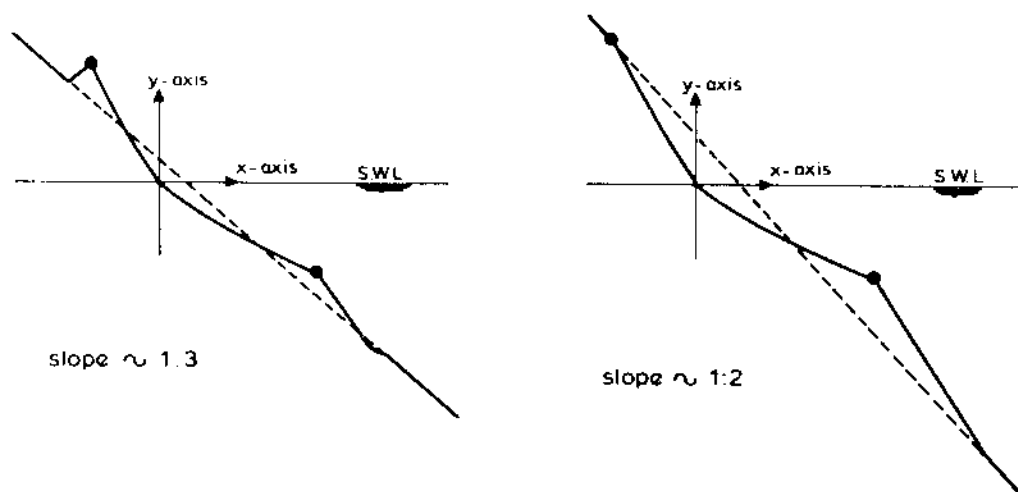
Figure 4.19 Schematized profiles on 1 : 3 and 1 : 2 initial slopes

Figure 4.20 shows the schematized model for a dynamic profile. A 1 : 5 uniform initial slope is shown with a high beach crest and a step. The profile is schematized by using a number of parameters all of which are related to the local origin or to the water level. The beach crest is described by the height, h_c, and the length, l_c. The transition to the step is described by the height, h_s, and the length, l_s. Curves, described by power functions, start at the local origin and go through these two points. The run-up length is described by the length, l_r. The step is described by two angles, β and γ. Finally, the transition from β to γ is described by the transition height, h_t.

Summarizing, the dynamic profile is defined by:

The runup length,	l_r
The crest height,	h_c
The crest length,	l_c
The step height,	h_s
The step length,	l_s
The transition height,	h_t
The angles,	β and γ
Power functions between h_c and h_s	

The profile described above is more or less independent of its location with respect to the initial slope. The location of the local origin determines the

shape of the profile completely. The location of the profile is obtained by means of an iteration process where the profile (the local origin) is moved along the still water level until the mass balance is fulfilled.
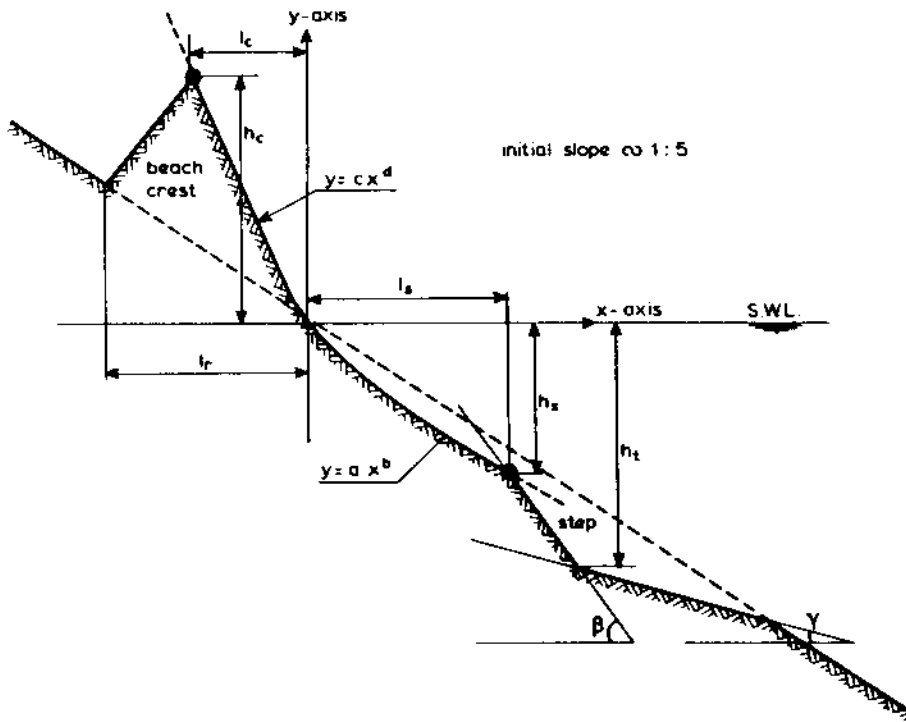
Figure 4.20 Schematized profile on 1 : 5 initial slope

4.4 Derivation of relationships

4.4.1 Basic functional relationships

The qualitative analysis in Section 4.2 using sets of profiles, resulted in the development of a schematic profile (Section 4.3). The profile parameters are only influenced by a relatively small number of governing variables. These governing variables are:

$$H_s/\Delta D_{n50}, \quad s_m, \quad h(x=toe)/H_s,$$

The final quantitative analysis should result in relationships which describe the profile parameters as a function of governing variables. The height and length parameters l_r, h_c, l_c, h_s, l_s and h_t can be related to the nominal diameter, D_{n50}, or to the wave height, H_s, in order to get dimensionless variables.

This Section, therefore, will mainly deal with curve fitting based on the governing variables established in the previous sections and summarized above.

The methods of curve fitting, the use of dimensionless variables and the possible errors in application by extrapolation of relationships have been described in Section 2.1.2 (the philosophy of approach of the research) and will not be repeated here.

The procedure starts with the influence of the storm duration, N. This storm duration is more or less independent of the other governing variables and is therefore taken first. Then the influence of the wave height, wave period and nominal diameter will be established. Finally the effect of the water depth and angle of wave attack on the relationships established will be analyzed.

First the influence of the storm duration will be analyzed. Long duration tests (in total eight tests) and the ratio of the parameters after 1000 and 3000 waves were used. For static stability two relationships were derived in order to describe the influence of the storm duration. One relationship (Equation 2.24) was based on theoretical considerations, taking into account an equilibrium after long wave attack. The other relationship (Equation 2.25) was applicable in a wide, but not the total, range and showed that the damage was simply related to the square root of the number waves.

The long duration tests performed by Van Hijum and Pilarczyk (1982), tests 503, 504 and 511 (Appendix III), had a total duration of more than 25,000 waves. The differences in profiles, especially the crest heights, were still substantial if N was increased from 10,000 to 25,000, see also Figure 4.6. Therefore, an equilibrium profile for random waves is only reached after very long wave attack. This means that it might be acceptable to use a power function between the profile parameters and the storm duration, which will be applicable in almost the entire range of possible storm durations. The influence of the storm duration can then be described by:

$$\text{par} = a_1 N^{b_1} \qquad \text{with } a_1 = f(H_s, T_m, D_{n50}) \tag{4.1}$$

where:

$\text{par} = l_r, h_c, l_c, h_s, l_s \text{ or } h_t$

a_1 and b_1 are curve-fitting coefficients.

A dimensionless parameter for the profile heights and lengths, including the storm duration, can be expressed by:

$$\text{par}/D_{n50}N^{b_1} \qquad \text{or} \qquad \text{par}/H_s N^{b_1}$$

The coefficient b_1 was established for each parameter.

For the height and length parameters this resulted in the following list of governing profile parameters:

- runup length : $l_r/D_{n50}N^{0.05}$ or $l_r/H_sN^{0.05}$
- crest height : $h_c/D_{n50}N^{0.15}$ or $h_c/H_sN^{0.15}$
- crest length : $l_c/D_{n50}N^{0.12}$ or $l_c/H_sN^{0.12}$
- step height : $h_s/D_{n50}N^{0.07}$ or $h_s/H_sN^{0.07}$
- step length : $l_s/D_{n50}N^{0.07}$ or $l_s/H_sN^{0.07}$
- transition height : $h_t/D_{n50}N^{0.04}$ or $h_t/H_sN^{0.04}$

The value of the coefficient b_1 was taken as the average of all tests. The coefficient showed no dependency on wave height, wave period, diameter or slope angle. The variation coefficient ranged between 0.3 and 1 (1 for the low values of b_1). A high value of b_1 means a large influence of storm duration. The parameter which is most influenced by the storm duration is the crest height h_c, where the power coefficient amounts to the highest value of 0.15. This conclusion was already reached by the analysis of the profiles (Section 4.2).

The wave height, period and diameter have a large influence on the profile parameters. The wave height parameter is given by $H_s/\Delta D_{n50}$ and the wave period parameter by the fictitious steepness, s_m. In Section 4.2.4 (Figure 4.7) it was concluded that for high $H_s/\Delta D_{n50}$ values some parts of the profile (for instance the crest height) were no longer influenced by the diameter but solely by the wave height and period.

In that case the profile parameters are only a function of the wave height and period. This means that governing variables should be used without the nominal diameter in the dimensionless form. For the profile parameter itself and the wave height this results in the parameter $par/H_sN^{b_1}$. The influence of the wave period is described by the fictitious wave steepness s_m. In the case that the diameter has no influence on the profile (which might be the case for high $H_s/\Delta D_{n50}$ values) the following basic relationship can be determined:

$$par/H_sN^{b_1} \propto f(s_m)$$

$$(4.2)$$

On the other hand, if the stone diameter influences the height or length parameter, it is reasonable to relate this height and length parameters to the nominal diameter, which results in $par/D_{n50}N^{b_1}$. Dynamic stability of rock slopes and gravel beaches is obtained for a large range of $H_s/\Delta D_{n50}$ values (roughly between $H_s/\Delta D_{n50} = 3 - 500$). The governing variable in this case is the nominal diameter, D_{n50}. The nominal diameter in prototype can cange from 1 m (berm breakwaters) to 0.004 m (fine shingle).

The profile parameters are related to the nominal diameter by $par/D_{n50}N^{b1}$. The wave height is related to the nominal diameter by $H_s/\Delta D_{n50}$. It is consistent if the wave period is also related to the nominal diameter. This is achieved by the parameter $\sqrt{g/D_{n50}} \; T_m$. If the diameter influences the profile then all governing variables are related to D_{n50}. This means that a relationship has to be established between the wave height parameter $H_s/\Delta D_{n50}$, the wave period parameter, $\sqrt{g/D_{n50}} \; T_m$ and the profile parameter $par/D_{n50}N^{b1}$. This leads to a second basic functional relationship which must hold for the whole range of $H_s/\Delta D_{n50}$:

$$par/D_{n50}N^{b1} = f(H_s/\Delta D_{n50}, \; \sqrt{g/D_{n50}} \; T_m) \qquad (4.3)$$

Moreover, from the analysis of the profiles (Section 4.2.2) it was concluded that wave height and period had similar effect on the profile. This conclusion can be used to define a combined parameter, H_oT_o, for the wave height and wave period:

$$H_oT_o = H_s/\Delta D_{n50} * \sqrt{g/D_{n50}} \; T_m \qquad (4.4)$$

where:

$H_o = H_s/\Delta D_{n50}$ = dimensionless wave height parameter

$T_o = \sqrt{g/D_{n50}} \; T_m$ = dimensionless wave period parameter related to D_{n50}

Using this parameter, H_oT_o, Equation 4.3 changes into:

$$par/D_{n50}N^{b1} = f(H_oT_o) \qquad (4.5)$$

The complete range for dynamic stability ($H_s/\Delta D_{n50} = 3 - 500$) can also be covered by the combined wave height-wave period parameter H_oT_o. The relationship between different types of structures and the parameters $H_s/\Delta D_{n50}$ and H_oT_o are listed below (see also Section 1.1).

structure	$H_s/\Delta D_{n50}$	H_oT_o
Statically stable breakwaters	1 - 4	< 100
Rock slopes and beaches	6 - 20	200 - 1500
Gravel beaches	15 - 500	1000 - 200,000
Sand beaches	> 500	> 200,000

4.4.2 The height and length parameters

Relationships with H_oT_o

Based on the qualitative conclusions derived in Sections 4.2 and 4.3, only two functional relationships are defined in the previous Section. The first one (Equation 4.2) holds for high $H_s/\Delta D_{n50}$ values and does not consider any influence of the diameter. A plot of par/H_sN^{b1} versus the wave steepness, s_m, for each length and height parameter will show the following possibilities:

- Data points for different diameters show the same curve. In this case the diameter indeed has no influence on the length or height parameter considered and a functional relationship as in Equation 4.2 can be established.

- Data points for different diameters show a shift and each diameter shows a different curve. In this case the influence of the diameter can not be ignored and Equation 4.2 can not be established. Then Equation 4.5 must be considered.

The second functional relationship (Equation 4.5) covers the whole area of dynamic stability, given by $H_s/\Delta D_{n50}$ = 3 - 500 or by the combined wave height-period parameter H_oT_o = 100 - 200,000. The values of H_oT_o during the complete test program ranged from H_oT_o = 100 to 70,000, see Appendix III. Figures can be drawn with the profile parameter $par/D_{n50}N^{b1}$ against H_oT_o. This is achieved by using a logarithmic scale.

The following conclusions can be derived from such a plot:

- If all data points lay on one smooth curve, the combined H_oT_o parameter gives a good representation of the influence of wave height and wave period. If shifted curves are found for each diameter, the wave height and period should be treated independently and not in the combined parameter H_oT_o.

- It is expected that for relatively large diameters ($H_s/\Delta D_{n50}$ < 10 - 15 or H_oT_o < 1000 - 2000) the initial profile will have influence on the profile parameters. A plot with both the data for a 1 : 3 and 1 : 5 uniform initial slope will show the range where the initial slope has influence on the profile.

Therefore all tests with initial slopes of 1 : 3 and 1 : 5 were plotted in one figure and this was done for each profile parameter. Figures 4.21 to 4.26 show these plots. The highest point in the figures was found using 4 mm

shingle with a wave height of 1.7 m (test 806). The lowest point was found using 0.026 m rock on a slope of 1 : 3 with a wave height of 0.15 m.

From Figures 4.21 - 4.26 it follows that the data points show smooth curves without shifts, which implies that the combined wave height-period parameter, $H_0 T_0$, gives the influence of wave height, period and diameter in a proper way. The initial slope becomes important when the $H_0 T_0$ value is smaller than 500 - 2000, depending on the profile parameter considered. This is according to the expectation. The influence is most pronounced for the parameters h_s and l_s, see Figures 4.24 and 4.25.
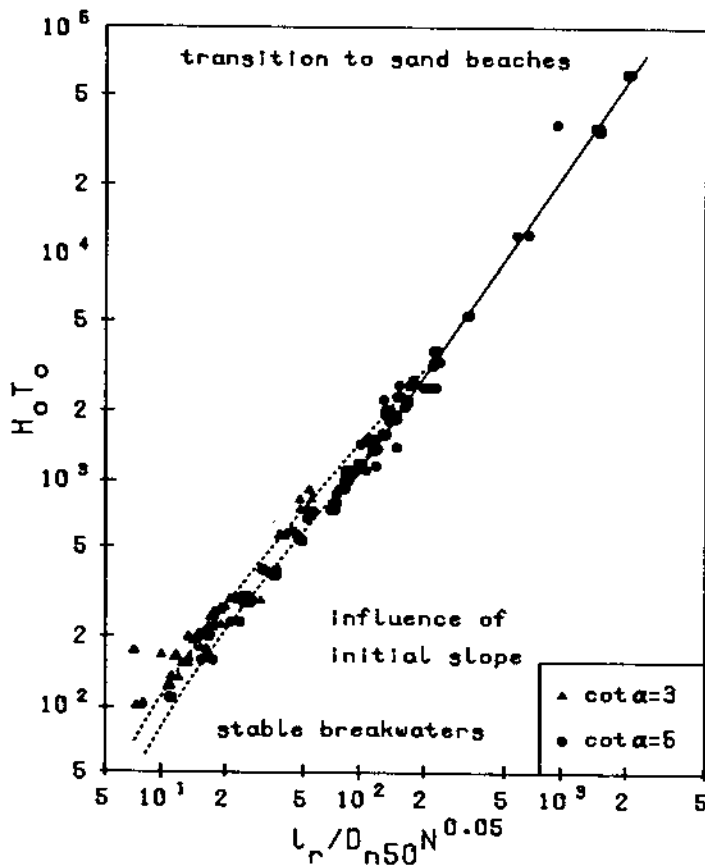
Figure 4.21 Relationship between runup length, l_r, and $H_0 T_0$
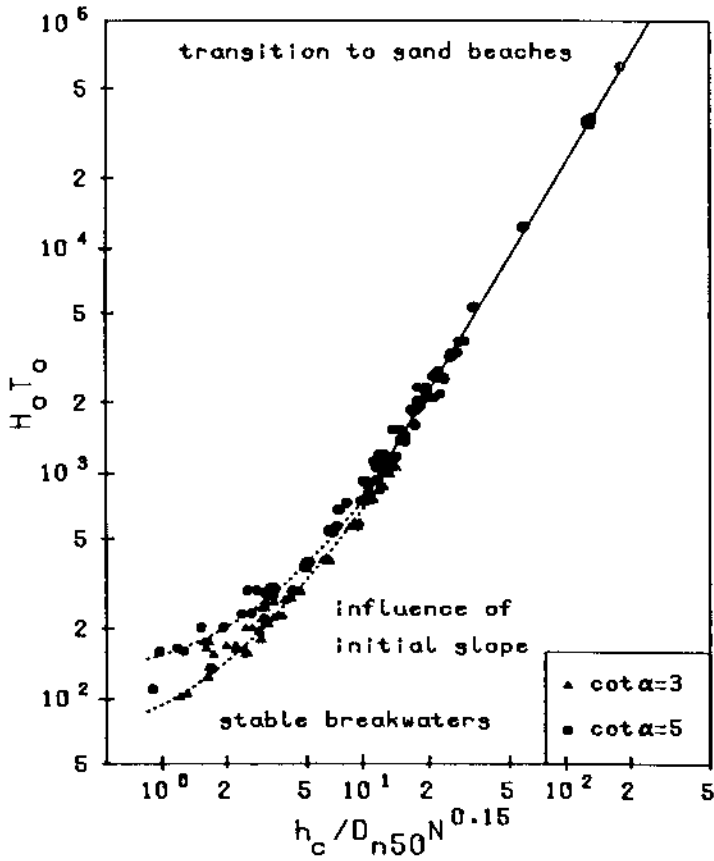
Figure 4.22 Relationship between crest height, h_c, and $H_o T_o$
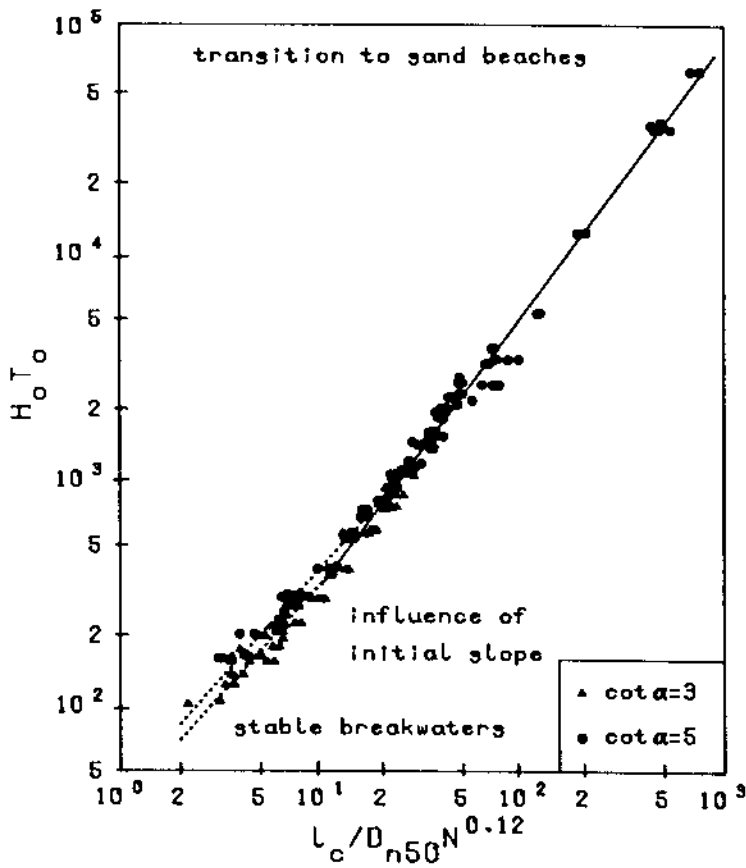
Figure 4.23 Relationship between crest length, l_c, and $H_o T_o$
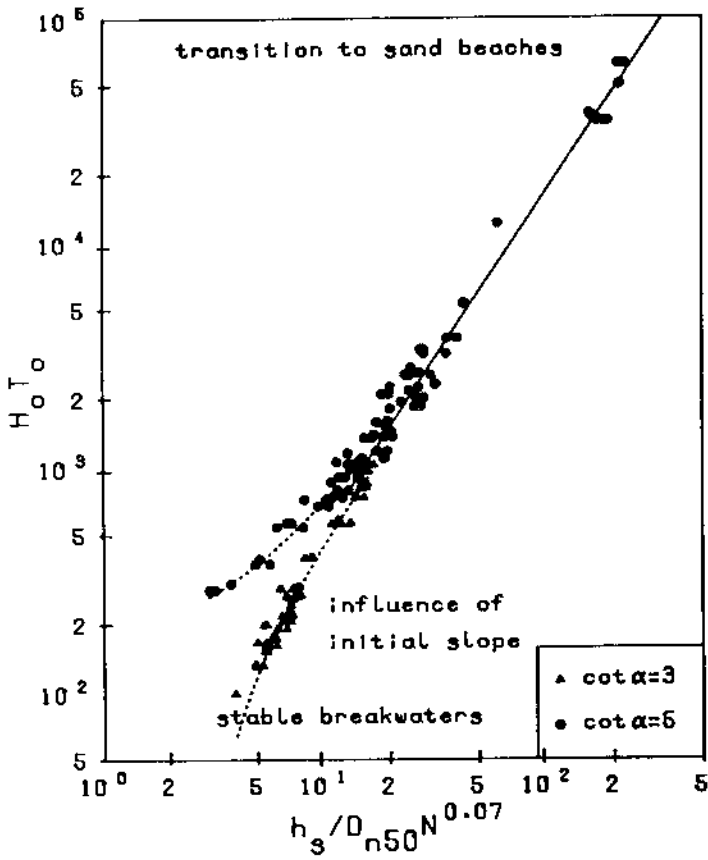
Figure 4.24 Relationship between step height, h_s, and H_oT_o
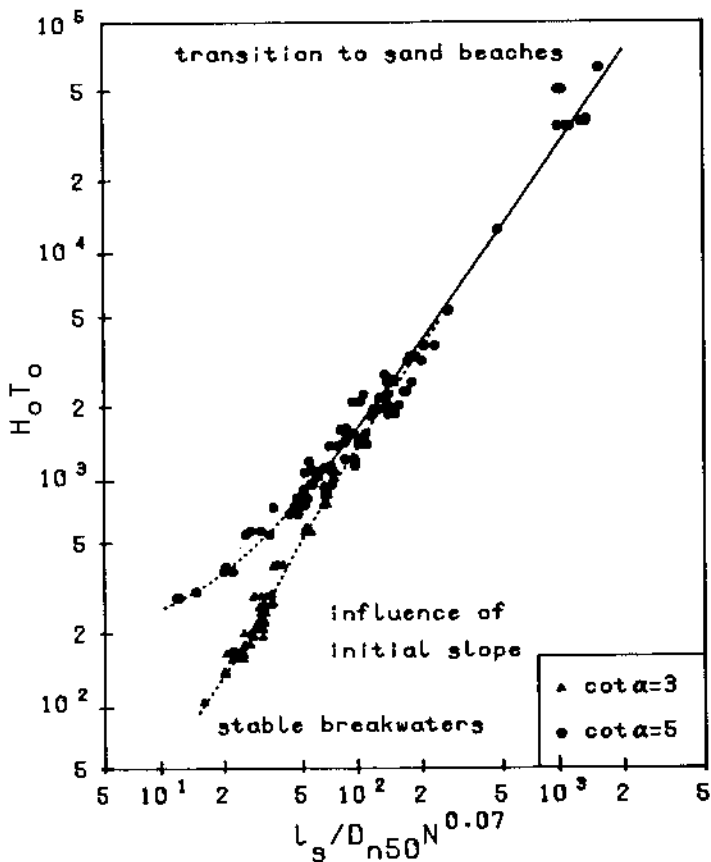
Figure 4.25 Relationship between step length, l_s, and H_oT_o
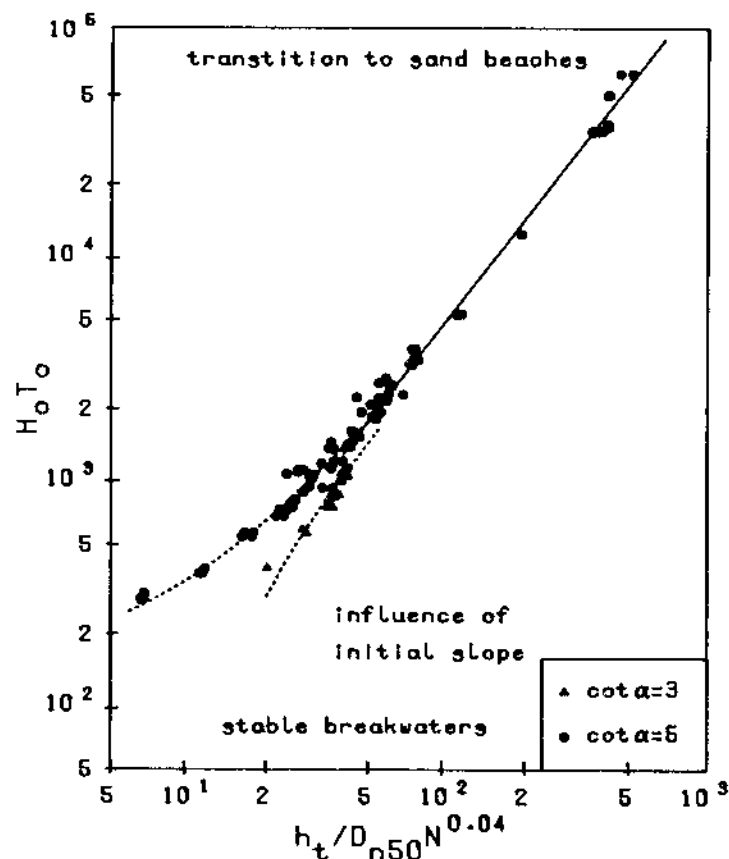
Figure 4.26 Relationship between transition height, h_t, and H_oT_o

For higher values of H_oT_o a relationship such as Equation 4.5 can be established. The relationships which were found with regression analysis were based on the power curve:

$$H_oT_o = a_2 \ (par/D_{n50}N^{b_1})^{c_2}, \tag{4.6}$$

where a_2 and c_2 are curve fitting coefficients. The established relationships are listed below for each profile parameter.

runup length	:	$H_oT_o = 2.9(l_r/D_{n50}N^{0.05})1.3$	Fig. 4.21	(4.7)
crest height	:	$H_oT_o = 25(h_c/D_{n50}N^{0.15})1.5$	Fig. 4.22	(4.8)
crest length	:	$H_oT_o = 22(l_c/D_{n50}N^{0.12})1.2$	Fig. 4.23	(4.9)
step height	:	$H_oT_o = 16.5(h_s/D_{n50}N^{0.07})1.5$	Fig. 4.24	(4.10)
step length	:	$H_oT_o = 3.8(l_s/D_{n50}N^{0.07})1.3$	Fig. 4.25	(4.11)
transition height:		$H_oT_o = 5(h_t/D_{n50}N^{0.04})1.5$	Fig. 4.26	(4.12)

Equations 4.7 - 4.12 were plotted in the Figures 4.21 - 4.26 (solid lines). For lower values ($H_0T_0 < 500 - 2000$) equivalent slope angles were introduced into the equations. The equivalent slope angles for the parameters l_r, h_c and l_c were based on the upper part of the initial profile. The equivalent slope angle for h_s and l_s was based on the profile around the still water level. Finally a third equivalent slope was based on the profile below the still water level and was used for determining h_t, $\tan\beta$ and $\tan\gamma$.

Equations 4.7 - 4.12 are independent on the initial slope and are all based on the same basic equation (Equation 4.6). They are valid for high H_0T_0 values. For lower values ($H_0T_0 < 500 - 2000$) the above mentioned equivalent slope angle has to be used for each length and height parameter. From Figures 4.21 - 4.26 it follows furthermore that in the low H_0T_0 region the relationships for some parameters can no longer be described by a power function (a uniform line in double logarithmic plots). See for example Figure 4.22. This means that various types of functional relationships have to be established in the low H_0T_0 region.

This curve fitting procedure is given in DELFT HYDRAULICS-M1983 (1988b) and will not be repeated here as it gives no further insight in the processes involved in dynamic stability. A summary, however, of the equations together with the method of establishing an equivalent slope angle is given in Appendix IV. The curves representing the equations are shown in Figures 4.21 - 4.26 with dotted lines.

Relationships with s_m

Equation 4.2 was analysed by plotting the profile parameter $par/H_sN^{b_1}$ versus the fictitious wave steepness s_m, for high H_0T_0 values ($H_0T_0 > 1000$). These plots are shown in Figures 4.27 - 4.32, where a distinction was made between various ranges of H_0T_0.

Figure 4.28 shows Equation 4.2 for the crest height, h_c, for several H_0T_0 values > 1000. Since all the H_0T_0 values lay on the one curve, irrespective of their individual values, this implies that different diameters fit the same relationship which in turn means that indeed the crest height is not influenced by the diameter for these particular H_0T_0 values.

A similar conclusion is reached for the other height parameters, h_s and h_t (Figures 4.30 and 4.32), although more variation in results is present in this case. Another conclusion can be drawn from the figures for the length parameters, l_r, l_c and l_s (Figures 4.27, 4.29 and 4.31). Here different diameters
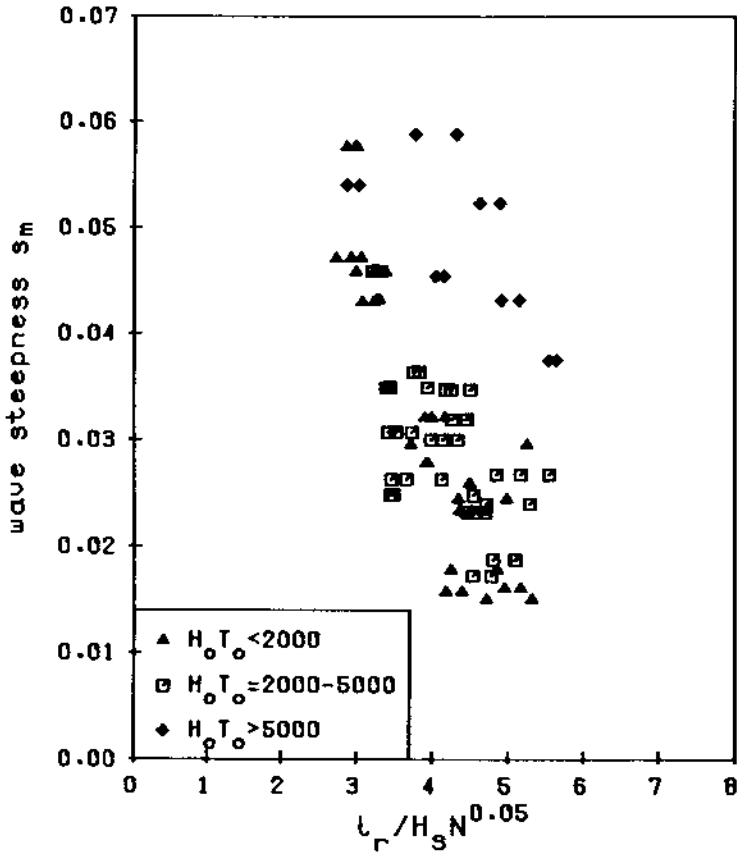
Figure 4.27 Relationship between runup length, l_r, and wave steepness, s_m
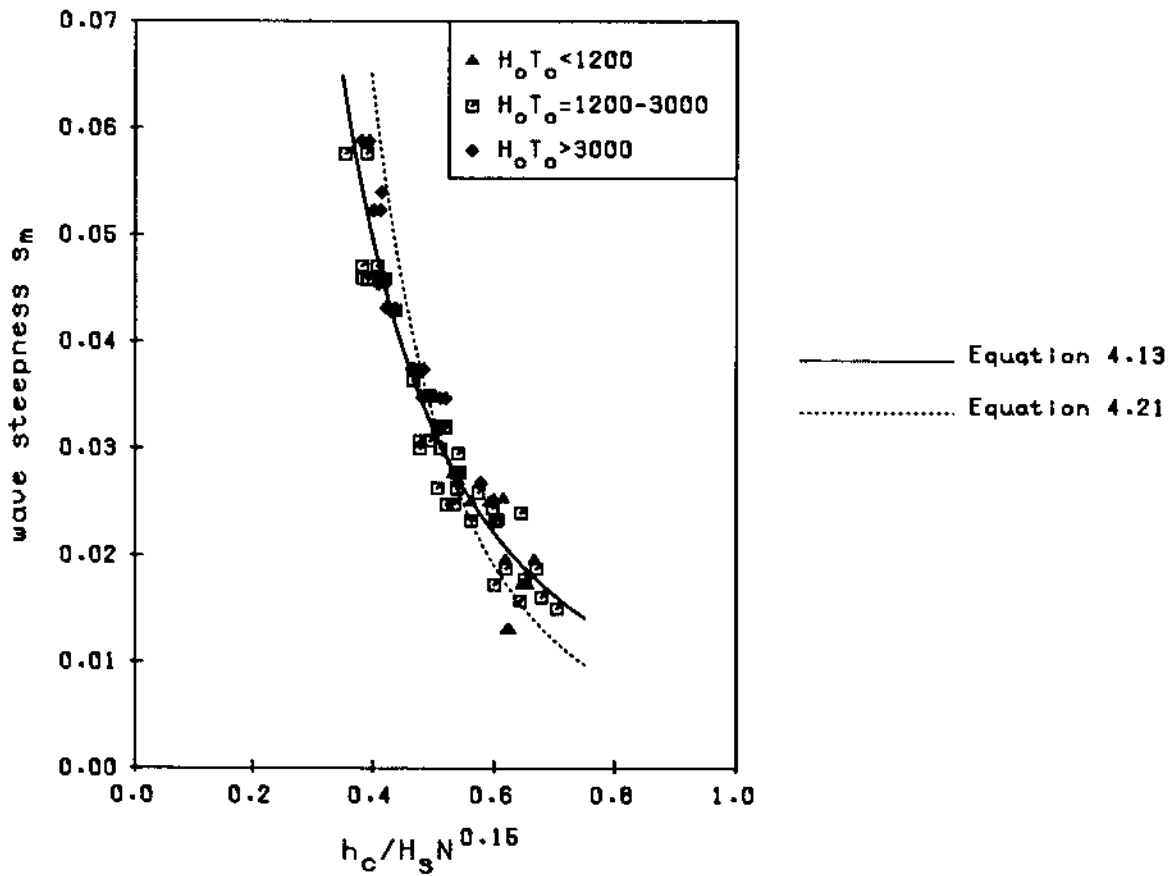
Figure 4.28 Relationship between crest height, h_c, and wave steepness, s_m
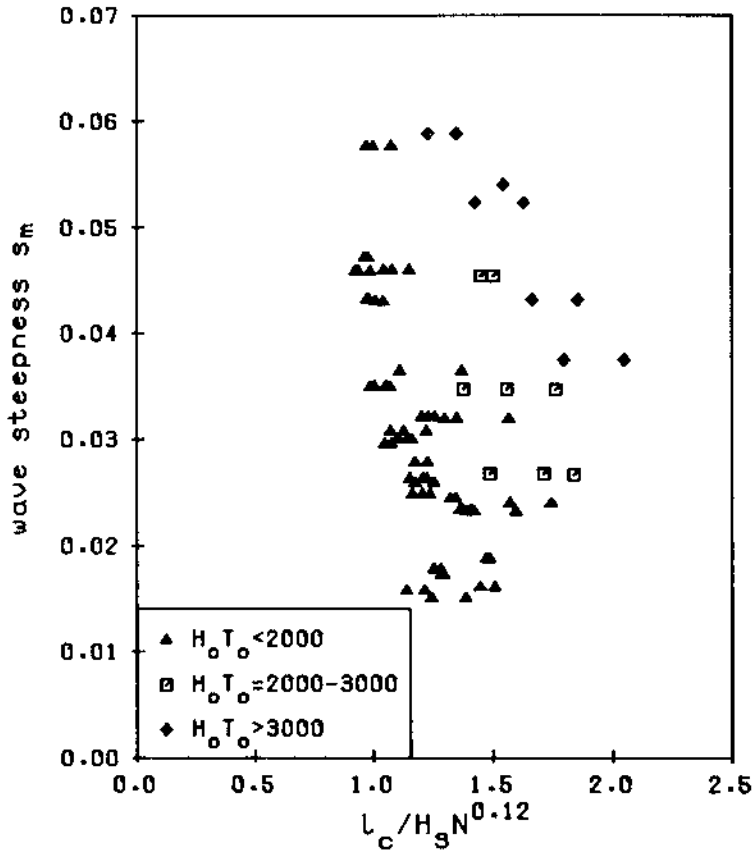
Figure 4.29 Relationship between crest length, l_c, and wave steepness, s_m
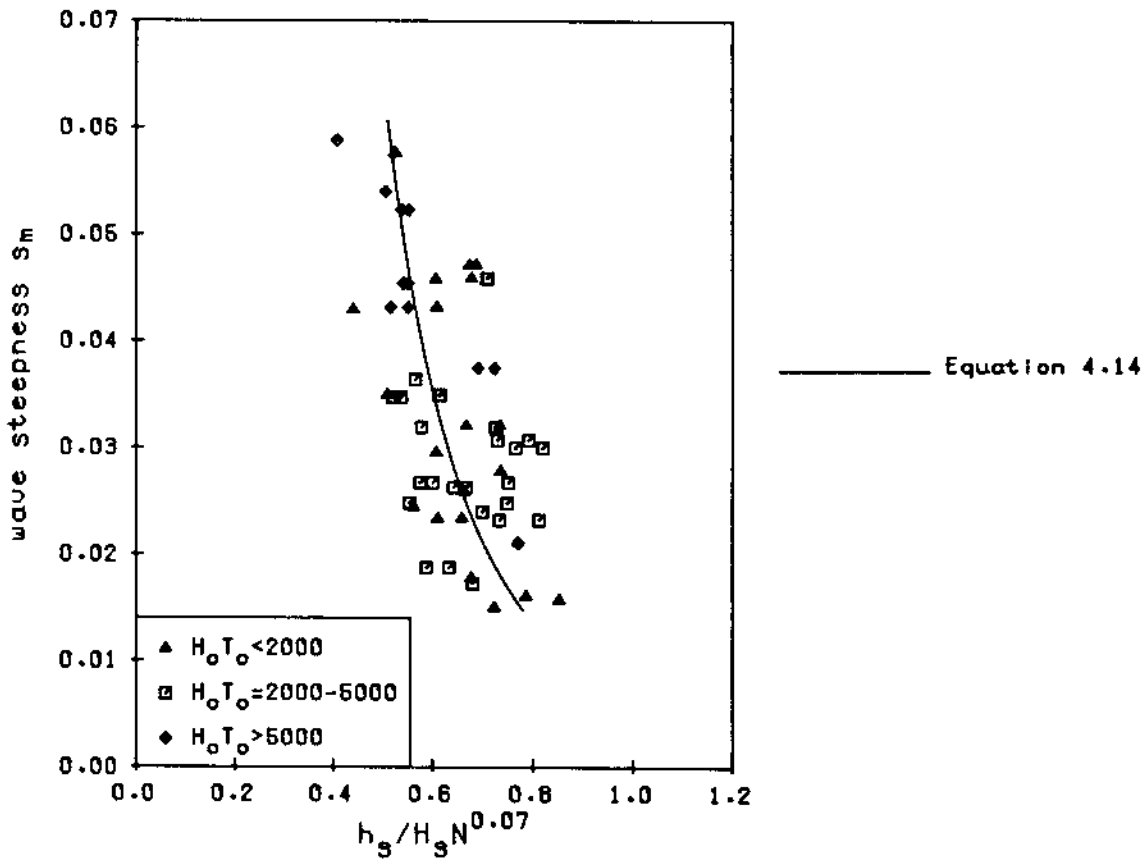
Figure 4.30 Relationship between step height, h_s, and wave steepness, s_m
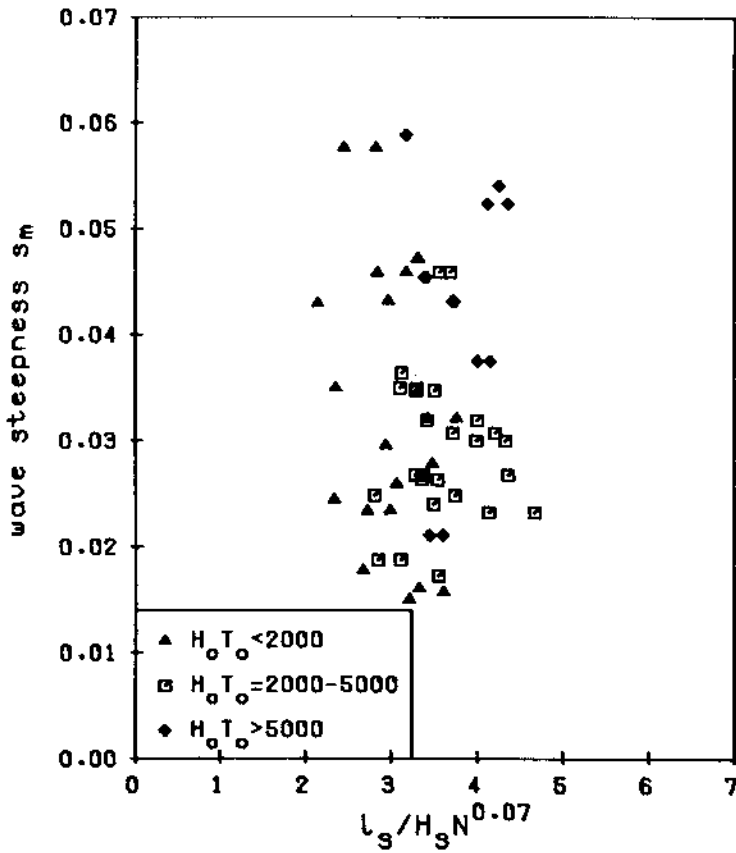
Figure 4.31 Relationship between step length, l_s, and wave steepness, s_m
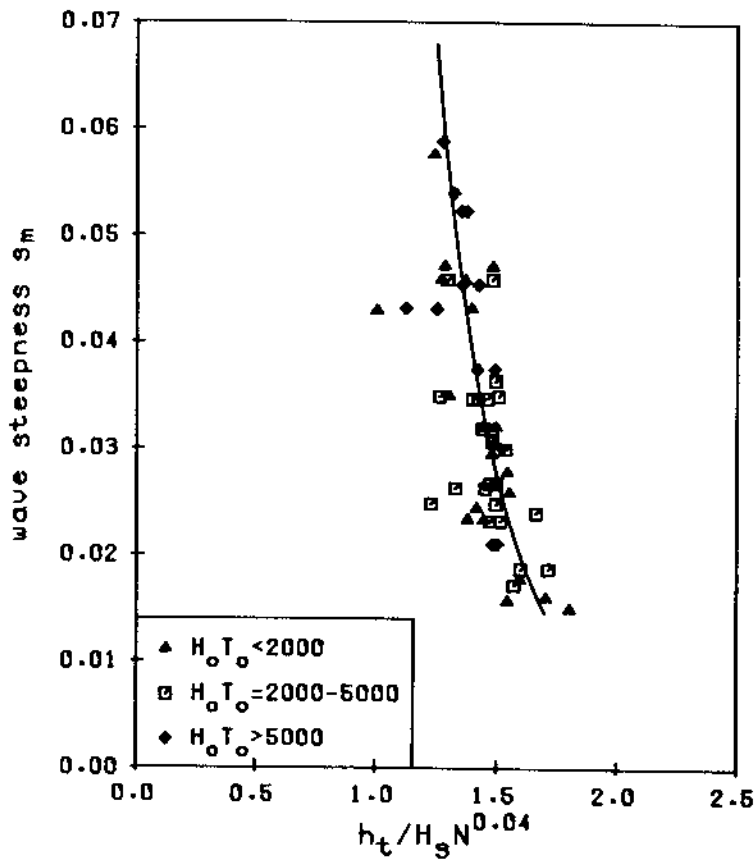
Figure 4.32 Relationship between transition height, h_t, and wave steepness, s_m

show a different relationship. It is clear that, for these length parameters, the influence of the diameter cannot be ignored, even not for very small grain sizes.

For all height parameters (h_c, h_s and h_t) a relationship such as Equation 4.2 was established for high H_oT_o values:

crest height : $h_c/H_sN^{0.15} = 0.089 \, s_m^{-0.5}$ Fig. 4.28   (4.13)

step height : $h_s/H_sN^{0.07} = 0.22 \, s_m^{-0.3}$ Fig. 4.30   (4.14)

transition height: $h_t/H_sN^{0.04} = 0.73 \, s_m^{-0.2}$ Fig. 4.32   (4.15)

Correlation between H_oT_o and s_m

Two types of relationships were established for the height parameters h_c, h_s and h_t. The first type uses the parameter H_oT_o and the profile parameter related to the nominal diameter, $par/D_{n50}N^{b1}$, see Equations 4.8, 4.10 and 4.12. The second type describes the profile parameter related to the wave height, par/H_sN^{b1}, as a function of the fictitious wave steepness, s_m, see Equations 4.13 - 4.15. In these latter equations the nominal diameter is not present.

The general form of Equations 4.7 - 4.12 can be written as:

$$H_oT_o = a_2 \, (par/D_{n50}N^{b_1})^{c_2} \qquad (4.6)$$

The general form of Equations 4.13 - 4.15 is:

$$par/H_sN^{b1} = d_1(s_m)^{e1} \qquad (4.16)$$

Although Equations 4.6 and 4.16 look rather different it is possible to re-write Equation 4.6 in the same form as Equation 4.16. This means that it is possible to prove that, under certain conditions, Equations 4.6 and 4.16 are strongly correlated. This procedure will be treated now. The power coefficient c_2 in Equation 4.6 is very important in the transformation. If this coefficient has a value of $c_2 = 1.5$, Equation 4.6 can be written as:

$$H_s/\Delta D_{n50} * \sqrt{g/D_{n50}} \, T_m = a_2 \, (par/N^{b1})^{1.5} \, D_{n50}^{-1.5} \qquad (4.17)$$

which gives:

$$H_sT_m\sqrt{g}/\Delta = a_2 \, (par/N^{b1})^{1.5} \qquad (4.18)$$

With some rearrangement Equation 4.18 becomes:

$$par/H_s N^{b_1} = a_3 \ s_m^{-1/3} \tag{4.19}$$

with: $a_3 = (\sqrt{2\pi}/\Delta a_2)$

Equation 4.19 has the same form as Equation 4.16. This transformation is possible only for $c_2 = 1.5$ in Equation 4.6. For other values of c_2 the nominal diameter will always remain in the equation.

Putting it in another way: if for a certain profile parameter $c_2 = 1.5$ is found in Equation 4.6, it should be possible to find a relationship as described in Equation 4.16. On the other hand, if no relationship as Equation 4.16 can be found, the coefficient c_2 in Equation 4.6 will differ from 1.5.

It follows from Equations 4.7 – 4.13 that for the height parameters h_c, h_s and h_t a coefficient of $c_2 = 1.5$ was found, where for the length parameters l_r, l_c and l_s values were found of $c_2 = 1.3$, 1.2 and 1.3, respectively. And a relationship as Equation 4.16 was only found for the three height parameters, which is according to the above mentioned remarks.

Equation 4.19 will be elaborated for the crest height, h_c, Figure 4.28. With $\Delta = 1.62$, Equation 4.19 becomes:

$$h_c/H_s N^{0.05} = 1.34 \ a_2^{-1/1.5} \ s_m^{-1/3} \tag{4.20}$$

Curve fitting gives $a_2 = 25.2$ which results in:

$$h_c/H_s N^{0.05} = 0.16 \ s_m^{-1/3} \tag{4.21}$$

The difference between Equations 4.13 and 4.21 is the fixed value of the power coefficient -1/3 in Equation 4.21, where the power coefficient of -0.5 in Equation 4.13 was found by curve fitting. In fact, if the diameter has no influence on a profile parameter the equation of the type 4.16 gives a better result than the type 4.6. This can also be concluded from Figure 4.28 where both Equations 4.13 and 4.21 were plotted.

4.4.3 Profile around still water level

Curves described by power functions start at the local origin, and go through the points described by h_c and l_c and by h_s and l_s, respectively, see Figure 4.20. These curves can be described by:

$$y = a_4 \ x^{b_4} \ \text{below SWL, and} \tag{4.22}$$

$$y = a_5 \ (-x)^{b_5} \ \text{above SWL,} \tag{4.23}$$

where the coefficients b_4 and b_5 are determined from regression analyses and where the coefficients a_4 and a_5 are determined by the values of h_c, l_c and h_s and l_s.

Equation 4.22 was also developed for the description of sand beaches. Dean (1977) derived a value of $b_4 = 2/3$ from theoretical considerations. Vellinga (1986) found a value of $b_4 = 0.78$ on the basis of extensive model research and evaluation of scale relationships.

The curves described by Equations 4.22 and 4.23 were fitted to all profiles measured, and the coefficients b_4 and b_5 were established for each profile. The analyses showed that the coefficients were independent of the storm duration, the wave height, the wave period, the diameter and the initial slope. From about 250 profiles the following values were established for the coefficients b_4 and b_5:

$b_4 = 0.83 \qquad (\sigma = 0.06)$
$b_5 = 1.15 \qquad (\sigma = 0.10)$

This results in the following power curves:

$$y = a_4 \ x^{0.83} \qquad \text{below SWL, and} \tag{4.24}$$

$$y = a_5 \ (-x)^{1.15} \qquad \text{above SWL} \tag{4.25}$$

The coefficient 0.83 in Equation 4.24 seems close to the value of 0.78 found by Vellinga (1986) for sand beaches. The difference, however, is equal to about the standard deviation found for the present 250 profiles. On the other hand the coefficient of 0.78 was based on scale relationships and on the erosion of dunes during storm surge and not really on the developed profiles. Furthermore, the number of tests was limited. Therefore, the standard deviation for the factor 0.78 is probably much larger than found for the present tests. The relationships found by Vellinga (1986) for the profiles during dune erosion will by compared with the present research in more detail in Section 4.5.

4.4.4 Angles β and γ

The transition from the gentle part of the profile below SWL to a steeper slope is modeled by a line with an angle β, see Figure 4.20. The transition to again a more gentle slope (if present) is modeled by a line with an angle γ.

From first analysis it followed that the angle β (or tanβ) was independent of the wave height, wave period and nominal diameter. The storm duration, however, and the initial slope had influence on tanβ which can be concluded from Table 4.1 where results of series of tests were combined.

tests	cotα	tanβ	σ	tanβ	σ
		N = 1000		N = 3000	
383 - 395	1.5	0.837	0.035	0.854	0.030
323 - 356 and 397 - 408	3.0	0.508	0.060	0.530	0.067
301 - 323	5.0	0.319	0.061	0.405	0.036
801 - 809	5.0	0.351	0.071	0.375	0.064

Table 4.1 Tanβ for various series of tests

In Table 4.1 the tests with a berm profile (tests 383 - 395) were considered to have a seaward slope of 1 : 1.5. From this table it follows that a steeper initial slope results in a higher value of tanβ and that the influence of the storm duration is more pronounced for gentler initial slopes. The influence of N on tanβ in the large scale tests 801 - 809 is less pronounced, however, but within the range of the small scale tests 301 - 323 for the same initial slope of cotα = 5.

This influence of N and cotα on tanβ can be explained in physical terms. A steep initial slope results in material falling down, forming more or less a slope with a natural angle of repose, see Figure 4.12 - slope 1 : 1.5. This is independent of the storm duration.

The natural angle of repose of the material (without any wave forces) is about φ = 45° - 50°. This results in tanφ = 1.0 - 1.2 which is larger than the maximum tanβ of 0.85 for a 1 : 1.5 initial slope. The difference is due to the wave forces acting on this part of the profile. Waves breaking on a gentle slope below the still water level form a step and the material is transported upwards, see Figure 4.12 - slope 1 : 5. The slope angle is small as the wave motion has still large influence on the stability of the material in that area. It takes also time to form this "hole" which means that the storm duration has more influence than on a steep initial slope.

It can be stated that $\tan\beta$ is larger than $\tan\alpha$. On the other hand, at the start of a test (or storm) $\tan\beta$ is equal to $\tan\alpha$ (theoretical lower boundary). Figure 4.33 shows a plot of $\tan\alpha$ versus $\tan\beta$ with this lower boundary and the data of Table 4.1.

▢ tests 301-408	N=1000	_____ N = 0
◇ tests 301-408	N=3000	_ _ __ __ N = 1000
⦿ tests Delta flume	N=1000	_ . __ . __ N = 3000
▵ tests Delta flume	N=3000	_ _ __ _ . N = ∞
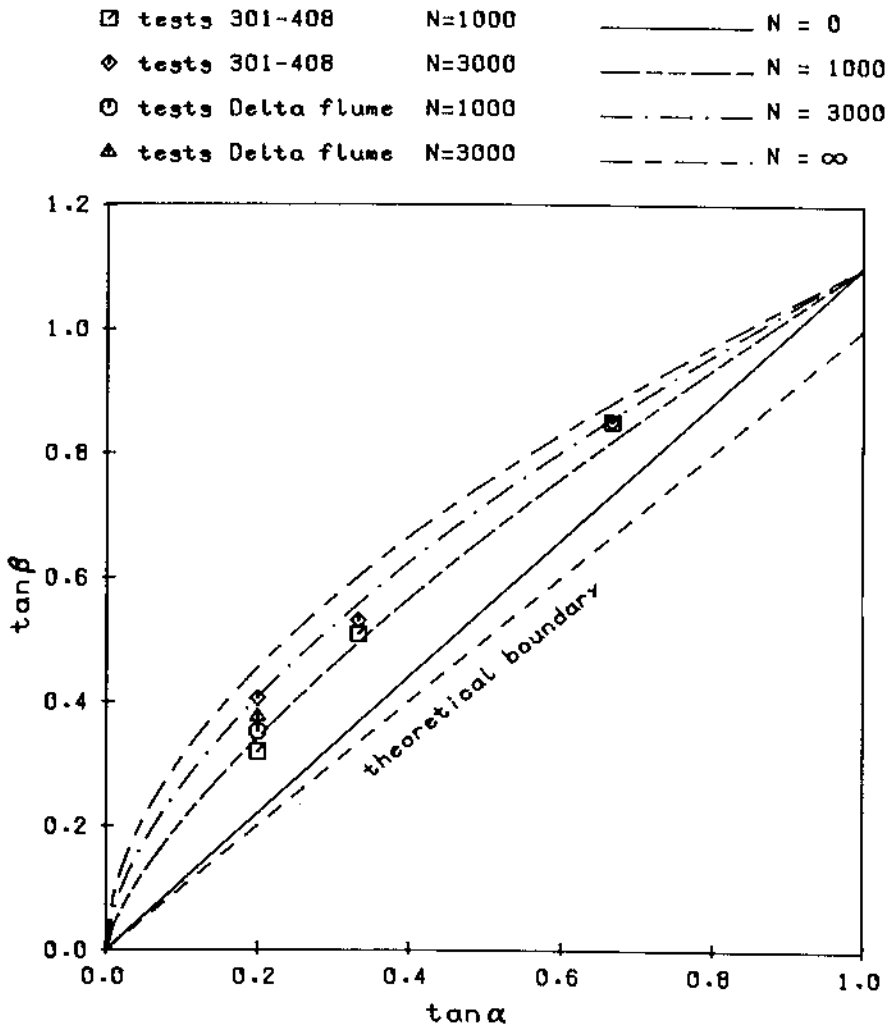
Figure 4.33 Tanβ as a function of tanα

The parameter $\tan\beta$ must be related to the number of waves, N, and the initial slope, $\tan\alpha$, (or an equivalent slope if the initial slope is not uniform). For low values of N the lower boundary should be reached and for very high values an equilibrium can be considered. The influence of N should be more pronounced for gentler slopes.

The following relationship meets this requirements and was chosen to describe $\tan\beta$:

$$\tan\beta = a_6 \, \tan\alpha^A \qquad\qquad 4.26)$$

with: $A = 1 - b_6 \exp(-c_6/N)$

It does not mean that this is the only relationship which can be chosen. This relationship can be compared with the influence of the storm duration on damage of statically stable structures, see Section 2.3.4. From regression analyses it followed that $a_6 = 1.1$, $b_6 = 0.45$ and $c_6 = 500$ which results in:

$$\tan\beta = 1.1 \tan\alpha^A \tag{4.27}$$

with: $A = 1 - 0.45 \exp(-500/N)$

Equation 4.27 is plotted in Figure 4.33 for $N = 0$, 1000, 3000 and ∞.

A slope with an angle γ is only found for initial slopes of $1 : 3$ and gentler. All values of $\tan\gamma$, established from the profiles, are shown in Figure 4.34. In this Figure $\tan\gamma$ is plotted versus H_0T_0. The values of $\tan\gamma$ are small (generally between -0.1 and 0.2) in comparison with $\tan\beta$ (between 0.3 and 0.8). The values of $\tan\gamma$ show large variation in this range measured. Difference was made between various initial slopes. The whole range of possible H_0T_0 values was measured only for $\cot\alpha = 5$. The range for $\cot\alpha = 3$ and 10 is much smaller.

From Figure 4.34 no clear dependency can be established for $\tan\gamma$ and an initial slope of $\cot\alpha = 5$, on the parameter H_0T_0. The average value of $\tan\gamma$ is more or less equal to the half of the initial slope angle, $\tan\alpha$. Therefore a simple relationship can be established for $\tan\gamma$:

$$\tan\gamma = 0.5 \tan\alpha \tag{4.28}$$

This relationship is plotted in Figure 4.34 for the three initial slopes with $\cot\alpha = 3$, 5 and 10 respectively.

4.4.5 Influence of water depth

On a shallow foreshore high waves will break and the wave heights will not be Rayleigh distributed. For static stability this effect was taken into account by using the 2 percent value of the wave height exceedance curve in the stability formulae, instead of the significant wave height (Section 3.3).

This means that the movement of stones around the still water level for static stability is initiated by the highest waves in a storm. This is different for dynamic stability where stones move during almost each wave.
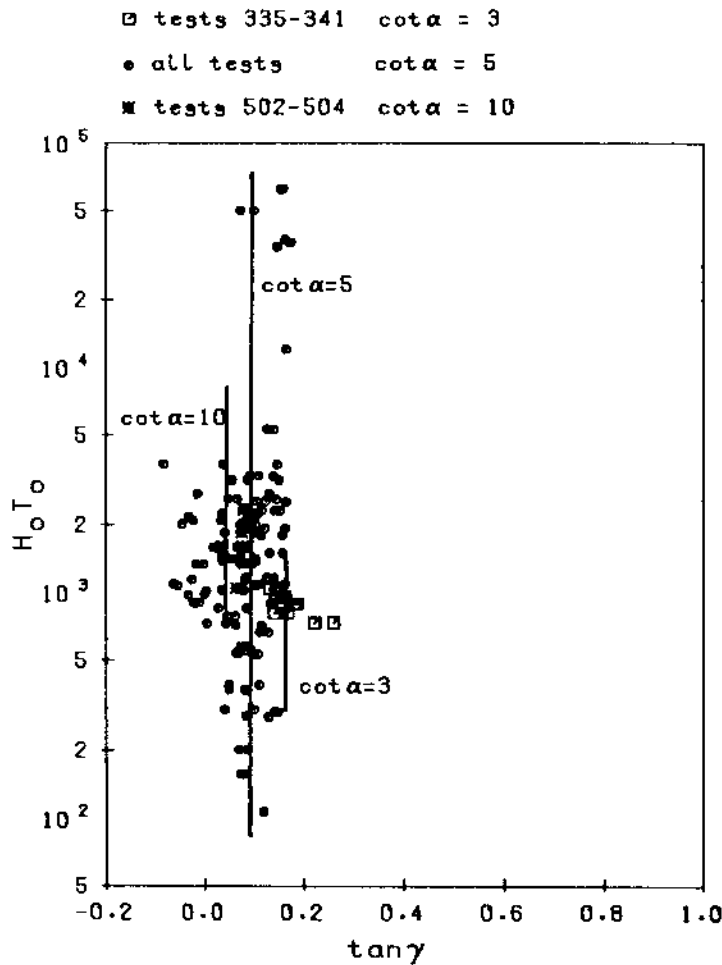
Figure 4.34 Tanγ as a function of H_oT_o

In Section 4.2 it was concluded by comparing different profiles, that a relatively small water depth results in a steeper profile below the still water level. This is probably due to higher water velocities below the still water level which is caused by the influence of the bottom. This assumption can simply be demonstrated by applying the Airy theory for linear, sinusoidal waves. The water depth in front of the structure varied between 0.2 and 0.4 m during these tests and was 0.8 m for all other tests. Assuming a wave period of 1.8 s and a wave height, H, the maximum horizontal water velocity at a depth of 0.20 can be calculated. This results in the following velocities for various water depths:

water depth (m)	velocity at 0.2 m depth (m/s)
0.20	6.95 H
0.30	4.61 H
0.40	3.49 H
0.80	1.92 H

The higher velocities near the bottom for a small water depth result in a shorter and steeper profile below the still water level. It is acceptable, therefore, to use the water depth related to the significant wave height as an additional parameter, and not the 2% wave height. The small water depths have influence on the profile parameters h_s and l_s. As discussed, the significant wave height in front of the structure, H_s, can be used for comparison.

The analysis of all profile parameters will not be given here. For sake of simplicity the results for the crest height, h_c, and the step height, h_s, will be given only. The results are shown in Figures 4.35 and 4.36 and are compared with the results with a water depth of 0.80 m.
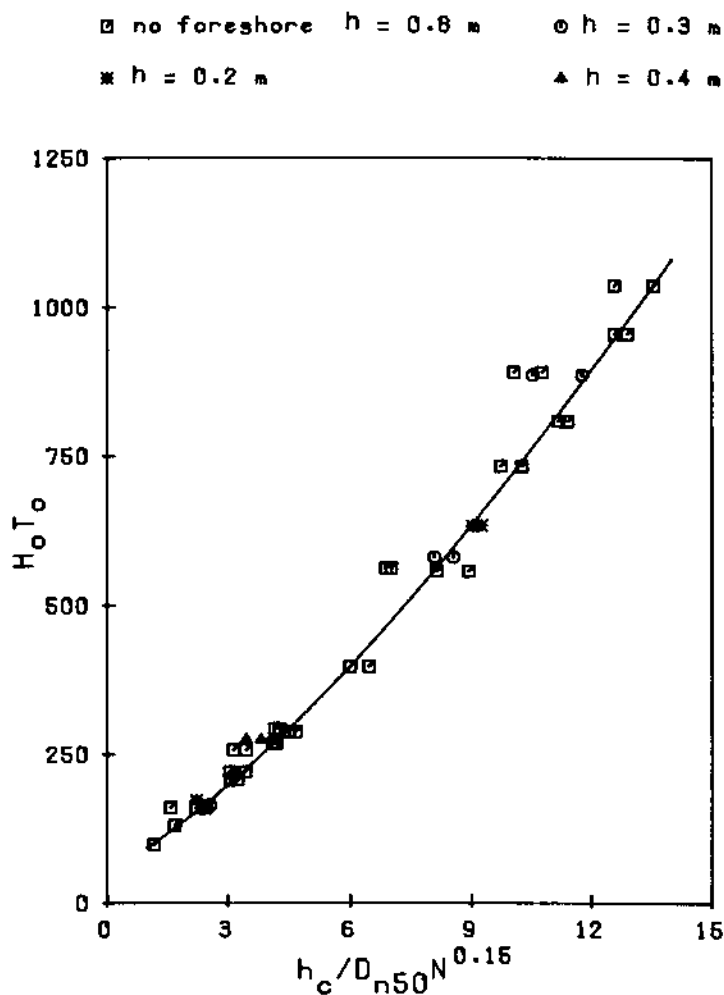
Figure 4.35   Influence of water depth on crest height, h_c

From Figure 4.35 it follows that, as already concluded before, the crest height is not influenced by a relatively small water depth in front of the structure. The same conclusion was found for the profile parameters l_r and l_c. In Figure 4.36 all results for the small water depth are located left of the results for a large water depth. This implies that the height, h_s, will be

shorter when the water depth is relatively small. The same effect was found for the length of the step, l_s.
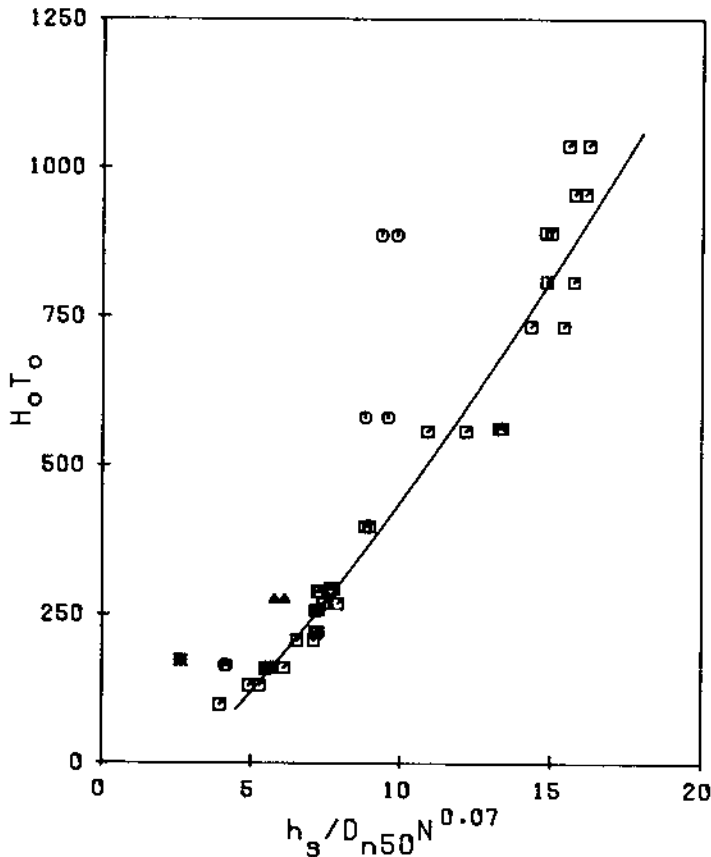
Figure 4.36   Influence of water depth on step height, h_s

The water depth was varied between 0.20 and 0.40 m during tests 416 – 421. From Figure 4.36 it can be concluded that the smallest water depth gave the largest relative difference in results for h_s (and l_s) in comparison with the water depth of 0.80 m. A reduction factor, r, for the profile parameters h_s and l_s can be developed by using the ratio of the water depth and wave height, h/H_s. The reduction factor, r, for each test can be calculated by using the average curve in Figure 4.36 as a reference (called h_s-reference). The actual value of h_s is than divided by h_s-reference.

A plot of h/H_s versus the reduction factor, r, is shown in Figure 4.37. This figure shows clearly the influence of the relatively water depth, h/H_s, on the parameter h_s. The following equation for the reduction factor was found to fit with the results:
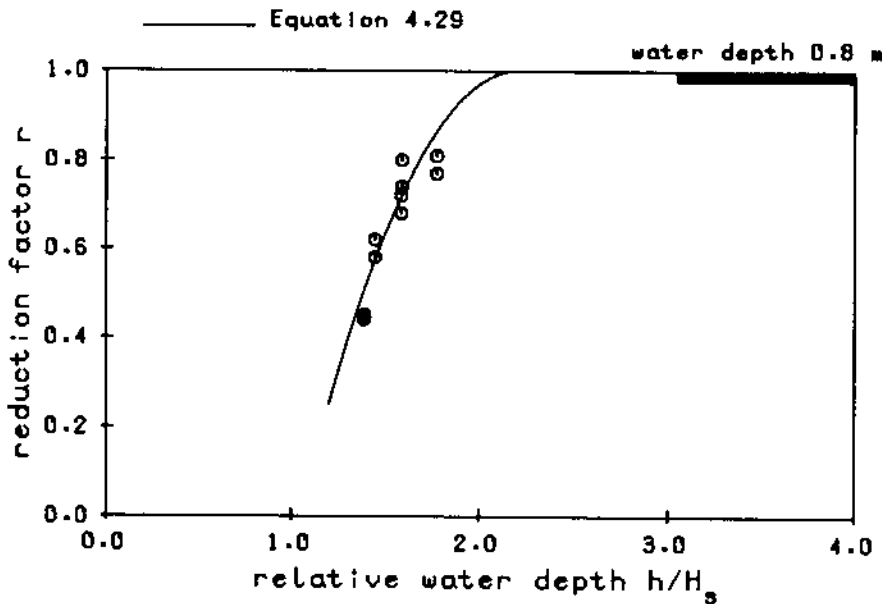
Figure 4.37 Reduction factor, r, as a function of relative water depth, h/H$_S$

$$r = 1 - 0.75 \ (2.2 - h/H_S)^2 \quad \text{for} \quad h/H_S < 2.2, \text{ and} \tag{4.29}$$

$$r = 1 \quad \text{for} \quad h/H_S > 2.2$$

The same relationship was found for the length parameter, l$_S$. This means that the influence of the water depth in front of the structure on the profile is given by Equation 4.29. The profile is not influenced by the water depth when h/H$_S$> 2.2.

4.4.6 Influence of angle of wave attack

Van Hijum and Pilarczyk (1982) concluded from their tests that the angle of wave attack was taken into account by using a reduction factor $\sqrt{\cos\psi}$ for all length and height parameters. The influence of the angle of wave attack on the wave run-up on slopes is described in various ways (TAW (1974), Tautenhain et al (1982)).

In order to investigate the influence of the angle of wave attack on the profile parameters, l$_r$, h$_c$, l$_c$, h$_s$, l$_s$, and h$_t$ a comparison was made with the results for perpendicular wave attack. The actual value of the profile parameter for oblique wave attack (ψ = 30°) was divided by the expected value for perpendicular wave attack (Equations 4.7 - 4.15). The average value of this ratio for each profile parameter is shown in Table 4.2, together with the standard deviation (based on about 20 figures - tests 551 - 560).

profile parameter	ratio of profile parameters for $\psi = 30°/\psi = 0°$	σ
l_r	0.90	0.10
h_c	0.86	0.11
l_c	1.06	0.13
h_s	0.82	0.12
l_s	0.87	0.14
h_t	0.92	0.12

Table 4.2   Influence of angle of wave attack

This table shows that the crest length, l_c, is not influenced by oblique wave attack. The ratio of 1.06 is even a little greater than 1.0 (1.0 means no influence). Tautenhain et al (1982) found that oblique wave attack with $\psi = 10° - 30°$ gave higher run-up than perpendicular wave attack. The results for l_c are in agreement with these results on run-up. If this length l_c is omitted, the other profile parameters have an overall ratio of 0.87. This value is equal to the value of $\cos 30°$ which is also 0.87. This means that the influence of the angle of wave attack on all profile parameters, except the crest length l_c, is given by a reduction factor $\cos\psi$.

The factor $\sqrt{\cos\psi}$ which was found by Van Hijum and Pilarczyk results in 0.93 for $\psi = 30°$ and this is higher than all of the values found in Table 4.2 (except for l_c). This means that a factor $\sqrt{\cos\psi}$ gives less reduction of the parameters than found in Table 4.2.

4.4.7   Summary of functional relationships

The shape of the dynamically stable profile (for relatively high H_0T_0 values of $H_0T_0 > 500 - 2000$) may be obtained from a set of equations which relate the profile parameters, shown in Figure 4.20, to the boundary conditions. In a second phase the location of the profile is found by means of an iteration process where the actual profile is moved along the still water level until the mass balance is fulfilled. The following set of equations were established in this Section.

The parameters s_m and H_0T_0

The profile parameters were related to the fictitious wave steepness s_m or to the combined wave height-wave period parameter H_0T_0:

$$s_m = 2\pi H_s/gT_m^2 \qquad\qquad (4.30)$$

$$H_oT_o = H_s/\Delta D_{n50} * \sqrt{g/D_{n50}} \; T_m \tag{4.4}$$

where:

$H_o = H_s/\Delta D_{n50}$ = dimensionless wave height parameter

$T_o = \sqrt{g/D_{n50}} \; T_m$ = dimensionless wave period parameter related to D_{n50}

The runup length, l_r

$$H_oT_o = 2.9 \; (l_r/D_{n50}N^{0.05})^{1.3} \tag{4.7}$$

The crest height, h_c

$$h_c/H_sN^{0.15} = 0.089 \; s_m^{-0.5} \tag{4.13}$$

The crest length, l_c

$$H_oT_o = 21 \; (l_c/D_{n50}N^{0.12})^{1.2} \tag{4.9}$$

The step height, h_s

$$h_s/H_sN^{0.07} = 0.22 \; s_m^{-0.3} \tag{4.14}$$

The step length, l_s

$$H_oT_o = 3.8 \; (l_s/D_{n50}N^{0.07})^{1.3} \tag{4.11}$$

The transition height, h_t

$$h_t/H_sN^{0.04} = 0.73 \; s_m^{-0.2} \tag{4.15}$$

The profile around the still water level

$$y = a_4 \; x^{0.83} \qquad\qquad \text{below SWL, and} \tag{4.24}$$

$$y = a_5 \; (-x)^{1.15} \qquad\qquad \text{above SWL,} \tag{4.25}$$

where the coefficients, a_4 and a_5, are determined by the values of h_c, l_c and h_s and l_s.

The slope $\tan\beta$

$$\tan\beta = 1.1 \; \tan\alpha^A \tag{4.27}$$

with: $A = 1 - 0.45 \exp(-500/N)$

The slope tanγ

$$\tan\gamma = 0.5 \tan\alpha \tag{4.28}$$

A relatively shallow foreshore

The influence of limited water depth is described by a reduction factor, r, which in fluences the profile parameters h_s and l_s only. This factor is given by:

$$r = 1 - 0.75 (2.2 - h/H_s)^2 \qquad \text{for} \qquad h/H_s < 2.2, \text{ and}$$

$$r = 1 \qquad \text{for} \qquad h/H_s > 2.2$$

Oblique wave attack

The influence of oblique wave attack is taken into account when all length and height parameters (except l_c) are reduced by a factor $\cos\psi$.

4.5 Comparison with dune erosion during storm surges

The model developed in the previous sections described the dynamic stability of loose materials (rock and gravel) under wave attack. The transition from gravel to sand beaches roughly corresponds to materials with diameters in the order of 4 mm. Scale effects in small scale tests on gravel beaches can not longer be ignored if diameters in the model become smaller than 4 - 6 mm (Van Hijum and Pilarczyk (1982)). Rock and gravel is described by the (nominal) diameter of the material and the transport of material is determined by bed load only. Sand is, besides the diameter, also characterized by the fall velocity in water, and the transport of material is determined by bed load and suspension. Scale relationships for dune erosion tests were obtained by using the fall velocity, w, of the material in water (Vellinga (1986)).

Vellinga (1986) developed a model for dune erosion during storm surges. The part of the profile below the still water level is given by the same equation as Equation 4.22:

$$y = a_4 \, x^{b_4} \tag{4.22}$$

It is interesting, therefore, to compare the results of the tests on dune erosion with the present tests on gravel and rock. On the basis of scale rela-

tions and model tests Vellinga found $b_4 = 0.78$ in Equation 4.22, where the present tests showed a value of $b_4 = 0.83$ (based on 250 profiles, Equation 4.24). According to Vellinga the coefficient a_4 in Equation 4.22 included the fall velocity of sand in water:

$$y = 0.39 \, w^{0.44} \, x^{0.78} \tag{4.31}$$

This equation can directly be related to the present tests on gravel and rock. For grains larger than 4 mm the fall velocity can be described by, (Vellinga (1986)):

$$w = 1.1 \, (\Delta gD)^{0.5} \tag{4.32}$$

With $\Delta = 1.6$, $g = 9.81$ and Equation 4.32 substituted in Equation 4.31, yields:

$$y = 0.75 \, D^{0.22} \, x^{0.78} \tag{4.33}$$

The profiles of tests 301 - 341 ($H_s/\Delta D_{n50} = 3 - 13$), 506 - 532 ($H_s/\Delta D_{n50} = 12 - 32$) and 801 - 809 (Delta flume: $H_s/\Delta D_{n50} = 25 - 260$) were used to analyze Equation 4.33 for gravel beaches. The coefficient, p, of all the profiles were established where p is given by:

$$y = p \, D^{0.22} \, x^{0.78} \tag{4.34}$$

For $p = 0.75$ Equation 4.33 is found. The values of p were plotted versus the fictitious wave steepness s_m in Figure 4.38. Difference was made between various ranges of $H_s/\Delta D_{n50}$.

Figure 4.38 shows that for $H_s/\Delta D_{n50} < 80 - 90$ no difference is found between the various ranges of $H_s/\Delta D_{n50}$. The values of p roughly range between 0.5 and 0.65 which is about 15 - 30 % less than the value of $p = 0.75$, found by Vellinga.

The tests on 4 mm gravel in the Delta flume are closest to the tests on dune erosion, although still a factor of about 20 exists between the diameters (gravel: $D_{n50} = 0.0041$ m, sand: $D_{n50} = 0.000225$ m). The values of p for these tests ($H_s/\Delta D_{n50} = 95 - 260$) differ from the values found for lower $H_s/\Delta D_{n50}$ ranges. In fact the average of the tests on 4 mm gravel is close to the value of 0.75. A clear influence of the wave steepness is found, however.

tests	D_{n50}	H_s/D_{n50}	$\cot\alpha$
◆ 801-803	0.0041	95-260	5
✕ 804-809	0.0187	25-50	5
▲ 501-533	0.0041	12-32	5
▣ 315-323	0.0110	7-13	5
+ 333-341	0.0110	7-13	3
♣ 307-314	0.0257	3-7	5
✻ 324-332	0.0257	3-7	3

$$p \text{ in } y = p \ D^{0.22} \ x^{0.78}$$
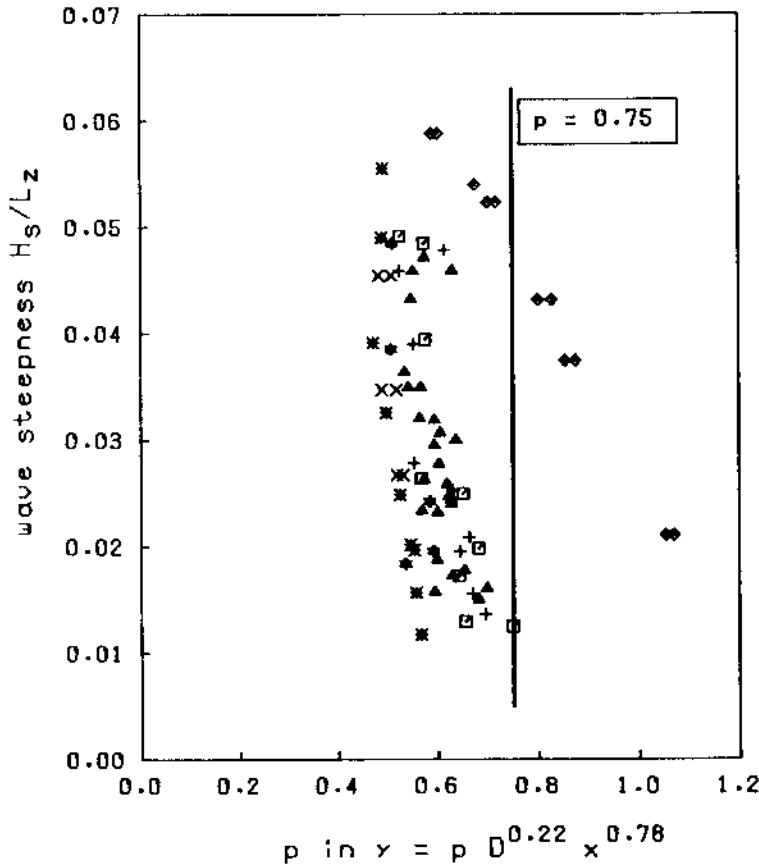
Figure 4.38 Comparison with dune erosion tests

It can be concluded that, if the influence of the wave steepness is ignored, Equation 4.33 which was found for dune erosion under storm surges, can be extrapolated into the area of gravel beaches upto a value of about $H_s/\Delta D_{n50} = 80 - 90$. For smaller values of $H_s/\Delta D_{n50}$ a coefficient p in Equation 4.34 is overestimated by Equation 4.33.

4.6 Verification and application of the model

All the relationships for the height and length parameters, the power curves, the two angles β and γ (and the method used to establish the equivalent slope angles for lower H_0T_0 values) were used to develop a computer program.

This program can be used to calculate the profile, starting from an arbitrary slope and with varying water levels (tide) and wave conditions.

The input required for the computation can be derived from the relationships developed:

The nominal diameter	D_{n50}
The grading of the stone	D_{85}/D_{15}
The relative mass density	Δ
The significant wave height in front of the structure	H_s
The average wave period	T_m
The number of waves	N
The water depth in front of the structure	h
The angle of wave attack	ψ

The (arbitrary) initial slope can be given by characteristic points in an x-y plot, connected by uniform lines. It is also possible to use a profile derived by a previous computation as the initial profile for the next computation. In that case a sequence of storms (including water level variations) can be simulated.

The verification of the model with the test results is very easy. Measured and computed profiles can directly be compared in a plot. A small number of tests is selected here for verification. The test numbers with some additional information is given in Table 4.3. Most of these tests were used to derive the functional relationships which means that verification on these tests is not independent. Tests 396 and 366, however, were not used and give an independent verification.

test	slope	remark
318	1 : 5	basic small scale test
336	1 : 3	basic small scale test
388	berm	non-uniform slope
396	arbitrary	test performed for verification model
508	1 : 5	test of Van Hijum and Pilarczyk
805	1 : 5	Delta flume test
366	1 : 3	storm surge

Table 4.3 Tests selected for verification of the model

The plots with both the measured and computed profiles are shown in Figures 4.39 - 4.45. Some of the boundary conditions are given in the figures.

The agreement between measured and computed profiles of test 318 (Figure 4.39) is very good. Almost no differences can be seen. The differences in Figure 4.40 are more pronounced, but the agreement is still good. The same conclusion can be drawn for the berm profile in Figure 4.41.
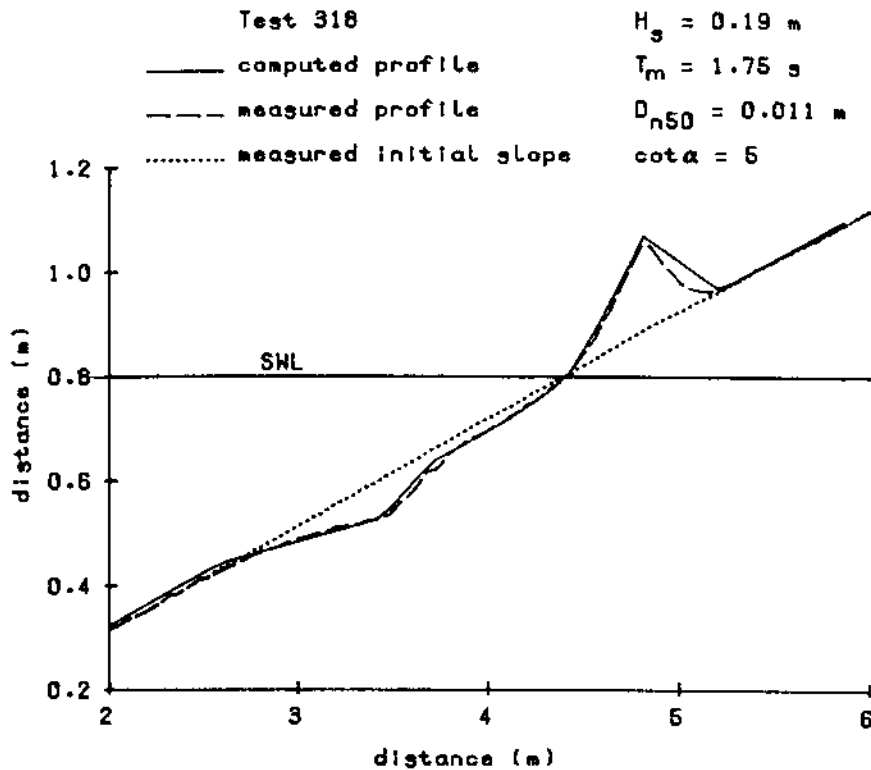
Figure 4.39 Verification of test 318

In test 396 the technician who built all the models was asked to build an arbitrary slope in the way he preferred. Figure 4.42 shows the slope he constructed and the measured and computed profile. The initial slope had an upper slope of 1 in 3 and a lower slope, with some irregularities, varying between 1 in 1.5 and 1 in 2. The agreement between measurement and computation is good.

Figure 4.43 shows the comparison of a test performed by Van Hijum and Pilarczyk (1982). The agreement is good for the lower part of the profile and reasonable for the upper part. Figure 4.44 shows a test in the Delta flume on 4 mm gravel. The differences are more pronounced, but are still acceptable.
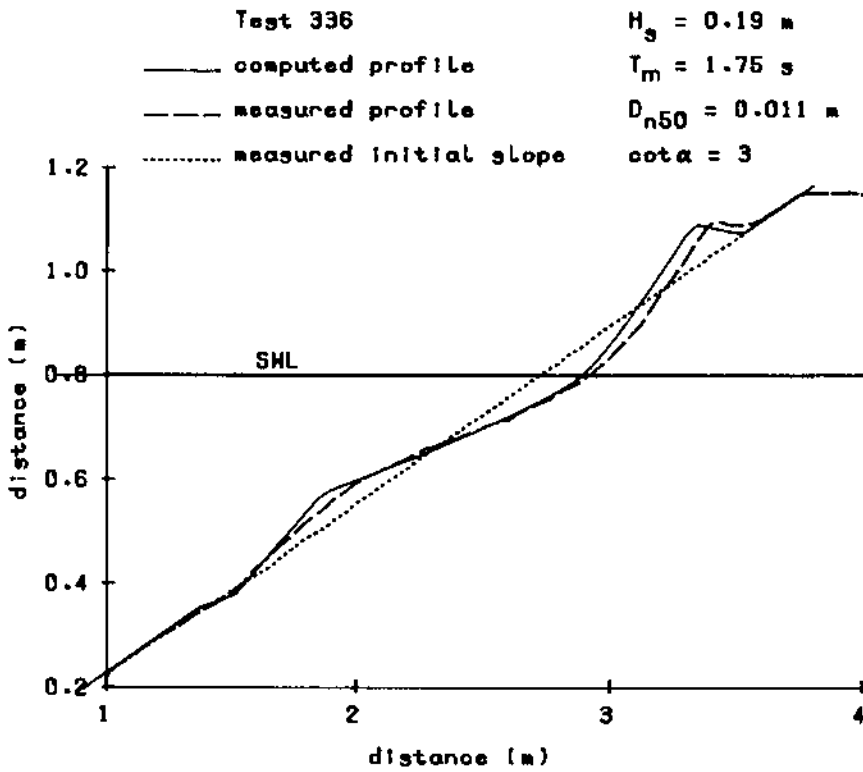
Figure 4.40 Verification of test 336
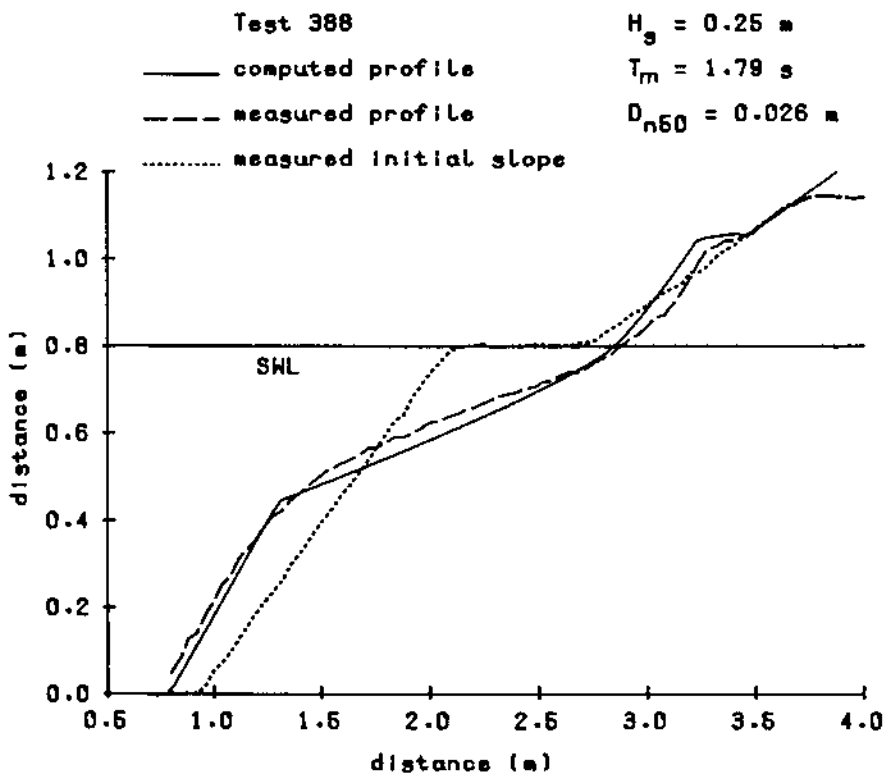
Figure 4.41 Verification of test 388

Test 396 H_s = 0.19 m

———— computed profile T_m = 1.79 s

——— measured profile D_{n50} = 0.026 m

········ measured initial slope
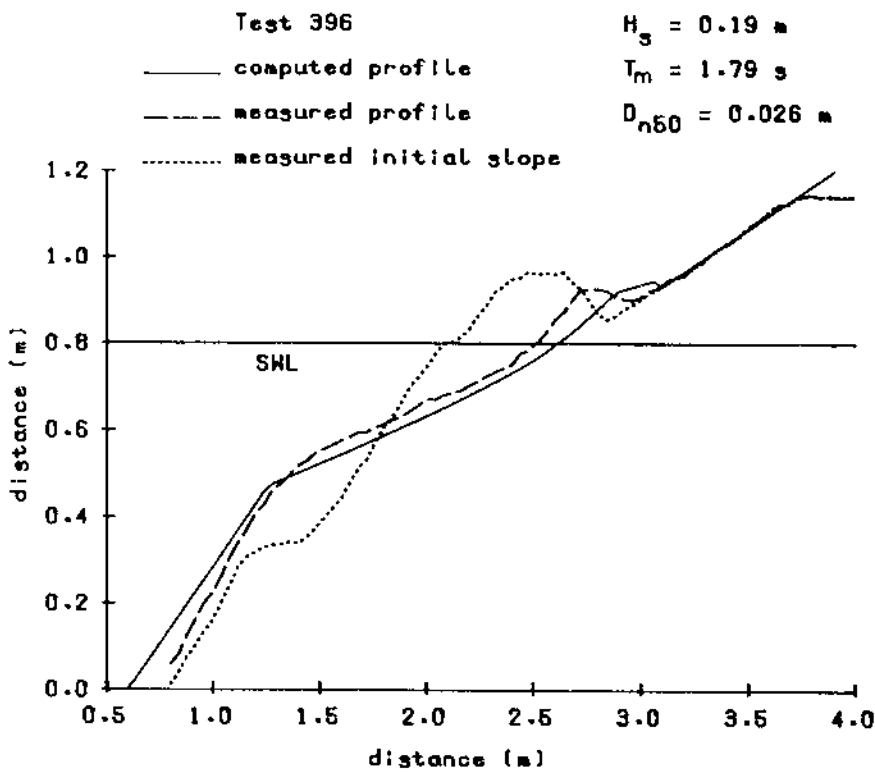
Figure 4.42   Verification of test 396

Test 508 H_s = 0.19 m

———— computed profile T_m = 1.62 s

——— measured profile D_{n50} = 0.004 m

——— initial slope $cot\alpha$ = 5
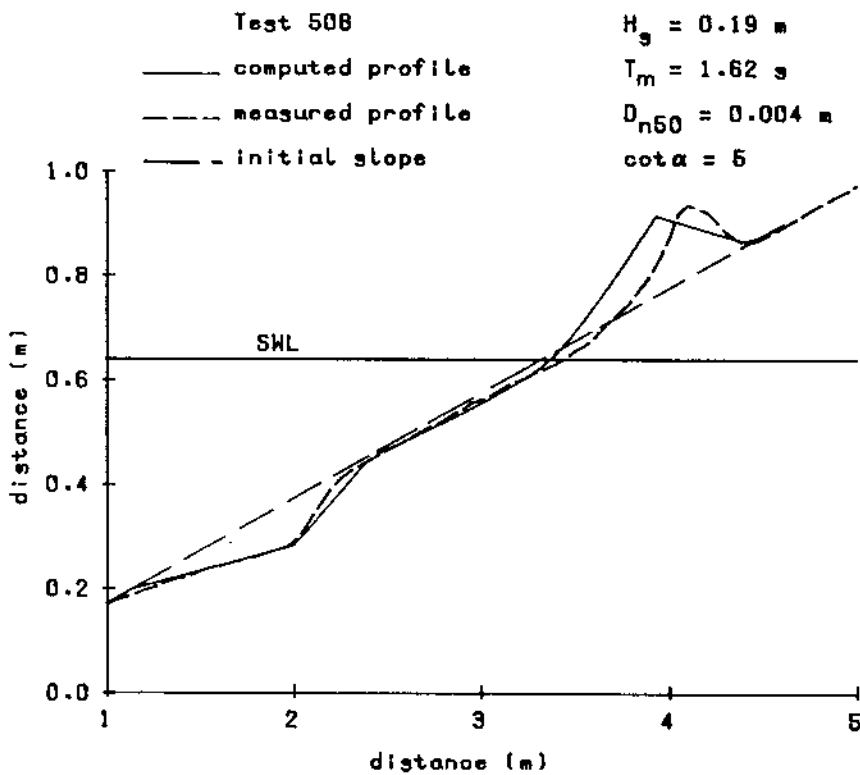
Figure 4.43   Verification of test 508
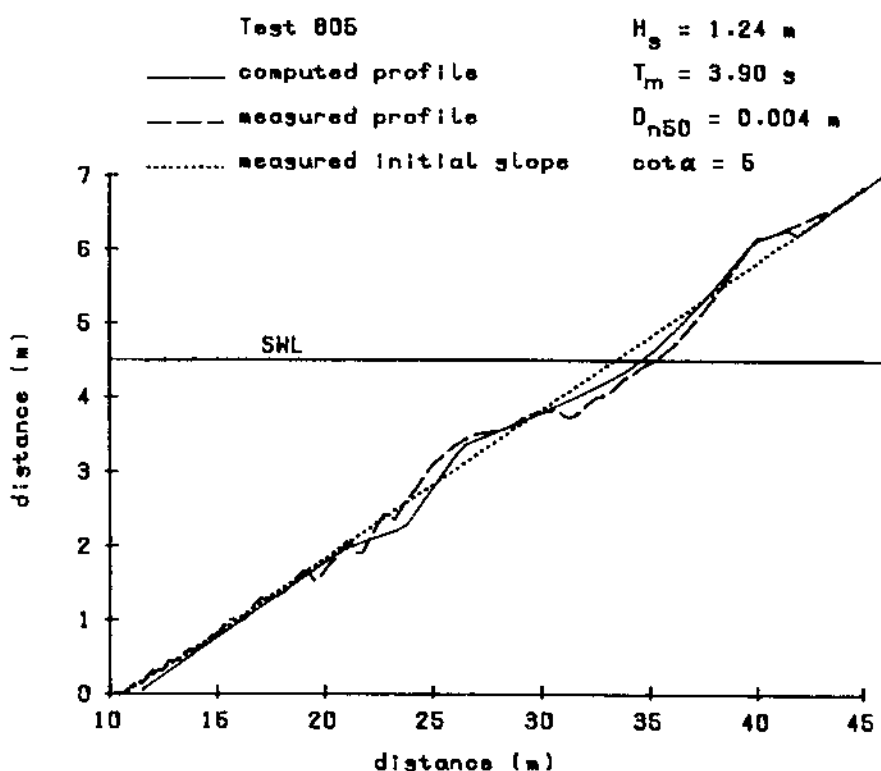
Figure 4.44 Verification of test 805

Above mentioned tests were all performed with constant water level and constant wave boundary conditions during the test. The profile was directly computed from the initial profile. Tests 360 - 378 were performed with varying water levels and wave boundary conditions, as described in Section 4.1 and Figure 4.2. Test 366 was selected for verification.

Four tides of 2 hours were performed in the model with the same wave boundary conditions for the first and fourth tide and also for the second and third tide, see Figure 4.2. The wave height was H_s = 0.13 m for the low tides and H_s = 0.19 m for the high tides. The wave period was T_m = 1.75 s during the whole test.

For the computation each tide was divided into six parts of 20 minutes (N = 20 x 60 / 1.75 = 686). During these parts the water level was kept constant at the average of the tidal curve for that particular part. The first computation was based on the 1 : 3 uniform initial slope. Later computations were based on the profile computed in the previous part of the tidal curve. This resulted in 4 tides x 6 parts = 24 computations, to establish the final profile after 8 hours.

This final profile after 8 hours is shown in Figure 4.45, together with the measured profile. Some differences exist between the two profiles, especially at the lowest part of the profile. The agreement, however, is reasonable.

Test 366 H_s = 0.13 and 0.19 m

_____ computed profile T_m = 1.75 s

_ _ _ measured profile D_{n50} = 0.011 m

.... measured initial slope   cot α = 3
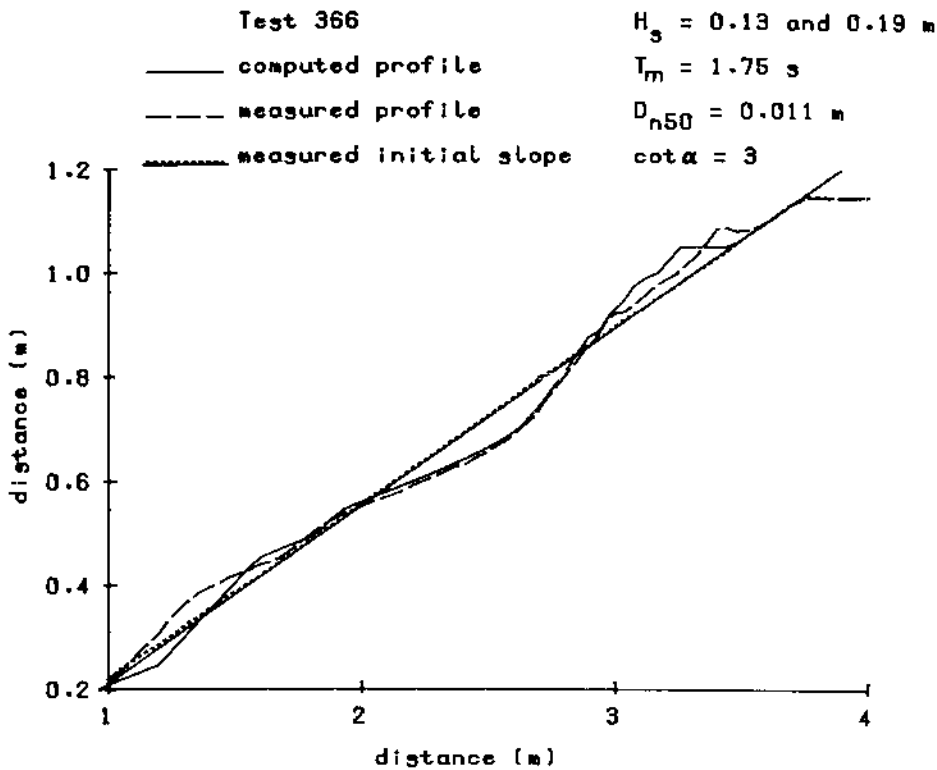
Figure 4.45 Verification of test 366

Tests 318, 336, 388, 508 and 805 were used to establish the relationships for the profile parameters, see Section 4.4. This means that the measured profiles of these tests are not independent of the computed ones. The development of the model was based on these tests. Verification of the model on these tests shows, in fact, the variation of the model with the test results, but only for the range tested.

Test 396, however, was not used in the derivation of relationships. This test with an arbitrary initial slope was solely performed for verification of the computational model. The measured and computed profiles are independent, therefore. Also none of the tests with varying water levels and storm surges (tests 360 - 378) were used in the derivation of relationships. This means that all these tests can be used for an independent verification of the computational model. Figure 4.45 shows the verification of one of these tests and was discussed already.

It can be concluded that the computational model was partly verified on tests which were used to derive the relationships for this model. The agreement between measurement and computation is good in this case. The computational model, however, was also verified on independent tests with arbitrary initial slopes or varying water levels and storm surges. Again verification gave good agreement between measurement and computation.

Prototype data are always scarce and especially on structures which are designed according to new developed concepts. Only a few berm breakwaters were built upto now. The papers presented at the Seminar on Unconventional Rubble Mound Breakwaters, Ottawa, 1987, contained a lot of data on berm breakwaters and gives a good impression of the state of the art of design, construction and behaviour.

The paper of Ryan et al (1987), presented at this Seminar described the behaviour of a prototype berm breakwater under design storm conditions which occurred within half a year after completion of the breakwater. One profile measured after the storm is shown in Figure 4.46 and is compared with a computed profile using the computational model. Differences are probably due to the uncertainty in the hindcasted wave height and the estimation of some parameters which were not given precisely in the paper. The development of storm surge with the corresponding wave heights were not given and also the nominal diameter was not given in the paper (only the grading). Only one wave height (no surge) with a fixed water level and a certain duration was used for the computation. Within these given uncertainties the comparison is fairly good.

It can be concluded, therefore, that the model has proved to be able to predict the behaviour of berm breakwaters.
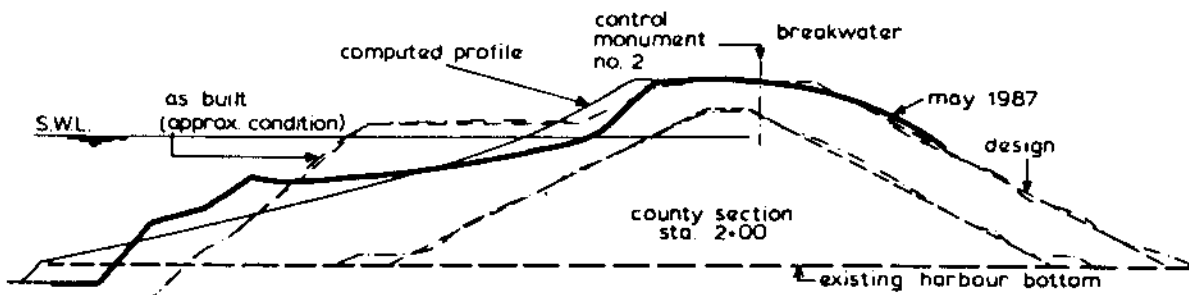
Figure 4.46   Verification on prototype berm breakwater measurements

Application

The model was developed for a large range of possible applications. Quantitatively speaking, the model can compute the profile in the range of $H_s/\Delta D_{n50}$ = 3 - 500 or H_0T_0 = 80 - 100,000. For large values ($H_s/\Delta D_{n50}$ > 10 - 15 or H_0T_0 > 300 - 1000) this results in prediction of the behaviour of rock slopes and gravel beaches during storm surges.

Applications in breakwater design will be limited to the lower regions of $H_s/\Delta D_{n50}$ and H_oT_o. Possible applications in this lower range are:

- The design of berm or mass armoured breakwaters.
- The design of S-shaped breakwaters
- The prediction of the behaviour of filter layers and core under yearly storm conditions for a breakwater under construction.
- The performance of a sensitivity analysis on a designed profile.

A first attempt to design a berm breakwater with the aid of the computational model was performed by the author (Van der Meer (1987-b)). An optimum shape of the initial profile was established under certain restrictions. After choosing the optimum initial profile a sensitivity analysis was performed on this profile. Other possible applications, as mentioned above, will not be treated in this thesis, but will be given in future publications.

REFERENCES

Ahrens, J.P., 1970
The influence of breaker type on riprap stability
Proc. of the 12th ICCE, Washington, USA, Chapter 95

Ahrens, J.P., 1975
Large wave tank tests of riprap stability
CERC, Technical Memorandum No. 51, USA

Ahrens, J.P., 1981
Design of riprap revetments for protection against wave attack
CERC, Technical paper No. 81-5, USA

Ahrens, J.P., 1984
Reef type breakwaters
Proc. 19th ICCE, Houston, USA, Chapter 178

Ahrens, J.P., 1987
Reef breakwater response to wave attack
Seminar on Unconventional Rubble-Mound Breakwaters, Ottawa, Canada

Ahrens, J.P. and McCartney, B.L., 1976
Wave period effect on the stability of riprap
Civil Engineering in the Oceans, pp. 1019 - 1034

Allsop, N.W.H., Bradbury, A.P. and Dibb, T.E., 1985
Rock durability in the marine environment
Hydraulics Research, Wallingford, Report No. SR 11, UK

Arhan, M. and Erzaty, R., 1978
Statistical relations between successive wave heights
Oceanologica Acta, Vol. 1, No. 2

Baird, W.F. and Hall, K.R., 1984
The design of breakwaters using quarried stones
Proc. of the 19th ICCE, Houston, USA, Chapter 173

Baird, W.F., Readshaw, J.S., Scott, R.D. and Turcke, D.J., 1986
A procedure for the analysis and design of concrete armor units
Proc. 20th ICCE, Taipei, Taiwan, Chapter 127

REFERENCES (continued)

Barends, F.B.J., 1985
Geotechnical aspects of rubble mound breakwaters
Developments in Breakwaters, ICE, Proc. Breakwaters '85 Conference, London, UK

Battjes, J.A., 1974a
Computation of set-up, longshore currents, run-up and overtopping due to
wind-generated waves
Comm. on Hydraulics, Dept. of Civil Eng., Delft Univ. of Technology,
Report 74-2, The Netherlands

Battjes, J.A., 1974b
Surf similarity
Proc. 14th ICCE, Copenhagen, Denmark, Chapter 26

Battjes, J.A., 1977
Probabilistic aspects of ocean waves
Delft University of Technology, Report No. 77-2, The Netherlands

Battjes, J.A., 1984
A review of methods to establish the wave climate for breakwater design
Coastal Eng., 8, pp. 141-160

Battjes, J.A. and Roos, A., 1975
Characteristics of flow in run-up of periodic waves
Delft University of Technology, Report No. 75-2, The Netherlands

Battjes, J.A. and Stive, M.J.F., 1985
Calibration and verification of a dissipation model for random breaking
waves
Journal of Geophysical Research, Vol. 90, C5, pp. 9159 - 9167

Battjes, J.A. and Van Vledder, G.Ph., 1984
Verification of Kimura's theory for wave group statistics
Proc. of the 19th ICCE, Houston, USA, Chapter 43

Bergh, H., 1984
Riprap protection of a road embankment exposed to waves
Hydraulic Laboratory, Royal Institute of Technology, Stockholm, Sweden,
Bulletin No. TRITA-VBI-123
In Swedish, with English summary

REFERENCES (contiuned)

Brampton, A.H. and Motyka, J.M., 1985
Modelling the plan shape of shingle beaches
Lecture Notes on Coastal and Estuarine Studies. Vol. 12: Offshore and Coastal
Modelling, England, Chapter 11

Bremner, W., Harper, B.A. and Foster, D.N., 1987
The design and construction of a mass armoured breakwater at Hay Point,
Australia
Seminar on Unconventional Rubble-Mound Breakwaters, Ottawa, Canada

Broderick, L.L., 1983
Riprap stability a progress report
Conf. on Coastal Structures 83, pp. 320 - 330

Broderick, L.L., 1984
Riprap stability versus monochromatic and irregular waves
M. thesis, George Washington University, USA

Broderick, L.L. and Ahrens, J.P., 1982
Riprap stability scale effects
CERC, Technical Paper No. 82-3, USA

Bruun, P., 1981
Port Engineering
The Gulf Publishing Company, Houston, USA

Bruun, P., 1984
Beach and dune erosion during storm surges
Discussion in Coastal Eng., 8, pp. 171 - 177

Bruun, P., 1985
Design and construction of mounds for breakwaters and coastal protection
Developments in geotechnical engineering, 37, Elsevier, Amsterdam,
The Netherlands

Bruun, P. and Johannesson, P., 1974
A critical review of the hydraulics of rubble mound structures
The University of Trondheim, Report R3, Norway

REFERENCES (continued)

Bruun, P. and Johannesson, P., 1976
Parameters affecting stability of rubble mounds
Proc. ASCE, Journal of WH and CED, Vol. 102, No. WW2, pp. 141 - 164

Burcharth, H.F., 1979
The effect of wave grouping on on-shore structures
Coastal Eng., 2, pp. 229 - 251

Burcharth, H.F., 1980
Full scale trials of Dolosse to destruction
Aalborg University Center, Bulletin No. 17, Denmark

Burcharth, H.F., 1981a
A comparison of nature waves and model waves with special reference to wave grouping
Coastal Eng., 4, pp. 303 - 318

Burcharth, H.F., 1981b
A design method for impact-loaded slender armour units
Aalborg University Center, Bulletin H2 18, Denmark

Burcharth, H.F., 1984
Fatigue in breakwater concrete armour units
Proc, 19th ICCE, Houston, USA, Chapter 174

Burcharth, H.F. and Frigaard, P., 1987
On the stability of berm breakwater roundheads and trunk erosion in oblique waves
Seminar on Unconventional Rubble-Mound Breakwater, Ottawa, Canada

Cartwright, D.E. and Longuet-Higgins, M.S., 1956
The statistical distribution of the maxima of a random function
Proc. Royal Soc., London, A, 237, pp. 212 - 232, UK

Carver, R.D., 1980
Effect of first underlayer weight on the stability of stone-armoured rubble mound breakwater trunks subjected to non-breaking waves with no overtopping
WES, Technical Report HL-80-1, USA

REFERENCES (continued)

CIAD, Project group breakwaters, 1985
Computer aided evaluation of the reliability of a breakwater design
Zoetermeer, The Netherlands

Coastal Engineering Research Center, 1984
Shore Protection Manual
U.S. Army Corps of Engineers, USA

Costa, F.V., 1980
Identification and quantification of individual scale effects in rubble
mound breakwater models
International Seminar, Santander, Spain

Dai, Y.B and Kamel, A.M., 1969
Scale effect tests for rubble-mound breakwaters
WES, Research Report H-69-2, USA

Dean, R.G., 1977
Equilibrium beach profiles: US Atlantic and Gulf Coasts
Newark, University of Delaware, Dep. of Civil Eng., Ocean Engineering Report
No. 12, USA

DELFT HYDRAULICS-ENDEC, 1986
ENDEC, wave propagation model. User's manual

DELFT HYDRAULICS-H24, 1987
Golfoverslag Afsluitdijk. Verslag modelonderzoek (Wave overtopping at the
Afsluitdijk. Report on model investigation), in Dutch

DELFT HYDRAULICS-M1216, 1974
Grindstranden. Evenwichtsprofiel bij loodrechte regelmatige golfaanval
Verslag modelonderzoek, deel I. (Gravel beaches. Equilibrium profile under
monochromatic and perpendicular wave attack. Report on model investigation,
Part I), in Dutch

DELFT HYDRAULICS-M1216, 1975
Grindstranden. Evenwichtsprofiel bij loodrechte regelmatige golfaanval
Verslag modelonderzoek, deel II. (Gravel beaches. Equilibrium profile under
monochromatic and perpendicular wave attack. Report on model investigation,
Part II), in Dutch

REFERENCES (continued)

DELFT HYDRAULICS-M1216, 1979
Grindstranden. Evenwichtsprofiel bij loodrechte onregelmatige golfaanval
Verslag modelonderzoek, deel III. (Gravel beaches. Equilibrium profile under
irregular and perpendicular wave attack. Report on model investigation, Part
III), in Dutch

DELFT HYDRAULICS-M1216, 1981
Grindstranden. Evenwichtsprofiel en langstransport bij scheve onregelmatige
golfaanval. Verslag modelonderzoek, deel IV. (Gravel beaches. Equilibrium
profile under irregular and oblique wave attack. Report on model
investigation, Part IV), in Dutch

DELFT HYDRAULICS-M1968, 1983a
Golfbrekers. Sterkte betonnen afdekelementen - Belastingen. (Breakwaters.
Strength of concrete armour units - Loads), confidential report in Dutch

DELFT HYDRAULICS-M1968, 1983b
Golfbrekers. Sterkte betonnen afdekelementen - Bloksterkte. (Breakwaters.
Strength of concrete armour units - Strength of block), confidential report
in Dutch

DELFT HYDRAULICS-M1809, 1984
Taluds van losgestorte materialen. Hydraulische aspecten van stortsteen,
grind en zandtaluds onder golfaanval. Verslag literatuurstudie. (Slopes of
loose materials. Hydraulic aspects of rock, gravel and sand slopes under
wave attack. Report on literature), in Dutch

DELFT HYDRAULICS-M2006, 1986
Taluds van losgestorte materialen. Stabiliteit van stortsteen-bermen en
teenkonstrukties. Verslag literatuurstudie en modelonderzoek. (Slopes of
loose materials. Stability of rubble mound berm and toe structures. Report
on literature and model investigation), in Dutch

DELFT HYDRAULICS-M1983, 1988a
Taluds van losgestorte materialen. Statische stabiliteit van stortsteen
taluds onder golfaanval. Onwerp formules. Verslag modelonderzoek, deel I
(Slopes of loose materials. Static stability of rubble mound slopes under
wave attack. Design formulae. Report on model investigation, Part I), in
Dutch

REFERENCES (continued)

DELFT HYDRAULICS-M1983, 1988b
Taluds van losgestorte materialen. Dynamische stabiliteit van grind- en
stortsteen taluds onder golfaanval. Model voor profielvorming. Verslag
modelonderzoek, deel II. (Slopes of loose materials. Dynamic stability of
gravel beaches and rubble mound slopes under wave attack. Model for profile
formation. Report on model investigation, Part II), in Dutch

Den Boer, K., 1985
Damage to armour units: Model Technique
Proc. ASCE, Journal of WPC and OE, Vol. 111, No. 5

Desai, H.C., 1976
Volume and strength of a dolos
Proc. ASCE, Journal of WHC and CED, Vol. 102, No. WW1

Foster, D.N. and Khan, S.P., 1984
Stability of overtopped rock armoured breakwaters
University of New South Wales, Water Research Laboratory, Australia,
Report No. 161

Funke, E.R. and Mansard, E.P.D., 1980
On the synthesis of realistic sea states
Proc. of the 17th ICCE, Hamburg, West Germany, Chapter 179

Givler, L.D. and Sorensen, R.M., 1986
An investigation of the stability of submerged homogeneous rubble-mound
structures under wave attack
Lehigh University, Imbt. Hydraulics Laboratory, Pennsylvania, Report IHL-110-
86, USA

Goda, Y., 1970
Numerical experiments on wave statistics with spectral simulation
Rept. Port and Harbour Research Institute, Vol. 9, No. 3, Japan

Goda, Y., 1976
On wave groups
BOSS 76, pp. 115 - 129

Gravesen, H., Jensen, O.J. and Sörensen, T., 1979
Stability of rubble mound breakwaters II
Conf. on Coastal Structures 79, Virginia, USA

REFERENCES (continued)

Günbak, A.L., 1978
Tests on a 1:2.5 rubble-mound breakwater; irregular waves
University of Trondheim, Norway, Report 2-1978

Günbak, A.L., 1979
Rubble-mound breakwaters
University of Trondheim, Norway, Report 1-1979

Hall, K.R., Baird, W.F. and Turcke, D.J., 1984
Structural design procedures for concrete armour units
Proc. 19th ICCE, Houston, USA, Chapter 172

Hedar, P.A., 1960
Stability of rock-fill breakwaters
Doctoral thesis, University of Goteborg, Sweden

Hedar, P.A., 1986
Armor layer stability of rubble-mound breakwaters
Proc. ASCE, Journal of WPC and OE, Vol. 112, No. 3

Heydra, G. and Den Boer, K., 1985
Rubble mound breakwaters in the Mediterranean
Proc. Symposium on Maritime Structures in the Mediterranean Sea, Athens, Greece

Hölscher, P. and Barends, F.B.J., 1986
Transport in porous media
Delft Geotechnics, internal report, The Netherlands

Hudson, R.Y., 1958
Design of quarry stone cover layers for rubble mound breakwaters
WES, Research Report No. 2-2, USA

Hudson, R.Y., 1959
Laboratory investigations of rubble mound breakwaters
WES Report, Vicksburg, USA

Hudson, R.Y., 1975
Reliability of rubble mound breakwater stability models
WES, Vicksburg, Miscellaneous Paper H-75-5, USA

REFERENCES (continued)

IAHR/PIANC, 1986
List of sea state parameters
Supplement of Bulletin No. 52 (1986)

Iribarren, R.C., 1938
Una formula para el calcula de los diques de escollera. (A formula for the calculation of rock-fill dikes)
Revista de Obras Publicas, Madrid
Translated by D. Heinrich, Technical Report HE-116-295, University of California, 1948, USA

Iribarren, R.C., 1950
Generalizacion de la formula para el calculo de los diques de escollera y comprobacion de sus coeficientes. (Generalization of the formula for calculation of rock fill dikes and verification of its coefficients)
Revista de Obras Publicas, Madrid
Translated by A. Haritos, WES Translation N. 51-4, 1951, USA

Jensen, O.J., 1984
A monograph on rubble mound breakwaters
Danish Hydraulic Institute, Denmark

Jensen, O.J. and Klinting, P., 1983
Evaluation of scale effects in hydraulic models by analysis of laminar and turbulent flows
Coastal Eng., 7, pp. 319 - 329

Klein Breteler, M. and Van der Meer, J.W., 1984
Stability of rubble mound breakwaters. Influence of contact friction and natural angle of repose of armour units. Report on basic research, S467
Volume III, DELFT HYDRAULICS, The Netherlands

Klinting, P. and Sand, S.E., 1987
Analysis of prototype freak waves
Proc. ASCE, Conf. on Coastral Hydrodynamics, Delaware, USA

Kobayashi, N. and Jacobs, B.K., 1985a
Riprap stability under wave action
Proc. ASCE, Journal of WPC and OE, Vol. 111, No. 3

REFERENCES (continued)

Kobayashi, N. and Jacobs, B.K., 1985b
Stability of armor units on composite slopes
Proc. ASCE, Journal of WPC and OE, Vol. 111, No. 5

Kobayashi, N., Roy, I. and Otta, A.K., 1986
Numerical simulation of wave runup and armor stability
Proc. 18th Annual OTC, Houston, pp. 51 - 60, USA

Kobayashi, N. and Otta, A.K., 1987
Hydraulic stability analysis of armor units
Proc. ASCE, Journal of WPC and OE, Vol. 113, No. 2

Kobayashi, N., Otta, A.K. and Roy, I., 1987
Wave reflection and run-up on rough slopes
Proc. ASCE, Journal of WPC and OE, Vol. 113, No. 3

Kogami, Y., 1978
Researches on stability of rubble mound structures
Kajima Institute of Constuction Technology, Tokyo, Report No. 29, Japan

Latham, J.P. and Poole, A.B., 1986
The quantification of breakwater armour profiles for design purposes
Coastal Eng., 10, pp. 253-273

Latham, J.P. and Poole, A.B., 1987
The application of shape descriptor analysis to the study of aggregate wear
Quarterly Journal of Engineering Geology, London, Vol. 21, UK

Lillevang, O.J. and Nickola, W.E., 1976
Experimental studies of stresses within the breakwater armour piece "Dolos"
Proc. 15th ICCE, Honolulu, Hawaii, Chapter 145

Losada, M.A. and Giménez-Curto, L.A., 1979a
The joint effect of the wave height and period on the stability of rubble
mound breakwaters using Iribarren's number
Coastal Eng., 3, pp. 77 - 96

Losada, M.A. and Giménez-Curto, L.A., 1979b
An approximation to the failure probability of maritime structures under a
seastate
Proc. POAC 1979, Spain, pp. 1269 -1281

REFERENCES (continued)

Losada, M.A. and Giménez-Curto, L.A., 1981
Flow characteristics on rough, permeable slopes under wave action
Coastal Eng., 4, pp. 187 - 206

Losada, M.A. and Giménez-Curto, L.A., 1982
Mound breakwaters under oblique wave attack; a working hypothesis
Coastal Eng., 6, pp. 83 - 92

Nielsen, S.R.K. and Burcharth, H.F., 1983
Stochasic design of rubble mound breakwaters
Proc. 11th IFIP Conf. on System Modelling and Optimization, Copenhagen,
Denmark

Nishigori, W., Endo, T. and Shimada, A., 1986
On stress in tetrapods under wave action
Proc. 20th ICCE, Taipei, Taiwan, Chapter 156

PIANC, 1976
Final Report of the International Commission for the study of waves, second
part
Annex to bulletin No. 25, Vol. III/1976

PIANC, 1980
Final Report of the International Commission for the study of waves, third
part
Annex to bulletin No. 36, Vol. II/1980

Pilarczyk, K.W. and Den Boer, K., 1983
Stability and profile development of coarse materials and their application in
coastal engineering
Proc. Int. Conf. on Coastal and Port Eng. in Developing Countries, Colombo,
Sri Lanka

Popov, I.J., 1960
Experimental research in formation by waves of stable profiles of upstream
faces of earth dams and reservoir shores
Proc. 7th ICCE, The Hague, The Netherlands, Chapter 16

REFERENCES (continued)

Powel, K.A., 1986
The hydraulic behaviour of shingle beaches under regular waves of normal incidence
Doctoral thesis, University of Southampton, Department of Civil Engineering, UK

Price, W.A., 1978
Some ideas on breakwaters
Proc. 16th ICCE, Hamburg, West Germany, Theme speech

Raichlen, F., 1974
The effect of waves on rubble-mound structures
Annual review of Fluid Mechanics, Vol. 7, 2975, pp. 327 - 356

Rice, S.O., 1945
Mathematical analysis of random noise
Vell System Tech. Journal, 23, pp. 282-332, 24, pp. 46-156

Ryan, L.W., Montgomery, R.J., Hofmeister, G.G. and Baird W.F., 1987
Implementation and performance of berm breakwater design at Racine, Wisconsin
Seminar on Unconventional Rubble-Mound Breakwaters, Ottawa, Canada

Rye, H. and Lervik, E., 1981
Wave grouping studied by means of correlation techniques
International Symposium on Hydrodynamics in Ocean Engineering, pp. 25 - 48

Ryu C.R. and Sawaragi, T., 1986
Wave control functions and design principles of composite slope rubble mound structures
Coastal Eng. in Japan, Vol. 29, pp.227 - 240

Sawaragi, T., Ruy, C.R. and Iwata, K., 1983
Considerations of the destruction mechanism of rubble mound breakwaters due to the resonance phenomenon
Proc. 8th Int. Harbour Congress, Antwerp, Belgium

Sawaragi, T., Ryu, C.R. and Kusumi, M., 1985
Destruction mechanism and design of rubble mound structures by irregular waves
Coastal Eng. in Japan, Vol. 28, pp. 173 - 189

REFERENCES (continued)

Scott, R.D., Turcke, D.J. and Baird, W.F., 1986
A unique instrumentation scheme for measuring loads in model dolos units
Proc. 20th ICCE, Taipei, Taiwan, Chapter 163

Shimada, A., Fujimoto, T., Saito, S., Sakakiyama, T. and Hirakuchi, H., 1986
Scale effects on stability and wave reflection regarding armor units
Proc. 20th ICCE, Taipei, Taiwan, Chapter 165

Siggurdson, G., 1962
Wave forces on breakwater capstones
Proc. ASCE, Journal of WHC and CED, Vol. 88, No. WW3

Smith, O.P., 1987
Cost-effectiveness of breakwater cross-sections
Proc. ASCE, Journal of WPC and OE, Vol. 113, No. 5

Sörensen, T. and Jensen, O.J., 1985
Reliability of hydraulic models of rubble-mound breakwaters as proven by
prototype measurements
The Dock & Harbour Authority, March, pp. 155 - 157

Stam, C.J.M., 1988
De korrelatieparameter in de twee-dimensionale Rayleigh kansdichtheidsfunktie
voor opeenvolgende golfhoogten. Een vergelijking van berekeningsmethoden. (The
correlation coefficient in the bivariate Rayleigh probability density function
of successive wave heights. A comparison of computation methods)
DELFT HYDRAULICS Report M1983/H198. Technical University Delft, The
Netherlands, in Dutch

Stive, M.J.F. and Battjes, J.A., 1984
A model for offshore sediment transport
Proc. 19th ICCE, Houston, USA, Chapter 97

Tautenhain, E., Kohlhase, S., Partenscky, H.W., 1982
Wave run-up at sea dikes under oblique wave approach
Proc. 18th ICCE, Cape Town, South Africa, Chapter 50

Technical Advisory Committee on Protection against Inundation (TAW), 1974
Wave run-up and overtopping
Covernment Publishing Office, The Hague, The Netherlands

REFERENCES (continued)

Thompson, D.M. and Shuttler, R.M., 1975
Riprap design for wind wave attack. A laboratory study in random waves
HRS, Wallingford, Report EX 707, UK

Thompson, D.M. and Shuttler, R.M., 1976
Design of riprap slope protection against wind waves
HRS, Wallingford, CIRIA Report 61, UK

Thompson, E.F. and Vincent, C.L., 1985
Significant wave height for shallow water design
Proc. ASCE, Journal of WPC and OE, Vol. 111, No. 5

Thomsen, A.L., Wohlt, P.E. and Harrison, 1972
Riprap stability on earth embankments tested in large- and small-scale wave tanks
CERC, Technical Memorandum No. 37, USA

Timco, G.W., 1983a
On the structural integrity of dolos under dynamic loading conditions
Coastal Eng., 7, pp. 91 -101

Timco, G.W., 1983b
An analysis of the breakage of concrete armour units on rubble-mound breakwaters
National Research Council, Canada, Technical Report 1983/09

Timco, G.W., 1984
On the stability criterion for fracture in dolos armoured breakwaters
Coastal Eng., 8, pp. 161 -171

Uhlenbeck, G.E., 1943
Theory of Random process
MIT Radiation Laboratory, Report 454

Van der Meer, J.W., 1985
Stability of rubble mound revetments and breakwaters under random wave attack
Development in Breakwaters, ICE, Proc. Breakwaters '85 Conference, London, UK

REFERENCES (continued)

Van der Meer, J.W., 1986a
Stability of rubble mound breakwaters. Stability formula for breakwaters
armoured with Cubes
DELFT HYDRAULICS. Report on basic research, S467 Volume VI, The Netherlands

Van der Meer, J.W., 1986b
Deterministic and probabilistic design of breakwater armour layers
The Dock & Harbour Authorithy, December, pp. 177 - 180

Van der Meer, J.W., 1987a
Stability of breakwater armour layers - Design formulae
Coastal Eng., 11, pp. 219 - 239

Van der Meer, J.W., 1987b
Application of computational model on berm breakwater design
Seminar on Unconventional Rubble-Mound Breakwaters, Ottawa, Canada

Van der Meer, J.W., 1987c
Stability of rubble mound breakwaters. Stability formula for breakwaters
armoured with Tetrapods
DELFT HYDRAULICS. Report on basic research, H462 Volume II, The Netherlands

Van der Meer, J.W., 1987d
Stability of rubble mound breakwaters. Stability formula for breakwaters
armoured with Accropode (R)
DELFT HYDRAULICS. Report on basic research, H546, The Netherlands

Van der Meer, J.W., 1988
Deterministic and probabilistic design of breakwater armor layers
Proc. ASCE, Journal of WPC and OE, Vol. 114, No. 1

Van der Meer, J.W. and Pilarczyk, K.W., 1984
Stability of rubble mound slopes under random wave attack
Proc. 19th ICCE, Houston, USA, Chapter 176

Van der Meer, J.W. and Pilarczyk, K.W., 1986
Dynamic stability of rock slopes and gravel beaches
Proc. 20th ICCE, Taipei, Taiwan, Chapter 125

REFERENCES (continued)

Van der Meer, J.W. and Pilarczyk, K.W., 1987
Stability of breakwater armour layers - Deterministic and probabilistic design
Delft Hydraulics Communication No. 378, The Netherlands

Van Hijum, E., 1974
Equilibrium profiles of coarse material under wave attack
Proc. 14th ICCE, Copenhagen, Denmark, Chapter 54

Van Hijum, E., 1976
Equilibrium profiles and longshore transport of coarse material under wave attack
Proc. 14th ICCE, Honolulu, Hawaii, Chapter 74

Van Hijum, E. and Pilarczyk, K.W., 1982
Equilibrium profile and longshore transport of coarse material under regular and irregular wave attack
DELFT HYDRAULICS, Publication No. 274, The Netherlands

Van Oorschot, J.H. and d'Angremond, K., 1968
The effect of wave energy spectra on wave run-up
Proc. 11th ICCE, London, UK, Chapter 68

Vellinga, P., 1982
Beach and dune erosion during storm surges
Coastal Eng., 6, pp. 361 - 387

Vellinga, P., 1984
A tentative description of a universal erosion profile for sandy beaches and rock beaches
Discussions in Coastal Eng., 8, pp. 177 - 188

Vellinga, P., 1986
Beach and dune erosion during storm surges
Delft University of Technology. Doctoral thesis, The Netherlands

Walton, I.L. and Weggel, J.R., 1981
Stability of rubble-mound breakwaters
Proc. ASCE, Journal of WPC and OE, Vol. 107, No. WW3, pp. 195 - 201

Whillock, A.F. and Price, W.A., 1976
Armour blocks as slope protection
Proc. 15th ICCE, Honolulu, Hawaii, Chapter 147

LIST OF SYMBOLS

A	=	erosion area in a cross-section
a_n	=	n-th amplitude in time series
$\overline{a^2}$	=	average of the squared amlitudes
C	=	coefficient
C_1	=	coefficient
C_2	=	coefficient
D	=	diameter

index:
n	=	nominal diameter, $(W/\rho_a)^{1/3}$
15	=	15 % value of sieve curve
50	=	50 % value of sieve curve
85	=	85 % value of sieve curve
90	=	90 % value of sieve curve
n50	=	nominal diameter, $(W_{50}/\rho_a)^{1/3}$
armour	=	diameter of stones of armour layer
filter	=	diameter of stones of filter layer
core	=	diameter of stones of core

F	=	wave force
F_N	=	wave force normal to the slope
F_p	=	wave force parallel to the slope
H	=	monochromatic wave height

index:
s	=	signicant wave height, average of the highest one-third of the waves
n%	=	n percent value of wave height exceedance curve
10	=	average of highest one-tenth of the waves
rms	=	rooth mean square wave height, $2\sqrt{2m_o}$

H_o	=	dimensionless wave height parameter, $H_s/\Delta D_{n50}$
H(t)	=	wave height envelope
$\overline{H^2}$	=	average of squared wave heights
H_oT_o	=	dimensionless wave height-wave period parameter, $H_s/\Delta D_{n50} * \sqrt{g/D_{n50}}\ T_m$
K	=	coefficient
K_1	=	coefficient
K_2	=	coefficient
K_D	=	stability coefficient in Hudson formula
L	=	wave length, $gT^2/2\pi$
N	=	number of waves
N_Δ	=	damage level defined by Thompson and Shuttler (1975)
P	=	permeability coefficient
Q	=	volume of water dissipating in core of breakwater, per wave period and meter width
R_c	=	crest height of structure

LIST OF SYMBOLS (continued)

Re	=	Reynolds number, $\sqrt{gH_s}\ D_{n50}/\nu$
R(t)	=	amplitude envelope
S	=	damage level, A/D_{n50}^2
S(f)	=	spectral density as a function of f
S_R	=	coefficient, $\mu \cos\alpha + \sin\alpha$
T	=	wave period

index: p = peak period

      s = significant period, average of periods belonging to highest one-third of the waves

      m = average wave period of a time signal

T_o	=	dimensionless wave height parameter related to D_{n50}, $\sqrt{g/D_{n50}}\ T_m$
W_{50}	=	average mass of stone class
W'	=	mass of stone under water

a	=	amplitude
a	=	coefficient in regression analysis
b	=	coefficient in regression analysis
c	=	coefficient in regression analysis
f	=	frequency
g	=	accelaration of gravity
h	=	water depth
h	=	height parameter in dynamically stable profile

index: c = crest height

      s = step height

      t = transition height

1	=	length parameter in dynamically stable profile

index: c = crest length

      r = runup length

      s = step length

m_n	=	n-th spectral moment
p	=	coefficient
par	=	one of the height of length parameters, h_c, h_s, h_t, l_c, l_r or l_s
s_m	=	ficticious wave steepness, $2\pi H_s/gT_m^2$
t	=	time
t_a	=	thickness of armour layer
u	=	velocity of water
w_c	=	crest width
w	=	fall velocity of sand in water
x	=	x-axis
y	=	y-axis

LIST OF SYMBOLS (continued)

α =   angle of seaward slope of structure

β =   angle in dynamically stable profile

γ =   angle in dynamically stable profile

Δ =   relative mass density, $(\rho_a - \rho)/\rho$

κ =   parameter of the bivariate Rayleigh probability density function

           index: f   = based on spectrum

                  aa.t = based on successive amplitudes in time domain

                  HH.t = based on successive wave heights in time domain

μ =   tangent of natural angle of repose, $\tan\phi$

ν =   dynamic fluid viscosity

ξ =   surf similarity parameter, $\tan\alpha/\sqrt{H/L}$

ξ_m =   surf similarity parameter using T_m, $\tan\alpha/\sqrt{2\pi H_s/gT_m^2}$

ξ_p =   surf similarity parameter using T_p, $\tan\alpha/\sqrt{2\pi H_s/gT_p^2}$

ρ =   mass density of water

ρ_a =   mass density of stone

ρ_b =   bulk density

σ =   standard deviation

τ =   time step

ϕ =   natural angle of repose

ψ =   angle of wave attack

LIST OF TABLES

LIST OF FIGURES

LIST OF FIGURES (continued)

APPENDIX I

Boundary conditions and damage for tests on static stability

parameters in columns

column	description

1   test number

2   remark: Rock imperm = impermeable rock slope with PM spectrum

               Rock perm   = permeable rock slope with PM spectrum

               Rock hom   = homogeneous structure with PM spectrum

               Spectrum   = spectrum different from PM spectrum

               Depth 0.4 m = structure with 1:30 foreshore and water depth
of 0.40 m at the toe of the structure

               Depth 0.2 m = structure with 1:30 foreshore and water depth
of 0.20 m at the toe of the structure

               Density   = rock with high or low mass density

               Large scale = tests in Delta flume

               Low crest 1 = crest at SWL

               Low crest 2 = crest 0.125 m above SWL

               Low crest 3 = crest 0.10 m below SWL

3   permeability: - = impermeable core

                 + = permeable core

                 H = homogeneous structure

4   nominal diameter, D_{n50} (m)

5   relative mass density, Δ

6   slope angle, $\cot\alpha$

7   grading, D_{85}/D_{15}

8   spectral shape: PM = Pierson Moskowitz spectrum

                     NA = narrow spectrum

                     WI = wide spectrum

9   significant wave height in front of the structure, H_s (m)

10   average wave period, T_m (s)

11   peak period, T_p (s)

12   wave height parameter: $H_s/\Delta D_{n50}$

13   surf similarity parameter: $\xi_m = \tan\alpha/\sqrt{2\pi H_s/gT_z^2}$

14   surf similarity parameter: $\xi_p = \tan\alpha/\sqrt{2\pi H_s/gT_p^2}$

15   damage, S, after 1000 waves

16   damage, S, after 3000 waves

1	2	3	4	5	6	7	8	9	10	11	12	13	14	15	16
2	Rock imperm	-	.0360	1.630	2.0	2.25	PM	.0858	1.85	2.08	1.46	3.95	4.44	3.45	6.39
3	Rock imperm	-	.0360	1.630	2.0	2.25	PM	.0464	1.85	2.13	.79	5.37	6.18	.35	.65
4	Rock imperm	-	.0360	1.630	2.0	2.25	PM	.0772	1.85	2.13	1.32	4.16	4.79	3.26	6.54
5	Rock imperm	-	.0360	1.630	2.0	2.25	PM	.0701	1.85	2.13	1.19	4.37	5.03	.81	1.57
6	Rock imperm	-	.0360	1.630	2.0	2.25	PM	.0733	2.19	2.56	1.25	5.05	5.91	2.04	2.45
7	Rock imperm	-	.0360	1.630	2.0	2.25	PM	.0827	2.18	2.53	1.41	4.74	5.50	4.78	9.20
8	Rock imperm	-	.0360	1.630	2.0	2.25	PM	.0657	2.19	2.60	1.12	5.34	6.34	1.17	1.49
9	Rock imperm	-	.0360	1.630	2.0	2.25	PM	.0557	2.19	2.56	.95	5.80	6.78	.56	.71
10	Rock imperm	-	.0360	1.630	2.0	2.25	PM	.0795	2.19	2.56	1.35	4.85	5.67	2.14	3.42
11	Rock imperm	-	.0360	1.630	2.0	2.25	PM	.0751	2.69	3.13	1.28	6.13	7.14	1.24	1.39
12	Rock imperm	-	.0360	1.630	2.0	2.25	PM	.0658	2.69	3.13	1.12	6.55	7.62	.56	62
13	Rock imperm	-	.0360	1.630	2.0	2.25	PM	.0553	2.69	3.13	.94	7.15	8.32	.76	1.09
14	Rock imperm	-	.0360	1.630	2.0	2.25	PM	.0841	2.68	3.17	1.43	5.77	6.83	3.59	5.85
15	Rock imperm	-	.0360	1.630	2.0	2.25	PM	.0931	2.68	3.17	1.59	5.49	6.49	32.63	-1.00
16	Rock imperm	-	.0360	1.630	2.0	2.25	PM	.0871	3.11	3.85	1.48	6.58	8.15	5.32	7.12
17	Rock imperm	-	.0360	1.630	2.0	2.25	PM	.0756	3.13	3.64	1.29	7.11	8.27	.32	.76
18	Rock imperm	-	.0360	1.630	2.0	2.25	PM	.0942	3.08	3.70	1.61	6.27	7.53	22.41	-1.00
19	Rock imperm	-	.0360	1.630	2.0	2.25	PM	.0818	3.13	3.70	1.39	6.84	8.08	2.78	3.43
21	Rock imperm	-	.0360	1.630	3.0	2.25	PM	.1177	2.18	2.53	2.01	2.65	3.07	10.09	23.80
22	Rock imperm	-	.0360	1.630	3.0	2.25	PM	.0995	2.21	2.56	1.70	2.92	3.38	3.02	6.71
23	Rock imperm	-	.0360	1.630	3.0	2.25	PM	.0858	2.19	2.53	1.46	3.11	3.60	1.47	3.09
24	Rock imperm	-	.0360	1.630	3.0	2.25	PM	.1085	2.19	2.53	1.85	2.77	3.20	4.89	9.16
25	Rock imperm	-	.0360	1.630	3.0	2.25	PM	.0705	2.17	2.53	1.20	3.40	3.97	.80	1.88
26	Rock imperm	-	.0360	1.630	3.0	2.25	PM	.1173	2.65	3.17	2.00	3.22	3.86	14.40	29.07
27	Rock imperm	-	.0360	1.630	3.0	2.25	PM	.0996	2.66	3.08	1.70	3.51	4.06	4.82	7.46
28	Rock imperm	-	.0360	1.630	3.0	2.25	PM	.0844	2.67	3.08	1.44	3.83	4.42	.78	1.47
29	Rock imperm	-	.0360	1.630	3.0	2.25	PM	.0920	2.65	3.13	1.57	3.64	4.30	1.94	2.35
30	Rock imperm	-	.0360	1.630	3.0	2.25	PM	.1059	2.67	3.08	1.80	3.42	3.94	4.75	11.39
31	Rock imperm	-	.0360	1.630	3.0	2.25	PM	1160	3.08	3.57	1.98	3.77	4.37	10.26	17 35
32	Rock imperm	-	.0360	1.630	3.0	2.25	PM	.1051	3.12	3.51	1.79	4.01	4.51	4.43	8.70
33	Rock imperm	-	.0360	1.630	3.0	2.25	PM	.0950	3.18	3.57	1.62	4.30	4.82	2.75	2.66
34	Rock imperm	-	.0360	1.630	3.0	2.25	PM	.0830	3.14	3.57	1.41	4.54	5.16	1.36	1.76
35	Rock imperm	-	.0360	1.615	3.0	1.25	PM	.1098	2.20	2.53	1.89	2.77	3.18	5.22	8.16
36	Rock imperm	-	.0360	1.615	3.0	1.25	PM	.1002	2.21	2.50	1.72	2.91	3.29	4.93	9.11
37	Rock imperm	-	.0360	1.615	3.0	1.25	PM	.0860	2.20	2.50	1.48	3.12	3.55	1.71	3.66
38	Rock imperm	-	.0360	1.615	3.0	1.25	PM	.0742	2.19	2.50	1.28	3.35	3.82	.89	1.48
39	Rock imperm	-	.0360	1.615	3.0	1.25	PM	.1188	2.20	2.47	2.04	2.66	2.98	8.09	15 15
40	Rock imperm	-	.0360	1.615	3.0	1.25	PM	.1285	2.20	2.50	2.21	2.56	2.90	13.98	-1.00
41	Rock imperm	-	.0360	1.615	3.0	1.25	PM	.1221	1.77	2.04	2.10	2.11	2.43	7.40	13.12
42	Rock imperm	-	.0360	1.615	3.0	1.25	PM	.1004	1.76	2.04	1.73	2.31	2.68	3.87	5.47
43	Rock imperm	-	.0360	1.615	3.0	1.25	PM	.0799	1.77	2.02	1.37	2.61	2.98	1.23	2 11
44	Rock imperm	-	.0360	1.615	3.0	1.25	PM	.1369	1.77	2.02	2.35	1.99	2.27	10.95	19.47
45	Rock imperm	-	.0360	1.615	3.0	1.25	PM	.1123	1.77	2.01	1.93	2.20	2.50	6.44	9.62
46	Rock imperm	-	.0360	1.615	3.0	1.25	PM	.0981	1.31	1.37	1.69	1.74	1.82	1.83	2.15
47	Rock imperm	-	.0360	1.615	3.0	1.25	PM	.1346	1.32	1.38	2.32	1.50	1.57	4.87	7.45
48	Rock imperm	-	.0360	1.615	3.0	1.25	PM	.1548	1.35	1.43	2.66	1.43	1.51	8.29	13.11
49	Rock imperm	-	.0360	1.615	3.0	1.25	PM	.1682	1.36	1.46	2.89	1.38	1.48	10.52	17.81
50	Rock imperm	-	.0360	1.615	3.0	1.25	PM	.1187	1.31	1.41	2.04	1.58	1.70	3.88	6.44
51	Rock imperm	-	.0360	1.615	3.0	1.25	PM	.1145	2.97	3.57	1.97	3.66	4.39	9.90	18.41
52	Rock imperm	-	.0360	1.615	3.0	1.25	PM	.1049	2.99	3.45	1.80	3.85	4.44	3.76	6.40
53	Rock imperm	-	.0360	1.615	3.0	1.25	PM	.0975	3.00	3.51	1.68	4.00	4.68	3.49	5.26
54	Rock imperm	-	.0360	1.615	3.0	1.25	PM	.0799	3.02	3.45	1.37	4.45	5.08	.83	1.50
55	Rock imperm	-	.0360	1.615	3.0	1.25	PM	.1120	2.98	3.45	1.93	3.71	4.29	7.02	9.14
56	Rock imperm	-	.0360	1.630	3.0	2.25	PM	.1256	1.86	2.11	2.14	2.19	2.48	7.31	12.34
57	Rock imperm	-	.0360	1.630	3.0	2.25	PM	.1004	1.86	2.11	1.71	2.44	2.77	5.03	6.63
58	Rock imperm	-	.0360	1.630	3.0	2.25	PM	.0691	1.85	2.08	1.18	2.93	3.30	.60	.77
59	Rock imperm	-	.0360	1.630	3.0	2.25	PM	.0868	1.84	2.13	1.49	2.60	3.01	.86	2.93
60	Rock imperm	-	.0360	1.630	3.0	2.25	PM	.1159	1.84	2.17	1.98	2.25	2.65	8.13	12.64
61	Rock imperm	-	.0360	1.630	3.0	2.25	PM	.1326	1.87	2.11	2.26	2.14	2.41	10.88	18.65
62	Rock imperm	-	.0360	1.630	4.0	2.25	PM	.1881	2.18	2.44	3.21	1.57	1.76	28.84	-1.00

1	2	3	4	5	6	7	8	9	10	11	12	13	14	15	16
63	Rock imperm	-	.0360	1.630	4.0	2.25	PH	.1661	2.17	2.50	2.83	1.66	1.92	20.45	32.97
64	Rock imperm	-	.0360	1.630	4.0	2.25	PH	.1365	2.18	2.56	2.33	1.84	2.16	8.68	18.32
65	Rock imperm	-	.0360	1.630	4.0	2.25	PH	.1162	2.20	2.50	1.98	2.02	2.29	5.35	8.78
66	Rock imperm	-	.0360	1.630	4.0	2.25	PH	.0893	2.20	2.44	1.52	2.30	2.55	1.55	3.24
67	Rock imperm	-	.0360	1.630	4.0	2.25	PH	.1343	2.67	3.13	2.29	2.28	2.67	18.80	29.88
68	Rock imperm	-	.0360	1.630	4.0	2.25	PH	.1189	2.68	3.10	2.03	2.43	2.81	11.24	19.17
69	Rock imperm	-	.0360	1.630	4.0	2.25	PH	.0874	2.69	3.13	1.49	2.84	3.31	3.62	5.11
70	Rock imperm	-	.0360	1.630	4.0	2.25	PH	.0721	2.69	3.17	1.23	3.13	3.69	1.15	1.25
71	rock imperm	-	.0360	1.630	4.0	2.25	PH	.1022	2.70	3.17	1.74	2.64	3.10	5.23	9.98
72	Rock imperm	-	.0360	1.630	4.0	2.25	PH	.1132	3.19	3.64	1.93	2.96	3.38	9.26	16.17
73	Rock imperm	-	.0360	1.630	4.0	2.25	PH	.0867	3.25	3.64	1.48	3.45	3.86	2.45	3.52
74	Rock imperm	-	.0360	1.630	4.0	2.25	PH	.0762	3.26	3.64	1.30	3.69	4.12	1.33	1.71
75	Rock imperm	-	.0360	1.630	4.0	2.25	PH	.0998	3.23	3.64	1.70	3.19	3.60	4.71	7.99
76	Rock imperm	-	.0360	1.630	4.0	2.25	PH	.1233	3.18	3.64	2.10	2.83	3.24	14.72	25.79
77	Rock imperm	-	.0360	1.630	4.0	2.25	PH	.1850	1.61	1.83	3.15	1.17	1.33	10.34	17.31
78	Rock imperm	-	.0360	1.630	4.0	2.25	PH	.1951	1.62	1.82	3.32	1.15	1.29	11.14	19.57
79	Rock imperm	-	.0360	1.630	4.0	2.25	PH	.1548	1.37	1.49	2.64	1.09	1.18	3.81	5.57
80	Rock imperm	-	.0360	1.630	4.0	2.25	PH	.1633	1.40	1.50	2.78	1.08	1.16	4.91	7.89
81	Rock imperm	-	.0360	1.630	4.0	2.25	PH	.1748	1.41	1.48	2.98	1.05	1.11	5.51	8.73
82	Rock imperm	-	.0360	1.630	4.0	2.25	PH	.1907	1.44	1.52	3.25	1.03	1.09	8.40	13.26
83	Rock imperm	-	.0360	1.615	4.0	1.25	PH	.1163	2.19	2.44	2.00	2.01	2.24	4.04	7.77
84	Rock imperm	-	.0360	1.615	4.0	1.25	PH	.1338	2.18	2.53	2.30	1.86	2.16	8.23	11.98
85	Rock imperm	-	.0360	1.615	4.0	1.25	PH	.0991	2.20	2.50	1.70	2.18	2.48	3.16	5.56
86	Rock imperm	-	.0360	1.615	4.0	1.25	PH	.0695	2.20	2.53	1.20	2.61	3.00	1.50	1.91
87	Rock imperm	-	.0360	1.615	4.0	1.25	PH	.1573	2.19	2.53	2.71	1.72	1.99	16.17	25.96
88	Rock imperm	-	.0360	1.615	4.0	1.25	PH	.1190	2.98	3.51	2.05	2.70	3.18	7.42	13.36
89	Rock imperm	-	.0360	1.615	4.0	1.25	PH	.0930	3.00	3.51	1.43	3.25	3.81	1.53	1.74
90	Rock imperm	-	.0360	1.615	4.0	1.25	PH	.1084	3.02	3.51	1.86	2.87	3.33	6.01	9.41
91	Rock imperm	-	.0360	1.615	4.0	1.25	PH	.0965	3.02	3.51	1.66	3.04	3.53	3.55	5.56
92	Rock imperm	-	.0360	1.615	4.0	1.25	PH	.1396	2.95	3.51	2.40	2.47	2.93	15.34	28.75
93	Rock imperm	-	.0360	1.615	4.0	1.25	PH	.1214	1.33	1.42	2.09	1.19	1.27	1.69	3.20
94	Rock imperm	-	.0360	1.615	4.0	1.25	PH	.1721	1.35	1.49	2.96	1.02	1.12	5.06	7.77
95	Rock imperm	-	.0360	1.615	4.0	1.25	PH	.1975	1.41	1.49	3.40	.99	1.05	7.26	10.88
96	Rock imperm	-	.0360	1.615	4.0	1.25	PH	.1481	1.35	1.42	2.55	1.10	1.15	4.45	6.46
97	Rock imperm	-	.0360	1.615	4.0	1.25	PH	.1333	1.32	1.42	2.29	1.13	1.21	2.47	3.90
98	Rock imperm	-	.0360	1.615	4.0	1.25	PH	.1521	1.77	1.96	2.62	1.42	1.57	8.01	10.76
99	Rock imperm	-	.0360	1.615	4.0	1.25	PH	.1168	1.75	1.92	2.01	1.60	1.76	3.42	4.67
100	Rock imperm	-	.0360	1.615	4.0	1.25	PH	.0884	1.75	1.96	1.52	1.84	2.06	1.09	2.15
101	Rock imperm	-	.0360	1.615	4.0	1.25	PH	.1356	1.76	1.94	2.33	1.49	1.65	5.06	8.53
102	Rock imperm	-	.0360	1.615	4.0	1.25	PH	.1804	1.76	1.96	3.10	1.29	1.44	13.84	20.08
103	Rock imperm	-	.0360	1.615	4.0	1.25	PH	.1533	1.77	1.96	2.64	1.41	1.56	3.73	3.93
104	Rock imperm	-	.0360	1.615	4.0	1.25	PH	.1806	1.77	2.00	3.11	1.30	1.47	3.60	6.02
105	Rock imperm	-	.0360	1.615	4.0	1.25	PH	.1543	1.78	2.00	2.65	1.42	1.59	6.64	11.64
106	Rock imperm	-	.0360	1.615	4.0	1.25	PH	.1529	1.78	1.96	2.63	1.42	1.57	7.50	11.13
107	Rock imperm	-	.0360	1.615	4.0	1.25	PH	.1532	1.77	1.96	2.64	1.41	1.56	6.64	10.47
108	Rock imperm	-	.0360	1.630	6.0	2.25	PH	.1709	2.17	2.53	2.91	1.09	1.27	3.29	6.64
109	Rock imperm	-	.0360	1.630	6.0	2.25	PH	.2273	2.15	2.50	3.87	.94	1.09	10.86	21.47
110	Rock imperm	-	.0360	1.630	6.0	2.25	PH	.1138	2.15	2.53	1.94	1.33	1.56	1.03	2.81
111	Rock imperm	-	.0360	1.630	6.0	2.25	PH	.2010	2.15	2.53	3.43	1.00	1.18	7.49	13.29
112	Rock imperm	-	.0360	1.630	6.0	2.25	PH	.2573	2.17	2.56	4.38	.89	1.05	15.06	-1.00
113	Rock imperm	-	.0360	1.630	6.0	2.25	PH	.1763	2.62	3.08	3.00	1.30	1.53	12.41	15.53
114	Rock imperm	-	.0360	1.630	6.0	2.25	PH	.1167	2.64	3.08	1.99	1.61	1.88	3.57	5.07
115	Rock imperm	-	.0360	1.630	6.0	2.25	PH	.1499	2.64	3.08	2.55	1.42	1.66	6.33	8.60
116	Rock imperm	-	.0360	1.630	6.0	2.25	PH	.0838	2.66	3.08	1.43	1.91	2.22	.80	1.25
117	Rock imperm	-	.0360	1.630	6.0	2.25	PH	.2017	2.59	3.17	3.44	1.20	1.47	14.52	23.83
118	Rock imperm	-	.0360	1.630	6.0	2.25	PH	.1523	3.14	3.92	2.60	1.68	2.09	15.13	19.92
119	Rock imperm	-	.0360	1.630	6.0	2.25	PH	.0907	3.08	3.85	1.55	2.13	2.66	4.04	4.41
120	Rock imperm	-	.0360	1.630	6.0	2.25	PH	.0685	3.23	3.85	1.17	2.57	3.06	1.59	2.53
121	Rock imperm	-	.0360	1.630	6.0	2.25	PH	.1135	3.23	3.85	1.93	2.00	2.38	4.00	6.19
122	Rock imperm	-	.0360	1.630	6.0	2.25	PH	.1325	3.06	3.77	2.26	1.75	2.16	7.96	10.48

1	2	3	4	5	6	7	8	9	10	11	12	13	14	15	16
123	Rock imperm	-	.0360	1.630	6.0	2.25	PM	.2347	1.85	2.15	4.00	.80	.92	10.66	17.42
124	Rock imperm	-	.0360	1.630	6.0	2.25	PM	.1792	1.82	2.15	3.05	.90	1.06	6.17	10.40
125	Rock imperm	-	.0360	1.630	6.0	2.25	PM	.1207	1.81	2.17	2.06	1.09	1.30	2.62	2.61
126	Rock imperm	-	.0360	1.630	6.0	2.25	PM	.1499	1.83	2.15	2.55	.98	1.16	5.25	6.56
127	Rock imperm	-	.0360	1.630	6.0	2.25	PM	.2526	1.89	2.17	4.30	.78	.90	11.66	20.81
128	Rock imperm	-	.0360	1.630	6.0	2.25	PM	.1915	1.60	1.79	3.26	.76	.85	6.81	10.73
129	Rock imperm	-	.0360	1.630	6.0	2.25	PM	2120	1.63	1.85	3.61	.74	.84	4.66	9.03
130	Rock imperm	-	.0360	1.630	6.0	2.25	PM	.2441	1.68	1.92	4.16	.71	.81	9.68	17.35
131	Rock imperm	-	.0360	1.630	6.0	2.25	PM	.1519	1.37	1.48	2.59	.73	.79	1.54	1.74
132	Rock imperm	-	.0360	1.630	6.0	2.25	PM	.1784	1.41	1.54	3.04	.70	.76	2.50	3.84
133	Rock imperm	-	.0360	1.630	6.0	2.25	PM	.2084	1.46	1.56	3.55	.67	.71	4.37	6.88
134	Rock imperm	-	.0360	1.630	6.0	2.25	PM	.1930	1.60	1.83	3.29	.76	.87	4.07	7.89
158	Spectrum	-	.0360	1.630	3.0	2.25	NA	0938	2.23	2.25	1.60	3.03	3.06	8.60	13.26
159	Spectrum	-	.0360	1.630	3.0	2.25	NA	.0621	2.22	2.25	1.06	3.71	3.76	.86	.74
160	Spectrum	-	.0360	1.630	3.0	2.25	NA	.0793	2.22	2.24	1.35	3.28	3.31	4.70	7.01
161	Spectrum	-	.0360	1.630	3.0	2.25	NA	.1108	2.22	2.24	1.89	2.78	2.80	9.69	17.48
162	Spectrum	-	.0360	1.630	3.0	2.25	NA	.0689	2.22	2.25	1.17	3.52	3.57	3.40	4.46
163	Spectrum	-	.0360	1.630	3.0	2.25	NA	.0837	1.79	1.79	1.43	2.58	2.58	2.75	3.55
164	Spectrum	-	0360	1.630	3.0	2.25	NA	1193	1.79	1.79	2.03	2.16	2.16	6.77	11.43
165	Spectrum	-	.0360	1.630	3.0	2.25	NA	.1006	1.78	1.79	1.71	2.34	2.35	2.72	3.56
166	Spectrum	-	.0360	1.630	3.0	2.25	NA	.1094	1.78	1.79	1.86	2.24	2.25	7.21	11.22
167	Spectrum	-	.0360	1.630	3.0	2.25	NA	.1354	1.78	1.80	2.31	2.01	2.04	13.02	23.10
168	Spectrum	-	.0360	1.630	3.0	2.25	WI	.1332	1.78	2.72	2.27	2.03	3.10	18.32	-1.00
169	Spectrum	-	.0360	1.630	3.0	2.25	WI	.0908	1.82	2.60	1.55	2.52	3.59	2.25	4.71
170	Spectrum	-	.0360	1.630	3.0	2.25	WI	.1065	1.82	2.47	1.81	2.32	3.15	6.33	10.63
171	Spectrum	-	.0360	1.630	3.0	2.25	WI	.1221	1.81	2.67	2.08	2.16	3.19	10.73	18.12
172	Spectrum	-	.0360	1.630	3.0	2.25	WI	.0736	1.81	2.47	1.25	2.78	3.79	1.21	2.62
173	Spectrum	-	.0360	1.630	3.0	2.25	WI	.0847	2.89	4.25	1.44	4.14	6.08	4.93	8.77
174	Spectrum	-	.0360	1.630	3.0	2.25	WI	.0632	2.92	4.25	1.09	4.84	7.04	1.88	2.65
175	Spectrum	-	.0360	1.630	3.0	2.25	WI	.1056	2.85	4.25	1.80	3.65	5.45	13.77	31.63
176	Spectrum	-	.0360	1.630	3.0	2.25	WI	.0745	2.91	4.25	1.27	4.44	6.49	1.80	4.37
177	Spectrum	-	.0360	1.630	3.0	2.25	WI	.0955	2.86	4.25	1.63	3.85	5.73	12.07	17.53
178	Spectrum	-	.0360	1.630	3.0	2.25	WI	.0886	2.16	3.00	1.51	3.02	4.20	6.83	11.66
179	Spectrum	-	.0360	1.630	3.0	2.25	WI	.0589	2.16	3.28	1.00	3.71	5.63	1.13	1.87
180	Spectrum	-	.0360	1.630	3.0	2.25	WI	.0746	2.17	3.23	1.27	3.31	4.93	4.38	7.24
181	Spectrum	-	.0360	1.630	3.0	2.25	WI	.1015	2.16	3.23	1.73	2.82	4.22	10.65	19.85
182	Spectrum	-	0360	1.630	3.0	2.25	WI	.1117	2.16	3.17	1.90	2.69	3.95	15.20	-1.00
183	Spectrum	-	.0360	1.630	3.0	2.25	NA	.0799	3.06	3.23	1.36	4.51	4.76	6.11	11.72
184	Spectrum	-	.0360	1.630	3.0	2.25	NA	.0593	3.10	3.23	1.01	5.30	5.52	.97	1.66
185	Spectrum	-	.0360	1.630	3.0	2.25	NA	.0696	3.09	3.23	1.19	4.88	5.10	2.65	4.37
186	Spectrum	-	.0360	1.630	3.0	2.25	NA	.0970	3.07	3.20	1.65	4.11	4.28	12.65	31.79
187	Spectrum	-	.0360	1.630	3.0	2.25	WI	.1070	1.39	1.54	1.82	1.77	1.96	4.83	8.06
188	Spectrum	-	.0360	1.630	3.0	2.25	WI	.1253	1.41	1.83	2.14	1.66	2.15	7.19	11.07
189	Spectrum	-	.0360	1.630	3.0	2.25	PM	.1069	3.09	3.64	1.82	3.94	4.64	11.41	20.64
190	Spectrum	-	.0360	1.630	3.0	2.25	WI	.0671	1.39	1.89	1.14	2.24	3.04	.86	.86
191	Spectrum	-	.0360	1.630	3.0	2.25	WI	.0867	1.37	1.89	1.48	1.94	2.67	1.12	1.98
192	Spectrum	-	.0360	1.630	3.0	2.25	WI	.1404	1.45	1.89	2.39	1.61	2.10	6.81	13.20
193	Spectrum	-	.0360	1.630	3.0	2.25	NA	.1090	1.41	1.40	1.86	1.78	1.77	3.94	6.84
194	Spectrum	-	.0360	1.630	3.0	2.25	NA	.0793	1.40	1.40	1.35	2.07	2.07	.65	1.11
195	Spectrum	-	.0360	1.630	3.0	2.25	NA	.1240	1.40	1.40	2.11	1.66	1.66	3.13	6.71
196	Spectrum	-	.0360	1.630	3.0	2.25	NA	.1391	1.41	1.40	2.37	1.57	1.56	6.71	11.59
197	Spectrum	-	.0360	1.630	3.0	2.25	NA	.1666	1.41	1.40	2.84	1.44	1.43	11.84	17.00
198	Rock perm	+	0360	1.615	3.0	1.25	PM	.0946	2.19	2.53	1.63	2.97	3.43	.43	.99
199	Rock perm	+	.0360	1.615	3.0	1.25	PM	.1044	2.21	2.53	1.80	2.85	3.26	1.64	2.55
200	Rock perm	+	0360	1.615	3.0	1.25	PM	.1213	2.17	2.53	2.09	2.60	3.03	3.09	5.06
201	Rock perm	+	.0360	1.615	3.0	1.25	PM	.1436	2.17	2.53	2.47	2.39	2.78	6.01	8.96
202	Rock perm	+	.0360	1.615	3.0	1.25	PM	.1792	2.17	2.53	3.08	2.14	2.49	12.75	20.92
203	Rock perm	+	.0360	1.615	3.0	1.25	PM	.1287	2.98	3.51	2.21	3.46	4.08	3.63	4.08
204	Rock perm	+	.0360	1.615	3.0	1.25	PM	.1631	2.90	3.51	2.81	2.99	3.62	10.54	20.39
205	Rock perm	+	.0360	1.615	3.0	1.25	PM	.1465	2.93	3.51	2.52	3.19	3.82	4.95	12.75

1	2	3	4	5	6	7	8	9	10	11	12	13	14	15	16
206	Rock perm	+	.0360	1.615	3.0	1.25	PM	.1132	3.00	3.51	1.95	3.71	4.35	1.93	3.07
207	Rock perm	+	.0360	1.615	3.0	1.25	PM	.1757	2.89	3.51	3.02	2.87	3.49	15.76	28.80
208	Rock perm	+	.0360	1.615	3.0	1.25	PM	.1520	1.33	1.46	2.61	1.42	1.56	2.37	3.63
209	Rock perm	+	.0360	1.615	3.0	1.25	PM	.1692	1.35	1.45	2.91	1.37	1.47	3.02	5.12
210	Rock perm	+	.0360	1.615	3.0	1.25	PM	.1279	1.33	1.44	2.20	1.55	1.68	1.19	2.04
211	Rock perm	+	.0360	1.615	3.0	1.25	PM	.1468	1.78	2.06	2.52	1.93	2.24	3.39	5.44
212	Rock perm	+	.0360	1.615	3.0	1.25	PM	.1778	1.79	2.04	3.06	1.77	2.02	9.37	13.80
213	Rock perm	+	.0360	1.615	3.0	1.25	PM	.1620	1.79	2.04	2.79	1.85	2.11	7.01	8.56
214	Rock perm	+	.0360	1.615	3.0	1.25	PM	.1305	1.77	2.06	2.24	2.04	2.38	2.47	4.18
215	Rock perm	+	.0360	1.615	3.0	1.25	PM	.1062	1.77	2.04	1.83	2.26	2.61	1.47	1.85
216	Rock perm	+	.0360	1.615	3.0	1.25	PM	.1856	1.77	2.04	3.19	1.71	1.97	12.19	18.31
217	Rock perm	+	.0360	1.615	2.0	1.25	PM	.0897	1.70	1.95	1.54	3.55	4.07	1.36	2.05
218	Rock perm	+	.0360	1.615	2.0	1.25	PM	.1028	1.69	1.94	1.77	3.29	3.78	3.83	4.20
219	Rock perm	+	.0360	1.615	2.0	1.25	PM	.1152	1.70	1.94	1.98	3.13	3.57	5.32	6.74
220	Rock perm	+	.0360	1.615	2.0	1.25	PM	.1381	1.69	1.95	2.38	2.84	3.28	9.27	15.35
221	Rock perm	+	.0360	1.615	2.0	1.25	PM	.1305	1.72	1.95	2.24	2.97	3.37	7.36	12.21
222	Rock perm	+	.0360	1.615	2.0	1.25	PM	.1127	2.16	2.52	1.94	4.02	4.69	3.73	5.66
223	Rock perm	+	.0360	1.615	2.0	1.25	PM	.0905	2.15	2.50	1.56	4.47	5.19	.99	1.67
224	Rock perm	+	.0360	1.615	2.0	1.25	PM	.1250	2.16	2.53	2.15	3.82	4.47	6.59	13.17
225	Rock perm	+	.0360	1.615	2.0	1.25	PM	.1038	2.15	2.52	1.79	4.17	4.89	2.55	4.06
226	Rock perm	+	.0360	1.615	2.0	1.25	PM	.1327	2.16	2.45	2.28	3.70	4.20	9.98	-1.00
227	Rock perm	+	.0360	1.615	2.0	1.25	PM	.1026	2.98	3.48	1.76	5.81	6.79	.83	.92
228	Rock perm	+	.0360	1.615	2.0	1.25	PM	.1166	2.94	3.51	2.01	5.38	6.42	1.67	3.67
229	Rock perm	+	.0360	1.615	2.0	1.25	PM	.1324	2.88	3.51	2.28	4.94	6.03	1.85	5.08
230	Rock perm	+	.0360	1.615	2.0	1.25	PM	.1597	2.81	3.48	2.75	4.39	5.44	10.90	22.93
231	Rock perm	=	.0360	1.615	2.0	1.25	PM	.1480	2.83	3.48	2.55	4.60	5.65	5.90	9.57
232	Rock perm	+	.0360	1.615	2.0	1.25	PM	.1142	1.31	1.39	1.96	2.47	2.57	3.20	2.85
233	Rock perm	+	.0360	1.615	2.0	1.25	PM	.1364	1.32	1.40	2.35	2.23	2.37	4.44	7.11
234	Rock perm	+	.0360	1.615	2.0	1.25	PM	.1590	1.35	1.46	2.73	2.12	2.29	8.46	16.13
235	Rock perm	+	.0360	1.615	2.0	1.25	PM	.0909	1.30	1.42	1.56	2.69	2.94	1.00	1.20
236	Rock perm	+	.0360	1.615	2.0	1.25	PM	.1236	1.32	1.41	2.13	2.35	2.51	2.01	4.10
237	Rock perm	+	.0360	1.615	1.5	1.25	PM	.1131	2.15	2.56	1.95	5.33	6.34	10.42	14.89
238	Rock perm	+	.0360	1.615	1.5	1.25	PM	.0861	2.16	2.53	1.48	6.13	7.18	2.39	2.73
239	Rock perm	+	.0360	1.615	1.5	1.25	PM	.0962	2.15	2.50	1.65	5.77	6.71	1.33	2.61
240	Rock perm	+	.0360	1.615	1.5	1.25	PM	.1048	2.15	2.56	1.80	5.53	6.59	3.09	4.22
241	Rock perm	+	.0360	1.615	1.5	1.25	PM	.1208	2.16	2.53	2.08	5.18	6.06	6.82	10.80
242	Rock perm	=	.0360	1.615	1.5	1.25	PM	.1154	1.72	1.98	1.98	4.22	4.86	8.18	15.20
243	Rock perm	+	.0360	1.615	1.5	1.25	PM	.0843	1.69	1.96	1.45	4.85	5.62	1.27	2.11
244	Rock perm	+	.0360	1.615	1.5	1.25	PM	.1011	1.71	1.96	1.74	4.48	5.13	3.08	7.04
245	Rock perm	+	.0360	1.615	1.5	1.25	PM	.1240	1.71	1.96	2.13	4.05	4.64	13.74	-1.00
246	Rock perm	+	.0360	1.615	1.5	1.25	PM	.1317	2.13	2.56	2.27	4.89	5.88	13.04	23.69
247	Rock perm	+	.0360	1.615	1.5	1.25	PM	.1084	1.31	1.43	1.86	3.31	3.62	5.15	9.65
248	Rock perm	+	.0360	1.615	1.5	1.25	PM	.0905	1.30	1.43	1.56	3.60	3.96	2.19	3.01
249	Rock perm	+	.0360	1.615	1.5	1.25	PM	.1230	1.32	1.42	2.12	3.14	3.37	6.79	13.58
250	Rock perm	=	.0360	1.615	1.5	1.25	PM	.1386	1.33	1.43	2.38	2.98	3.20	12.19	20.45
251	Rock perm	+	.0360	1.615	1.5	1.25	PM	.1004	1.30	1.43	1.73	3.42	3.76	2.24	3.04
252	Rock perm	+	.0360	1.615	1.5	1.25	PM	.0921	1.70	1.98	1.58	4.67	5.43	1.61	2.67
253	Rock perm	+	.0360	1.615	1.5	1.25	PM	.1050	2.95	3.45	1.81	7.58	8.87	1.42	1.87
254	Rock perm	+	.0360	1.615	1.5	1.25	PM	.1220	2.92	3.51	2.10	6.96	8.37	1.84	3.83
255	Rock perm	+	.0360	1.615	1.5	1.25	PM	.1387	2.87	3.51	2.39	6.42	7.85	5.94	16.36
256	Rock perm	+	.0360	1.615	1.5	1.25	PM	.1507	2.82	3.51	2.59	6.05	7.53	25.08	-1.00
257	Rock perm	+	.0360	1.615	1.5	1.25	PM	.1302	2.88	3.51	2.24	6.65	8.10	4.32	8.02
258	Rock hom	H	.0360	1.615	2.0	1.25	PM	.1049	2.15	2.60	1.80	4.15	5.02	1.57	1.86
259	Rock hom	H	.0360	1.615	2.0	1.25	PM	.1384	2.14	2.60	2.38	3.60	4.37	4.83	8.77
260	Rock hom	H	.0360	1.615	2.0	1.25	PM	.1715	2.14	2.63	2.95	3.23	3.97	17.68	30.80
261	Rock hom	H	.0360	1.615	2.0	1.25	PM	.1532	2.14	2.60	2.64	3.42	4.15	10.02	15.33
262	Rock hom	H	.0360	1.615	2.0	1.25	PM	.1346	1.70	2.00	2.32	2.90	3.41	4.84	7.99
263	Rock hom	H	.0360	1.615	2.0	1.25	PM	.1805	1.71	1.98	3.10	2.52	2.91	16.48	27.30
264	Rock hom	H	.0360	1.615	2.0	1.25	PM	.1583	1.71	2.00	2.72	2.69	3.14	11.45	17.68
265	Rock hom	H	.0360	1.615	2.0	1.25	PM	.1053	1.69	2.00	1.81	3.26	3.85	2.60	2.47

1	2	3	4	5	6	7	8	9	10	11	12	13	14	15	16
266	Rock hom	H	.0360	1.615	2.0	1.25	PM	.1420	1.33	1.40	2.44	2.21	2.32	3.00	4.79
267	Rock hom	H	.0360	1.615	2.0	1.25	PM	.1697	1.37	1.47	2.92	2.08	2.23	5.96	12.04
268	Rock hom	H	.0360	1.615	2.0	1.25	PM	.1009	1.31	1.45	1.74	2.58	2.85	1.13	1.30
269	Rock hom	H	.0360	1.615	2.0	1.25	PM	.1882	1.40	1.47	3.24	2.02	2.12	10.64	18.76
270	Rock hom	H	.0360	1.615	2.0	1.25	PM	.1385	2.90	3.64	2.38	4.87	6.11	2.07	3.77
271	Rock hom	H	.0360	1.615	2.0	1.25	PM	.1613	2.82	3.70	2.77	4.39	5.76	6.07	10.30
272	Rock hom	H	.0360	1.615	2.0	1.25	PM	1762	2.76	3.64	3.03	4.11	5.42	10.80	14.00
273	Rock hom	H	.0360	1.615	2.0	1.25	PM	.1111	2.97	3.57	1.91	5.57	6.69	1.09	1.29
274	Depth 0.4m	+	.0360	1.615	2.0	1.25	PM	.1253	1.68	2.04	2.16	2.97	3.60	8.51	12.69
275	Depth 0.4m	+	.0360	1.615	2.0	1.25	PM	.0900	1.69	2.00	1.55	3.52	4.17	.86	1.56
276	Depth 0.4m	+	.0360	1.615	2.0	1.25	PM	.1088	1.68	2.04	1.87	3.18	3.87	2.85	4.05
277	Depth 0.4m	+	.0360	1.615	2.0	1.25	PM	.1359	1.67	1.96	2.34	2.83	3.32	10.15	18.15
278	Depth 0.4m	+	.0360	1.615	2.0	1.25	PM	.1286	2.19	2.60	2.21	3.82	4.53	6.04	9.85
279	Depth 0.4m	+	.0360	1.615	2.0	1.25	PM	.1052	2.19	2.56	1.81	4.22	4.93	1.16	2.15
280	Depth 0.4m	+	.0360	1.615	2.0	1.25	PM	.1555	2.18	2.60	2.67	3.46	4.12	8.78	20.04
281	Depth 0.4m	+	.0360	1.615	2.0	1.25	PM	.1215	2.20	2.56	2.09	3.94	4.59	4.78	7.19
282	Depth 0.2m	+	.0360	1.615	2.0	1.25	PM	.1345	2.18	2.53	2.31	3.72	4.31	4.50	6.29
283	Depth 0.2m	+	.0360	1.615	2.0	1.25	PM	.1275	2.17	2.50	2.19	3.80	4.38	3.05	3.00
284	Depth 0.2m	+	.0360	1.615	2.0	1.25	PM	.1415	2.17	2.56	2.43	3.61	4.25	5.13	6.43
285	Depth 0.2m	+	.0360	1.615	2.0	1.25	PM	.1445	2.18	2.53	2.49	3.58	4.16	6.52	12.45
286	Depth 0.2m	+	.0360	1.615	2.0	1.25	PM	.1270	1.70	2.04	2.18	2.98	3.58	2.27	3.63
287	Depth 0.2m	+	.0360	1.615	2.0	1.25	PM	.1320	1.73	2.00	2.27	2.98	3.44	4.97	7.97
288	Depth 0.2m	+	.0360	1.615	2.0	1.25	PM	.1350	1.74	2.04	2.32	2.96	3.47	6.65	11.03
289	Depth 0.2m	+	.0360	1.615	2.0	1.25	PM	.1350	1.77	2.08	2.32	3.01	3.54	8.65	11.38
901	Density	+	.0332	.920	2.0	-1.0	PM	0735	1.25	1.35	2.13	2.88	3.11	1.98	3.17
902	Density	+	.0332	.920	2.0	-1.0	PM	.0929	1.27	1.33	2.69	2.60	2.73	6.77	9.20
903	Density	+	.0332	.920	2.0	-1.0	PM	.0829	1.25	1.35	2.40	2.71	2.93	4.41	6.03
904	Density	+	.0332	920	2.0	-1.0	PM	.0597	1.25	1.33	1.73	3.20	3.40	1.82	2.33
905	Density	+	.0332	.920	2.0	-1.0	PM	.0461	1.24	1.36	1.34	3.61	3.96	.61	.44
906	Density	+	.0332	.920	2.0	-1.0	PM	.0730	1.57	1.80	2.12	3.63	4.16	2.17	4.68
907	Density	+	.0332	.920	2.0	-1.0	PM	.0868	1.57	1.72	2.52	3.33	3.65	6.08	10.27
908	Density	+	.0332	.920	2.0	-1.0	PM	.0599	1.57	1.71	1.74	4.01	4.37	1.56	1.85
909	Density	+	.0332	.920	2.0	-1.0	PM	.0800	1.56	1.72	2.32	3.45	3.80	4.09	7.07
910	Density	+	.0332	.920	2.0	-1.0	PM	.0931	1.57	1.72	2.70	3.22	3.52	6.84	13.06
911	Density	+	.0358	2.050	2.0	-1.0	PM	.1422	1.90	2.17	1.94	3.15	3.60	3.26	3.90
912	Density	+	.0358	2.050	2.0	-1.0	PM	.1668	1.91	2.22	2.27	2.92	3.40	4.84	8.21
913	Density	+	.0358	2.050	2.0	-1.0	PM	.1122	1.90	2.15	1.53	3.55	4.01	.70	1.73
914	Density	+	.0358	2.050	2.0	-1.0	PM	.1841	1.92	2.20	2.51	2.80	3.20	12.82	19.92
915	Density	+	.0358	2.050	2.0	-1.0	PM	.1292	1.90	2.22	1.76	3.30	3.86	3.18	6.96
916	Density	+	.0358	2.050	2.0	-1.0	PM	.1330	2.36	2.86	1.81	4.04	4.90	1.29	2.88
917	Density	+	.0358	2.050	2.0	-1.0	PM	.1651	2.36	2.86	2.25	3.63	4.40	7.56	11.00
918	Density	+	.0358	2.050	2.0	-1.0	PM	.1490	2.36	2.86	2.03	3.82	4.63	3.13	3.30
919	Density	+	.0358	2.050	2.0	-1.0	PM	.1184	2.36	2.86	1.61	4.29	5.19	1.13	1.47
920	Density	+	.0358	2.050	2.0	-1.0	PM	.1566	2.35	2.86	2.13	3.71	4.52	5.14	7.29
930	Large scale	+	.2100	1.700	3.0	1.38	PM	.9600	4.40	5.10	2.69	1.87	2.17	4.03	6.55
931	Large scale	+	.2100	1.700	3.0	1.38	PM	1.0600	4.40	5.10	2.97	1.78	2.06	5.91	11.24
932	Large scale	+	.2100	1.700	3.0	1.38	PM	.7700	4.40	5.10	2.16	2.09	2.39	1.82	3.22
933	Large scale	+	.2100	1.700	3.0	1.38	PM	1.0700	4.40	5.10	3.00	1.77	2.05	8.03	-1.00
934	Large scale	+	.2100	1.700	3.0	1.38	PM	.8700	4.40	5.10	2.44	1.96	2.27	3.97	5.82
935	Large scale	+	.2100	1.700	3.0	1.38	PM	1.1800	4.40	5.10	3.31	1.69	1.96	11.59	21.08
936	Large scale	-	.2100	1.700	3.0	1.38	PM	.6400	4.40	5.10	1.79	2.29	2.65	3.84	6.31
937	Large scale	-	.2100	1.700	3.0	1.38	PM	.7000	4.40	5.10	1.96	2.19	2.54	4.55	7.70
938	Large scale	-	.2100	1.700	3.0	1.38	PM	.7700	4.40	5.10	2.16	2.09	2.42	8.77	13.86
939	Large scale	-	.2100	1.700	3.0	1.38	PM	.5000	4.40	5.10	1.40	2.59	3.00	1.97	2.78
940	Large scale	-	.2100	1.700	3.0	1.38	PM	.8500	4.40	5.10	2.38	1.99	2.31	11.83	16.35
941	Low crest 1	+	.0344	1.604	2.0	1.25	PM	.1050	1.70	1.96	1.90	3.28	3.78	1.48	2.47
942	Low crest 1	+	.0344	1.604	2.0	1.25	PM	.1250	1.71	1.96	2.27	3.02	3.46	4.20	4.40
943	Low crest 1	+	.0344	1.604	2.0	1.25	PM	.1450	1.72	1.98	2.63	2.82	3.25	2.87	8.63
944	Low crest 1	+	.0344	1.604	2.0	1.25	PM	.1740	1.72	1.96	3.15	2.58	2.94	13.53	20.54
945	Low crest 1	+	.0344	1.604	2.0	1.25	PM	.0830	1.70	1.96	1.50	3.69	4.25	1.28	1.72

1	2	3	4	5	6	7	8	9	10	11	12	13	14	15	16
946	Low crest 1	+	.0344	1.604	2.0	1.25	PM	.1340	2.21	2.56	2.43	3.77	4.37	3.85	4.66
947	Low crest 1	+	.0344	1.604	2.0	1.25	PM	.1590	2.22	2.56	2.88	3.48	4.01	3.52	5.52
948	Low crest 1	+	.0344	1.604	2.0	1.25	PM	.1960	2.19	2.56	3.55	3.09	3.61	16.91	46.38
949	Low crest 1	+	.0344	1.604	2.0	1.25	PM	.1110	2.22	2.56	2.01	4.16	4.80	2.01	2.92
950	Low crest 1	+	.0344	1.604	2.0	1.25	PM	.0770	2.21	2.53	1.40	4.98	5.70	.86	1.02
951	Low crest 1	+	.0344	1.604	2.0	1.25	PM	.1760	2.21	2.56	3.19	3.29	3.81	9.62	17.87
952	Low crest 2	+	.0344	1.604	2.0	1.25	PM	.1370	2.21	2.60	2.48	3.73	4.39	3.27	5.64
953	Low crest 2	+	.0344	1.604	2.0	1.25	PM	.1620	2.20	2.60	2.94	3.42	4.04	13.04	21.98
954	Low crest 2	+	.0344	1.604	2.0	1.25	PM	.1120	2.19	2.56	2.03	4.09	4.78	3.05	3.59
955	Low crest 2	+	.0344	1.604	2.0	1.25	PM	.0780	2.21	2.50	1.41	4.95	5.59	.68	.75
956	Low crest 2	+	.0344	1.604	2.0	1.25	PM	.1490	2.22	2.56	2.70	3.59	4.15	8.66	14.54
957	Low crest 2	+	.0344	1.604	2.0	1.25	PM	.1280	1.70	1.94	2.32	2.97	3.39	6.69	12.27
958	Low crest 2	+	.0344	1.604	2.0	1.25	PM	.1050	1.68	1.96	1.90	3.24	3.78	2.45	3.54
959	Low crest 2	+	.0344	1.604	2.0	1.25	PM	.0830	1.68	1.94	1.50	3.64	4.21	1.16	1.84
960	Low crest 2	+	.0344	1.604	2.0	1.25	PM	.1480	1.70	1.96	2.68	2.76	3.18	14.07	45.66
961	Low crest 3	+	.0344	1.604	2.0	1.25	PM	.1470	1.72	1.96	2.66	2.80	3.20	1.59	2.53
962	Low crest 3	+	.0344	1.604	2.0	1.25	PM	.1750	1.72	1.94	3.17	2.57	2.90	4.64	7.02
963	Low crest 3	+	.0344	1.604	2.0	1.25	PM	.1960	1.72	1.96	3.55	2.43	2.77	4.63	6.77
964	Low crest 3	+	.0344	1.604	2.0	1.25	PM	.2160	1.74	1.96	3.91	2.34	2.64	10.10	13.54
965	Low crest 3	+	.0344	1.604	2.0	1.25	PM	.1160	1.70	1.94	2.10	3.12	3.56	1.45	1.71
966	Low crest 3	+	.0344	1.604	2.0	1.25	PM	.1610	1.72	1.98	2.92	2.66	3.08	1.81	2.95
967	Low crest 3	+	.0344	1.604	2.0	1.25	PM	.1930	2.18	2.53	3.50	3.10	3.60	7.66	11.66
968	Low crest 3	+	.0344	1.604	2.0	1.25	PM	.1610	2.18	2.56	2.92	3.40	3.99	4.23	7.43
969	Low crest 3	+	.0344	1.604	2.0	1.25	PM	.1370	2.18	2.56	2.48	3.68	4.32	2.00	3.11
970	Low crest 3	+	.0344	1.604	2.0	1.25	PM	.1100	2.18	2.56	1.99	4.11	4.82	.97	1.20
971	Low crest 3	+	.0344	1.604	2.0	1.25	PM	.2190	2.16	2.60	3.97	2.88	3.47	13.47	16.96

APPENDIX II

Results established from fixed damage levels in damage curves

The procedure was described in Section 3.2 and Figure 3.15

Tests on static stability

parameters in columns

column   **description**

1   number (not test number)
2   slope angle, $\cot\alpha$
3   grading, D_{85}/D_{15}
4   permeability or type of structure

                                − = impermeable core

                                + = permeable core

                                H = homogeneous structure

                                V = foreshore; water depth at structure 0.40 m

                                B = foreshore; water depth at structure 0.20 m

                                C = crest height at 0.125 m above SWL

                                D = crest height at SWL

                                E = crest height at 0.10 m below SWL

5   relative mass density, Δ
6   average wave period, T_m (s)
7   nominal diameter, D_{n50} (m)
8   damage level, S
9   ξ_m value for N = 1000
10       $H_s/\Delta D_{n50}$ value for N = 1000
11   ξ_m value for N = 3000
12       $H_s/\Delta D_{n50}$ value for N = 3000

1	2	3	4	5	6	7	8	9	10	11	12
1	2.0	2.25	-	1.700	1.00	.0164	2	3.15	1.41	3.49	1.15
2	2.0	2.25	-	1.700	1.00	.0164	3	3.01	1.55	3.32	1.27
3	2.0	2.25	-	1.700	1.00	.0164	5	2.87	1.70	3.08	1.48
4	2.0	2.25	-	1.700	1.00	.0164	8	2.77	1.83	2.86	1.71
5	2.0	2.25	-	1.700	1.00	.0246	2	2.49	1.51	2.65	1.33
6	2.0	2.25	-	1.700	1.00	.0246	3	2.40	1.62	2.54	1.45
7	2.0	2.25	-	1.700	1.00	.0246	5	2.28	1.79	2.42	1.60
8	2.0	2.25	-	1.700	1.00	.0246	8	2.22	1.89	2.32	1.74
9	2.0	2.25	-	1.700	1.00	.0328	2	2.08	1.62	2.21	1.43
10	2.0	2.25	-	1.700	1.00	.0328	3	2.01	1.73	2.17	1.49
11	2.0	2.25	-	1.700	1.16	.0164	2	3.85	1.27	4.05	1.15
12	2.0	2.25	-	1.700	1.16	.0164	3	3.63	1.43	3.92	1.23
13	2.0	2.25	-	1.700	1.16	.0164	5	3.37	1.66	3.70	1.38
14	2.0	2.25	-	1.700	1.16	.0164	8	3.25	1.78	3.50	1.54
15	2.0	2.25	-	1.700	1.16	.0246	2	3.00	1.40	3.58	.98
16	2.0	2.25	-	1.700	1.16	.0246	3	2.85	1.55	3.31	1.15
17	2.0	2.25	-	1.700	1.16	.0246	5	2.66	1.77	2.93	1.46
18	2.0	2.25	-	1.700	1.16	.0246	8	0.00	0.00	2.69	1.74
19	2.0	2.25	-	1.700	1.16	.0328	2	2.46	1.56	2.56	1.44
20	2.0	2.25	-	1.700	1.16	.0328	3	2.38	1.67	2.49	1.52
21	2.0	2.25	-	1.700	1.31	.0164	2	4.27	1.32	4.37	1.26
22	2.0	2.25	-	1.700	1.31	.0164	3	4.09	1.44	4.22	1.35
23	2.0	2.25	-	1.700	1.31	.0164	5	3.95	1.54	4.09	1.44
24	2.0	2.25	-	1.700	1.31	.0164	8	0.00	0.00	4.00	1.50
25	2.0	2.25	-	1.700	1.31	.0246	2	3.47	1.33	3.65	1.20
26	2.0	2.25	-	1.700	1.31	.0246	3	3.34	1.44	3.47	1.33
27	2.0	2.25	-	1.700	1.31	.0246	5	3.21	1.56	3.34	1.44
28	2.0	2.25	-	1.700	1.31	.0246	8	0.00	0.00	3.25	1.52
29	2.0	2.25	-	1.700	1.31	.0328	2	2.87	1.46	3.02	1.32
30	2.0	2.25	-	1.700	1.31	.0328	3	2.74	1.60	2.88	1.45
31	2.0	2.25	-	1.700	1.31	.0328	5	0.00	0.00	2.73	1.61
32	2.0	2.25	-	1.700	1.31	.0328	8	0.00	0.00	2.68	1.67
33	2.0	2.25	-	1.630	1.85	.0360	2	4.20	1.29	4.41	1.17
34	2.0	2.25	-	1.630	1.85	.0360	3	4.05	1.39	4.25	1.26
35	2.0	2.25	-	1.630	1.85	.0360	5	3.94	1.47	4.08	1.37
36	2.0	2.25	-	1.630	1.85	.0360	8	0.00	0.00	0.00	0.00
37	2.0	2.25	-	1.630	2.19	.0360	2	5.01	1.27	5.25	1.16
38	2.0	2.25	-	1.630	2.19	.0360	3	4.90	1.33	5.03	1.26
39	2.0	2.25	-	1.630	2.19	.0360	5	4.76	1.41	4.85	1.36
40	2.0	2.25	-	1.630	2.19	.0360	8	0.00	0.00	4.76	1.41
41	2.0	2.25	-	1.630	2.69	.0360	2	5.95	1.36	6.06	1.31
42	2.0	2.25	-	1.630	2.69	.0360	3	5.82	1.42	5.91	1.38
43	2.0	2.25	-	1.630	2.69	.0360	5	5.74	1.46	5.82	1.42
44	2.0	2.25	-	1.630	2.69	.0360	8	5.74	1.46	5.80	1.43
45	2.0	2.25	-	1.630	3.11	.0360	2	6.88	1.36	6.96	1.33
46	2.0	2.25	-	1.630	3.11	.0360	3	6.78	1.40	6.88	1.36
47	2.0	2.25	-	1.630	3.11	.0360	5	6.62	1.47	6.69	1.44
48	2.0	2.25	-	1.630	3.11	.0360	8	6.49	1.53	6.55	1.50
49	3.0	2.25	-	1.700	.99	.0164	2	1.88	1.73	2.37	1.09
50	3.0	2.25	-	1.700	.99	.0164	3	1.78	1.92	2.03	1.48
51	3.0	2.25	-	1.700	.99	.0164	5	1.70	2.11	1.79	1.90
52	3.0	2.25	-	1.700	.99	.0164	8	1.65	2.24	1.68	2.15
53	3.0	2.25	-	1.700	.99	.0164	12	0.00	0.00	1.61	2.35
54	3.0	2.25	-	1.700	.99	.0246	2	1.47	1.88	1.57	1.66
55	3.0	2.25	-	1.700	.99	.0246	3	1.42	2.02	1.52	1.77
56	3.0	2.25	-	1.700	.99	.0246	5	0.00	0.00	1.46	1.91
57	3.0	2.25	-	1.700	.99	.0246	8	0.00	0.00	1.39	2.10
58	3.0	2.25	-	1.700	1.15	.0164	2	2.38	1.46	2.48	1.34
59	3.0	2.25	-	1.700	1.15	.0164	3	2.16	1.77	2.29	1.57
60	3.0	2.25	-	1.700	1.15	.0164	5	1.97	2.12	2.13	1.82

1	2	3	4	5	6	7	8	9	10	11	12
61	3.0	2.25	-	1.700	1.15	.0164	8	1.88	2.34	2.03	2.00
62	3.0	2.25	-	1.700	1.15	.0246	2	1.70	1.89	1.95	1.45
63	3.0	2.25	-	1.700	1.15	.0246	3	1.66	2.00	1.82	1.66
64	3.0	2.25	-	1.700	1.15	.0246	5	1.59	2.16	1.68	1.95
65	3.0	2.25	-	1.700	1.15	.0246	8	1.55	2.28	1.63	2.07
66	3.0	2.25	-	1.700	1.15	.0246	12	0.00	0.00	1.60	2.15
67	3.0	2.25	-	1.700	1.30	.0164	2	2.68	1.46	3.00	1.17
68	3.0	2.25	-	1.700	1.30	.0164	3	2.56	1.60	2.82	1.32
69	3.0	2.25	-	1.700	1.30	.0164	5	2.39	1.84	2.59	1.57
70	3.0	2.25	-	1.700	1.30	.0164	8	2.25	2.07	2.40	1.82
71	3.0	2.25	-	1.700	1.30	.0164	12	2.17	2.24	2.24	2.10
72	3.0	2.25	-	1.700	1.30	.0246	2	2.15	1.52	2.34	1.29
73	3.0	2.25	-	1.700	1.30	.0246	3	2.02	1.72	2.12	1.56
74	3.0	2.25	-	1.700	1.30	.0246	5	1.93	1.89	1.99	1.77
75	3.0	2.25	-	1.700	1.30	.0246	8	1.82	2.12	1.96	1.83
76	3.0	2.25	-	1.700	1.30	.0246	12	1.77	2.25	1.83	2.09
77	3.0	2.25	-	1.700	1.30	.0328	2	1.79	1.65	1.85	1.54
78	3.0	2.25	-	1.700	1.30	.0328	3	0.00	0.00	1.75	1.71
79	3.0	2.25	-	1.630	1.84	.0360	2	2.56	1.53	2.68	1.39
80	3.0	2.25	-	1.630	1.84	.0360	3	2.46	1.65	2.59	1.49
81	3.0	2.25	-	1.630	1.84	.0360	5	2.31	1.87	2.46	1.66
82	3.0	2.25	-	1.630	1.84	.0360	8	2.19	2.08	2.33	1.84
83	3.0	2.25	-	1.630	1.84	.0360	12	2.10	2.28	2.23	2.02
84	3.0	2.25	-	1.630	2.19	.0360	2	3.03	1.55	3.38	1.24
85	3.0	2.25	-	1.630	2.19	.0360	3	2.91	1.68	3.18	1.40
86	3.0	2.25	-	1.630	2.19	.0360	5	2.78	1.84	3.00	1.58
87	3.0	2.25	-	1.630	2.19	.0360	8	2.68	1.97	2.86	1.73
88	3.0	2.25	-	1.630	2.19	.0360	12	2.65	2.02	2.79	1.82
89	3.0	2.25	-	1.630	2.66	.0360	2	3.66	1.56	3.72	1.51
90	3.0	2.25	-	1.630	2.66	.0360	3	3.56	1.65	3.69	1.54
91	3.0	2.25	-	1.630	2.66	.0360	5	3.45	1.76	3.59	1.62
92	3.0	2.25	-	1.630	2.66	.0360	8	3.35	1.87	3.49	1.72
93	3.0	2.25	-	1.630	2.66	.0360	12	3.27	1.96	3.40	1.81
94	3.0	2.25	-	1.630	3.13	.0360	2	4.37	1.52	4.49	1.44
95	3.0	2.25	-	1.630	3.13	.0360	3	4.23	1.62	4.38	1.51
96	3.0	2.25	-	1.630	3.13	.0360	5	4.04	1.78	4.22	1.63
97	3.0	2.25	-	1.630	3.13	.0360	8	3.86	1.95	4.04	1.78
98	3.0	2.25	-	1.630	3.13	.0360	12	3.80	2.01	3.93	1.88
99	4.0	2.25	-	1.700	.99	.0164	2	1.27	2.12	1.31	2.00
100	4.0	2.25	-	1.700	.99	.0164	3	1.22	2.32	1.26	2.16
101	4.0	2.25	-	1.700	.99	.0164	5	1.16	2.57	1.20	2.38
102	4.0	2.25	-	1.700	.99	.0164	8	0.00	0.00	1.16	2.56
103	4.0	2.25	-	1.700	1.15	.0164	2	0.00	0.00	0.00	0.00
104	4.0	2.25	-	1.700	1.15	.0164	3	1.45	2.21	1.62	1.76
105	4.0	2.25	-	1.700	1.15	.0164	5	1.31	2.72	1.44	2.23
106	4.0	2.25	-	1.700	1.15	.0164	8	1.24	2.99	1.33	2.60
107	4.0	2.25	-	1.700	1.15	.0164	12	0.00	0.00	1.27	2.88
108	4.0	2.25	-	1.700	1.15	.0164	17	0.00	0.00	1.23	3.05
109	4.0	2.25	-	1.700	1.15	.0246	2	1.18	2.20	1.39	1.60
110	4.0	2.25	-	1.700	1.15	.0246	3	0.00	0.00	1.28	1.88
111	4.0	2.25	-	1.700	1.31	.0164	2	1.80	1.85	0.00	0.00
112	4.0	2.25	-	1.700	1.31	.0164	3	1.73	2.01	1.78	1.90
113	4.0	2.25	-	1.700	1.31	.0164	5	1.60	2.34	1.72	2.04
114	4.0	2.25	-	1.700	1.31	.0164	8	1.48	2.73	1.64	2.24
115	4.0	2.25	-	1.700	1.31	.0164	12	0.00	0.00	1.55	2.50
116	4.0	2.25	-	1.700	1.31	.0164	17	0.00	0.00	1.45	2.84
117	4.0	2.25	-	1.700	1.31	.0246	2	1.41	2.02	1.50	1.79
118	4.0	2.25	-	1.700	1.31	.0246	3	1.36	2.18	1.42	1.98
119	4.0	2.25	-	1.700	1.31	.0246	5	1.29	2.39	1.33	2.28
120	4.0	2.25	-	1.700	1.31	.0246	8	0.00	0.00	1.26	2.54

1	2	3	4	5	6	7	8	9	10	11	12
121	4.0	2.25	-	1.700	1.31	.0246	12	0.00	0.00	0.00	0.00
122	4.0	2.25	-	1.700	1.31	.0328	2	1.22	2.01	1.31	1.74
123	4.0	2.25	-	1.700	1.31	.0328	3	1.18	2.15	1.25	1.93
124	4.0	2.25	-	1.700	1.31	.0328	5	0.00	0.00	1.17	2.18
125	4.0	2.25	-	1.700	1.31	.0328	8	0.00	0.00	1.11	2.44
126	4.0	2.25	-	1.700	1.31	.0328	12	0.00	0.00	0.00	0.00
127	4.0	2.25	-	1.630	1.40	.0360	5	1.08	2.82	1.14	2.53
128	4.0	2.25	-	1.630	1.40	.0360	8	1.00	3.23	1.07	2.84
129	4.0	2.25	-	1.630	1.40	.0360	12	0.00	0.00	1.02	3.16
130	4.0	2.25	-	1.630	1.63	.0360	5	0.00	0.00	0.00	0.00
131	4.0	2.25	-	1.630	1.63	.0360	8	1.19	3.11	0.00	0.00
132	4.0	2.25	-	1.630	1.63	.0360	12	1.17	3.24	1.24	2.87
133	4.0	2.25	-	1.630	1.63	.0360	17	1.14	3.40	1.18	3.16
134	4.0	2.25	-	1.630	2.19	.0360	2	2.24	1.59	2.43	1.35
135	4.0	2.25	-	1.630	2.19	.0360	3	2.11	1.79	2.34	1.46
136	4.0	2.25	-	1.630	2.19	.0360	5	2.00	1.99	2.11	1.79
137	4.0	2.25	-	1.630	2.19	.0360	8	1.88	2.27	2.03	1.94
138	4.0	2.25	-	1.630	2.19	.0360	12	1.80	2.47	1.94	2.12
139	4.0	2.25	-	1.630	2.19	.0360	17	1.73	2.68	1.88	2.27
140	4.0	2.25	-	1.630	2.69	.0360	2	2.95	1.38	3.06	1.29
141	4.0	2.25	-	1.630	2.69	.0360	3	2.83	1.50	2.96	1.37
142	4.0	2.25	-	1.630	2.69	.0360	5	2.67	1.69	2.83	1.50
143	4.0	2.25	-	1.630	2.69	.0360	8	2.52	1.89	2.69	1.66
144	4.0	2.25	-	1.630	2.69	.0360	12	2.41	2.08	2.57	1.82
145	4.0	2.25	-	1.630	2.69	.0360	17	2.32	2.24	2.47	1.97
146	4.0	2.25	-	1.630	3.22	.0360	2	3.52	1.39	3.62	1.32
147	4.0	2.25	-	1.630	3.22	.0360	3	3.33	1.56	3.47	1.43
148	4.0	2.25	-	1.630	3.22	.0360	5	3.19	1.70	3.35	1.54
149	4.0	2.25	-	1.630	3.22	.0360	8	3.03	1.88	3.19	1.70
150	4.0	2.25	-	1.630	3.22	.0360	12	2.92	2.03	3.07	1.83
151	4.0	2.25	-	1.630	3.22	.0360	17	2.83	2.15	2.98	1.94
152	6.0	2.25	-	1.700	1.15	.0164	2	.96	2.22	1.00	2.07
153	6.0	2.25	-	1.700	1.15	.0164	3	.89	2.59	.95	2.28
154	6.0	2.25	-	1.700	1.15	.0164	5	.82	3.09	.86	2.80
155	6.0	2.25	-	1.700	1.31	.0164	2	.95	2.98	1.33	1.52
156	6.0	2.25	-	1.700	1.31	.0164	3	.88	3.44	1.08	2.28
157	6.0	2.25	-	1.700	1.31	.0164	5	.84	3.83	.93	3.11
158	6.0	2.25	-	1.700	1.31	.0164	8	.81	4.11	.87	3.52
159	6.0	2.25	-	1.700	1.31	.0164	12	0.00	0.00	.82	4.00
160	6.0	2.25	-	1.630	1.40	.0360	2	.71	2.86	0.00	0.00
161	6.0	2.25	-	1.630	1.40	.0360	3	.68	3.13	.73	2.72
162	6.0	2.25	-	1.630	1.40	.0360	5	.63	3.70	.66	3.28
163	6.0	2.25	-	1.630	1.63	.0360	2	0.00	0.00	0.00	0.00
164	6.0	2.25	-	1.630	1.63	.0360	3	.82	2.90	.90	2.44
165	6.0	2.25	-	1.630	1.63	.0360	5	.77	3.34	.85	2.70
166	6.0	2.25	-	1.630	1.63	.0360	8	.71	3.94	.77	3.35
167	6.0	2.25	-	1.630	1.63	.0360	12	0.00	0.00	.73	3.64
168	6.0	2.25	-	1.630	1.63	.0360	17	0.00	0.00	.69	4.14
169	6.0	2.25	-	1.630	1.85	.0360	2	0.00	0.00	0.00	0.00
170	6.0	2.25	-	1.630	1.85	.0360	3	1.09	2.13	1.11	2.07
171	6.0	2.25	-	1.630	1.85	.0360	5	.97	2.68	1.03	2.40
172	6.0	2.25	-	1.630	1.85	.0360	8	.87	3.38	.96	2.72
173	6.0	2.25	-	1.630	1.85	.0360	12	.76	4.43	.88	3.28
174	6.0	2.25	-	1.630	1.85	.0360	17	0.00	0.00	.81	3.88
175	6.0	2.25	-	1.630	2.16	.0360	2	1.23	2.28	0.00	0.00
176	6.0	2.25	-	1.630	2.16	.0360	3	1.13	2.69	1.31	2.00
177	6.0	2.25	-	1.630	2.16	.0360	5	1.06	3.08	1.17	2.54
178	6.0	2.25	-	1.630	2.16	.0360	8	.98	3.59	1.07	3.00
179	6.0	2.25	-	1.630	2.16	.0360	12	.92	4.08	1.01	3.40
180	6.0	2.25	-	1.630	2.16	.0360	17	.89	4.36	.97	3.70

1	2	3	4	5	6	7	8	9	10	11	12
181	6.0	2.25	-	1.630	2.63	.0360	2	1.72	1.72	1.81	1.57
182	6.0	2.25	-	1.630	2.63	.0360	3	1.63	1.92	1.70	1.76
183	6.0	2.25	-	1.630	2.63	.0360	5	1.49	2.30	1.57	2.08
184	6.0	2.25	-	1.630	2.63	.0360	8	1.38	2.69	1.45	2.44
185	6.0	2.25	-	1.630	2.63	.0360	12	1.28	3.14	1.35	2.80
186	6.0	2.25	-	1.630	2.63	.0360	17	1.21	3.52	1.29	3.08
187	6.0	2.25	-	1.630	3.15	.0360	2	2.36	1.32	2.64	1.05
188	6.0	2.25	-	1.630	3.15	.0360	3	2.14	1.60	2.39	1.28
189	6.0	2.25	-	1.630	3.15	.0360	5	1.99	1.86	2.11	1.65
190	6.0	2.25	-	1.630	3.15	.0360	8	1.79	2.30	1.90	2.04
191	6.0	2.25	-	1.630	3.15	.0360	12	1.72	2.48	1.78	2.31
192	6.0	2.25	-	1.630	3.15	.0360	17	1.67	2.64	1.74	2.43
193	3.0	1.25	-	1.615	1.33	.0360	2	1.73	1.76	1.77	1.68
194	3.0	1.25	-	1.615	1.33	.0360	3	1.63	2.00	1.70	1.83
195	3.0	1.25	-	1.615	1.33	.0360	5	1.52	2.30	1.61	2.05
196	3.0	1.25	-	1.615	1.33	.0360	8	1.41	2.65	1.52	2.30
197	3.0	1.25	-	1.615	1.33	.0360	12	1.33	2.98	1.43	2.57
198	3.0	1.25	-	1.615	1.77	.0360	2	2.51	1.49	2.60	1.38
199	3.0	1.25	-	1.615	1.77	.0360	3	2.41	1.61	2.53	1.46
200	3.0	1.25	-	1.615	1.77	.0360	5	2.25	1.84	2.40	1.63
201	3.0	1.25	-	1.615	1.77	.0360	8	2.10	2.13	2.25	1.85
202	3.0	1.25	-	1.615	1.77	.0360	12	1.97	2.42	2.13	2.06
203	3.0	1.25	-	1.615	2.20	.0360	2	3.10	1.50	3.28	1.34
204	3.0	1.25	-	1.615	2.20	.0360	3	2.97	1.64	3.19	1.42
205	3.0	1.25	-	1.615	2.20	.0360	5	2.81	1.83	3.00	1.61
206	3.0	1.25	-	1.615	2.20	.0360	8	2.66	2.04	2.86	1.77
207	3.0	1.25	-	1.615	2.20	.0360	12	2.58	2.17	2.73	1.94
208	3.0	1.25	-	1.615	2.99	.0360	2	4.14	1.56	4.31	1.44
209	3.0	1.25	-	1.615	2.99	.0360	3	4.02	1.65	4.16	1.54
210	3.0	1.25	-	1.615	2.99	.0360	5	3.83	1.82	3.95	1.71
211	3.0	1.25	-	1.615	2.99	.0360	8	3.69	1.96	3.78	1.87
212	3.0	1.25	-	1.615	2.99	.0360	12	3.62	2.04	3.69	1.96
213	4.0	1.25	-	1.615	1.35	.0360	2	1.19	2.17	0.00	0.00
214	4.0	1.25	-	1.615	1.35	.0360	3	1.14	2.35	1.23	2.02
215	4.0	1.25	-	1.615	1.35	.0360	5	1.02	2.93	1.11	2.50
216	4.0	1.25	-	1.615	1.35	.0360	8	.93	3.53	1.02	2.95
217	4.0	1.25	-	1.615	1.35	.0360	12	0.00	0.00	0.00	0.00
218	4.0	1.25	-	1.615	1.76	.0360	2	1.72	1.75	1.88	1.47
219	4.0	1.25	-	1.615	1.76	.0360	3	1.63	1.97	1.75	1.70
220	4.0	1.25	-	1.615	1.76	.0360	5	1.51	2.27	1.60	2.03
221	4.0	1.25	-	1.615	1.76	.0360	8	1.41	2.62	1.49	2.35
222	4.0	1.25	-	1.615	1.76	.0360	12	1.33	2.96	1.39	2.68
223	4.0	1.25	-	1.615	1.76	.0360	17	1.26	3.28	1.33	2.96
224	4.0	1.25	-	1.615	2.19	.0360	2	2.31	1.51	2.55	1.24
225	4.0	1.25	-	1.615	2.19	.0360	3	2.17	1.71	2.38	1.42
226	4.0	1.25	-	1.615	2.19	.0360	5	1.99	2.03	2.15	1.75
227	4.0	1.25	-	1.615	2.19	.0360	8	1.88	2.28	2.00	2.01
228	4.0	1.25	-	1.615	2.19	.0360	12	1.78	2.55	1.88	2.28
229	4.0	1.25	-	1.615	2.19	.0360	17	1.72	2.72	1.81	2.47
230	4.0	1.25	-	1.615	2.99	.0360	2	3.16	1.50	3.28	1.40
231	4.0	1.25	-	1.615	2.99	.0360	3	3.06	1.60	3.16	1.50
232	4.0	1.25	-	1.615	2.99	.0360	5	2.89	1.80	3.05	1.61
233	4.0	1.25	-	1.615	2.99	.0360	8	2.71	2.04	2.90	1.78
234	4.0	1.25	-	1.615	2.99	.0360	12	2.53	2.34	2.75	1.98
235	4.0	1.25	-	1.615	2.99	.0360	17	2.48	2.44	2.65	2.14
236	1.5	1.25	+	1.615	1.31	.0360	2	3.56	1.62	3.62	1.56
237	1.5	1.25	+	1.615	1.31	.0360	3	3.42	1.75	3.55	1.63
238	1.5	1.25	+	1.615	1.31	.0360	5	3.24	1.95	3.42	1.75
239	1.5	1.25	+	1.615	1.31	.0360	8	3.07	2.17	3.28	1.90
240	1.5	1.25	+	1.615	1.71	.0360	2	4.61	1.64	4.87	1.47

1	2	3	4	5	6	7	8	9	10	11	12
241	1.5	1.25	♦	1.615	1.71	.0360	3	4.53	1.70	4.78	1.53
242	1.5	1.25	♦	1.615	1.71	.0360	5	4.37	1.83	4.60	1.65
243	1.5	1.25	♦	1.615	1.71	.0360	8	4.22	1.96	4.43	1.78
244	1.5	1.25	♦	1.615	2.16	.0360	2	5.69	1.72	5.90	1.60
245	1.5	1.25	♦	1.615	2.16	.0360	3	5.52	1.83	5.76	1.68
246	1.5	1.25	♦	1.615	2.16	.0360	5	5.29	1.99	5.56	1.80
247	1.5	1.25	♦	1.615	2.16	.0360	8	5.09	2.15	5.36	1.94
248	1.5	1.25	♦	1.615	2.89	.0360	2	7.01	2.03	7.28	1.88
249	1.5	1.25	♦	1.615	2.89	.0360	3	6.84	2.13	7.12	1.97
250	1.5	1.25	♦	1.615	2.89	.0360	5	6.54	2.33	6.81	2.15
251	1.5	1.25	♦	1.615	2.89	.0360	8	6.36	2.47	6.60	2.29
252	2.0	1.25	♦	1.615	1.32	.0360	2	2.43	1.98	2.58	1.76
253	2.0	1.25	♦	1.615	1.32	.0360	3	2.32	2.17	2.45	1.95
254	2.0	1.25	♦	1.615	1.32	.0360	5	2.19	2.43	2.32	2.12
255	2.0	1.25	♦	1.615	1.32	.0360	8	2.08	2.70	2.20	2.42
256	2.0	1.25	♦	1.615	1.32	.0360	12	0.00	0.00	2.11	2.62
257	2.0	1.25	♦	1.615	1.70	.0360	2	3.45	1.63	3.59	1.51
258	2.0	1.25	♦	1.615	1.70	.0360	3	3.33	1.75	3.45	1.63
259	2.0	1.25	♦	1.615	1.70	.0360	5	3.11	2.01	3.24	1.85
260	2.0	1.25	♦	1.615	1.70	.0360	8	2.92	2.27	3.06	2.07
261	2.0	1.25	♦	1.615	1.70	.0360	12	0.00	0.00	2.93	2.26
262	2.0	1.25	♦	1.615	2.16	.0360	2	4.27	1.72	4.44	1.59
263	2.0	1.25	♦	1.615	2.16	.0360	3	4.12	1.85	4.28	1.71
264	2.0	1.25	♦	1.615	2.16	.0360	5	3.93	2.03	4.09	1.87
265	2.0	1.25	♦	1.615	2.16	.0360	8	3.77	2.21	3.92	2.04
266	2.0	1.25	♦	1.615	2.16	.0360	12	3.67	2.33	3.83	2.14
267	2.0	1.25	♦	1.615	2.89	.0360	2	5.12	2.14	5.43	1.90
268	2.0	1.25	♦	1.615	2.89	.0360	3	5.01	2.24	5.26	2.03
269	2.0	1.25	♦	1.615	2.89	.0360	5	4.78	2.46	4.99	2.25
270	2.0	1.25	♦	1.615	2.89	.0360	8	4.60	2.65	4.79	2.45
271	2.0	1.25	♦	1.615	2.89	.0360	12	4.48	2.79	4.64	2.61
272	3.0	1.25	♦	1.615	1.34	.0360	2	1.46	2.53	1.56	2.20
273	3.0	1.25	♦	1.615	1.34	.0360	3	1.37	2.86	1.47	2.47
274	3.0	1.25	♦	1.615	1.78	.0360	2	2.12	2.10	2.26	1.86
275	3.0	1.25	♦	1.615	1.78	.0360	3	2.00	2.36	2.10	2.14
276	3.0	1.25	♦	1.615	1.78	.0360	5	1.89	2.66	1.97	2.44
277	3.0	1.25	♦	1.615	1.78	.0360	8	1.79	2.94	1.85	2.75
278	3.0	1.25	♦	1.615	1.78	.0360	12	1.73	3.17	1.78	2.98
279	3.0	1.25	♦	1.615	2.18	.0360	2	2.70	1.94	2.84	1.76
280	3.0	1.25	♦	1.615	2.18	.0360	3	2.61	2.09	2.72	1.97
281	3.0	1.25	♦	1.615	2.18	.0360	5	2.46	2.35	2.58	2.14
282	3.0	1.25	♦	1.615	2.18	.0360	8	2.30	2.68	2.44	2.39
283	3.0	1.25	♦	1.615	2.18	.0360	12	2.17	3.01	2.30	2.68
284	3.0	1.25	♦	1.615	2.94	.0360	2	3.60	1.99	3.76	1.83
285	3.0	1.25	♦	1.615	2.94	.0360	3	3.48	2.13	3.59	2.00
286	3.0	1.25	♦	1.615	2.94	.0360	5	3.28	2.40	3.45	2.17
287	3.0	1.25	♦	1.615	2.94	.0360	8	3.11	2.67	3.36	2.28
288	3.0	1.25	♦	1.615	2.94	.0360	12	2.99	2.88	3.22	2.49
289	2.0	1.25	H	1.615	1.35	.0360	2	2.38	2.16	2.54	1.90
290	2.0	1.25	H	1.615	1.35	.0360	3	2.24	2.44	2.40	2.12
291	2.0	1.25	H	1.615	1.35	.0360	5	2.10	2.79	2.24	2.45
292	2.0	1.25	H	1.615	1.35	.0360	8	1.99	3.09	2.11	2.76
293	2.0	1.25	H	1.615	1.35	.0360	12	1.93	3.30	2.02	3.01
294	2.0	1.25	H	1.615	1.74	.0360	2	3.41	1.75	3.49	1.67
295	2.0	1.25	H	1.615	1.74	.0360	3	3.23	1.95	3.34	1.82
296	2.0	1.25	H	1.615	1.74	.0360	5	2.99	2.27	3.14	2.06
297	2.0	1.25	H	1.615	1.74	.0360	8	2.80	2.59	2.96	2.32
298	2.0	1.25	H	1.615	1.74	.0360	12	2.66	2.87	2.82	2.56
299	2.0	1.25	H	1.615	2.18	.0360	2	4.09	1.91	4.21	1.80
300	2.0	1.25	H	1.615	2.18	.0360	3	3.94	2.06	4.09	1.91

1	2	3	4	5	6	7	8	9	10	11	12
301	2.0	1.25	H	1.615	2.18	.0360	5	3.70	2.33	3.88	2.12
302	2.0	1.25	H	1.615	2.18	.0360	8	3.53	2.56	3.73	2.30
303	2.0	1.25	H	1.615	2.18	.0360	12	3.38	2.79	3.55	2.54
304	2.0	1.25	H	1.615	2.86	.0360	2	4.85	2.34	5.17	2.06
305	2.0	1.25	H	1.615	2.86	.0360	3	4.77	2.42	4.85	2.34
306	2.0	1.25	H	1.615	2.86	.0360	5	4.54	2.67	4.74	2.45
307	2.0	1.25	H	1.615	2.86	.0360	8	4.35	2.91	4.48	2.74
308	2.0	1.25	H	1.615	2.86	.0360	12	4.22	3.08	4.32	2.95
309	2.0	1.25	U	1.615	1.68	.0360	2	3.30	1.74	3.42	1.62
310	2.0	1.25	U	1.615	1.68	.0360	3	3.19	1.86	3.32	1.72
311	2.0	1.25	U	1.615	1.68	.0360	5	3.03	2.06	3.18	1.87
312	2.0	1.25	U	1.615	1.68	.0360	8	2.94	2.20	3.05	2.04
313	2.0	1.25	U	1.615	1.68	.0360	12	2.85	2.34	2.95	2.18
314	2.0	1.25	U	1.615	2.19	.0360	2	4.12	1.90	4.24	1.79
315	2.0	1.25	U	1.615	2.19	.0360	3	4.02	1.99	4.16	1.86
316	2.0	1.25	U	1.615	2.19	.0360	5	3.85	2.17	4.02	1.99
317	2.0	1.25	U	1.615	2.19	.0360	8	3.67	2.39	3.87	2.15
318	2.0	1.25	U	1.615	2.19	.0360	12	3.49	2.65	3.71	2.34
319	2.0	1.25	B	1.615	1.74	.0360	2	3.07	2.16	3.11	2.11
320	2.0	1.25	B	1.615	1.74	.0360	3	3.03	2.22	3.08	2.15
321	2.0	1.25	B	1.615	1.74	.0360	5	2.99	2.27	3.03	2.21
322	2.0	1.25	B	1.615	1.74	.0360	8	2.95	2.34	2.99	2.27
323	2.0	1.25	B	1.615	1.74	.0360	12	0.00	0.00	2.96	2.32
324	2.0	1.25	B	1.615	2.17	.0360	2	0.00	0.00	0.00	0.00
325	2.0	1.25	B	1.615	2.17	.0360	3	3.79	2.22	3.81	2.18
326	2.0	1.25	B	1.615	2.17	.0360	5	3.64	2.39	3.72	2.29
327	2.0	1.25	B	1.615	2.17	.0360	8	3.52	2.55	3.62	2.41
328	2.0	1.25	B	1.615	2.17	.0360	12	0.00	0.00	3.54	2.53
349	2.0	1.25	C	1.604	1.70	.0344	2	3.48	1.69	3.62	1.56
350	2.0	1.25	C	1.604	1.70	.0344	3	3.31	1.87	3.47	1.70
351	2.0	1.25	C	1.604	1.70	.0344	5	3.09	2.14	3.27	1.91
352	2.0	1.25	C	1.604	1.70	.0344	8	2.91	2.41	3.08	2.15
353	2.0	1.25	C	1.604	1.70	.0344	12	2.79	2.63	2.95	2.35
354	2.0	1.25	C	1.604	2.20	.0344	2	4.26	1.89	4.44	1.74
355	2.0	1.25	C	1.604	2.20	.0344	3	4.05	2.09	4.24	1.91
356	2.0	1.25	C	1.604	2.20	.0344	5	3.78	2.40	3.96	2.19
357	2.0	1.25	C	1.604	2.20	.0344	8	3.58	2.68	3.75	2.44
358	2.0	1.25	C	1.604	2.20	.0344	12	3.44	2.90	3.58	2.67
359	2.0	1.25	D	1.604	1.70	.0344	2	3.25	1.94	3.45	1.72
360	2.0	1.25	D	1.604	1.70	.0344	3	3.05	2.20	3.25	1.94
329	2.0	1.25	+	.924	1.25	.0345	2	3.12	1.97	3.28	1.79
330	2.0	1.25	+	.924	1.25	.0345	3	2.97	2.18	3.11	1.99
331	2.0	1.25	+	.924	1.25	.0345	5	2.78	2.48	2.91	2.27
332	2.0	1.25	+	.924	1.25	.0345	8	2.63	2.79	2.73	2.58
333	2.0	1.25	+	.924	1.25	.0345	12	.00	0.00	0.00	0.00
334	2.0	1.25	+	.924	1.57	.0345	2	3.90	1.99	4.14	1.77
335	2.0	1.25	+	.924	1.57	.0345	3	3.74	2.17	3.95	1.94
336	2.0	1.25	+	.924	1.57	.0345	5	3.52	2.44	3.73	2.18
337	2.0	1.25	+	.924	1.57	.0345	8	3.36	2.67	3.56	2.40
338	2.0	1.25	+	.924	1.57	.0345	12	3.35	2.70	3.40	2.61
339	2.0	1.25	+	2.050	1.97	.0358	2	3.28	1.81	3.43	1.65
340	2.0	1.25	+	2.050	1.97	.0358	3	3.14	1.97	3.28	1.81
341	2.0	1.25	+	2.050	1.97	.0358	5	2.98	2.18	3.09	2.04
342	2.0	1.25	+	2.050	1.97	.0358	8	2.86	2.38	2.94	2.25
343	2.0	1.25	+	2.050	1.97	.0358	12	2.78	2.52	2.84	2.40
344	2.0	1.25	+	2.050	2.36	.0358	2	3.98	1.87	4.12	1.75
345	2.0	1.25	+	2.050	2.36	.0358	3	3.87	1.98	3.96	1.89
346	2.0	1.25	+	2.050	2.36	.0358	5	3.71	2.15	3.78	2.08
347	2.0	1.25	+	2.050	2.36	.0358	8	3.61	2.28	3.65	2.22
348	2.0	1.25	+	2.050	2.36	.0358	12	0.00	0.00	3.62	2.26

1	2	3	4	5	6	7	8	9	10	11	12
361	2.0	1.25	D	1.604	1.70	.0344	5	2.84	2.54	3.01	2.76
362	2.0	1.25	D	1.604	1.70	.0344	8	2.67	2.87	2.81	2.60
363	2.0	1.25	D	1.604	1.70	.0344	12	2.56	3.11	2.67	2.87
365	2.0	1.25	D	1.604	2.20	.0344	2	4.05	2.09	4.21	1.93
366	2.0	1.25	D	1.604	2.20	.0344	3	3.83	2.34	3.96	2.19
367	2.0	1.25	D	1.604	2.20	.0344	5	3.55	2.72	3.68	2.53
368	2.0	1.25	D	1.604	2.20	.0344	8	3.35	3.06	3.46	2.87
369	2.0	1.25	D	1.604	2.20	.0344	12	3.20	3.35	3.31	3.12
370	2.0	1.25	E	1.604	1.70	.0344	2	2.69	2.83	2.80	2.61
371	2.0	1.25	E	1.604	1.70	.0344	3	2.56	3.11	2.69	2.82
372	2.0	1.25	E	1.604	1.70	.0344	5	2.43	3.46	2.54	3.16
373	2.0	1.25	E	1.604	1.70	.0344	8	2.33	3.78	2.41	3.50
374	2.0	1.25	E	1.604	1.70	.0344	12	2.27	3.97	2.32	3.80
375	2.0	1.25	E	1.604	2.20	.0344	2	3.76	2.42	3.96	2.18
376	2.0	1.25	E	1.604	2.20	.0344	3	3.57	2.69	3.80	2.37
377	2.0	1.25	E	1.604	2.20	.0344	5	3.34	3.07	3.55	2.72
378	2.0	1.25	E	1.604	2.20	.0344	8	3.15	3.46	3.31	3.13
379	2.0	1.25	E	1.604	2.20	.0344	12	2.99	3.83	3.11	3.54
380	3.0	1.38	+	1.700	4.40	.2100	2	2.05	2.55	2.22	1.91
381	3.0	1.38	+	1.700	4.40	.2100	3	1.94	2.51	2.10	2.13
382	3.0	1.38	+	1.700	4.40	.2100	5	1.84	2.79	1.96	2.44
383	3.0	1.38	+	1.700	4.40	.2100	8	1.75	3.06	1.86	2.73
384	3.0	1.38	+	1.700	4.40	.2100	12	1.68	3.32	1.78	2.97
386	3.0	1.38	-	1.700	4.40	.2100	2	2.50	1.50	2.76	1.24
387	3.0	1.38	-	1.700	4.40	.2100	3	2.35	1.70	2.53	1.47
388	3.0	1.38	-	1.700	4.40	.2100	5	2.21	1.93	2.33	1.73
389	3.0	1.38	-	1.700	4.40	.2100	8	2.09	2.15	2.20	1.95
385	3.0	1.38	-	1.700	4.40	.2100	12	2.06	2.21	2.16	2.01

APPENDIX III

Boundary conditions for tests on dynamic stability

parameters in columns

| column | description |

1   test number

2   description:

	gravel	= slope with gravel (shingle)
	rock basic	= basic tests with rock slope
	spectrum	= tests with narrow spectrum
	rounded	= slope with rounded gravel (shingle)
	flat rock	= slope with flat rock
	berm type	= initial slope with berm
	arbitrary	= structure with arbitrary initial slope
	grading	= slope with narrow or wide grading
	low crest	= structure with low crest
	depth 0.4m	= structure with 1:30 foreshore and water depth of 0.40m at the toe of structure
	depth 0.3m	= structure with 1:30 foreshore and water depth of 0.30m at the toe of structure
	depth 0.2m	= structure with 1:30 foreshore and water depth of 0.20m at the toe of structure
	gravel-1982	= two-dimensional tests of Van Hijum and Pilarczyk (1982)
	3dim-1982	= three-dimensional tests of Van Hijum and Pilarczyk (1982)
	delta flume	= large scale tests in the Delta flume

3   nominal diameter, D_{n50} (m)

4   relative mass density, Δ

5   slope angle, $\cot\alpha$

6   grading, D_{85}/D_{15}

7   spectral shape:

	PM	= Pierson Moskowitz spectrum
	NA	= narrow spectrum
	SL	= narrow spectrum, different from NA spectrum
	TR	= Triton spectrum
	JO	= Jonswap spectrum

8   significant wave height in front of the structure, H_s (m)

9   average wave period, T_m (s)

10   peak period, T_p (s)

11   wave height parameter: $H_s/\Delta D_{n50}$

12   fictitious wave steepness: $s_m = 2\pi H_s/gT_m^2$

13   fictitious wave steepness: $2\pi H_s/gT_p^2$

14   combined wave heigt-wave period parameter: $H_oT_o = H_s/\Delta D_{n50} * \sqrt{g/D_{n50}}\, T_m$

15   combined wave heigt-wave period parameter: $H_oT_o = H_s/\Delta D_{n50} * \sqrt{g/D_{n50}}\, T_p$

1	2	3	4	5	6	7	8	9	10	11	12	13	14	15
301	gravel	.0115	1.573	5.0	1.50	PM	.1319	1.33	1.37	7.29	.0478	.0450	283.	292.
302	gravel	.0115	1.573	5.0	1.50	PM	.1298	1.77	2.04	7.18	.0265	.0200	371.	428.
303	gravel	.0115	1.573	5.0	1.50	PM	.1900	1.76	2.04	10.50	.0393	.0292	540.	626.
304	gravel	.0115	1.573	5.0	1.50	PM	.1879	2.41	2.99	10.39	.0207	.0135	731.	907.
305	gravel	.0115	1.573	5.0	1.50	PM	.2326	1.78	2.04	12.86	.0470	.0358	668.	766.
306	gravel	.0115	1.573	5.0	1.50	PM	.2374	2.35	3.17	13.12	.0275	.0151	901.	1215.
307	rock basic	.0257	1.615	5.0	1.50	PM	.1281	1.77	2.04	3.09	.0262	.0197	107.	123.
308	rock basic	.0257	1.615	5.0	1.50	PM	.1303	2.63	3.23	3.14	.0121	.0080	161.	198.
309	rock basic	.0257	1.615	5.0	1.50	PM	.1882	1.77	2.04	4.53	.0385	.0290	157.	181.
310	rock basic	.0257	1.615	5.0	1.50	PM	.1904	2.58	3.28	4.59	.0183	.0113	231.	294.
311	rock basic	.0257	1.615	5.0	1.50	PM	.1945	3.20	4.25	4.69	.0122	.0069	293.	389.
312	rock basic	.0257	1.615	5.0	1.50	PM	.2394	1.78	2.04	5.77	.0484	.0368	201.	230.
313	rock basic	.0257	1.615	5.0	1.50	PM	.2380	2.51	3.33	5.73	.0242	.0137	281.	373.
314	rock basic	.0257	1.615	5.0	1.50	PM	.2289	2.74	3.51	5.51	.0195	.0119	295.	378.
315	rock basic	.0110	1.586	5.0	1.50	PM	.1336	1.32	1.38	7.66	.0491	.0449	302.	316.
316	rock basic	.0110	1.586	5.0	1.50	PM	.1288	1.77	2.04	7.38	.0263	.0198	390.	450.
317	rock basic	.0110	1.586	5.0	1.50	PM	.1236	2.52	3.23	7.08	.0125	.0076	533.	683.
318	rock basic	.0110	1.586	5.0	1.50	PM	.1884	1.75	2.02	10.80	.0394	.0296	564.	651.
319	rock basic	.0110	1.586	5.0	1.50	PM	.1870	2.46	3.13	10.72	.0198	.0122	787.	1002.
320	rock basic	.0110	1.586	5.0	1.50	PM	.1938	3.10	4.25	11.11	.0129	.0069	1028.	1410.
321	rock basic	.0110	1.586	5.0	1.50	PM	.2369	1.77	2.08	13.58	.0484	.0351	718.	843.
322	rock basic	.0110	1.586	5.0	1.50	PM	.2338	2.45	3.23	13.40	.0249	.0144	980.	1293.
323	rock basic	.0110	1.586	5.0	1.50	PM	.2192	2.86	4.20	12.56	.0172	.0080	1073.	1576.
324	rock basic	.0257	1.615	3.0	1.50	PM	.1556	1.34	1.45	3.75	.0555	.0474	98.	106.
325	rock basic	.0257	1.615	3.0	1.50	PM	.1574	1.76	2.00	3.79	.0325	.0252	130.	148.
326	rock basic	.0257	1.615	3.0	1.50	PM	.1285	2.65	3.08	3.10	.0117	.0087	160.	186.
327	rock basic	.0257	1.615	3.0	1.50	PM	.1912	1.77	2.04	4.61	.0391	.0294	159.	184.
328	rock basic	.0257	1.615	3.0	1.50	PM	.1900	2.46	3.13	4.58	.0203	.0124	220.	280.
329	rock basic	.0257	1.615	3.0	1.50	PM	.1937	2.82	3.57	4.67	.0156	.0097	257.	326.
330	rock basic	.0257	1.615	3.0	1.50	PM	.2449	1.79	2.15	5.90	.0490	.0339	206.	248.
331	rock basic	.0257	1.615	3.0	1.50	PM	.2327	2.45	3.08	5.61	.0248	.0157	268.	337.
332	rock basic	.0257	1.615	3.0	1.50	PM	.2283	2.73	3.57	5.50	.0196	.0115	293.	384.
333	rock basic	.0110	1.586	3.0	1.50	PM	.1265	1.33	1.42	7.25	.0458	.0402	288.	307.
334	rock basic	.0110	1.586	3.0	1.50	PM	.1328	1.75	2.02	7.61	.0278	.0208	398.	459.
335	rock basic	.0110	1.586	3.0	1.50	PM	.1319	2.49	3.13	7.56	.0136	.0086	562.	707.
336	rock basic	.0110	1.586	3.0	1.50	PM	.1861	1.75	2.04	10.67	.0389	.0286	557.	650.
337	rock basic	.0110	1.586	3.0	1.50	PM	.1937	2.44	3.08	11.10	.0208	.0131	809.	1021.
338	rock basic	.0110	1.586	3.0	1.50	PM	.1873	2.78	3.57	10.74	.0155	.0094	891.	1145.
339	rock basic	.0110	1.586	3.0	1.50	PM	.2392	1.79	2.04	13.71	.0478	.0368	733.	835.
340	rock basic	.0110	1.586	3.0	1.50	PM	.2307	2.42	3.08	13.22	.0252	.0156	956.	1216.
341	rock basic	.0110	1.586	3.0	1.50	PM	.2236	2.71	3.57	12.82	.0195	.0112	1037.	1366.
342	spectrum	.0257	1.615	3.0	1.50	NA	.1573	1.79	1.79	3.79	.0314	.0314	133.	133.
343	spectrum	.0257	1.615	3.0	1.50	NA	.1296	2.48	2.53	3.12	.0135	.0130	151.	154.
344	spectrum	.0257	1.615	3.0	1.50	NA	.1960	1.79	1.80	4.72	.0392	.0387	165.	166.
345	spectrum	.0257	1.615	3.0	1.50	NA	.1884	2.45	2.50	4.54	.0201	.0193	217.	222.
346	spectrum	.0257	1.615	3.0	1.50	NA	.2373	1.77	1.80	5.72	.0485	.0469	198.	201.
347	spectrum	.0257·	1.615	3.0	1.50	NA	.2322	2.42	2.50	5.59	.0254	.0238	265.	273.
348	rounded	.0272	1.588	3.0	1.50	PM	.1300	1.77	2.04	3.01	.0266	.0200	101.	117.
349	rounded	.0272	1.588	3.0	1.50	PM	.1954	1.77	2.06	4.52	.0399	.0295	152.	177.
350	rounded	.0272	1.588	3.0	1.50	PM	.2434	1.79	2.06	5.64	.0487	.0367	192.	220.
351	rounded	.0272	1.588	3.0	1.50	PM	.0898	3.01	3.45	2.08	.0063	.0048	119.	136.
352	rounded	.0272	1.588	3.0	1.50	PM	.1325	2.95	3.51	3.07	.0098	.0069	172.	204.
353	rounded	.0272	1.588	3.0	1.50	PM	.1942	2.85	3.57	4.50	.0153	.0098	243.	305.
354	flat rock	.0242	1.608	3.0	1.50	PM	.1304	1.77	2.06	3.35	.0267	.0197	119.	139.
355	flat rock	.0242	1.608	3.0	1.50	PM	.1922	1.77	2.06	4.94	.0393	.0290	176.	205.
356	flat rock	.0242	1.608	3.0	1.50	PM	.2423	1.79	2.06	6.23	.0484	.0366	224.	258.

1	2	3	4	5	6	7	8	9	10	11	12	13	14	15
380	berm type	.0257	1.615	1.5	1.50	PM	.0576	.98	2.09	1.39	.0384	.0084	27.	52.
381	berm type	.0257	1.615	1.5	1.50	PM	.0829	1.26	1.41	2.60	.0734	.0262	49.	55.
382	berm type	.0257	1.615	1.5	1.50	PM	.1016	1.28	1.41	2.45	.0397	.0327	61.	67.
383	berm type	.0257	1.615	1.5	1.50	PM	.1028	1.81	2.05	2.48	.0201	.0157	88.	99.
384	berm type	.0257	1.615	1.5	1.50	PM	.1599	1.34	1.39	3.85	.0570	.0530	101.	105.
385	berm type	.0257	1.615	-1.	1.50	PM	.1586	1.81	2.06	3.82	.0310	.0239	135.	154.
386	berm type	.0257	1.615	-1.	1.50	PM	.1903	1.80	2.12	4.58	.0376	.0271	161.	190.
387	berm type	.0257	1.615	-1.	1.50	PM	.1863	2.51	2.98	4.49	.0169	.0134	229.	261.
388	berm type	.0257	1.615	-1.	1.50	PM	.2462	1.79	2.01	5.93	.0492	.0390	207.	233.
389	berm type	.0257	1.615	-1.	1.50	PM	.2500	2.51	2.96	6.02	.0254	.0163	295.	346.
390	berm type	.0257	1.615	-1.	1.50	PM	.1594	1.81	2.05	3.84	.0312	.0243	136.	154.
391	berm type	.0257	1.615	-1.	1.50	PM	.1695	1.80	2.08	4.57	.0275	.0281	161.	186.
392	berm type	.0257	1.615	-1.	1.50	PM	.2450	1.83	2.04	5.90	.0469	.0377	211.	235.
393	berm type	.0257	1.615	-1.	1.50	PM	.1605	1.80	2.05	3.87	.0317	.0245	136.	155.
394	berm type	.0257	1.615	-1.	1.50	PM	.1907	1.80	2.07	4.59	.0377	.0285	162.	186.
395	berm type	.0257	1.615	-1.	1.50	PM	.2438	1.82	2.03	5.87	.0471	.0329	209.	233.
396	arbitrary	.0257	1.615	-1.	1.50	PM	.1917	1.79	2.06	4.62	.0383	.0289	162.	186.
397	grading	.0110	1.605	3.0	1.25	PM	.1310	1.29	1.42	7.42	.0564	.0416	286.	315.
398	grading	.0110	1.605	3.0	1.25	PM	.1300	1.78	2.11	7.36	.0263	.0187	391.	464.
399	grading	.0110	1.605	3.0	1.25	PM	.1910	1.80	2.13	10.82	.0328	.0270	582.	686.
400	grading	.0110	1.605	3.0	1.25	PM	.2015	2.46	2.94	11.41	.0213	.0149	838.	1032.
401	grading	.0110	1.605	3.0	1.25	PM	.2401	1.81	2.17	13.60	.0469	.0327	735.	881.
402	grading	.0110	1.605	3.0	1.25	PM	.2437	2.47	3.00	13.80	.0256	.0173	1018.	1237.
403	grading	.0110	1.605	3.0	2.25	PM	.1312	1.29	1.42	7.43	.0505	.0417	286.	315.
404	grading	.0110	1.605	3.0	2.25	PM	.1291	1.77	2.08	7.31	.0264	.0191	387.	454.
405	grading	.0110	1.605	3.0	2.25	PM	.1894	1.81	2.11	10.73	.0279	.0272	580.	676.
406	grading	.0110	1.605	3.0	2.25	PM	.1994	2.45	3.03	11.29	.0213	.0139	826.	1022.
407	grading	.0110	1.605	3.0	2.25	PM	.2394	1.81	2.17	13.56	.0468	.0326	733.	879.
408	grading	.0110	1.605	3.0	2.25	PM	.2403	2.47	3.00	13.61	.0252	.0171	1004.	1219.
409	low crest	.0257	1.615	1.5	1.50	PM	.1295	1.33	1.45	3.12	.0469	.0394	81.	58.
410	low crest	.0257	1.615	1.5	1.50	PM	.1770	1.78	2.08	4.26	.0358	.0262	148.	173.
411	low crest	.0257	1.615	1.5	1.50	PM	.1648	2.64	3.64	4.46	.0171	.0040	231.	268.
412	low crest	.0257	1.615	1.5	1.50	PM	.2391	1.80	2.12	5.76	.0473	.0341	207.	239.
413	low crest	.0257	1.615	1.5	1.50	PM	.1323	1.32	1.43	3.19	.0426	.0414	70.	84.
414	low crest	.0257	1.615	1.5	1.50	PM	.1785	1.79	2.04	4.30	.0357	.0275	150.	171.
415	low crest	.0257	1.615	1.5	1.50	PM	.2489	1.83	2.13	5.80	.0462	.0348	208.	242.
416	depth 0.4m	.0257	1.591	3.0	1.50	PM	.2250	2.55	3.03	5.50	.0222	.0152	274.	326.
417	depth 0.3m	.0257	1.591	3.0	1.50	PM	.1890	1.81	2.02	4.62	.0376	.0292	163.	192.
418	depth 0.2m	.0257	1.591	3.0	1.50	PM	.1437	2.51	3.03	3.51	.0146	.0100	172.	206.
419	depth 0.3m	.0110	1.581	3.0	1.50	PM	.2074	2.49	3.08	11.93	.0214	.0140	887.	1092.
420	depth 0.3m	.0110	1.581	3.0	1.50	PM	.1886	1.79	2.11	10.84	.0378	.0272	580.	683.
421	depth 0.2m	.0110	1.581	3.0	1.50	PM	.1486	2.49	3.03	8.51	.0153	.0103	633.	770.
501	gravel-1982	.0041	1.570	10.	1.30	SL	.1080	1.27	1.46	16.78	.0429	.0325	1042.	1198.
502	gravel-1982	.0041	1.570	10.	1.30	SL	.1630	1.29	1.48	25.32	.0627	.0477	1598.	1833.
503	gravel-1982	.0041	1.570	10.	1.30	SL	.1540	1.59	1.83	23.92	.0390	.0295	1861.	2142.
504	gravel-1982	.0041	1.570	10.	1.30	SL	.1900	1.63	1.88	29.52	.0458	.0344	2353.	2714.
506	gravel-1982	.0041	1.570	5.0	1.30	SL	.1520	1.30	1.50	23.61	.0576	.0433	1502.	1733.
507	gravel-1982	.0041	1.570	5.0	1.30	SL	.1080	1.27	1.46	16.78	.0429	.0325	1042.	1198.
508	gravel-1982	.0041	1.570	5.0	1.30	SL	.1880	1.62	1.86	29.21	.0459	.0348	2314.	2657.
509	gravel-1982	.0041	1.570	5.0	1.30	SL	.1470	1.61	1.85	22.84	.0363	.0275	1799.	2067.
510	gravel-1982	.0041	1.570	5.0	1.30	SL	.0950	1.58	1.82	14.76	.0244	.0184	1141.	1314.
511	gravel-1982	.0041	1.570	5.0	1.30	SL	.2050	2.03	2.33	31.85	.0319	.0242	3162.	3630.
512	gravel-1982	.0041	1.570	5.0	1.30	SL	.1450	1.97	2.27	22.53	.0239	.0180	2171.	2501.
513	gravel-1982	.0041	1.570	5.0	1.30	SL	.1030	2.03	2.33	16.00	.0160	.0122	1589.	1824.
514	gravel-1982	.0041	1.570	5.0	1.30	SL	.0880	1.27	1.46	13.67	.0349	.0264	849.	976.
515	gravel-1982	.0041	1.570	5.0	1.30	SL	.1190	1.29	1.48	18.49	.0458	.0348	1167.	1338.

1	2	3	4	5	6	7	8	9	10	11	12	13	14	15
516	gravel-1982	.0041	1.570	5.0	1.30	SL	.1150	1.63	1.88	17.87	.0277	.0208	1424.	1643.
517	gravel-1982	.0041	1.570	5.0	1.30	SL	.1500	1.77	2.04	23.30	.0307	.0231	2018.	2325.
518	gravel-1982	.0069	1.570	5.0	1.30	SL	.1640	1.56	1.79	15.14	.0432	.0328	891.	1022.
519	gravel-1982	.0069	1.570	5.0	1.30	SL	.1930	1.62	1.86	17.82	.0471	.0357	1088.	1250.
520	gravel-1982	.0069	1.570	5.0	1.30	SL	.1580	1.98	2.28	14.58	.0258	.0195	1089.	1254.
521	gravel-1982	.0069	1.570	5.0	1.30	TR	.1960	1.98	2.28	18.09	.0320	.0241	1351.	1556.
522	gravel-1982	.0041	1.570	5.0	1.30	TR	.0950	1.97	2.56	14.76	.0157	.0093	1422.	1848.
523	gravel-1982	.0041	1.570	5.0	1.30	TR	.1500	1.97	2.56	23.30	.0248	.0147	2246.	2918.
524	gravel-1982	.0041	1.570	5.0	1.30	TR	.1520	2.38	3.10	23.61	.0172	.0101	2749.	3581.
525	gravel-1982	.0041	1.570	5.0	1.30	TR	.2050	2.38	3.10	31.85	.0232	.0137	3708.	4829.
526	gravel-1982	.0041	1.570	5.0	1.30	JO	.0790	1.69	1.86	12.27	.0177	.0146	1015.	1117.
527	gravel-1982	.0041	1.570	5.0	1.30	JO	.1040	1.69	1.86	16.16	.0233	.0193	1336.	1470.
528	gravel-1982	.0041	1.570	5.0	1.30	JO	.1000	2.07	2.28	15.53	.0149	.0123	1573.	1733.
529	gravel-1982	.0041	1.570	5.0	1.30	JO	.1300	2.11	2.32	20.20	.0187	.0155	2084.	2292.
530	gravel-1982	.0041	1.570	5.0	1.30	TR	.1690	2.03	2.64	26.25	.0263	.0155	2607.	3390.
531	gravel-1982	.0041	1.570	5.0	1.30	TR	.1150	1.58	2.05	17.87	.0295	.0175	1381.	1792.
532	gravel-1982	.0041	1.570	5.0	1.30	TR	.1520	1.67	2.17	23.61	.0349	.0207	1929.	2507.
533	gravel-1982	.0041	1.570	5.0	1.30	SL	.1400	1.73	1.99	21.75	.0300	.0226	1841.	2117.
551	3dim-1982	.0040	1.590	5.0	1.30	PM	.0740	.89	1.02	11.64	.0598	.0456	513.	588.
552	3dim-1982	.0040	1.590	5.0	1.30	JO	.0860	.85	.93	13.52	.0762	.0637	569.	623.
553	3dim-1982	.0040	1.590	5.0	1.30	JO	.0780	1.25	1.37	12.26	.0320	.0266	759.	832.
554	3dim-1982	.0040	1.590	5.0	1.30	JO	.1260	1.25	1.37	19.81	.0516	.0430	1226.	1344.
555	3dim-1982	.0040	1.590	5.0	1.30	PM	.0880	1.11	1.28	13.84	.0457	.0344	761.	877.
556	3dim-1982	.0040	1.590	5.0	1.30	PM	.1220	1.11	1.28	19.18	.0634	.0477	1055.	1216.
557	3dim-1982	.0040	1.590	5.0	1.30	PM	.0830	1.37	1.58	13.05	.0283	.0213	885.	1021.
558	3dim-1982	.0040	1.590	5.0	1.30	PM	.1220	1.37	1.58	19.18	.0416	.0313	1301.	1501.
559	3dim-1982	.0040	1.590	5.0	1.30	PM	.1700	1.78	2.05	26.73	.0344	.0259	2356.	2714.
560	3dim-1982	.0040	1.590	5.0	1.30	PM	.1620	1.78	2.05	25.47	.0327	.0247	2245.	2586.
801	delta flume	.0187	1.600	5.0	1.64	SL	.7700	4.30	5.00	25.74	.0267	.0197	2535.	2947.
802	delta flume	.0187	1.600	5.0	1.64	SL	1.000	4.30	5.00	33.42	.0347	.0256	3292.	3828.
803	delta flume	.0187	1.600	5.0	1.64	PM	1.500	4.60	5.50	50.13	.0454	.0318	5282.	6315.
804	delta flume	.0041	1.600	5.0	1.85	PM	.6200	2.60	2.98	94.51	.0588	.0473	12020	13407
805	delta flume	.0041	1.600	5.0	1.85	PM	1.240	3.90	4.50	189.0	.0523	.0393	36060	41608
806	delta flume	.0041	1.600	5.0	1.85	PM	1.680	5.00	5.70	256.1	.0431	.0331	62635	71404
807	delta flume	.0041	1.600	5.0	1.85	PM	1.280	3.90	4.50	195.1	.0540	.0405	37223	42950
808	delta flume	.0041	1.600	5.0	1.85	PM	1.020	4.30	5.10	164.6	.0374	.0266	34628	41070
809	delta flume	.0041	1.600	5.0	1.85	PM	1.140	5.90	7.60	173.8	.0210	.0127	50153	64604

Boundary conditions for tests with varying water level

parameters in columns

column	description
1	test number: last figure gives the part of the test
2	description: variation swl = varying water level with constant wave boundary conditions, see Figure 4.2
	storm tide = tests simulating storm surges, see Figure 4.2
3	nominal diameter, D_{n50} (m)
4	relative mass density, Δ
5	slope angle, $\cot\alpha$
6	grading, D_{85}/D_{15}
7	spectral shape: PM = Pierson Moskowitz spectrum
8	water level at beginning and end of part of test
9	significant wave height in front of the structure, H_s (m)
10	average wave period, T_m (s)
11	peak period, T_p (s)
12	wave height parameter: $H_s/\Delta D_{n50}$
13	fictitious wave steepness: $s_m = 2\pi H_s/g T_m^2$
14	combined wave heigt-wave period parameter: $H_oT_o = H_s/\Delta D_{n50} * \sqrt{g/D_{n50}}\, T_m$

1	2	3	4	5	6	7	8	9	10	11	12	13	14
3601	variation swl	.0110	1.586	3.0	1.50	PM	.72-.72M	.1271	1.31	1.45	7.29	.0475	285.0
3602	variation swl	.0110	1.586	3.0	1.50	PM	.72-.64M	.1265	1.33	1.56	7.25	.0458	289.0
3603	variation swl	.0110	1.586	3.0	1.50	PM	.64-.72M	.1266	1.30	1.40	7.26	.0480	282.0
3611	variation swl	.0110	1.586	3.0	1.50	PM	.72-.72M	.1281	1.73	2.03	7.34	.0274	379.0
3612	variation swl	.0110	1.586	3.0	1.50	PM	.72-.64M	.1284	1.72	2.07	7.36	.0278	378.0
3613	variation swl	.0110	1.586	3.0	1.50	PM	.64-.72M	.1283	1.73	2.02	7.35	.0275	380.0
3621	variation swl	.0110	1.586	3.0	1.50	PM	.72-.72M	.1888	1.74	2.02	10.62	.0409	562.0
3622	variation swl	.0110	1.586	3.0	1.50	PM	.72-.64M	.1863	1.76	1.90	10.68	.0385	561.0
3623	variation swl	.0110	1.586	3.0	1.50	PM	.64-.72M	.1899	1.76	1.98	10.89	.0393	572.0
3631	variation swl	.0110	1.586	3.0	1.50	PM	.72-.72M	.1819	2.47	3.05	10.43	.0191	769.0
3632	variation swl	.0110	1.586	3.0	1.50	PM	.72-.64M	.1826	2.45	3.00	10.47	.0195	766.0
3633	variation swl	.0110	1.586	3.0	1.50	PM	.64-.72M	.1847	2.46	2.99	10.59	.0196	778.0
3641	variation swl	.0110	1.586	3.0	1.50	PM	.72-.72M	.2406	1.80	2.66	14.10	.0476	758.0
3642	variation swl	.0110	1.586	3.0	1.50	PM	.72-.64M	.2276	1.80	2.08	13.04	.0450	701.0
3643	variation swl	.0110	1.586	3.0	1.50	PM	.64-.72M	.2408	1.82	2.99	13.80	.0466	750.0
3651	variation swl	.0110	1.586	3.0	1.50	PM	.72-.72M	.2330	2.44	3.10	13.36	.0251	973.0
3652	variation swl	.0110	1.586	3.0	1.50	PM	.72-.64M	.2259	2.43	3.10	12.95	.0245	940.0
3653	variation swl	.0110	1.586	3.0	1.50	PM	.64-.72M	.2335	2.43	3.03	13.38	.0254	971.0
3661	storm tide	.0110	1.586	3.0	1.50	PM	.64-.72M	.1305	1.73	1.99	7.48	.0280	386.0
3662	storm tide	.0110	1.586	3.0	1.50	PM	.68-.80M	.1920	1.75	2.03	11.00	.0402	575.0
3663	storm tide	.0110	1.586	3.0	1.50	PM	.68-.80M	.1928	1.74	2.00	11.05	.0408	574.0
3664	storm tide	.0110	1.586	3.0	1.50	PM	.64-.72M	.1317	1.73	1.97	7.55	.0282	390.0
3671	storm tide	.0110	1.586	3.0	1.50	PM	.64-.72M	.1142	2.40	3.03	6.55	.0127	469.0
3672	storm tide	.0110	1.586	3.0	1.50	PM	.68-.80M	.2053	2.44	3.03	11.77	.0221	858.0
3673	storm tide	.0110	1.586	3.0	1.50	PM	.68-.80M	.2032	2.49	3.05	11.65	.0210	866.0
3674	storm tide	.0110	1.586	3.0	1.50	PM	.64-.72M	.1288	2.50	3.03	7.38	.0132	551.0
3681	storm tide	.0110	1.586	3.0	1.50	PM	.64-.72M	.1589	1.73	2.00	9.10	.0340	470.0
3682	storm tide	.0110	1.586	3.0	1.50	PM	.68-.80M	.2437	1.79	2.05	13.97	.0488	747.0
3683	storm tide	.0110	1.586	3.0	1.50	PM	.68-.80M	.2446	1.78	1.99	14.02	.0495	745.0
3684	storm tide	.0110	1.586	3.0	1.50	PM	.64-.72M	.1590	1.73	1.98	9.11	.0341	471.0
3691	variation swl	.0110	1.586	5.0	1.50	PM	.72-.72M	.1901	1.73	2.01	10.90	.0407	563.0
3692	variation swl	.0110	1.586	5.0	1.50	PM	.72-.64M	.1924	1.74	2.01	11.03	.0407	573.0
3693	variation swl	.0110	1.586	5.0	1.50	PM	.64-.72M	.1903	1.75	2.01	10.91	.0398	570.0
3701	variation swl	.0110	1.586	5.0	1.50	PM	.72-.72M	.1871	2.50	3.13	10.72	.0192	800.0
3702	variation swl	.0110	1.586	5.0	1.50	PM	.72-.64M	.1896	2.46	3.05	10.87	.0201	799.0
3703	variation swl	.0110	1.586	5.0	1.50	PM	.64-.72M	.1852	2.50	3.01	10.62	.0190	793.0
3711	variation swl	.0110	1.586	5.0	1.50	PM	.72-.72M	.2401	1.78	2.12	13.76	.0486	731.0
3712	variation swl	.0110	1.586	5.0	1.50	PM	.72-.64M	.2294	1.81	2.23	13.15	.0449	711.0
3713	variation swl	.0110	1.586	5.0	1.50	PM	.64-.72M	.2401	1.79	2.16	13.76	.0480	736.0
3721	variation swl	.0110	1.586	5.0	1.50	PM	.72-.72M	.2344	2.44	3.13	13.44	.0252	979.0
3722	variation swl	.0110	1.586	5.0	1.50	PM	.72-.64M	.2263	2.38	3.17	12.97	.0256	922.0
3723	variation swl	.0110	1.586	5.0	1.50	PM	.64-.72M	.2336	2.41	3.15	13.39	.0258	964.0
3731	storm tide	.0110	1.586	5.0	1.50	PM	.64-.72M	.1335	1.74	2.01	7.65	.0288	398.0
3732	storm tide	.0110	1.586	5.0	1.50	PM	.68-.80M	.1908	1.74	2.08	10.94	.0404	568.0
3733	storm tide	.0110	1.586	5.0	1.50	FM	.68-.80M	.1918	1.74	1.99	11.00	.0406	572.0
3734	storm tide	.0110	1.586	5.0	1.50	PM	.64-.72M	.1345	1.74	1.97	7.71	.0284	401.0
3741	storm tide	.0110	1.586	5.0	1.50	PM	.64-.72M	.1614	1.74	2.00	9.25	.0342	481.0
3742	storm tide	.0110	1.586	5.0	1.50	PM	.68-.80M	.2412	1.77	2.10	13.83	.0494	731.0
3743	storm tide	.0110	1.586	5.0	1.50	PM	.68-.80M	.2421	1.77	2.00	13.86	.0495	734.0
3744	storm tide	.0110	1.586	5.0	1.50	PM	.64-.72M	.1634	1.73	1.98	9.37	.0350	484.0
3751	variation swl	.0062	1.483	5.0	1.50	PM	.72-.72M	.1916	1.74	2.03	20.84	.0406	1442.0
3752	variation swl	.0062	1.483	5.0	1.50	PM	.72-.64M	.1878	1.75	1.99	20.43	.0393	1422.0
3753	variation swl	.0062	1.483	5.0	1.50	PM	.64-.72M	.1917	1.75	1.99	20.85	.0401	1451.0
3761	variation swl	.0062	1.483	5.0	1.50	PM	.72-.72M	.1936	2.49	3.03	21.06	.0200	2086.0
3762	variation swl	.0062	1.483	5.0	1.50	PM	.72-.64M	.1908	2.49	3.03	20.75	.0197	2058.0
3763	variation swl	.0062	1.483	5.0	1.50	PM	.64-.72M	.1940	2.48	3.01	21.10	.0202	2081.0
3771	storm tide	.0062	1.483	5.0	1.50	PM	.64-.72M	.1301	1.74	2.01	14.15	.0276	979.0
3772	storm tide	.0062	1.483	5.0	1.50	PM	.68-.80M	.1921	1.74	2.04	20.89	.0407	1446.0
3773	storm tide	.0062	1.483	5.0	1.50	PM	.68-.80M	.1934	1.74	2.01	21.03	.0410	1456.0
3774	storm tide	.0062	1.483	5.0	1.50	PM	.64-.72M	.1346	1.73	2.00	14.64	.0289	1007.0

APPENDIX IV

Equivalent slope angle and the low H_0T_0 region

Equivalent slope angle

The method to establish equivalent slope angles for an arbitrary initial slope is described below and is shown in Figure Al.

1. Draw a uniform line through the points $+H_s$ and $-1.5 H_s$.
2. Establish the center of gravity of the figure between $+H_s$ and $-1.5 H_s$ formed by the uniform line and the initial slope (shaded figure).
3. A line through $+H_s$ and the center of gravity gives $\cot\alpha_1$. This equivalent slope angle should be used for l_r, h_c and l_c.
4. A line through $-1.5 H_s$ and the centre of gravity gives $\cot\alpha_2$ which should be used for h_s and l_s.
5. A line through $-H_s$ and $-3 H_s$ gives $\cot\alpha_3$. This equivalent slope angle should be used for $\tan\beta$, h_t, and $\tan\gamma$.
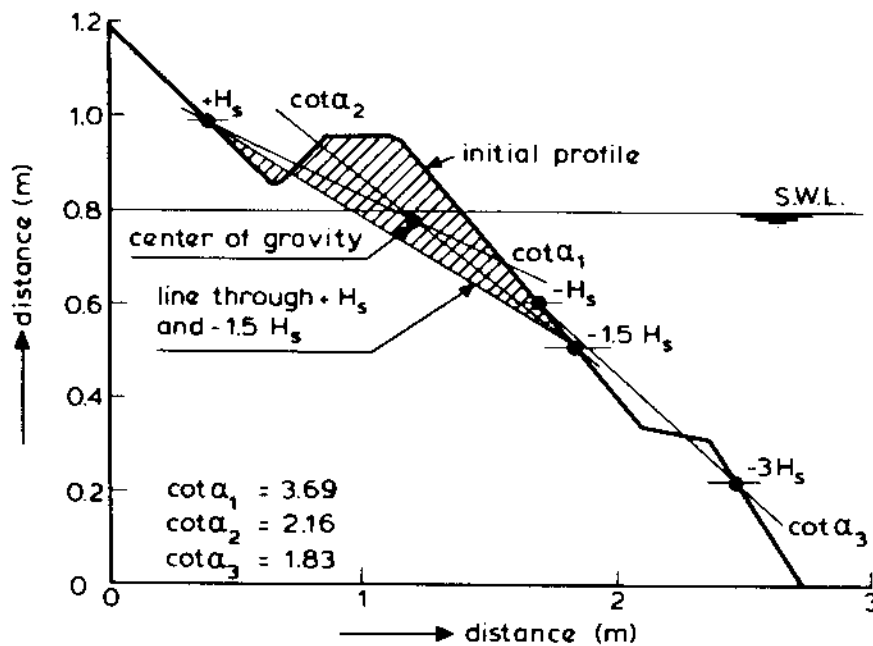

Figure A.1 Equivalent slope angle

Equations for the low H_0T_0 region

The equations for $H_0T_0 > 500 - 2000$ are independent of the slope angle and are given in Section 4.4. The equations for the low H_0T_0 region and the transition to the equations mentioned above, will be described here.

The run-up length, l_r

$$H_0T_0 = (20 - 1.5 \cot\alpha_1) \, l_r/D_{n50}N^{0.05} - 40 \qquad (A.1)$$

The intersection with Equation 4.7 gives the transition.

The crest height, h_c

$$H_0 T_0 = 33 (h_c/D_{n50}N^{0.15})^{1.3} + 30 \cot \alpha_1 - 30 \qquad (A.2)$$

Equation A.2 yields for $H_0 T_0 < 900$ and 4.13 for $H_0 T_0 > 900$.

The crest length, l_c

$$H_0 T_0 = (3 \cot \alpha_1 + 25) \, l_c/D_{n50}N^{0.12} \qquad (A.3)$$

The intersection with Equation 4.9 gives the transition.

The step height, h_s

$$H_0 T_0 = 27 (h_s/D_{n50}N^{0.07}) + 1.25 \cot \alpha_2 - 475 \qquad (A.4)$$

Equation A.4 yields for $H_0 T_0 < 300 \cot \alpha_2$ and 4.14 for $H_0 T_0 > 300 \cot \alpha_2$.

The step length, l_s

$$H_0 T_0 = 2.6 (l_s/D_{n50}N^{0.07})^{1.3} + 70 \cot \alpha_2 - 210 \qquad (A.5)$$

The intersection with Equation 4.11 gives the transition.

The transition height, h_t

$$H_0 T_0 = 10 (h_t/D_{n50}N^{0.04})^{1.3} + 175 \cot \alpha_3 - 725 \qquad (A.6)$$

Equation A.6 yields for $H_0 T_0 < 400 \cot \alpha_3$ and 4.15 for $H_0 T_0 > 400 \cot \alpha_3$.

CURRICULUM VITAE

Jentsje Wouter van der Meer werd geboren op 27 februari 1955 te Leeuwarden. Na een jaar MULO te Akkrum werd het middelbaar onderwijs voortgezet aan het Lienward College te Leeuwarden alwaar hij het HBS-b diploma behaalde in 1972. Daarna studeerde hij Bouwkunde aan de HTS te Leeuwarden. Deze opleiding werd voltooid in 1976. Van 1976 tot 1981 studeerde hij Civiele Techniek aan de Technische Hogeschool te Delft. Het afstudeerwerk behelsde een onderzoek naar het gedrag van betonnen opslagtanks voor vloeibaar gemaakte gassen onder explosie belasting. Het onderzoek werd afgesloten met een verslag en een publikatie. Het diploma voor Civiel Ingenieur werd behaald in 1981.

In september 1981 trad van der Meer in dienst bij Waterloopkundig Laboratorium - WL, in de Noordoostpolder, eerst bij de afdeling Maritieme Konstrukties en thans bij de sektor Havens, Kusten en Offshore. Hij verrichtte projekt gericht en fundamenteel onderzoek op het gebied van golfbrekers, taludverdedigingen en grindstranden. Tevens schreef hij een aantal publikaties over deze onderwerpen.

In begin 1987 trad hij tijdelijk als Universitair Docent voor 0,2 dagtaak in dienst bij de Technische Universiteit Delft, vakgroep Waterbouwkunde. In 1987 kreeg hij voor één van zijn publikaties de Halcrow Premium van het engelse instituut van civiele ingenieurs (ICE).